Studies on the interaction of Streptomyces subtilisin inhibitor with proteinases(Dissertation_全文)

AUTHOR(S):

Inoue, Kuniyo

Studies on the Interaction of *Streptomyces* Subtilisin Inhibitor with Proteinases

Kuniyo Inouye

1977

Studies on the Interaction of *Streptomyces* Subtilisin Inhibitor with Proteinases

Kuniyo Inouye

1977

Preface

The studies presented in this dissertation have been carried out under the direction of Professor Keitaro Hiromi at Kyoto University during 1972 - 1977.

During the last half of this century there has been a rapid development in the fields of protein chemistry and enzyme chemistry. It has been the author's eagerness to understand the specific interaction between proteins at the molecular level, namely, molecular recognition of proteins by proteins, because he believes that it plays significant roles in the biological phenomena.

In 1972, a unique protein was isolated by Professor Sawao Murao and Dr. Sakae Sato from the culture broth of a strain of *Streptomyces*. This protein inhibits strongly and specifically only alkaline serine proteinases. The studies presented here are concerned with the characterization of the protein, *Streptomyces* subtilisin inhibitor, and with the molecular aspects of the interaction of the inhibitor and proteinases especially subtilisin BPN'. This inhibitor provides us with a suitable entity not only for studying the protein-protein interaction but also for making clear an obscure phenomenon that a protein inhibits a proteinase.

November 1977

Kuniyo Inouye

Strong Son of God, immortal Love,
Whom we, that have not seen thy face,
By faith, and faith alone, embrace,
Believing where we cannot prove,

——— Tennyson, In Memoriam

Contents

Abbreviations and Symbols

AcTrpOEt	*N*-acetyl-L-tryptophan ethyl ester
AcTyrOEt	*N*-acetyl-L-tyrosine ethyl ester
BA	*N*-benzoyl-L-arginine
BEPCI	black-eyed pea chymotrypsin and trypsin inhibitor
BEPTI	black-eyed pea trypsin inhibitor
BPTI	basic pancreatic trypsin inhibitor (Kunitz)
CMC	critical micelle concentration
DIP	diisopropyl phosphoridate-inhibited
D_2O	deuterium oxide
EG	ethylene glycol
Met	methanol
MW	molecular weight
pCMB	*p*-chloromercuribenzoate
PEG	polyethylene glycol #300
PF	proflavine
pNPA	*p*-nitrophenyl acetate
PSTI	pancreatic secretory trypsin inhibitor (Kazal)
RTIC	rotor-temperature indicator and control
SDS	sodium dodecyl sulfate
SSI	*Streptomyces* subtilisin inhibitor
STI	soybean trypsin inhibitor (Kunitz)
TAME	tosyl-L-arginine methyl ester
tCI	*N-trans*-cinnamoyl imidazole
ZAGPCK	*N*-carbobenzoxy-L-alanyl-glycyl-L-phenylalanine chloromethyl ketone-treated

A	absorbance
B	second virial constant
C	concentration
D	diffusion coefficient (cm^2 sec^{-1})
D	(effective) dielectric constant
d	purity of the proteinase preparation
E	extinction, absorbance; enzyme
G	Gibbs free energy

g	gravity; centrifugal force
I	inhibitor; SSI
K_a	apparent acidic dissociation constant ($pK_a = - \log K_a$)
K_d	enzyme-inhibitor dissociation constant
K_i	enzyme-inhibitor dissociation constant (inhibitor constant)
K_m	Michaelis constant
K_s	enzyme-substrate dissociation constant (substrate constant)
k	rate constant
Mw	weight average molecular weight
Mw*	apparent (cell average) weight average molecular weight
N	Avogadro's number (6.02×10^{23} $mole^{-1}$)
n	refractive index
P	product
R	gas constant (8.31 $JK^{-1}mole^{-1} = 1.987$ cal $mole^{-1}deg^{-1}$)
r	radius
r	distance
S	Svedverg unit (10^{-13} sec)
s	sedimentation coefficient (S)
T	absolute temperature (K)
t	time
$t_{1/2}$	half-life period
v	(initial) velocity of reaction
$\bar{v}$	partial specific volume (ml/g)
Z	valence
Δ	measurable increment
δ	gram of detergent bound per gram of protein (g/g)
ε	molar extinction coefficient; the proton unit of charge (4.80×10^{-10} esu)
λ	wavelength (nm)
π	magnitude of initial burst
ρ	density of solution (g/ml)
Ψ	potential
ϕ'	effective partial specific volume (ml/g)
ω	angular velocity (rad)
$[\ ]_o$	initial concentration

Chapter One

General Introduction

The naturally occurring protein inhibitors of proteolytic enzymes are unique materials in biological science. They have the capacity of combining with and inactivating those proteins that have the capacity of hydrolyzing and degrading one of their own species. The inhibitor, proteolytic enzyme, and protein substrate have very different roles in the inhibitory process.

Within an individual, many homologous and analogous forms of these inhibitors may exist in different tissues and secretions. The homology and analogy is carried further, and indeed is thereby more interesting scientifically, in that the different inhibitors may react with different analogous and homologous forms of proteolytic enzymes. These homologous and analogous forms of the inhibitors and the enzymes provide a unique opportunity for studying the relationship between the structures of the proteins and the properties required for their interactions. The reaction between enzyme and inhibitor results in the formation of a complex of the two proteins that is usually stable over a wide pH range. Such a system has many characteristics that lend themselves well to physical-chemical studies and thus provide a useful tool for the fundamental study of specific protein-protein interaction.

Proteinase inhibitors are widely distributed in both animals and plants. In plants they are particularly plentiful in the legumes. The principal plant inhibitors that have been studied are those from soybeans, lima beans, pea, potatoes and eggplants; the principal animal

inhibitors that have been studied are those from pancreas, colostrum, blood plasma, and avian egg white. Inhibitors have also been found in seminal fluid, urine, and certain intestinal parasites. Some of these inhibitors may have an important function in biological control mechanisms and may have practical significance in animal and human nutrition.

The discovery of the inhibitors of proteolytic enzymes have been closely related to the history of the proteolytic enzymes that they inhibit. Inhibitors of bovine trypsin and α-chymotrypsin were reported as early as 1900. However, the first real understanding of the fundamental nature of the problem began with the crystallization of a trypsin inhibitor from bovine pancreas and crystallization of its complex with trypsin by Kunitz and Northrop (*1*) in the mid-1930's. Approximately a decade later the trypsin inhibitory activity was noticed in soybeans by Ham and Sandstedt (*2*), and by Bowman (*3*). This was followed several years later by the crystallization of a soybean inhibitor by Kunitz (*4*). Ovomucoid from chicken egg white had been regarded as a distinct protein until 1947, when Lineweaver and Murray detected a trypsin-inhibitory activity in chicken ovomucoid (*5*). During the next few years inhibitory activities against proteinases were found in many biological materials and an excellent review of inhibitors of proteolytic enzymes was published in 1954 by Laskowski, Sr. and Laskowski, Jr. (*6*). Methods for the assay and isolation of a number of inhibitor was published in 1955 by Laskowski, Sr. (*7*). During the last decade there have been many investigations on these inhibitors. The most recent work is an attempt to understand the enzyme-inhibitor interaction and specificity in molecular terms. This approach is recent because, only within the last decade, the molecular aspects of the enzymes was enough learned about and suffi-

ciently sensitive physical and chemical probes were developed.

In 1970 the tertiary structure of the bovine pancreatic trypsin inhibitor (Kunitz) was reported by Huber *et al.* (*8,9*). The tertiary structures of the complex formed by bovine pancreatic trypsin inhibitor (Kunitz) and bovine trypsin and that formed by soybean trypsin inhibitor (Kunitz) and porcine trypsin were reported by Huber and his coworkers (*10*) and Blow and his coworkers (*11*), respectively.

There are several current reviews of the nutritional (*12,13*), pharmacological (*14*), and general (*15-17*) aspects of proteinase inhibitors. The largest collection of references is the review by Vogel *et al.* (*18*). The international conferences on protein proteinase inhibitors have considered the physical-chemical properties of protein-protein interaction and the molecular evolution of proteins, as well as their physiological role especially in blood coagulation and fertilization (*19,20*).

In 1972 a protein proteinase inhibitor was isolated and crystallized from the culture broth of *Streptomyces albogriseolus* S-3253 by Murao and Sato (*21,22*). The inhibitor is one of the first protein proteinase inhibitors obtained from microbe and has a unique inhibitory specificity towards various proteinases. It was reported that it inhibits only microbial alkaline serine proteinases represented by subtilisin BPN', but not other serine proteinases including trypsin, chymotrypsin, plasmin and thrombin. It does not inhibit plant proteinases, ficin and papain, and also acid proteinases including pepsin and microbial acid proteinases (Table 1.1) (*23*). The inhibitor has been named *Streptomyces* Subtilisin Inhibitor (abbreviated in the following as SSI) after its inhibitory specificity.

Table 1.1. Inhibitory Activity of SSI.[a]

Proteinase	pH	Substrate	Inhibition
1. Subtilisin BPN'	9.5	casein	+
2. *B. subtilis* SO4 alkaline proteinase	9.5	casein	+
3. *B. subtilis* var. *amylosaccharitticus* alkaline proteinase	9.5	casein	+
4. *Streptomyces* sp. alkaline proteinase	9.5	casein	+
5. *Cephalosporium* sp. alkaline proteinase	9.5	casein	+
6. Trypsin	7.0	casein	-
7. α-Chymotrypsin	7.0	casein	-
8 Thrombin	7.2	TAME	-
9. Plasmin	7.2	fibrin	-
10. Papain	7.0	casein	-
11. Ficin	7.0	casein	-
12. *Pseudomonas aeruginosa* neutral proteinase	7.0	casein	-
13. Pepsin	1.6	casein	-
14. *Rhodotorula glutinis* acid proteinase	2.5	casein	-
15. *Cladosporium* sp. acid proteinase	2.5	casein	-

[a] cited from Sato and Murao (1973) (*23*).

TAME: tosyl-L-arginine methyl ester

Subtilisin BPN' is one of the best characterized proteinases, as well as α-chymotrypsin and trypsin, in the sense that the information on the primary (*24,25*) and tertiary (*26*) structures has been obtained. As to SSI, the amino acid sequence was determined in 1974 by Ikenaka *et al.* (Fig. 1.1) (*27*), and the tertiary structure was recently determined from X-ray analysis by Mitsui *et al.* on the basis of an electron density map at 2.3 A resolution (*28,29*). As shown in Fig. 1.1, SSI is a single polypeptide of 113 amino acid residues including two disulfide bridges. This protein has no isoleucine but contains a large number of alanine and valine. Based on the experiments with α-chymotrypsin, the susceptible

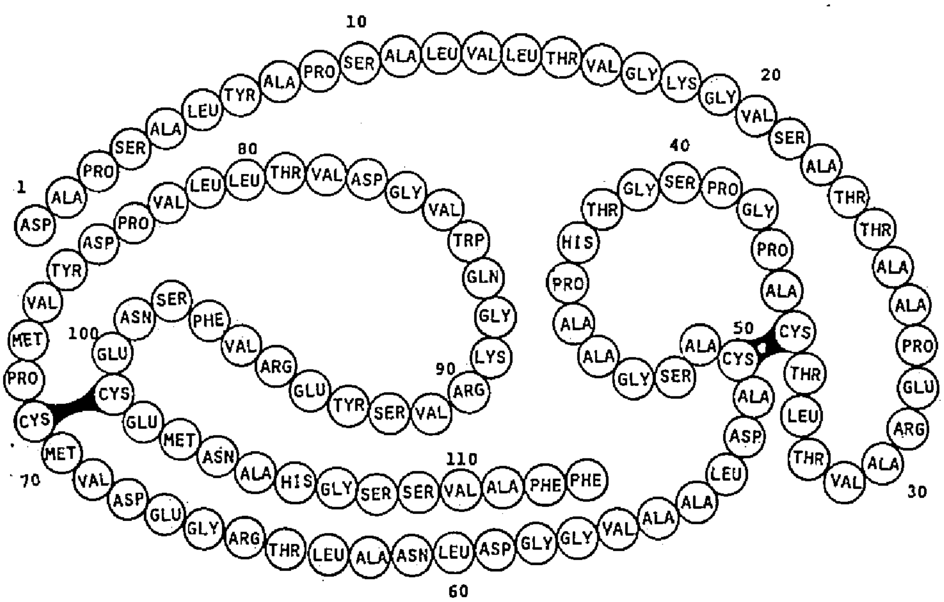

Fig. 1.1. The amino acid sequence of *Streptomyces* Subtilisin Inhibitor, SSI, cited from Ikenaka *et al.* (1974) (*27*). The reactive site is considered to be Met 73-Val 74 (*27*).

---

peptide bond to the active site of proteinase has been considered to be Met 73-Val 74 and the methionine to be a reactive (anti-proteinase) site residue (*27*). The interaction of SSI and subtilisin BPN' can thus be an excellent model system for studying the molecular aspects of the strong and specific interaction between proteins which play important roles in the biological phenomena. It can also provide some information about the catalytic mechanism of proteolytic enzymes, since the studies on the reaction by proteolytic enzymes have so far been made exclusively by using synthetic small substrates, and not physiologically significant natural substrates.

In the present thesis are described physical-chemical properties of *Streptomyces* Subtilisin Inhibitor, SSI, and the interaction between the inhibitor and proteinases, especially subtilisin BPN', at the molec-

ular level revealed by using enzyme kinetic and spectrophotometric methods.

In Chapter Two, the stoichiometry of the inhibition and binding of SSI against subtilisin BPN' is described. A molecule of SSI (of 113 amino acid residues) combines with one molecule of the enzyme and strongly inhibits it. The inhibitor constant was estimated to be less than 10^{-9} M.

In Chapter Three is depicted the determination of the molecular weights of SSI and the complex of SSI and subtilisin BPN' by sedimentation method. SSI was shown to exist in solution as a dimer of identical subunits. It was indicated from the molecular weight of the complex that a dimer molecule of SSI combines with two molecules of subtilisin BPN'.

In Chapter Four, however, SSI is shown to dissociate into monomers with low concentration of sodium dodecyl sulfate without loss of the inhibitory activity.

In Chapter Five is described the interaction of SSI with α-chymotrypsin and trypsin which have been reported not to be inhibited by SSI (Table 1.1) (*23*). The homology between the active-site structures of α-chymotrypsin and subtilisin BPN' has been shown by substrate specificity (*30*) and by X-ray crystallography (*31,32*) notwithstanding the much differences in the origin and the amino acid sequence. This homology has been explained by virtue of the convergence in evolution (*31-33*). SSI has been shown in the present study to bind α-chymotrypsin and inhibits its activity to a much less extent. SSI appears to recognize the subtle difference between the active site of the both enzymes.

In Chapter Six, the investigation of the states of tyrosyl and

tryptophyl residues of SSI by means of solvent perturbation and spectrophotometric titration at alkaline pH region are described. Three tyrosyl residues are all accessible to all of the solvent used. One tryptophyl residue is not accessible to polyethylene glycol, and partially accessible to methanol and ethylene glycol. The apparent pK_a values of the three tyrosyl residues were determined separately to be 9.66, 11.02, and 12.33.

In Chapter Seven, the interaction of SSI and subtilisin BPN' is described. On the formation of the complex between SSI and the enzyme, 4 to 5 tyrosyl and a tryptophyl residues become inaccessible to ethylene glycol, and simultaneously a typical and big absorption difference spectrum due to pK_a-shift of a tyrosyl residue of apparent pK_a 9.7 upwards to > 11.5 is observed.

In Chapter Eight, by chemical modification studies, it is shown that this tyrosyl residue belongs to subtilisin BPN' and the pK_a-shift is resulted from the approach of carboxyl group(s) of SSI on the formation of the complex between subtilisin BPN' and SSI.

In Chapter Nine, the interaction of the tyrosyl residue and carboxyl group(s) in SSI-subtilisin BPN' system is compared with that in SSI-thiolsubtilisin BPN' system. Thiolsubtilisin BPN' is an artificial enzyme obtained by converting the serine residue at the catalytic site of subtilisin BPN' into cysteine. The binding of SSI and this "cysteine" enzyme was shown to be ten thousands or more weaker than that of SSI and subtilisin BPN'. On the binding of thiolsubtilisin BPN' and SSI, the apparent pK_a value of a tyrosyl residue of the enzyme changes from 9.7 to 10.2. Differences in the dissociation constants and the degrees of pK_a-shift between the bindings of subtilisin BPN' and thiolsubtilisin

BPN' with SSI are considered to be due to a subtle difference in geography of the active sites between those enzymes. The significance of good fitness between the active site of subtilisin BPN' and the reactive site of SSI for their strong binding is discussed.

Chapter Two

The Stoichiometry of Inhibition and Binding of *Streptomyces* Subtilisin Inhibitor to Subtilisin BPN' *

2.1 Introduction

A protein proteinase inhibitor of unique properties, *Streptomyces* subtilisin inhibitor, inhibits almost exclusively the hydrolytic activity of the alkaline serine proteinases (*23*). The author believes that this protein is a good object for the comparative study of specific protein-protein interaction between subtilisin BPN' and α-chymotrypsin whose three-dimensional structures have been elucidated in detail (*26,34*) (see Chapter Four).

The term "protein proteinase inhibitor" refers to a protein which may associate reversibly with one or more proteinases to form complexes of *descrete* stoichiometry in which *all* of the catalytic functions of the proteinase are *competitively* inhibited (*15*).

In this Chapter the stoichiometry of inhibition and binding of SSI to subtilisin BPN' and some characteristics of the inhibition are described.

2.2 Experimental Procedures

---

* A part of this study was presented at the Annual Meeting of the Agricultural Chemical Society of Japan (Tokyo, April 1973), and published in *J. Biochem.* (1977) 82, 961-967 (*a*).

Inhibitor. A three times crystallized and lyophilized preparation of *Streptomyces* subtilisin inhibitor, SSI, obtained from the culture broth of *Streptomyces albogriseolus* S-3253 according to the previously reported method (*22,23*) was a generous gift from Professor S. Murao. The preparation showed a single band on polyacrylamide gel electrophoresis either at pH 2.3, 6.6, or 9.5 (*23*). The minimal molecular weight calculated from the amino acid composition (*27*) is 11,500 (Fig. 1.1). This value was used throughout the study.

Enzyme. A three times crystallized preparation of subtilisin BPN' [EC 3.4.21.14] was purchased from Nagase & Co. Ltd., Osaka (Lot No. 01026) and used without further purification. The purity of the enzyme preparation was determined as described later. The molecular weight was taken to be 27,500 on the basis of the amino acid composition (*24,25*).

Substrates. *p*-Nitrophenyl acetate (pNPA) (Tokyo Kasei Kogyo Co. Ltd.) and *N-trans*-cinnamoyl imidazole (Sigma Chemical Co.) were used without further purification. The concentration of pNPA (pK_a = 7.14) and *N-trans*-cinnamoyl imidazole solutions were determined spectrophotometrically at pH 7.00 with $\varepsilon_{405} = 7.73 \times 10^3\ M^{-1}cm^{-1}$ and $\varepsilon_{335} = 9.04 \times 10^3\ M^{-1}cm^{-1}$, respectively, after complete hydrolysis.

Determination of protein concentration. The concentration of subtilisin BPN' and SSI were determined spectrophotometrically at pH 7.00 with a Shimadzu UV-200 recording spectrophotometer. The absorptivity of subtilisin BPN' was assumed to be $E_{1\ cm}^{0.1\%}$(278 nm) = 1.063 and $E_{1\ cm}^{0.1\%}$(280 nm) = 1.041, and that of SSI to be $E_{1\ cm}^{0.1\%}$(276 nm) = 0.829 and $E_{1\ cm}^{0.1\%}$(280 nm) = 0.796. These values were calculated on the basis of the amino acid compositions of these proteins (*24,27*). The values of absorptivity of these protein preparations observed by the author were as follows: $E_{1\ cm}^{0.1\%}$(278

nm) = 1.078 and $E_{1\ cm}^{0.1\%}$(280 nm) = 1.066 for subtilisin BPN', and $E_{1\ cm}^{0.1\%}$(276 nm) = 0.822 and $E_{1\ cm}^{0.1\%}$(280 nm) = 0.810 for SSI.

Determination of the purity of subtilisin BPN' preparation. The purity of the subtilisin BPN' preparation used was determined by the active-site titration essentially according to the method of Bender *et al.* (1966) (*35*) with slight modifications. Two kinds of titrant, *p*-nitrophenyl acetate (pNPA) and *N-trans*-cinnamoyl imidazole were used.

Equal volumes of an enzyme solution in 20 mM pyrophosphate buffer, pH 8.50 and a pNPA solution in water containing 10.0% (v/v) isopropanol were mixed in a Union SF-70 stopped-flow apparatus. Changes in transmittance and absorbance at 405 nm due to the liberation of *p*-nitrophenol were monitored on an Iwatsu MS-5019A storage oscilloscope, and the reaction profile was recorded with a camera (as Fig. 2.1). The final concentration of the enzyme was in the range of 0.70 - 2.0 mg/ml (25.5 - 72.7 μM assuming the enzyme preparation to be 100% pure) and that of pNPA was in the range between 0.364mM and 1.82 mM. The molar absorptivity difference between pNPA and *p*-nitrophenol, $\Delta\varepsilon_{405}$, was determined to be $1.76 \times 10^4\ M^{-1}cm^{-1}$ at pH 8.50.

The stoichiometric basis of the active-site titration of the hydrolytic enzyme may be represented by the reaction scheme 2.1, which represents the overall pathway for α-chymotrypsin, trypsin, elastase, subtilisin, papain, and acetylcholinesterase reactions (*35,36*).

$$E + S \underset{}{\overset{K_s}{\rightleftharpoons}} ES \xrightarrow{k_2} \underset{+\ P_1}{ES'} \xrightarrow{k_3} \underset{+\ P_2}{E} \qquad (2.1)$$

Here, in the present case, E is subtilisin BPN'; S, the substrate, pNPA; ES, the Michaelis complex; ES', acyl-enzyme intermediate; P_1, *p*-nitrophenol; and P_2, acetate. The conversion of E and S into ES' and P_1 can be

considered a stoichiometric reaction with respect to an individual active site. If this process can be observed before the turnover (regeneration) of the enzyme occurs, then a direct measurement of the active enzyme concentration may be made.

The most common set of conditions for observation of enzymatic processes, and the most important set for the determination of the enzyme concentration, utilizes $[S]_o >> [E]_o$, where $[S]_o$ and $[E]_o$ is the initial concentrations of substrate (pNPA) and enzyme (subtilisin BPN'), respectively. Under these conditions a pre-steady state (acylation) and a steady state (deacylation) may be observed, the former often being too fast to measure, and the concentration of P_1 liberated in the pre-steady state, π (the magnitude of the apparent initial burst), is related to the concentration of active site of the enzyme. For the reaction scheme 2.1, when $[S]_o >> [E]_o$, the concentration of *p*-nitrophenol liberated in time t, $[P_1]$, can be described by

$$[P_1] = At + \pi(1 - e^{-bt}) \tag{2.2}$$

where $A = k_{cat}[E]_o[S]_o / ([S]_o + K_m)$ (the steady-state rate) (2.3)

$b = \{(k_2 + k_3)[S]_o + k_3K_s\} / (K_s + [S]_o)$ (an apparent rate constant for the burst) (2.4)

and π may be expressed as

$$\pi = [E]_o\{k_2/(k_2 + k_3)\}^2 / \{1 + (K_m/[S]_o)\}^2 \tag{2.5}$$

Here, K_m and k_{cat} are, respectively, the apparent Michaelis constant and the catalytic rate constant (molecular activity) $\{k_2k_3/(k_2 + k_3)\}$ obtained for the steady state phase of the reaction curve.

At time when $t >> b$ holds, the exponential term of Eq. 2.2 approaches zero and P_1 can be described as a linear function of t,

$$[P_1] = \pi + At \tag{2.6}$$

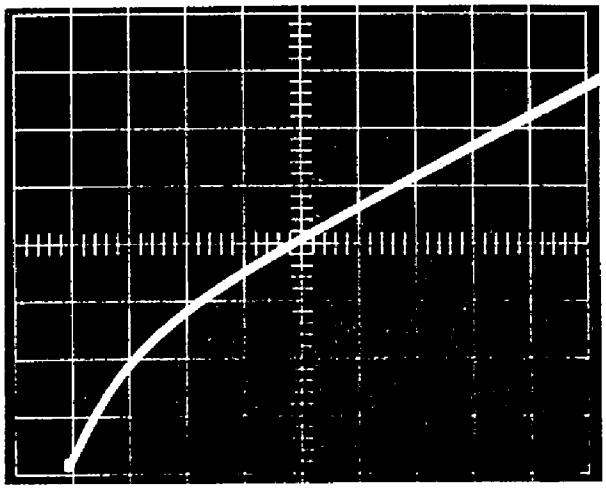

Fig. 2.1. Stopped-flow oscillogram of the liberation of *p*-nitrophenol during the hydrolysis of *p*-nitrophenyl acetate by subtilisin BPN'. [subtilisin BPN']$_o$ = 2.0 mg/ml, and [pNPA]$_o$ = 3.2 mM in 20 mM pyrophosphate buffer, pH 8.5, containing 5.0% (v/v) isopropanol, 25°C. Wavelength, 405 nm. Scale: horizontal, 0.5 sec/div.; vertical, 0.05 Abs./div.

Since π is the intercept of a plot of $[P_1]$ vs. t at $t = 0$, it was measured from the stopped-flow traces of the reaction profiles. Equation 2.5 may be transformed into Eq. 2.7,

$$\pi^{-1/2} = [E]_o^{-1/2} \{(k_2 + k_3)/k_2\}(1 + K_m/[S]_o) \qquad (2.7)$$

From Eq. 2.7, the plot of $\pi^{-1/2}$ vs. $[S]_o^{-1}$ is expected to give a straight line whose intercept is $[E]_o^{-1/2} \{(k_2 + k_3)/k_3\}$. If the condition is met that $k_2 >> k_3$, the intercept of such a plot (as Fig. 2.2) would give $[E]_o^{-1/2}$ and hence $[E]_o$ directly.

Since for the hydrolysis of pNPA by subtilisin BPN', the ratio of k_2/k_3 has not been reported, it was calculated as follows. The pre-steady state phase of the reaction curve was analysed with the Guggenheim plot (*37*), and the first-order rate constant, b, was obtained (1.64

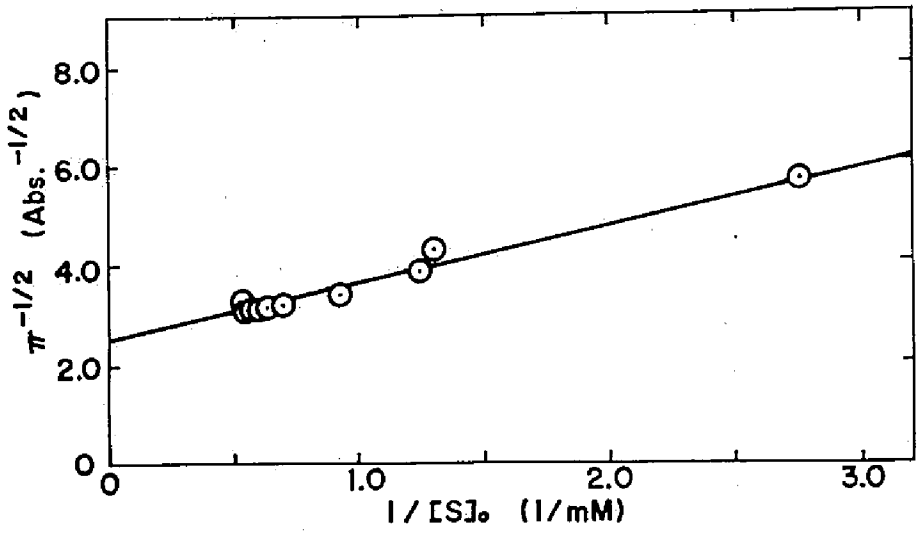

Fig. 2.2. Dependence of the *p*-nitrophenol "burst", π, on the initial concentration of substrate, $[S]_o$, in the active-site titration of subtilisin BPN' by *p*-nitrophenyl acetate. Subtilisin BPN'; 2.0 mg/ml (72.7 μM assuming 100% pure) in 20 mM pyrophosphate buffer, pH 8.5, containing 5.0% (v/v) isopropanol, 25°C.

---

sec^{-1}). The ratio of k_2/k_3 was calculated to be 50 from

$$k_2/k_3 = \{b\pi_o(1 + [S]_o/K_m)\} / \{V(1 + [S]_o/K_m) - b\pi_o\} \qquad (2.8)$$

where V is the maximum velocity obtained for the steady state phase of the reaction curve, and π_o is the magnitude of the initial burst, π, extrapolated to $[S]_o \longrightarrow \infty$ in Eq. 2.5 (Fig. 2.2). The active enzyme concentration, $[E]_o$, was obtained from $[E]_o = \pi_o(1 + k_3/k_2)^2$; and the purity of the enzyme preparation was calculated to be 74.7%.

The active-site of subtilisin BPN' was titrated also with *N-trans*-cinnamoyl imidazole. Equal volumes of the enzyme solution in 25 mM phosphate buffer, pH 7.00, ionic strength 0.1 M (NaCl), and the titrant solution in the same buffer containing acetonitrile at 6.4% (v/v) were mixed with a Union MX-7 sample mixing unit. The final concentration of the

enzyme was 0.54 mg/ml (19.6 μM assuming the enzyme preparation to be 100% pure) and that of *N-trans*-cinnamoyl imidazole was in the range between 13.2 μM and 76.9 μM. The ratio of k_2/k_3 for the hydrolysis of *N-trans*-cinnamoyl imidazole by subtilisin Novo, which is believed to be identical with subtilisin BPN' (*38,39*), has been reported to be 186 ± 20 (*35*) satisfying the requirement of $k_2 >> k_3$. Accordingly, the magnitude of the burst, π_o, was considered to be the same as the active enzyme concentration in this case; and the purity of the subtilisin BPN' preparation was calculated to be 74.6%.

The values of the purity of the subtilisin BPN' preparation thus determined by the two different titrants are in good agreement with each other, and 74.7% is used throughout this study.

Enzyme activity measurement. The esterolytic activity of subtilisin BPN' was measured spectrophotometrically with pNPA as substrate. The reaction was initiated by mixing equal volumes of the enzyme solution in 20 mM pyrophosphate buffer, pH 8.50 and the substrate solution in water containing isopropanol at 10.0% (v/v). Increase in absorption at 405 nm due to the liberation of *p*-nitrophenol was followed at 25°C with a Shimadzu UV-200 recording spectrophotometer. The molar absorptivity at 405 nm of *p*-nitrophenol at pH 8.50 was taken to be 1.76×10^4 $M^{-1}cm^{-1}$.

Measurement of inhibitor activity. The inhibitory activity of SSI against subtilisin BPN' was assayed spectrophotometrically under the same conditions as the enzyme activity measurement with pNPA as substrate. The enzyme and the inhibitor were mixed first, and after keeping the mixture at 25°C for ten minutes the reaction was started by adding the substrate solution. For the measurement with a stopped-flow

apparatus, however, the substrate and the inhibitor were mixed first, and the reaction was started by mixing the substrate-inhibitor mixture and the enzyme solution (also refer to the section of *Determination of the purity of subtilisin BPN' preparation*).

Titration of subtilisin BPN' with SSI by ultraviolet absorption difference spectrophotometry. Difference spectra observed on the binding of SSI and subtilisin BPN' were recorded with a Hitachi Model 323-2000 recording spectrophotometer with an expanded scale (0.04 Abs./full scale). Two pairs of matched cuvettes of 1 cm light path length were used. To an enzyme solution, 1.65 mg/ml (44.8 μM taking into account the purity of the enzyme preparation) in 25 mM phosphate buffer, pH 7.0 (the ionic strength was adjusted to 0.1 M with NaCl) was added the equal volume of SSI solution in the same buffer at various concentrations up to 2.0 mg/ml (0.174 mM). The ultraviolet absorption difference spectra were recorded after holding the mixture at 25°C for 10 min.

2.3 Results

Absorption spectrum of SSI. Figure 2.3 shows the ultraviolet absorption spectrum of SSI in 25 mM phosphate buffer, pH 7.0, ionic strength 0.1 M (NaCl). The absorption maximum is at 276 nm, and the ratio A_{250}/A_{276} is 0.431 and A_{280}/A_{276}, 0.985.

Inhibition of subtilisin BPN' by SSI. The inhibition by SSI of the hydrolysis of pNPA by subtilisin BPN' is shown in Fig. 2.4. A good linear relationship is observed between the remaining enzyme activity and the inhibitor concentration. There is the distinct point of complete inhibition, at which the concentration ratio of subtilisin BPN' to

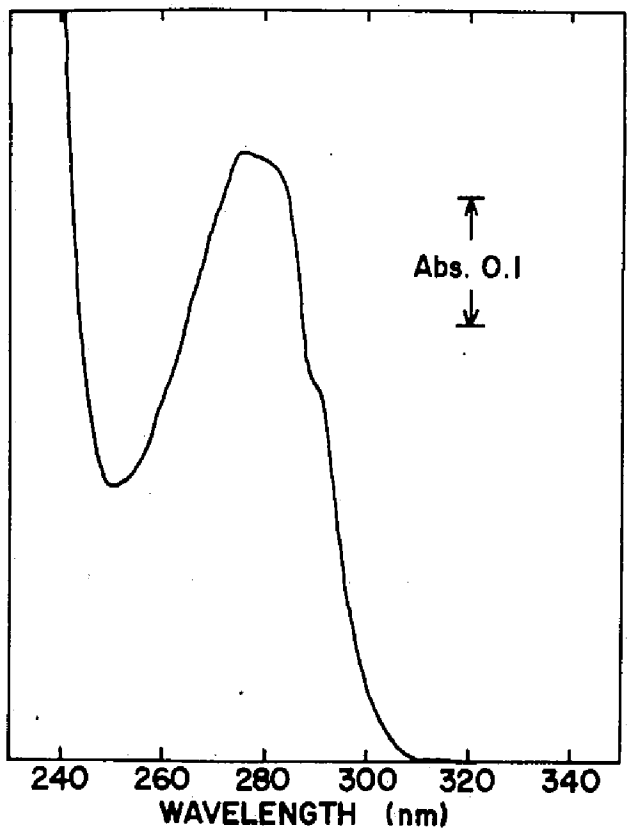

Fig. 2.3. Ultraviolet absorption spectrum of SSI. SSI: 0.572 mg/ml (49.4 μM) in 25 mM phosphate buffer, pH 7.0, ionic strength 0.1 M (NaCl), 25°C.

SSI is 3.15 : 1.00 (in mg/ml units).

Inhibition of the pre-steady state as observed by the stopped-flow method. The inhibition experiment was carried out also with a stopped-flow apparatus. The oscilloscope traces of the reaction curves are shown in Fig. 2.5. In the absence of the inhibitor (Fig. 2.5, a), a clear bi-phasic curve with a initial burst and the steady state phase is recorded. As the inhibitor concentration increases (Fig. 2.5, b,c), there are observed not only decreases in the rate of the steady state phase but

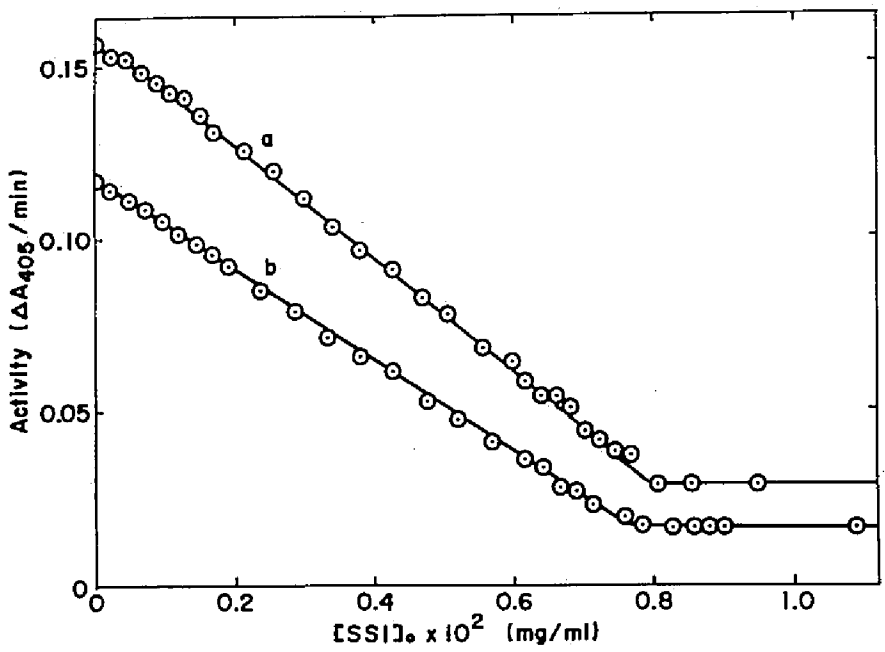

Fig. 2.4. Inhibition of subtilisin BPN'-catalyzed hydrolysis of *p*-nitrophenyl acetate by SSI. Subtilisin BPN': 2.30×10^{-2} mg/ml (0.826 μM assuming 100% pure); *p*-nitrophenyl acetate: (a), 0.710 mM and (b), 0.406 mM. 20 mM pyrophosphate buffer, pH 8.50, containing 5.0% (v/v) isopropanol, 25°C. $[\text{subtilisin BPN'}]_o/[\text{SSI}]_o = 3.15$ (w/w) at the saturation point. The residual activity beyond the saturation point is due to the non-enzymatic hydrolysis of the substrate.

---

also the disappearance of the initial burst.

Titration of subtilisin BPN' with SSI by ultraviolet absorption difference spectra. Figure 2.6 shows the ultraviolet absorption difference spectra produced on the mixing of SSI with subtilisin BPN'. The spectra reflect some changes in the environment of both tryptophyl and tyrosyl residues caused by the these proteins.

Figure 2.7 represents the plot of the difference between ΔA_{288} and ΔA_{294} of the spectra as shown in Fig. 2.6 against the concentration of

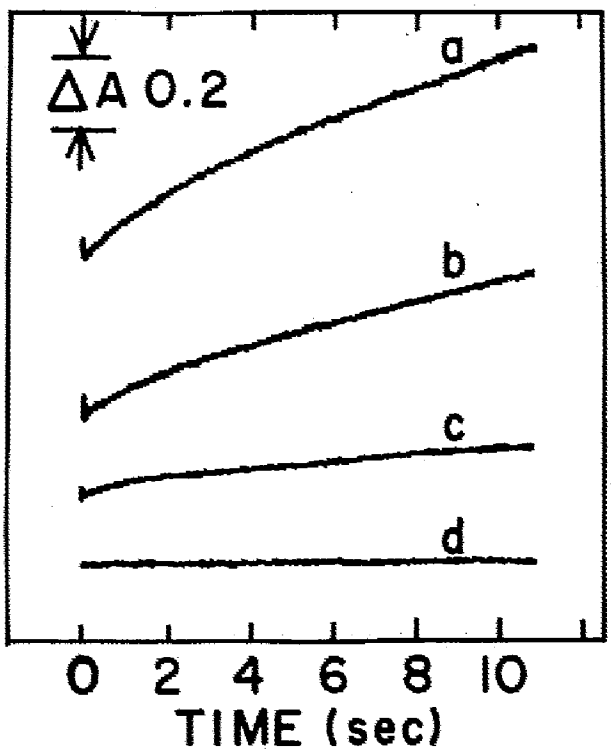

Fig. 2.5. Stopped-flow oscillograms showing the effect of SSI on the subtilisin BPN'-catalyzed hydrolysis of *p*-nitrophenyl acetate. [subtilisin BPN']$_o$ = 0.803 mg/ml (21.8 μM taking the purity, 74.7%, into account). [*p*-nitrophenyl acetate]$_o$ = 0.922 mM. [SSI monomer]$_o$ = (a), 0; (b), 7.88 μM; (c), 15.8 μM; and (d), 23.7 μM. 20 mM pyrophosphate buffer, pH 8.50, containing 5.0% (v/v) isopropanol, 25°C. Wavelength, 405 nm.

SSI. There is the distinct point of saturation, at which the concentration ratio of subtilisin BPN' to SSI is 3.16 : 1.00 (in mg/ml units).

Evaluation of inhibition and binding equivalence. The concentration ratio of subtilisin BPN' to SSI at the point of complete inhibition (Fig. 2.4) and the value at the point of saturation in binding (Fig. 2.7) agree very well with each other indicating the stoichiometric binding of SSI to a specific site of the enzyme. The average of the two values

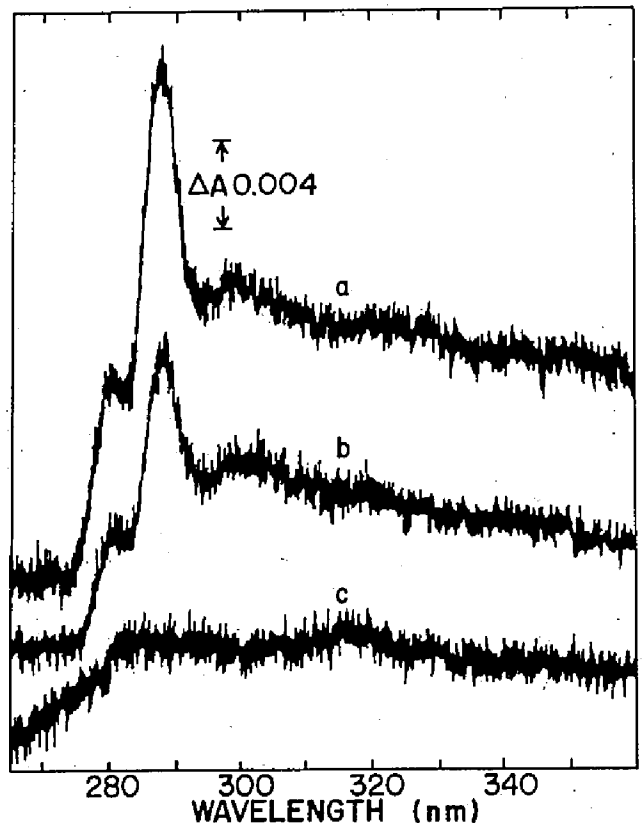

Fig. 2.6. Ultraviolet absorption difference spectra observed on the binding of SSI and subtilisin BPN'. $[\text{subtilisin BPN'}]_o$ = 0.735 mg/ml (26.7 μM assuming 100% pure); $[\text{SSI}]_o$ = (a), 0.550 mg/ml; (b), 0.150 mg/ml; and (c), 0. 25 mM phosphate buffer, pH 7.0, ionic strength 0.1 M (NaCl), 25°C.

---

gives subtilisin BPN' : SSI = 3.15 : 1.00 (in mg/ml units). When the purity of the enzyme preparation, 74.7% and the molecular weights of the two proteins (subtilisin BPN', 27,500; SSI, 11,500) are taken into account, the ratio turns out to be 0.99 : 1.00 in molar basis. It is concluded accordingly that one molecule of SSI stoichiometrically binds and inhibits one molecule of subtilisin BPN' (see Discussion 2.4).

The type of inhibition and estimation of K_i. The linear plots of

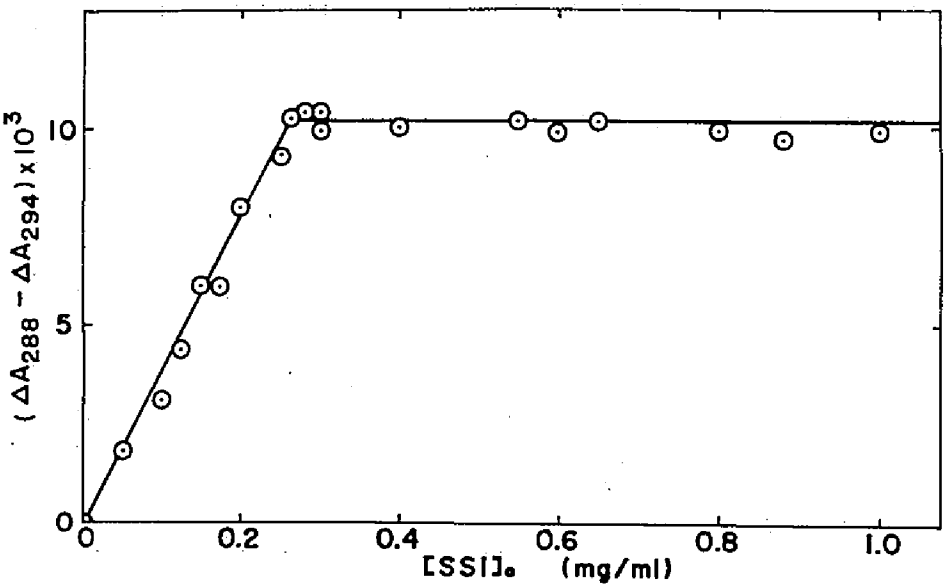

Fig. 2.7. Difference spectral titration of subtilisin BPN' with SSI at pH 7.0, 25°C. Conditions are as in Fig. 2.6. [subtilisin BPN']$_o$/[SSI]$_o$ = 3.16 (w/w) at the saturation point.

---

the kinetic data of subtilisin BPN' with and without SSI exhibited apparently a typical noncompetitive type inhibition profile (Fig. 2.8). Determination of the inhibitor constant, K_i, of SSI against subtilisin BPN' was attempted by the method of Green and Work (1953) (*40*) and other methods of linear plotting. A value (3.8 ± 1.5) x 10^{-10} M was obtained using the equation of Henderson (1972) (*41*) which describes the steady state kinetics of the enzyme with tightly bound inhibitors; however, enzyme concentrations of the order of 10^{-7} M had to be used in the present assay system, which are somewhat too high to obtain a very accurate K_i value. It is safely stated, at present, that K_i of SSI against subtilisin BPN' is less than 10^{-9} M at pH 8.5. The K_i determination with more sensitive assay methods have been under investigation (kinetic investi-

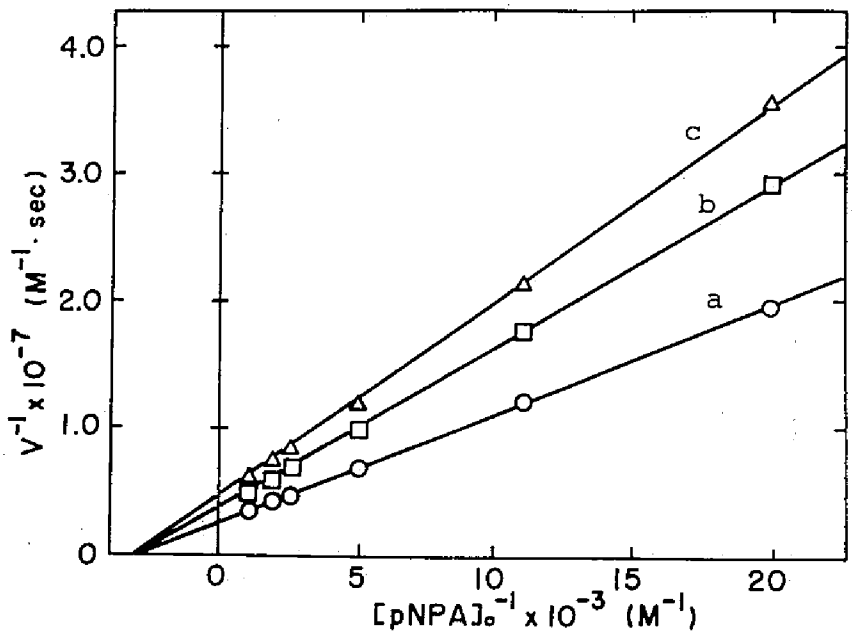

Fig. 2.8. Apparent noncompetitive inhibition of subtilisin BPN'-catalyzed hydrolysis of *p*-nitrophenyl acetate by SSI. $[\text{subtilisin BPN'}]_o$ = 5.0×10^{-2} mg/ml (1.36 μM taking the purity, 74.7%, into account. $[SSI]_o$ = (a), 0 mg/ml; (b), 5.0×10^{-3} mg/ml; (c), 7.0×10^{-3} mg/ml. 20 mM pyrophosphate buffer, pH 8.5, containing 5.0% (v/v) isopropanol, 25°C.

---

gation: Tonomura, B., Azuma, T., and Hiromi, K., unpublished results; fluorescence titration: Uehara, Y., Tonomura, B., and Hiromi, K., unpublished results).

2.4 Discussion

Determination of absorptivity of proteins. In the present study the absorptivity, $E_{1\ cm}^{0.1\%}$, of each protein calculated from its amino acid composition was used throughout. Ratios of the observed values to the calculated values of the absorptivity for SSI are 0.991 (276 nm) and

1.018 (280 nm); and for subtilisin BPN', 1.014 (278 nm) and 1.024 (280 nm). These figures fall in the range of the ratios for some other proteins listed by Wetlaufer (*42*). A value $E_{1\ cm}^{0.1\%}$(278 nm) = 1.17 obtained for diisopropyl phosphoridate-inhibited (DIP) subtilisin BPN' by Matsubara *et al.* (*43*) has been used widely in the literature as the absorptivity of this enzyme. If this value is employed in the present case, the purity of the enzyme preparation will be 82.2%, and the molar ratio of the inhibition and binding equivalence will be 1.08 : 1.00; the present inference that a mole of SSI (monomer) binds and inhibits one mole of subtilisin BPN' need not be changed by this.

Competitive inhibition of SSI against subtilisin BPN'. The inhibition of the pre-steady state observed by the stopped-flow method suggests that SSI inhibits the hydrolysis of pNPA by subtilisin BPN' either at or before the step of the acyl-enzyme (ES') formation in the reaction scheme 2.1. This is interpreted, for the reasons described below, as that SSI competes with pNPA for the active site of the enzyme, though the apparent noncompetitive inhibition mentioned in Results 2.4 may seem to suggest the formation of the inactive ternary complex, IES. It has been recognized that an inhibitor with a high affinity to an enzyme exhibits apparently the noncompetitive type inhibition even if its inhibition mechanism is competitive with the substrate (*44*).

The apparent noncompetitive inhibition is evident especially when the activity assay is started by adding a substrate into the pre-mixed solution of the enzyme and the inhibitor, as was done in this study. This is believed to be due to the slow dissociation of the enzyme-inhibitor complex in the final reaction mixture, which results in the decrease of the actual initial concentration of the active enzyme. This view is

endorsed by the observations that the degree of inhibition was lower when the activity assay was started by adding the enzyme into the mixture of the substrate and the inhibitor allowing the competition between them, and that this phenomenon was more clearly seen at the low concentration of the inhibitor and hard to detect when a better substrate like casein was used instead of pNPA.

The above conclusion of competitive inhibition is supported by the fact that DIP-subtilisin BPN' and carbobenzoxy-L-alanyl-glycyl-L-phenylalanine chloromethyl ketone-inhibited (ZAGPCK) subtilisin BPN' fail to produce the complex with SSI as monitored by gel filtration with Sephadex G-100 (*45*). In this connection, it has been demonstrated that SSI competitively inhibits bovine α-chymotrypsin with K_i of $(3.0 \pm 0.7) \times 10^{-6}$ M (see Chapter Five). The above interpretation seems reasonable also on the analogy of the cases of bovine pancreatic trypsin inhibitor (Kunitz)-bovine trypsin (*10*) and soybean trypsin inhibitor (Kunitz)-porcine trypsin (*11*), for which the X-ray crystallographic analyses have suggested that the inhibitors are bound to the catalytic site of the enzyme in the form of tetrahedral intermediate.

SSI as an active-site titrant of subtilisin BPN'. Since the stoichiometry of the binding and inhibition has been accurately determined here (Figs. 2.4 and 2.7), SSI can be recommended as a useful titrant of the active-site of subtilisins in view of the present status that there is no good active-site titrant for these proteinases: in the case of pNPA, k_2/k_3 is not large enough as determined in this study (Experimental Procedures 2.2), and in the case of *N-trans*-cinnamoyl imidazole, which has been used widely for subtilisins (*35*), the large absorbance change due to the intermediate, cinnamoyl-enzyme, may possibly prevent one from

the accurate determination; moreover, considerable degree of spontaneous hydrolysis of these titrants in the pH region optimal for subtilisins makes the active-site titration troublesome.

The recommended method for the active-site titration of subtilisin BPN' by the use of SSI is as follows. The esterolytic activity of subtilisin BPN' is measured spectrophotometrically with pNPA as substrate. A pNPA solution of about 1.0 mM in water containing 10.0% (v/v) isopropanol and a pre-mixed solution of enzyme and SSI (subtilisin BPN', 0.05 mg/ml, 1.82 μM assuming the enzyme preparation to be 100% pure; SSI, 0 - 0.02 mg/ml, 0 - 1.82 μM as monomer) in 50 mM phosphate buffer, pH 7.0 are prepared. The reaction is initiated by mixing equal volumes of the pNPA solution and the SSI-subtilisin BPN' mixture solution in the optical cuvette at 25°C, and the initial velocity, v, for the reaction can be directly determined from the progress curve at 405 nm, for the spontaneous hydrolysis of the substrate is almost negligible at pH 7.0. The initial velocity of the reaction must be determined at least two SSI concentrations; in addition, the blanck must be taken ($[SSI]_o$ = 0 M). When v is plotted against final SSI concentration, $[SSI]_o$, (as Fig. 2.4), v is expressed as $v = v_o + a[SSI]_o$, where v_o is v at $[SSI]_o$ = 0 M and a is a constant describing the slope. The extrapolated value of $[SSI]_o$ to $v \longrightarrow 0$, $- v_o/a$, corresponds to the active-site concentration of the preparation used of subtilisin BPN'.

The absorption difference spectrum observed on the binding of SSI and subtilisin BPN'. The difference spectra observed on the mixing of SSI and subtilisin BPN' (Fig. 2.6) are attributable to the specific interaction between the two proteins. The shape of the difference spectra suggests some change in the environment of both tyrosyl and trypto-

phyl residues. The environmental change may include the electrostatic one of tryptophyl residues as indicated from the small peak at 300 nm (*46-48*). The states of these aromatic amino acid residues and their changes on the enzyme-inhibitor complex formation will be dealt with in detail in Chapter Six and Chapter Seven, respectively.

2.5 Summary

The stoichiometry of inhibition and binding of *Streptomyces* subtilisin inhibitor, a protein proteinase inhibitor produced by *Streptomyces albogriseolus* S-3253 (*21-23*) towards subtilisin BPN' was studied. The inhibition of the hydrolysis of *p*-nitrophenyl acetate by subtilisin BPN' was measured, at the pre-steady state and at the steady state. The stopped-flow study of the pre-steady state demonstrated the disappearance of the initial burst of the enzyme reaction. The ultraviolet absorption difference spectra were observed on mixing the inhibitor and the enzyme, suggesting some change in the environment of tryptophyl and tyrosyl residues in the proteins. Titration by means either of the degree of inhibition at the steady state or of the magnitude of the ultraviolet difference absorbance revealed that one protomer (molecular weight, 11,500) of the inhibitor binds and inhibits one molecule of subtilisin BPN'. The inhibitor constant, K_i, for subtilisin BPN' was estimated to be less than 10^{-9} M at pH 8.5. A new method for active-site titration of subtilisin BPN' with SSI was proposed.

Chapter Three

The Determination of Molecular Weights of *Streptomyces* Subtilisin Inhibitor and the Complex of *Streptomyces* Subtilisin Inhibitor and Subtilisin BPN' *

3.1 Introduction

In the previous Chapter, it was described that one monomer unit of SSI of molecular weight 11,500 binds and inhibits one molecule of subtilisin BPN' stoichiometrically. This molecular weight of SSI was calculated from the amino acid composition (Fig. 1.1) (*27*).

The molecular weight of SSI, however, was first reported to be 27,000 by gel filtration on a Sephadex G-100 column (*23*) and to be 12,000 by SDS polyacrylamide gel electrophoresis (*49*). From this discrepancy was suggested the possibility of dimerization of SSI molecule in solution. The dimeric structure of SSI in crystal was also suggested from X-ray crystallography (*28*). The view that SSI exists as a dimer (I_2) composed of identical subunits is consistent with the results of binding and inhibition equivalence shown in the previous Chapter. However, the possibility remains to be examined that SSI dissociates into monomer (I_1) upon binding of the enzyme (E) and that the enzyme-inhibitor complex is in the form of one molecule of enzyme with a monomer of inhibitor (E_1I_1) as in the case of plasminostreptin (Sugino, H. and Kakinuma, A., unpublished results).

---

* A part of this study was presented at the Annual Meeting of the Biophysical Society of Japan (Tokyo, October 1973) (*b*).

The present study in this Chapter was initiated to determine the molecular weight of SSI in solution and that of the enzyme-inhibitor complex by using sedimentation equilibrium method. Especially, in order to detect the dissociation of SSI into monomer, the molecular weight of SSI was measured at the low protein concentration.

3.2 Experimental Procedures

Proteins. A three times crystallized and lyophilized preparation of *Streptomyces* subtilisin inhibitor, SSI, was kindly supplied by Professor S. Murao. A three times crystallized preparation of soybean trypsin inhibitor (Kunitz) (Lot No. 54B-0720) was a product of Sigma Chemical Co. A three times crystallized preparation of subtilisin BPN' [EC 3.4.21.14] was purchased from Nagase Co. & Ltd., Osaka (Lot No. 01026). The purity of the preparation was determined to be 74.7% by the method described in the previous Chapter (Experimental Procedures 2.2).

Protein concentrations were determined spectrophotometrically with a Shimadzu UV-200 recording spectrophotometer. The absorptivities, $E_{1\ cm}^{0.1\%}$(280 nm), of 1.066, 0.810, and 1.004 were used for subtilisin BPN', SSI (Experimental Procedures 2.2) and soybean trypsin inhibitor (Kunitz) (*50*), respectively.

Proteins were dissolved in 25 mM phosphate buffer, pH 7.0, ionic strength 0.1 M (NaCl).

The complex of subtilisin BPN' and SSI. A crystallized and lyophilized preparation of the complex of subtilisin BPN' and SSI obtained according to the previously reported method (*45*) was generously supplied by Professor S. Murao. The preparation showed a single band on polyacryl

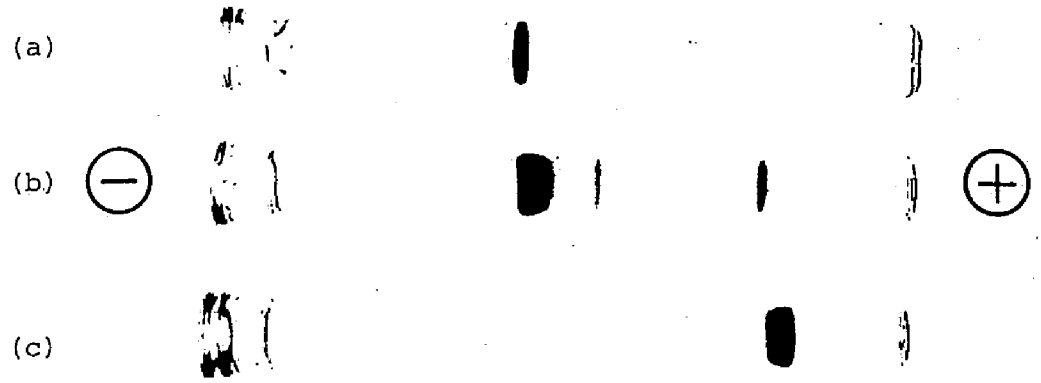

Fig. 3.1. Polyacrylamide gel electrophoresis of (a) subtilisin BPN'-SSI complex, (b) mixture of subtilisin BPN' and SSI, and (c) SSI. Sample solutions were applied to polyacrylamide separating gels at pH 9.5. The gels were stained with Coomassie Brilliant Blue R-250 and destained by leaching with 7.5% acetic acid.

---

amide gel electrophoresis at pH 9.5 (Fig. 3.1, a).

Determination of the partial specific volume of SSI. The partial specific volume, $\bar{v}$, of SSI used in the ultracentrifugal experiments was measured with a 5-ml Ostwald pycnometer (*51*). Meniscus was adjusted in a water bath at 25.0±0.1°C, and room temperature was adjusted to 24.0°C. A Sartorius 2442 chemical balance was used for weighing. The measurements with pycnometer were carried out at six different concentrations of the inhibitor between 5.3 mg/ml and 0.5 mg/ml, and the measurement was repeated at least 10 times at each concentration.

The $\bar{v}$ of SSI was also theoretically calculated based on the amino acid compositions (*27*) and the values of partial specific volume of each amino acid according to the method of McMeekin (*52, 53*).

Ultracentrifugal methods. All experiments were performed either with a Beckman Spinco Model E analytical ultracentrifuge or with a

Hitachi UCA-1A analytical ultracentrifuge. The Beckman Spinco Model E was equipped with an electronic speed control, a rotor temperature indicator and control (RTIC) unit, and phase-plate schlieren-Rayleigh interference optical system; and the Hitachi UCA-1A was equipped with an electronic speed control, an RTIC unit, and a split-beam photoelectric scanning apparatus (*54*), Hitachi UVC with a differential circuit and an absorbance scale expander (2.5 - 20 times) made by the author. The expander is equipped with an external circuit to apply the off-set voltage, with which the Hitachi UVC photoelectric scanning apparatus is improved to record the absorbance change of 0.05 - 0.25 in the full scale.

When the initial protein concentration was over about 0.6 in absorbance at 280 nm, the Beckman Spinco Model E was used, and schlieren and Rayleigh interference patterns were photographed on Fuji spectroscopic plates, Process Panchro Type. When the initial protein concentration was below about 0.6 in absorbance at 280 nm, the Hitachi UCA-1A was employed and sedimentation patterns were recorded with a photoelectric scanning apparatus Hitachi UVC. All photographic plates were read on a Nikon Model 6C two dimensional microcomparator.

Fluorocarbon FC-43 was used as a bottom liquid.

Sedimentation velocity. Sedimentation velocity studies were performed to determine the sedimentation coefficients of SSI and the complex of SSI and subtilisin BPN'. Ultracentrifugation was run at 25.0°C using 12-mm valve type synthetic boundary cells. For SSI, the schlieren otpics of the Beckman Spinco Model E was applied and photographs were taken on Fuji spectroscopic plates, Process Panchro Type with an appropriate time interval. Subtilisin BPN'-SSI complex has very low solubil-

ity; it dissolved in buffer solution at about 0.5 mg/ml at maximum under the conditions used. The schlieren optics is not sensitive enough to detect this low concentration of protein, therefore, ultraviolet absorption scanning optics was used on the Hitachi UCA-1A analytical ultracentrifuge at 280 nm at 25.0°C. Absorbances at 280 nm were scanned throughout a liquid column in the cell and were recorded at appropriate time intervals during the sedimentation process. Sedimentation coefficients $s_{20,w}$ were calculated according to Schachman (*51*).

Sedimentation equilibrium. With the Beckman Spinco Model E analytical ultracentrifuge, all experiments were performed with five different protein concentrations at one run at 25.0°C, with double sector cells having a 12-mm light path and fitted with quartz windows on an An-G rotor.

Synthetic boundary experiments using the capillary-type synthetic boundary cell were made with each solution to give the concentration in terms of area on the photographic plate.

The experiments were also performed with a simple 12-mm aluminium double-sector cell and quartz windows in the Hitachi UCA-1A analytical ultracentrifuge.

Determination of molecular weights using the high speed sedimentation technique (*55*) was performed at initial concentrations of less than 1.0 mg/ml. The attainment of equilibrium was checked at 2 hr intervals near the end of the experiment until an equilibrium distribution was observed. Low speed sedimentation equilibrium studies (*56,57*) were performed with solutions having an initial protein concentrations of 1.0 - 3.0 mg/ml. In all such experiments, overspeeding rotation to reduce the time to reach equilibrium was employed (*57*).

Before the use of the Hitachi UCA-1A ultracentrifuge with the initial concentration of protein below 0.1 mg/ml, the fidelity of the apparatus was tested by performing the similar experiments with a protein of known molecular weight; soybean trypsin inhibitor (Kunitz) was chosen as the reference protein and its molecular weight was determined with the initial concentration of 0.0292 mg/ml.

Weight average molecular weight (Mw*) and local weight average molecular weight (Mw(r)) were obtained by Eqs. 3.1 and 3.2, respectively *(58, 59)*.

$$Mw^* = \frac{2RT(C_b - C_a)}{(1 - \bar{v}\rho)\ \omega^2\ C_o(r_b^2 - r_a^2)} \tag{3.1}$$

$$Mw(r) = \frac{2RT}{(1 - \bar{v}\rho)\ \omega^2} \frac{d\{\ln C(r)\}}{d(r^2)} \tag{3.2}$$

where r_a : position of the meniscus from the center of rotation,

r_b : position of the bottom from the center of rotation,

C_a : protein concentration at the meniscus in mg/ml,

C_b : protein concentration at the bottom in mg/ml,

ω : angular velocity of the rotor,

ρ : density of the solvent,

C_o : initial protein concentration in mg/ml,

R : gas constant,

T : absolute temperature in Kelvin.

Sedimentation equilibrium of the mixture of SSI and subtilisin BPN'. The molecular weight of the subtilisin BPN'-SSI complex was determined, in addition to the sedimentation equilibrium of the subtilisin BPN'-SSI complex preparation, by applying the treatment of sedimentation equilibrium of multicomponent-polydisperse system to the mixture solu-

tion of the enzyme and SSI. In the mixture solution, subtilisin BPN' and SSI were dissolved at the ratio of 2.17 : 1.00 (in mg/ml units). Sedimentation equilibrium measurements were conducted with six different concentrations of total protein between 2.67 - 0.0666 mg/ml. Taking into account the purity of the enzyme preparation used, 74.7%, and the strong binding between the enzyme and the inhibitor, $K_i < 10^{-9}$ M, the weight fractions of the species contained in the mixture solution were determined to be 72.13% for subtilisin BPN'-SSI complex, 10.61% for excess SSI, and 17.26% for inactivated enzyme. The polyacrylamide gel electrophoretic pattern of the mixture solution used for the sedimentation experiments is shown in Fig. 3.1 (b). The middle band is the inactive form of subtilisin BPN'.

Sedimentation analysis of multicomponent-polydisperse system. For a system in polymerization equilibrium, the quantity Mw* obtained by sedimentation equilibrium is not identical with Mw value which would indicate for the same solution if it were not redistributed in the centrifugal field, even if all species behave ideally. In other words, it cannot simply be assumed that the Mw* value obtained corresponds to that in a solution of a concentration C_o, which would be

$$Mw = \frac{\Sigma\, C_{o_i} M_i}{\Sigma\, C_{o_i}} \tag{3.3}$$

$$C_o = \Sigma\, C_{o_i} \tag{3.4}$$

where C_{o_i} represents the equilibrium concentration of the species, i, in the absence of a centrifugal field. As Adams pointed out (*60,61*), the conservation of mass, even in the case of chemical equilibrium, is for a sector-shaped cell,

$$C_o = \Sigma \int_a^b C_i(r)\, r\, dr.$$

If the solution is ideal, this is transformed to

$$C_o = \Sigma \frac{C_i(r_a)\ \{\exp[AM_i(r_b^2 - r_a^2)] - 1\}}{AM_i(r_b^2 - r_a^2)}$$

where $A = \omega^2(1 - \bar{\nu}\rho)/2RT$. If a quantity g_i is defined as,

$$g_i = \Sigma \frac{C_i(r_a)\ \{\exp[AM_i(r_b^2 - r_a^2)] - 1\}}{AM_i(r_b^2 - r_a^2)} \quad ,$$

an apparent weight average molecular weight is described as;

$$Mw^* = \frac{\Sigma\ g_i M_i}{\Sigma\ g_i} \tag{3.5}$$

and $C_o = \Sigma\ g_i$. It should be noted that g_i's are not identical with C_{o_i}'s; but the equation for Mw* for an ideal polymerizing system have the same form with respect to g_i as do the expressions for Mw with respect to C_{o_i}. When the polymerization or complex formation of proteins is too small to be experimentally detectable and each species of the proteins approaches to equilibrium independently, Mw* is described by the same equation as Eq. 3.3.

Generally, globular proteins are unique among macromolecules in having such a small excluded volume that the virial coefficient, B, is very small; thus many of the expressions described for thermodynamically ideal systems can be applied without significant error to protein systems. As would be described later, the molecular weight of SSI measured is almost independent on its concentration, and if any, too small to be detected ultracentrifugally, in a wide concentration range, indicating the monodisperse system. Therefore, the author need not apply the treatment of a mixed-solute system or a self-associating system to SSI. In the mixture system of subtilisin BPN' and SSI, there would be the

subtilisin BPN'-SSI complex, free SSI, and inactive enzyme fragments whose molecular weight would be between that of intact enzyme (Mw = 27,500) and that of amino acids (Mw ≃ 100). It is assumed that the mixture system behaves as an ideal mixed-solute system, since the very small dissociation constant of subtilisin BPN'-SSI complex ($K_i < 10^{-9}$ M) and homogeneity of SSI in the concentration range used are taken into account.

3.3 Results

Partial specific volume. The partial specific volume of SSI was measured by using a pycnometer and the value was obtained to be (0.730 ± 0.004) ml/g (Fig. 3.2). This value is in good agreement with that of 0.729 which was obtained theoretically by calculation according to McMeekin's method (*52*). For the subtilisin BPN'-SSI complex, the value of 0.730 was used for molecular weight calculation. Because the partial specific volume, $\bar{v}$, of subtilisin BPN' is 0.731, which is calculated from the amino acid composition of the enzyme (*24,25*), and this value is identical with that of SSI, the average value of $\bar{v}$'s of SSI and subtilisin BPN' 0.730 is reasonable, assuming that the value of $\bar{v}$ for each protein does not change appreciably upon complex formation.

Sedimentation velocity of SSI. SSI shows a single synthetic schlieren boundary at 51,200 rpm, at 20°C in 25 mM phosphate buffer at pH 7.0, ionic strength 0.1 M (NaCl), showing the homogeneity of the preparation and giving the sedimentation coefficient $s^{\circ}_{20,w}$ 2.30 S (Figure not shown).

Monodisperse behavior of SSI in a wide concentration range. Sedi-

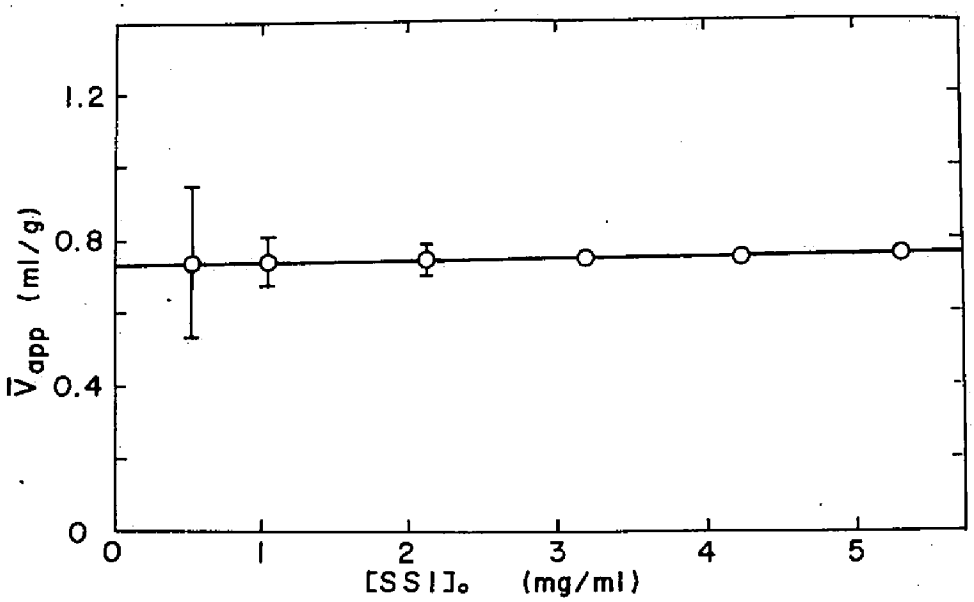

Fig. 3.2. Determination of the partial specific volume, $\bar{v}$, of SSI by the density measurement in 25 mM phosphate buffer, pH 7.0, ionic strength 0.1 M (NaCl), 25.0±0.1°C. The $\bar{v}$ value was determined to be (0.730 ± 0.004) ml/g from the intercept on the ordinate-axis.

---

mentation equilibrium experiments were performed in a wide range of SSI concentration which covers those used in kinetic and chemical measurements.

Rayleigh interference optical system was applied to the initial concentrations of SSI between 4.0 and 0.8 mg/ml, and the plots of the logarithms of the concentration of SSI against the square of the distance from the center of rotation (log $C_i(r)$ vs. r^2) (Fig. 3.3) are linear and indicate that the protein behaves ideally and in a monodispersed manner with the concentration of 10 mg/ml at the cell bottom. The weight average molecular weight was found to be 24,000.

Photoelectric ultraviolet absorption scanning optics was used for the lower initial concentration range of SSI from 0.8 to 0.025 mg/ml.

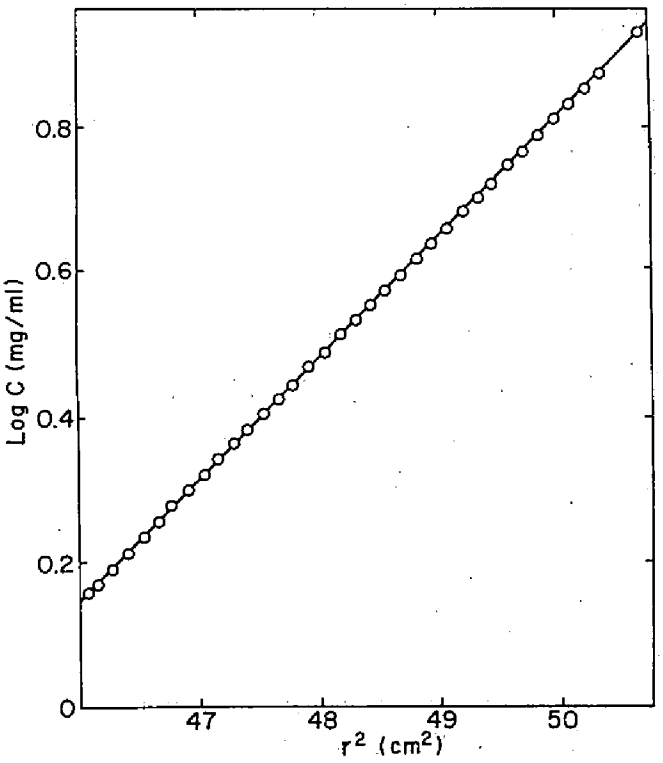

Fig. 3.3. Sedimentation equilibrium run of SSI. Log $C_i(r)$ vs. r^2 plot. sample run in 25 mM phosphate buffer, pH 7.0, ionic strength 0.1 M (NaCl), 25.0°C at 16,200 rpm with the Rayleigh interference optics on the Beckman Spinco Model E analytical ultracentrifuge. $[SSI]_o$ = 3.99 mg/ml. The weight average molecular weight, Mw*, was determined to be 24,000.

In order to examine the validity of the results at such a dilute concentration, soybean trypsin inhibitor (Kunitz) was selected as a reference protein, for its molecular weight is almost the same as that of SSI (*62*) and exists as monomer in this concentration range. The plot of log $C_i(r)$ vs. r^2 is linear and the molecular weight was determined to be 22,400 at the initial concentration of 0.0292 mg/ml, which is in good agreement with other determinations (*50, 62*). Thus it was confirmed that the system of a Hitachi UCA-1A analytical ultracentrifuge and a Hitachi

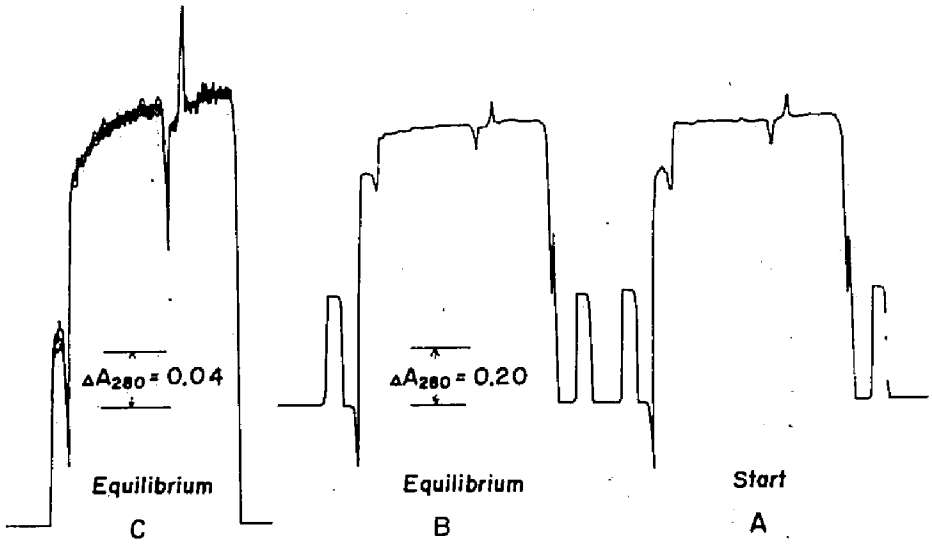

Fig. 3.4. Sedimentation equilibrium run of SSI. Run in 25 mM phosphate buffer, pH 7.0, ionic strength 0.1 M (NaCl), 25.0°C at 16,880 rpm with the photoelectric scanning optics on the Hitachi UCA-1A analytical ultracentrifuge. $[SSI]_o$ = 0.025 mg/ml. Sedimentation profile: (A), at the start of sedimentation; (B), at the equilibrium; (C), at the equilibrium expanded 5 times.

UVC photoelectric scanning apparatus is good for the present purpose.

Figure 3.4 shows the sedimentation equilibrium patterns recorded with a photoelectric scanning apparatus when initial concentration of SSI was 0.025 mg/ml. Figure 3.4 (A) was recorded immediately when the rotor speed attained the prescribed speed, 16,880 rpm. Figure 3.4 (B) is a sedimentation profile at equilibrium, and Fig. 3.4 (C) is that expanded five times with the expanding device (see Experimental Procedures 3.2). The plot of log $C_i(r)$ vs. r^2 is shown in Fig. 3.5, which is characteristic for meniscus depletion method (*55*). The weight average molecular weight was determined to be 22,400 ± 800 in the concentration range from 0.01 to 0.1 mg/ml.

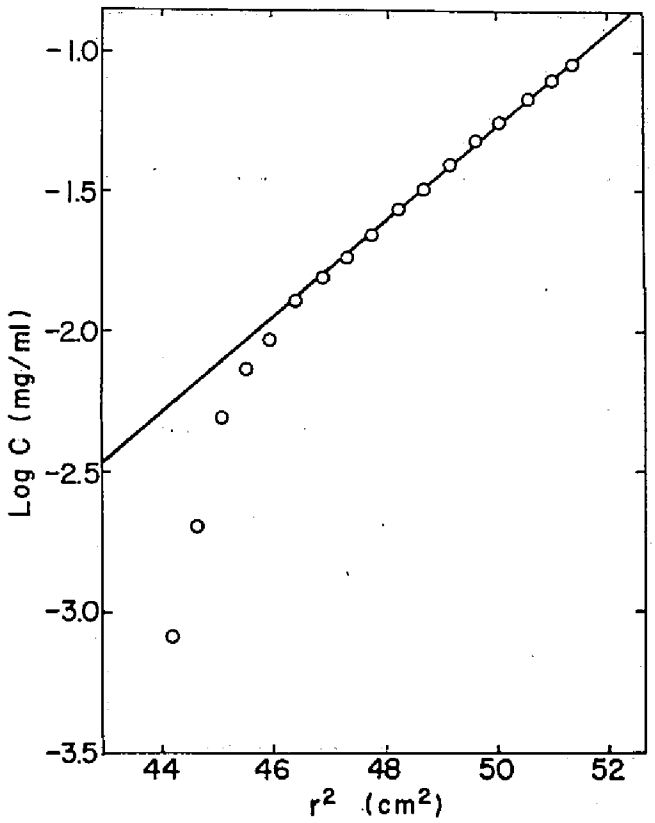

Fig. 3.5. Sedimentation equilibrium run of SSI. Log $C_i(r)$ vs. r^2 plot. Conditions are as in Fig. 3.4. $[SSI]_o$ = 0.025 mg/ml. The weight average molecular weight, Mw*, was determined to be 23,300.

From the results obtained by using Rayleigh interference optics and ultraviolet absorption scanning optics, it was concluded that the molecular weight of SSI is 23,000 in the concentration range of 10 - 0.01 mg/ml.

Figure 3.6 depicts the dependence of the weight average molecular weight, Mw*, on the cell average concentration, $(C_a + C_b)/2$, where C_a and C_b are the concentration of SSI at meniscus and cell bottom, respectively. In general, the apparent weight average molecular weight,

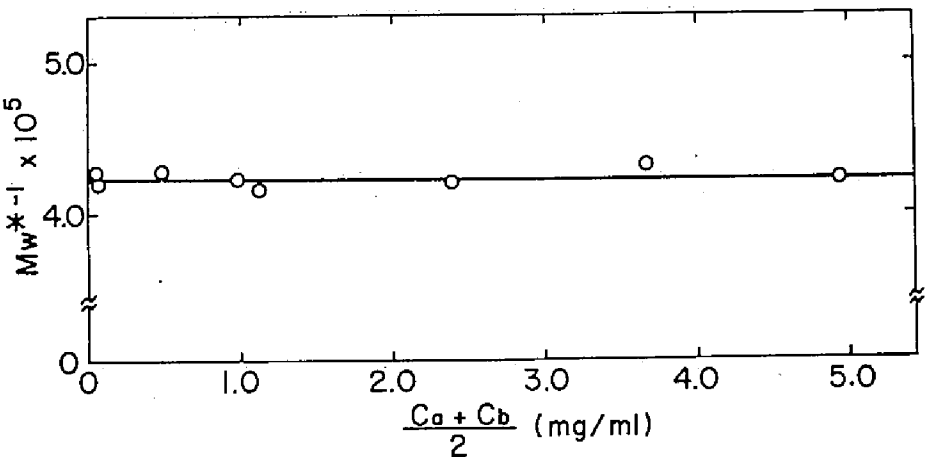

Fig. 3.6. Dependence of weight average molecular weight of SSI, Mw*, on cell average protein concentration, $(C_a + C_b)/2$. Each point of Mw* was obtained from the run in 25 mM phosphate buffer, pH 7.0, ionic strength 0.1 M (NaCl), 25.0°C with the Rayleigh interference optics or the photoelectric scanning optics. From the intercept on the ordinate-axis, the molecular weight of SSI was determined to be 23,165 ± 211.

Mw*, is defined as

$$Mw^{*-1} = Mw^{-1} + (B + \bar{v}\ Mw^{*-1})(C_a + C_b)/2 + \cdots\cdots \quad (3.6)$$

where Mw is the molecular weight of protein, and B, the secondary virial coefficient. The intercept on the ordinate-axis in Fig. 3.6 gives the molecular weight of SSI, Mw = 23,165 ± 211, in the concentration range between 10 and 0.01 mg/ml covering the concentration used in kinetic and chemical measurements. The value 23,165 ± 211 is twice of the molecular weight calculated based on the amino acid composition (27). Therefore, SSI was concluded to exist as a dimer under the conditions employed in the concentration range of SSI 10 - 0.01 mg/ml, namely, the dimer is the essential form of SSI.

Sedimentation velocity of the subtilisin BPN'-SSI complex. Sedi-

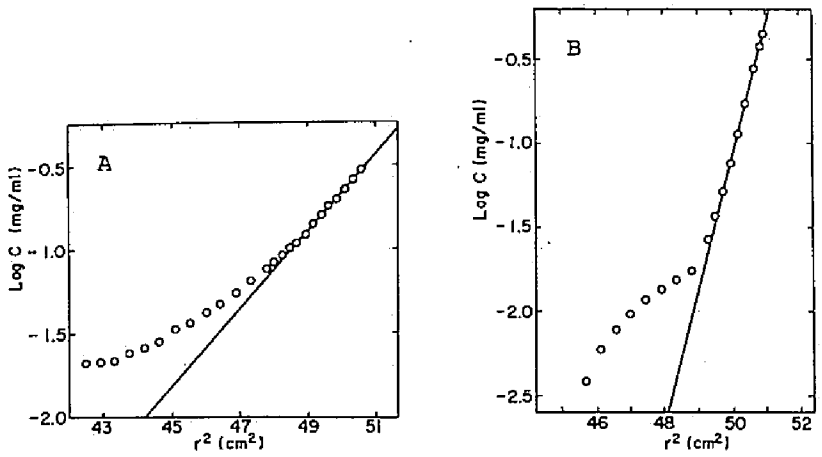

Fig. 3.7. Sedimentation equilibrium runs of subtilisin BPN'-SSI complex. Sample runs in 25 mM phosphate buffer, pH 7.0, ionic strength 0.1 M (NaCl), 25.0°C, with the photoelectric scanning optics on the Hitachi UCA-1A analytical ultracentrifuge. (A): $[complex]_o$ = 0.0855 mg/ml at 10,490 rpm. (B): $[complex]_o$ = 0.0362 mg/ml at 19,780 rpm. (A): weight average molecular weight (cell average), Mw* = 51,620; weight average molecular weight (at cell bottom), Mw(b) = 75,810. (B): Mw* = 70,600, Mw(b) = 76,760.

---

mentation velocity measurement for the subtilisin BPN'-SSI complex was carried out on a Hitachi UCA-1A analytical ultracentrifuge with a Hitachi UVC scanning apparatus using the differentiating circuit, at 51,200 rpm, 20°C (Figure not shown). The sedimentation coefficient $s^{\circ}_{20,w}$ was obtained to be 5.45 S.

Sedimentation equilibrium of the subtilisin BPN'-SSI complex. Since the lyophilized powder of the subtilisin BPN'-SSI complex is sparingly soluble, the maximum solubility being 0.3 mg/ml in 25 mM phosphate buffer, pH 7.0, ionic strength 0.1 M (NaCl), at 25.0°C, the sedimentation equilibrium measurements were carried out with ultraviolet absorption photoelectric scanning optics on a Hitachi UCA-1A analytical ultra-

centrifuge. Figure 3.7 shows the sedimentation equilibrium patterns of the complex; Fig. 3.7 (A), a conventional method at low speed, and Fig. 3.7 (B), a meniscus depletion method at high speed, which reveal distinctly two parts. Consequently, the lyophilized preparation of the complex appeared to be composed of at least two molecular species, though it shows a single band on polyacrylamide gel electrophoresis at pH 9.5 (Fig. 3.1, a). The smaller species, whose molecular weight is estimated less than 10,000, might have been generated during the lyophilization. For the main species, the molecular weight is given to be 76,800, which indicates that the subtilisin BPN'-SSI complex is composed of a mole of SSI dimer (Mw: 23,000, I_2) and two moles of subtilisin BPN' (Mw: 27,500, 2 x E), thus being represented as E_2I_2.

Sedimentation equilibrium of the mixture solution of subtilisin BPN' and SSI. In order to prove that the lyophilized preparation of the subtilisin BPN'-SSI complex whose molecular weight has turned out to be 76,800 is a genuine complex, sedimentation equilibrium experiments were performed on the mixture of subtilisin BPN' and SSI solutions. This mixture solution, as described in Experimental Procedures 3.2, contained subtilisin BPN'-SSI complex, free SSI, and inactive enzyme fragments at 72.13%, 10.61%, and 17.26%, respectively, in weight fraction. These values were calculated based on the active site purity of the enzyme preparation used (74.7%) and assuming that the equilibrium between the complex and both SSI and subtilisin BPN' extremely weighted toward the the complex formation. This assumption is justified by very small dissociation constant ($< 10^{-9}$ M) of the complex. Figure 3.8 shows the typical sedimentation equilibrium patterns of the mixture using the Rayleigh interference optics (Fig. 3.8, A) and the ultraviolet absorption

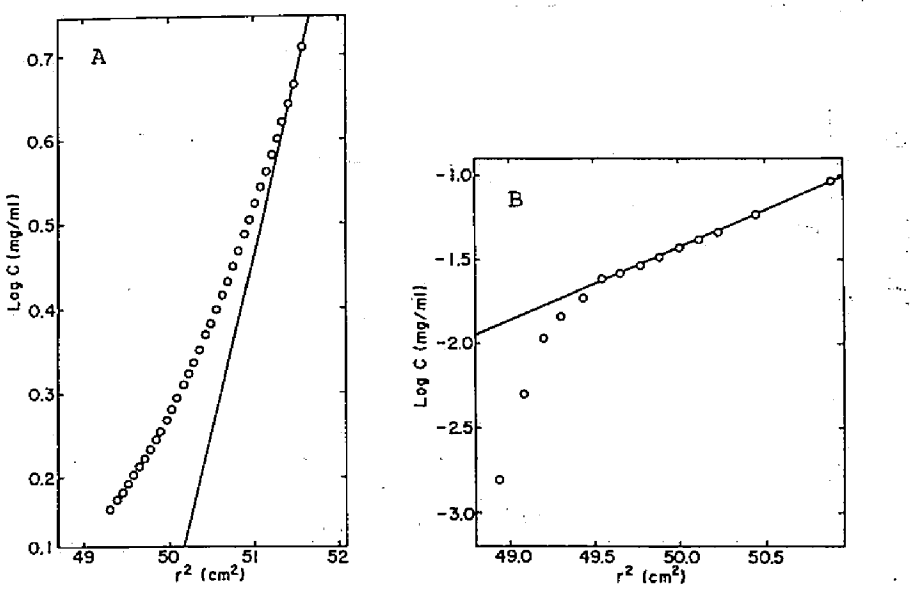

Fig. 3.8. Sedimentation equilibrium runs of the mixture solution of SSI and subtilisin BPN'. Sample runs in 25 mM phosphate buffer, pH 7.0, ionic strength 0.1 M (NaCl), 25.0°C. (A): $[SSI]_o$ = 0.841 mg/ml, [subtilisin BPN']$_o$ = 1.83 mg/ml, the Rayleigh interference optics on the Beckman Spinco Model E analytical ultracentrifuge at 14,290 rpm. (B): $[SSI]_o$ = 0.0210 mg/ml, [subtilisin BPN']$_o$ = 0.0456 mg/ml, the photoelectric scanning optics on the Hitachi UCA-1A analytical ultracentrifuge at 14,400 rpm. (A): weight average molecular weight (cell average), Mw* = 48,540; weight average molecular weight (at cell bottom), Mw(b) = 77,110. (B): Mw* = 51,310, Mw(b) = 77,300.

---

photoelectric scanning optics (Fig. 3.8, B). At the cell bottom, the molecular weight was obtained to be 74,000 - 78,000. Apparent weight average molecular weight (cell average, weight average molecular weight; Mw*) was also calculated simultaneously. The inverse of apparent molecular weight of the mixture of subtilisin BPN' and SSI solutions against the cell average concentration, $(C_a + C_b)/2$, is plotted in accord with Eq. 3.6 (Fig. 3.9). The reading of intercept gives the molecular weight

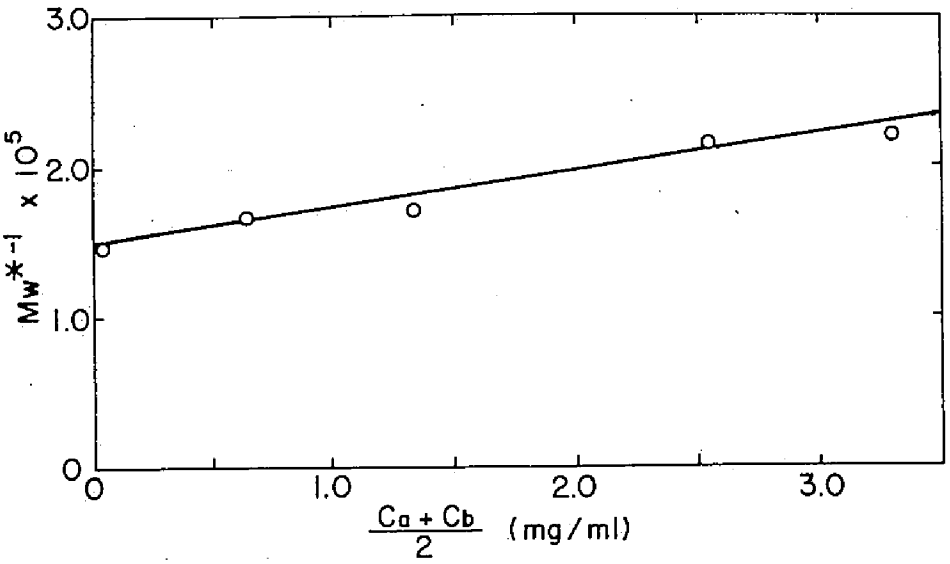

Fig. 3.9. Dependence of apparent weight average molecular weight (cell average, weight average molecular weight), Mw*, of the mixture of subtilisin BPN' and SSI solutions on the cell average protein concentration, $(C_a + C_b)/2$. Each point of Mw* was obtained from the run in 25 mM phosphate buffer, pH 7.0, ionic strength 0.1 M (NaCl), 25.0°C with the Rayleigh interference optics or the photoelectric scanning optics. From the intercept, the molecular weight of the mixture, 65,360 ± 1,200, was obtained.

---

of the mixture Mw as 65,360 ± 1,200. In this case, Eq. 3.3 is applicable to determine the molecular weight of subtilisin BPN'-SSI complex. Equation 3.3 is transformed to

$$Mw = \gamma_{EI} M_{EI} + \gamma_{I_2} M_{I_2} + \gamma_{E'} M_{E'} \qquad (3.7)$$

where Mw is the weight average molecular weight of the mixture; γ_{EI}, γ_{I_2}, and $\gamma_{E'}$ are weight fraction of subtilisin BPN'-SSI complex, SSI, and inactive enzyme, respectively; M_{EI}, M_{I_2}, and $M_{E'}$ are the molecular weights of the complex, SSI, and inactive enzyme, respectively.

The values of these terms are assumed, based on the active site purity of the enzyme preparation used and the binding equivalence of SSI to the enzyme (see Chapter One), to be as follows; $\gamma_{EI} = 0.721$, $\gamma_{I_2} = 0.106$, $\gamma_{E'} = 0.173$, $M_{I_2} = 23{,}000$, $M_{E'} = 27{,}500 - 100$. M_{EI} is calculated to be 80,700 when $M_{E'}$ is assumed to be identical with the molecular weight of native and intact enzyme (27,500), and M_{EI} to be 87,300 when $M_{E'}$ is taken to be 100 due to the autolysis of the enzyme to amino acids. It is not practical to believe that all inactive enzyme is autolyzed to amino acids. Thus, it is concluded that the molecular weight of the subtilisin BPN'-SSI complex is in the range of 77,300 (Fig. 3.8, B) to 80,700 (above calculation) (see Discussion 3.4).

3.4 Discussion

Dimeric form of SSI. The molecular weight of SSI has been reported by Sato and Murao (1973, 1974) to be 27,000 by gel filtration on a Sephadex G-100 column (*23*), and 12,000 by polyacrylamide gel electrophoresis in the presence of SDS (*49*). They concluded that SSI must exist in dimer under the usual conditions. It has been also suggested by X-ray crystallographic study that SSI may consist of two identical subunits in a crystalline state (*28*). Based on the amino acid composition (*27*), the minimal molecular weight of SSI is calculated to be 11,500.

One of the purpose of the present study is to determine the molecular weight of the essential unit of SSI in the concentration range used in enzyme kinetic, spectrophotometric, and binding measurements. The molecular weight of SSI was measured in the present study by sedimentation equilibrium method with accuracy in the wide concentration range of

0.01 - 10 mg/ml in 25 mM phosphate buffer, at pH 7.0, ionic strength 0.1 M (NaCl), 25.0°C. The concentration range covers the concentrations used for various measurements mentioned above. The concentration of 0.01 mg/ml is one of the lowest ones which has been applied to sedimentation equilibrium. The molecular weight was determined to be 23,000 constantly in the concentration range used. From this evidence, it is confirmed that SSI composed of two identical subunits and a dimer form is an essential unit in 1×10^{-6} - 1×10^{-3} M (as monomer), where neither monomer nor more aggregated form than dimer was detected.

Molecular weight of the subtilisin BPN'-SSI complex. Homogeneity of the crystallized complex preparation was examined by polyacrylamide gel electrophoresis (Fig. 3.1). However, the sedimentation equilibrium patterns shown in Fig. 3.7 are not linear indicating multicomponent system. As shown in Fig. 3.7 (B), near cell bottom, the main species is sedimenting with molecular weight of 76,760. Other than this, a minor species of molecular weight of less than 10,000 is detected. As previously described in Chapter Two, the binding and inhibition of SSI against subtilisin BPN' is strictly stoichiometric. So, the molecular weight of the complex may be 39,000 by simply adding the molecular weight of SSI (11,500) and that of subtilisin BPN' (27,500), or integral multiple values. The molecular weight 76,760 indicates that the complex is composed of a mole of dimeric SSI and two moles of the enzyme, but another species of low molecular weight remains unidentified. As the dissociation constant of the complex is very small, 10^{-9} M, the dissociated inhibitor and/or enzyme is difficult to detect in the concentration range used. It is most reasonable to attribute the low molecular weight protein to the damage during lyophilization.

Molecular weight determination of the subtilisin BPN'-SSI complex in the mixture solution of the both proteins. As described above, the molecular weight of the subtilisin BPN'-SSI complex using the crystallized and lyophilized preparation was not determined unambiguously. In order to overcome the disadvantage arising from the low solubility of the complex preparation and the presence of low molecular weight protein, the molecular weight was measured in polydisperse-multicomponent system (Fig. 3.8). From the sedimentation equilibrium pattern shown in Fig. 3.8, the biggest species in the mixture solution was found at the cell bottom having molecular weight of 77,300.

From the sedimentation equilibrium of the mixture solution of subtilisin BPN' and SSI, the molecular weight of the complex was suggested to fall on the range of 80,700 - 87,300 in accord with the treatment of pclydisperse-multicomponent system. It is clear that this molecular weight is the average one of some species, if any, of the complex.

In connection with that the maximum value is 77,300, that the average value is 80,700 (see the section of *Sedimentation equilibrium of the mixture solution of subtilisin BPN' and SSI* in Results 3.3), and that these values are almost the same, the number of the species of the complex must be only one. Among the possible combination of SSI and subtilisin BPN' (E_1I_1, E_1I_2, E_2I_2, ...), only the species of E_2I_2, E_1I_4, and E_1I_5 can have a molecular weight that conforms to the above values. Since the previous data on binding and inhibition stoichiometry show that the complex has a composition of E_nI_n, the species of E_2I_2 (MW 78,000) is concluded to be the complex.

Subunits interaction of SSI. Reversible subunit self-assembly of low molecular weight protein proteinase inhibitors from plant is well

established (*50,63*). In the absence of proteinase, monomer-dimer equilibria exist in the lima bean trypsin inhibitor (*64-66*), the Bowman-Birk soybean inhibitor (*67,68*), and the Ventura black-eyed pea inhibitor (*69*). Monomer-dimer-tetramer equilibria have been observed in various potato inhibitors (*70-72*), and black-eyed pea trypsin inhibitor (BEPTI) and black-eyed pea chymotrypsin and trypsin inhibitor (BEPCI) (*73,74*). When these self-associable inhibitors bind enzymes, only proteinase-bound monomers have been reported in the monomer-dimer system described above (*65,69,75*), and in the monomer-dimer-tetramer system, only proteinase-bound tetramer (*70*) or proteinase-bound monomers and dimers (*72*) have been reported. These indirect evidence suggest that subunit interaction (half-site reactivity) is important during complex formation of inhibitor and proteinase.

In the present Chapter, the reversible subunit-association of SSI which may be concentration dependent has not been observed. SSI exists in a stable dimer (I_2) in a wide concentration range (1×10^{-6} - 1×10^{-3} M as monomer). Even when it binds subtilisin BPN' (E_1), SSI is observed only as a proteinase-bound dimer (E_2I_2). From these results, the intersubunit binding of SSI seems stronger than that of other self-associating proteinase inhibitors previously reported, such as Bowman-Birk soybean inhibitor, lima bean inhibitor, and potato inhibitor. In this point, SSI is an interesting and unique protein proteinase inhibitor as well as in its origin and its inhibitory specificity. There have been some well known proteinase inhibitors that inhibit more than one enzyme (*15*), and Rhode *et al.* (*76*) coined the very descriptive term "multiheaded" to describe the inhibitors with several nonoverlapping independent sites. Apparently, SSI is not a multiheaded inhibitor.

However, it must be remembered that a SSI molecule binds two subtilisin BPN' molecules under usual conditions. This point should be taken into account especially in equilibrium and kinetic studies of this inhibitor.

The subunit interaction of SSI is probably one of the strongest ones which have been examined. Schachman and Edelstein (*54*) made the interesting observation that at neutral pH and at very low concentration of protein (0.002 mg/ml) in 0.1 M phosphate buffer solution, the hemoglobin tetramer dissociates all the way into monomers, by the sedimentation experiments using the photoelectric scanning optics. Their experiments with such a low protein concentration were made possible due to the big extinction coefficient of the hemoglobin Soret band, $E_{1\ cm}^{0.1\%}$ (410 nm) = 8.4. On the other hand, it was found in this study that SSI does not dissociate into monomers at the low concentration of 0.01 mg/ml. Roughly, the dissociation constant of SSI dimer into monomers may be estimated to be less than 4×10^{-7} M.

There remain interesting problems to be examined: under what conditions, SSI dissociates into subunits; whether the isolated subunit retains the strong inhibitory activity against subtilisin BPN'; by what kind of force, SSI subunits associate so strongly. These points will be described in the following Chapter.

3.5 Summary

The molecular weight of *Streptomyces* subtilisin inhibitor, SSI, and that of the complex of SSI and subtilisin BPN' were measured by the sedimentation equilibrium method in 25 mM phosphate buffer, at pH 7.0, ionic strength 0.1 M (NaCl), 25.0°C. The molecular weight of SSI was

determined to be 23,000 over the wide concentration range, 0.01 - 10 mg/ml (1×10^{-6} - 1×10^{-3} M as monomer) covering the range used for inhibitory, spectrophotometric, and kinetic measurements. Based on the amino acid composition of SSI, the molecular weight has been calculated to be 11,500, therefore the molecular weight of 23,000 obtained above suggests that SSI is dimer under the usual conditions.

The molecular weight of the subtilisin BPN'-SSI complex was determined to be 78,000 (77,300 - 87,300) by two ways; sedimentation equilibrium of the crystallized and lyophilized complex preparation and that of the mixture solution of subtilisin BPN' and SSI applying the treatment of multicomponent-polydisperse system. The molecular weight obtained here, combining with the evidence as shown in Chapter One that a mole of SSI (MW 11,500) binds to a mole of the enzyme (MW 27,500) tightly ($K_d < 10^{-9}$ M), demonstrates that one mole of dimeric SSI binds two moles of the enzyme to form a stable complex, E_2I_2.

Chapter Four

The Effect of Sodium Dodecyl Sulfate on the Structure and Function of *Streptomyces* Subtilisin Inhibitor *

4.1 Introduction

It has been known that SSI is a single polypeptide of molecular weight of 11,500 from the primary structure (*27*). As shown in the previous Chapters, one mole of SSI binds and inhibits stoichiometrically one mole of subtilisin BPN' with the inhibitor constant $K_i < 10^{-9}$ M, and under the usual conditions (at neutral pH, in the concentration range of 0.01 - 10 mg/ml), SSI exists as a dimer of molecular weight of 23,000. In the presence of subtilisin BPN', it forms a complex with two moles of the enzyme per mole of dimer. Neither monomer-dimer equilibrium of SSI even at the very low concentration as 0.01 mg/ml (1 μM) nor dissociation of SSI into monomers on the complex formation with the enzyme has been observed, in contrast with other reversibly self-associating protein proteinase inhibitors such as Bowman-Birk soybean trypsin inhibitor (*67, 68*), lima bean trypsin inhibitor (*64-66*), black-eyed pea inhibitors (*73, 74*), and potato inhibitors (*70-72*). Thus, the subunits interaction of SSI seems to be very strong in comparison with other self-associating inhibitors.

The interaction of detergents with proteins has been a subject of basic and practical interest. Anionic detergents are extensively used

---

* A part of this study was presented at the Annual Meeting of the Agricultural Chemical Society of Japan (Kyoto, April 1976) (*c*).

in biochemical preparations and they are classified as effective denaturing agents of proteins at remarkably low reagent concentrations (*77*). However, the mechanism of their action on protein conformation remains unsolved. It has been inferred chiefly from optical rotatory dispersion studies that denaturation by sodium dodecyl sulfate, SDS, of ovalbumin (*78*), and β-casein, histone fraction F_1, and chymotrypsinogen (*79*) may actually result in forming new helical regions that are not present in the native molecule. Such conversion of the unordered into the helical conformation by "amphiphilic" substances (*80*) was clearly indicated and confirmed later by circular dichroism (*81-85*).

The term "denaturation" is usually considered as a synonym of "disorganization" of the native three-dimensional structure of a protein or other macromolecule.

It is known that the interaction of proteins with SDS causes the formation of protein-SDS complexes and also subunit formation when the protein consists of subunits (*86-89*).

In the present Chapter will be described the dissociation of SSI dimer into subunits at the low concentration of SDS without the loss of inhibitory activity against subtilisin BPN' and the conformational change observed on the binding of SDS and SSI.

4.2 Experimental Procedures

Proteins. A three times crystallized and lyophilized preparation of *Streptomyces* subtilisin inhibitor, SSI, was a generous gift from Professor S. Murao. A three times crystallized preparation of subtilisin BPN' [EC 3.4.21.14] was purchased from Nagase & Co. Ltd., Osaka (Lot No.

206006). The purity of the preparation was determined to be 75.4% according to the method described in Experimental Procedures 2.2.

Concentrations of the protein solutions were determined spectrophotometrically using the following absorptivities at pH 7.0: $E_{1\ cm}^{0.1\%}$(276 nm) = 0.829 for SSI and $E_{1\ cm}^{0.1\%}$(278 nm) = 1.063 for subtilisin BPN' (Experimental Procedures 2.2).

Chemicals. Sodium dodecyl sulfate, SDS, (99% purity) (Lot No. M3N 5078) of specially prepared reagent and methylene blue (Lot No. V5T2345) of guaranteed reagent were purchased from Nakarai Chemicals Ltd., Kyoto. *p*-Nitrophenyl acetate, pNPA, (Lot No. FCF01) was the product of Tokyo Kasei Kogyo Co. Ltd., Tokyo. The concentration of pNPA was determined spectrophotometrically by the method described in Experimental Procedures 2.2.

A 25 mM sodium phosphate buffer, pH 7.0, ionic strength adjusted to 0.1 M with NaCl, at 25.0°C was used exclusively in the present study.

All the spectrophotometric measurements were made with a Shimadzu UV-200 or a Union SM-401 recording spectrophotometer.

Determination of the critical micelle concentration, CMC. The critical micelle concentration of SDS in the buffer solution used was determined to be 0.035% (w/v) at 25°C by the measurement of the surface tension using a Shimadzu ST-1 surface tensometer (the vertical method) (*90*).

The binding of SDS to SSI. The binding of SDS to SSI was measured with the equilibrium dialysis technique using a dializer manufactured by the author. The dialysis unit was composed of a pair of acrylic plastic blocks (50 mm x 50 mm x 15 mm thick) with a cylindrical hole (20 mm ϕ, 10 mm depth) bored in each. The pair was positioned so that the holes

were facing each other, and a sheet of Visking membrane, Type 27/32 was placed between them. The Visking membrane had been treated with 2% NaOH for 15 min at room temperature, rinsed with water, immersed in 1.5% SDS solution overnight, and finally washed with distilled water. It was soaked in distilled water. Five dialysis units were placed in a reciprocating shaker (130 reciprocating per min) at 25°C. In order to reduce the time to attain equilibrium, in the cases where SDS concentration was larger than the CMC, the dialysis was started with an protein solution (inner solution) containing appropriate amount of SDS. The concentration of SSI in inner solution was 1.0 mg/ml (87.0 μM as monomer).

Determination of SDS concentration. The concentration of SDS after dialysis was determined in both inner (protein) and outer (dialysate) solutions by extraction of an alkyl sulfate-methylene blue complex into chloroform and by reading the absorption of the chloroform layer at 655 nm (*89,91*).

One milliliter of 0.007% methylene blue in 1.0% aqueous Na_2SO_4, which had been washed with chloroform in a separating funnel, was placed into a test tube with a stopper. Five milliliter of chloroform was added to the test tube, and after addition of 0.1 ml of a sample solution containing SDS (0.1 - 0.5 mM; 0.003 - 0.015% (w/v)), the test tube was vigorously stirred with a flash mixer for one minute to extract the methylene blue-SDS complex into the chloroform layer. After the upper water layer had been carefully pipetted out, the chloroform layer was transferred into an optical cuvette with a stopper through a small funnel with a plug of adsorbent cotton to remove contaminating water droplets. The absorption at 655 nm was measured, and the SDS concentration was read from a calibration curve. The calibration curve for the SDS-

SSI mixture solution was substantially the same as that for SDS solution. It was found that the above procedure quantitatively removed the bound SDS from the protein.

Sedimentation equilibrium in the presence of SDS. The molecular weight of a protein in solution can be determined unambiguously with sedimentation equilibrium if the experimental data are treated in accord with the equations appropriate for multicomponent system (*92*) (also refer to the section of *Sedimentation analysis of multicomponent-polydisperse system* in Experimental Procedures 3.2). The protein should be highly purified, and it is assumed that measurements can be made at sufficiently low concentrations to avoid problems arising from reversible self-aggregation or thermodynamic nonideality (Linearity of the plot of log C(r) vs. r^2, when plotted according to Eq. 4.1 indicates that this condition is fulfilled) (see Chapter Three). The sedimentation experiment yields a value for buoyant molecular weight, $Mw(r)\cdot(1 - \phi'\rho)$, for the SDS-SSI complex. The extent of SDS binding, δ_D, is most conveniently expressed as grams of SDS per gram of protein. The molecular weight, Mw(r), that is to be measured is the local weight average molecular weight of pure protein, *excluding bound detergent and other solvent components*, and it is related to the experimentally determined protein concentration, C(r), as a function of radial position, r, by the relation

$$(2RT/\omega^2)\ \{d[\ln C(r)]/\ d(r^2)\} = Mw(r)\cdot(1 - \phi'\rho) \qquad (4.1)$$

where ω is the radial velocity of rotation, ρ is the density of the solvent, and ϕ' is the *effective partial specific volume* which includes both the true partial specific volume and the effects of the interaction with detergent and other solvent components.

The quantity ϕ' in Eq. 4.1 can be measured directly by determining

the density of protein solutions that have been dialyzed to equilibrium against a detergent solution of the desired concentration. This method requires great care (e.g., precise concentration measurements are required) and demands relatively large amounts of protein.

A more convenient procedure than measurement of ϕ' is to use a calculated buoyant density factor, as was first done for protein-detergent complexes by Hersh and Schachman (*93*). To do this, the factor $Mw(r)\cdot(1 - \phi'\rho)$ of Eq. 4.1 is replaced by

$$Mw(r)\cdot(1 - \phi'\rho) = Mw(r)\cdot\{(1 - \bar{v}_P\rho) + \delta_D(1 - \bar{v}_D\rho) + \Sigma\ \delta_i(1 - \bar{v}_i\rho)\} \tag{4.2}$$

where $\bar{v}_P$ is the partial specific volume of the protein and $\bar{v}_D$, the partial specific volume of the detergent *when bound to the protein* (*92*). The last term in the equation allows for binding of other substances, which does not exist in the present study. Since δ_D and any important δ_i are known parameters, Eq. 4.2 permits the determination of molecular weight without measurement of ϕ', provided that the $\bar{v}$ values are known. The value of $\bar{v}_D$ is 0.815 cm^3/g below CMC, and 0.870 cm^3/g above CMC, ρ = 1.00 g/cm^3 at the SDS concentration range used (*94*) and $\bar{v}_P$ is 0.730 ± 0.004 obtained by density measurement and 0.729 calculated on the basis of the amino acid composition (see Chapter Three). With the use of these values, the molecular weight of SSI in the complex with SDS, Mw(r) can be computed from the following expression;

$$Mw(r) = \frac{Mw(r)\cdot(1 - \phi'\rho)_{complex}}{(1 - \bar{v}_P\rho) + \delta_D(1 - \bar{v}_D\rho)} \tag{4.3}$$

where the numerator is the buoyant molecular weight term calculated experimentally. In the calculation, additivity of refractive index and molar volumes are assumed. This point has been discussed by Carusi and

Sinsheimer in connection with a similar calculation (*95*).

The apparent weight average molecular weight (cell average, weight average molecular weight) of pure protein, Mw*, was obtained by Eq. 4.4.

$$\{(2RT/\omega^2)(C_b - C_a)\} / \{C_o(r_b^2 - r_a^2)\} = Mw^* (1 - \phi'\rho) \qquad (4.4)$$

where C_o is the initial protein concentration, C_a and C_b are the protein concentrations at the meniscus and the cell bottom, respectively, and r_a and r_b are the radial positions of the meniscus and the cell bottom, respectively.

The sedimentation equilibrium experiment of SSI in the presence of SDS was carried out at 25.0°C in a Beckman Spinco Model E analytical ultracentrifuge equipped with a Rayleigh interference optical system, and a rotor-temperature control (RTIC) unit. A double-sector cell was used in all experiments. All measurements on the photographic plate were made with a Nikon Model 6C two-dimensional micro-comparator equipped with a rotational stage. A capillary-type synthetic boundary cell was used to determine the refractive index for initial protein concentration, C_o.

The SSI concentration used in the sedimentation equilibrium experiment was 1.00 mg/ml (87.0 μM as monomer) in 25 mM phosphate buffer, pH 7.0, ionic strength 0.1 M (NaCl). From the preliminary sedimentation equilibrium experiments by the author, it was found that SDS forms micelles of molecular weight of 30,000 above CMC under the present conditions. All samples to be analyzed with sedimentation analysis should be dialyzed first to equilibrium against the buffer, and the dialysate should be used as the reference solvent. It takes 3 - 4 days, however, to attain an dialysis equilibrium especially at the SDS concentration above CMC (see the section of *Determination of SDS concentration* of

this Experimental Procedures 4.2). As no antiseptic reagent (such as NaN_3) was used in the sample solutions for equilibrium dialysis, it was not practical to use the dialyzed solutions as sample solutions for sedimentation equilibrium because of the infection of the sample solutions during dialysis. Therefore, the SDS concentrations of the sample cell and reference cell in most of the sedimentation experiments were calculated on the basis of binding isotherm of SDS to SSI determined according to the method shown above. In some cases at the SDS concentration below CMC, the samples and reference solvents were prepared by equilibrium dialysis.

Ultraviolet absorption difference spectra observed on the binding of SDS with SSI. Absorption difference spectra measurements were carried out on a Union SM-401 high sensitivity recording spectrophotometer equipped with a Union SM-4012 spectral data processor at 25.0°C. A pair of quartz cuvettes devided into two compartments of 4-mm light path length was used. To a SSI solution, 2.00 mg/ml (174.0 μM as monomer) in 25 mM phosphate buffer, pH 7.0, ionic strength 0.1 M (NaCl) was added the equal volume of SDS solution in the same buffer at various concentrations up to 10.0% (w/v). The ultraviolet absorption spectra were measured after holding the mixture at 25.0°C for 6 hr. The base line was compensated by recording the difference between the difference spectrum produced by SDS-SSI binding and the base line memorized in a Union SM-4012 spectral data processor. The time dependence of the difference spectra was also measured immediately after mixing by scanning from 240 nm to 340 nm in 50 sec.

Absorption and absorption differential spectra of SSI-SDS complex. Ultraviolet absorption and its differential spectra (or derivative spec-

tra) (*96*) were measured with a Union SM-401 high sensitivity recording spectrophotometer equipped with a Union SM-4012 spectral data processor at 25.0°C. A differential spectrum was obtained by subtracting electronically the absorption spectrum measured in 240 - 340 nm region from that in 241 - 341 nm region; the former and the latter had been stored separately in the spectral data processor. The samples were prepared as those used in difference spectra.

Inhibitory activity of SSI against subtilisin BPN' in the presence of SDS. A pNPA solution (containing finally 5.0% (v/v) isopropanol) of 1.63 mM in 0.1 M NaCl aqueous solutios; a SSI solution of 13.0 μM (as monomer); a subtilisin BPN' solution of 139 μM; and SDS solutions of various concentration from 0 to 1.03% (w/v) in 25 mM phosphate buffer, pH 7.0, ionic strength 0.1 M (NaCl) were prepared. Two milliliter of a 1 : 1 (in volume) mixture of the pNPA and SDS solutions was mixed with the same volume of a 1 : 1 (in volume) mixture of the SDS and SSI solutions. To a 3.0 ml of the SDS-SSI-pNPA mixture, 0.1 ml of the enzyme solution was added in an optical cuvette to initiate the enzymatic reaction. The progress of the enzyme reaction was monitored at 405 nm on a Shimadzu UV-200 recording spectrophotometer at 25.0°C. Transferring and mixing of solutions were done immediately to avoid the non-enzymatic hydrolysis of pNPA at pH 7.0. The dependence on SDS concentration of the initial rate (v_i) of pNPA hydrolysis by subtilisin BPN' in the presence of SSI was determined in this way. On the other hand, the dependence of the enzymatic activity (v_o) on SDS concentration in the absence of SSI was determined by carrying out the same measurement using the buffer in the place of the SSI solution. The relative inhibitory activity of SSI at a certain SDS concentration was defined as $(1 - v_i/v_o)$ x

100 (%).

Inhibition stoichiometry of SSI against subtilisin BPN' in the presence of SDS was also examined by mixing the solutions in the same way. The final concentration of SDS of 0.10% (w/v), subtilisin BPN' of 1.86 μM, pNPA of 0.393 mM, and SSI monomer of various concentration up to 5.0 μM were used.

4.3 Results

The critical micelle concentration (CMC). Figure 4.1 shows the dependence of surface tension of SDS solution on SDS concentration in 25 mM phosphate buffer, at pH 7.0, ionic strength 0.1 M (NaCl), 25°C. From the minimum point, the CMC was determined to be 0.035% (w/v) in the condition used throughout this study.

The binding isotherm between SDS and SSI. The binding isotherm between SDS and SSI is shown in Fig. 4.2, which was determined with equilibrium dialysis. The extent of SDS binding increases gradually with SDS concentration, and reaches the maximum value, δ_D = 1.2 g SDS per 1.0 g SSI, above the SDS concentration 0.12% (w/v).

Sedimentation equilibrium of SSI in the presence of SDS. In Fig. 4.3 is shown a plot of log C(r) vs. r^2 of the sedimentation equilibrium at 0.09% (w/v) of SDS initial concentration, $[SDS]_o$, according to Eq. 4.1. From its non-linearity, it is clear that SSI in SDS solution is polydisperse and multicomponent, i.e., it demonstrates the existence of dissociation-association of SSI. From this plot, the buoyant molecular weight, $Mw(r)\cdot(1 - \phi'\rho)$, was shown to be between 9,000 and 4,540. The effective partial specific volume, ϕ', was determined to be 0.612, thus;

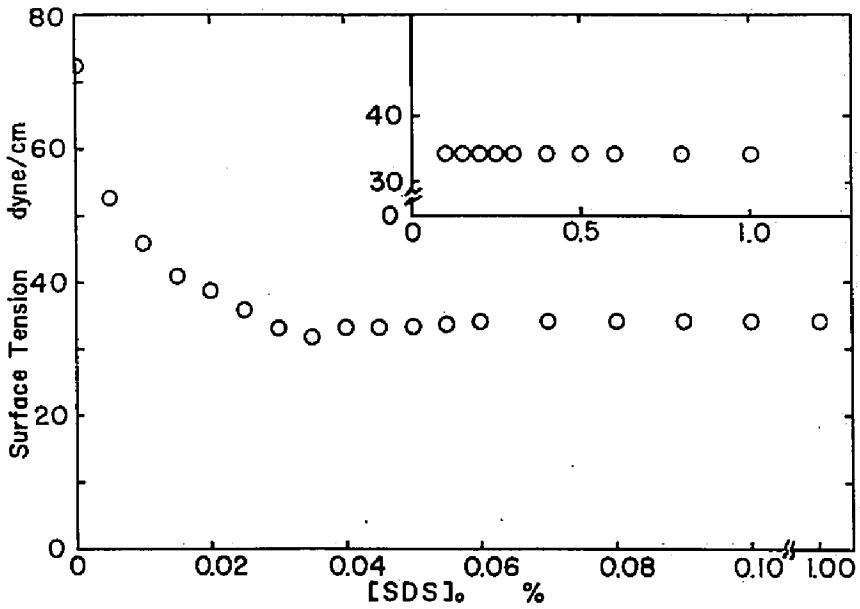

Fig. 4.1. Dependence of the surface tension of SDS solution on the SDS concentration in 25 mM phosphate buffer, at pH 7.0, ionic strength 0.1 M (NaCl), 25°C. The critical micelle concentration (CMC) of SDS solution was determined to be 0.035% (w/v) under the condition used.

---

from Eq. 4.3 the molecular weight of SSI, Mw(r), was turned out to be between 23,210 at cell bottom and 11,700 at meniscus, and the cell average molecular weight, Mw*, was 16,700.

The plot of log C(r) vs. r^2 was demonstrated to be linear in the SDS concentration ranges 0 - 0.03% (w/v) and 0.12 - 0.4% (w/v) (Figures not shown), and in the range of 0.03 - 0.12% (w/v), the plot was of more than one phase indicating the existence of more than one component. When the plot is linear, both cell local molecular weight, Mw(r), and cell average molecular weight, Mw*, of SSI give the same value; in the SDS concentration range of 0 - 0.03% (w/v), the value was about 23,000 and in that of 0.12 - 0.4% (w/v), about 10,000. In the SDS concentration range of 0.03 - 0.12% (w/v), the value of the cell average molecu-

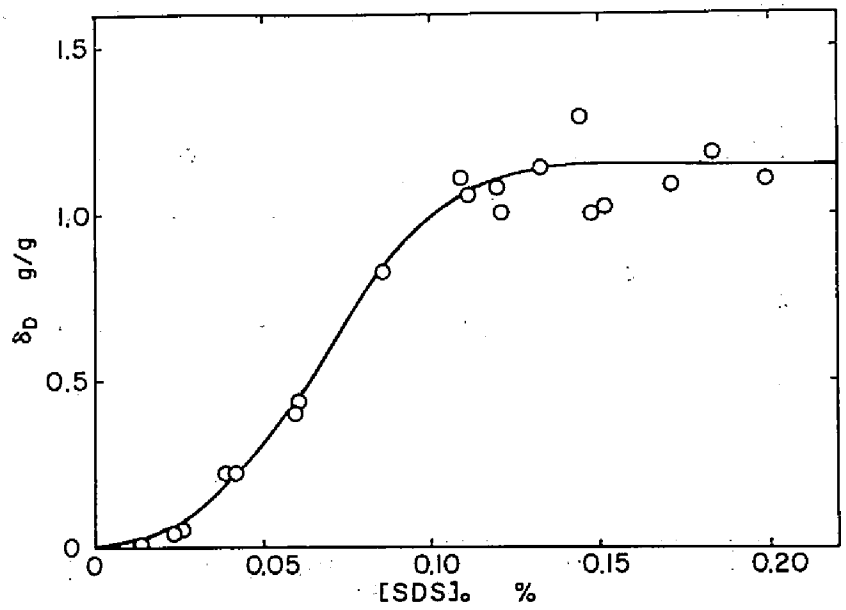

Fig. 4.2. The isotherm of binding of SDS toward SSI. $[SSI]_o$ = 1.00 mg/ml (87.0 μM as monomer), in 25 mM phosphate buffer at pH 7.0, ionic strength 0.1 M (NaCl), 25°C.

---

lar weight, Mw*, decreases gradually from about 23,000 to about 10,000 with the increase of the SDS concentration. The dependence of the cell average molecular weight, Mw*, on the SDS concentration is shown in Fig. 4.4. As reported previously, the molecular weight of SSI is 11,500 calculated on the basis of amino acid composition, and in the buffer system used in the present study at 25.0°C, the molecular weight is 23,000 from the sedimentation equilibrium study (see Chapter Three). From the data shown in Fig. 4.4, it is demonstrated that SSI (87.0 μM as monomer) exists as a dimer in SDS concentration from 0% up to 0.03% (w/v), the dissociation into monomers occurs between 0.03 and 0.12% (w/v), where monomer and dimer co-exist, and above 0.12% (w/v) of SDS, there is only monomer of molecular weight 11,500.

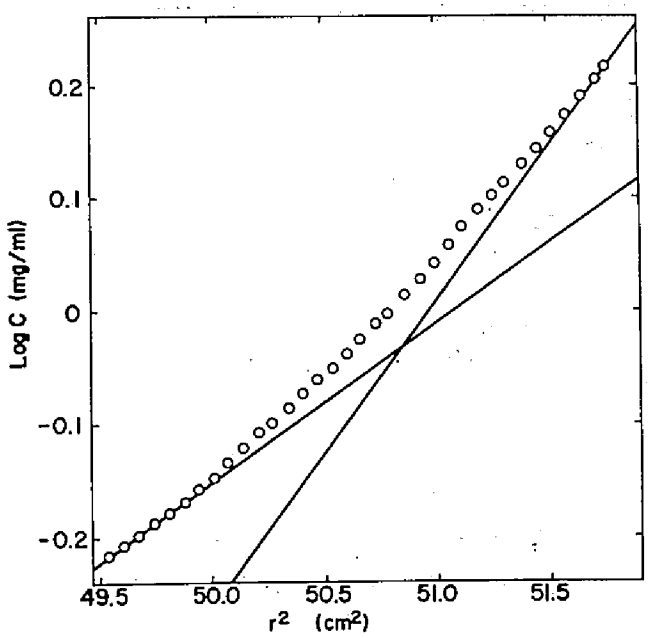

Fig. 4.3. Sedimentation equilibrium run of SSI in the presence of SDS. Log C(r) vs. r^2 plot. $[SSI]_o$ = 1.00 mg/ml (87.0 μM as monomer); $[SDS]_o$ = 0.09% (w/v) in 25 mM phosphate buffer at pH 7.0, ionic strength 0.1 M (NaCl), 25.0°C. $1 - \phi'\rho = 0.388$, fringe magnifying coefficient: 1.9619. The weight average molecular weight at cell bottom, Mw(b) = 23,210; the weight average molecular weight at meniscus, Mw(a) = 11,700; the apparent weight average molecular weight (cell average molecular weight), Mw* = 16,670 are determined.

Absorption difference spectra observed on the binding of SSI and SDS. Figure 4.5 depicts the absorption difference spectra observed on the binding of SSI and SDS, which were obtained after keeping the SSI-SDS mixture solution for 6 hr at 25.0°C. In the SDS concentration range used (0 - 0.3% (w/v) in 25 mM phosphate buffer, pH 7.0, ionic strength 0.1 M (NaCl)) were shown the red shifts of difference spectra most probably due to phenylalanyl residues in 255 - 275 nm region and those due to tryptophyl and/or tyrosyl residues in 275 - 290 nm region. On the

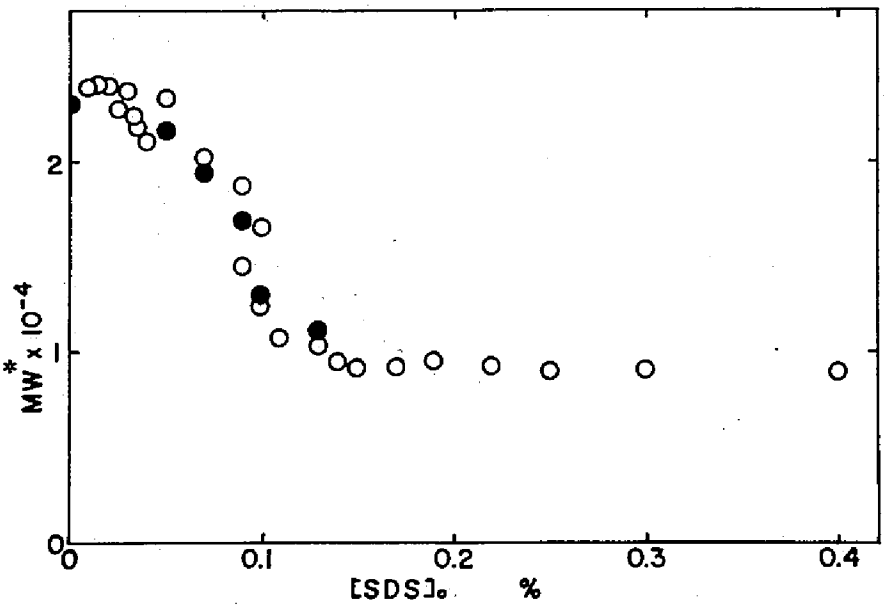

Fig. 4.4. Dependence of the apparent weight average molecular weight (cell average, weight average molecular weight), Mw*, of SSI on the concentration of SDS. $[SSI]_o$ = 1.00 mg/ml (87.0 μM as monomer) in 25 mM phosphate buffer at pH 7.0, ionic strength 0.1 M (NaCl), 25.0°C. $[SDS]_o$: the total concentration of SDS in the sample cell, i.e., the concentration of SDS bound to SSI plus that of free SDS. Sample and reference solutions were obtained after complete dialysis (closed circle) or prepared according to the binding isotherm, Fig. 4.1 (open circle) (see Experimental Procedures 4.2).

---

other hand, in 290 - 310 nm region, there are large change depending on the SDS concentration; in the SDS concentration of 0 - 0.09% (w/v), there is a characteristic trough at 300 nm, but above 0.09% (w/v) SDS, another trough at 293 nm appears and becomes deeper, as SDS concentration increases. At last, the 293 nm band overcomes the 300 nm band, and the latter apparently dimishes. This spectral change can not be considered to be a shift of a single difference spectral band from 300 nm to 293 nm, but it seems that there are substantially two bands at 300 nm

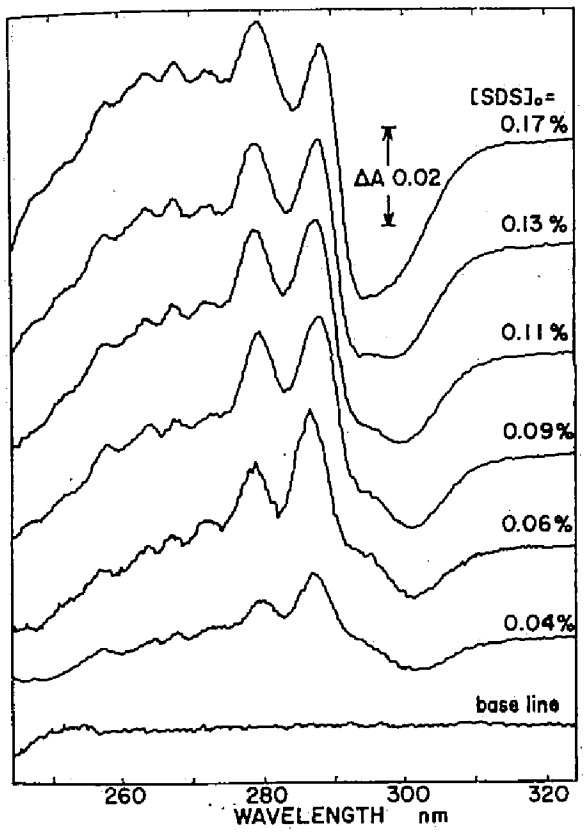

Fig. 4.5. Ultraviolet absorption difference spectra observed on the binding of SSI and SDS. $[SSI]_0$ = 1.00 mg/ml (87.0 μM as monomer) in 25 mM phosphate buffer, pH 7.0, ionic strength 0.1 M (NaCl), 25.0°C.

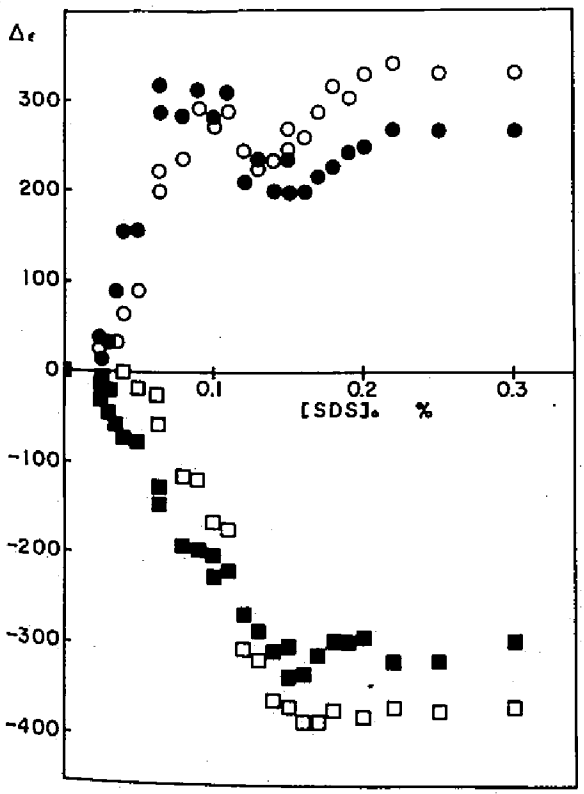

Fig. 4.6. Dependence of the molar absorptivity difference of the difference spectra observed on the binding of SSI and SDS on the concentration of SDS. $[SSI]_0$ = 1.00 mg/ml (87.0 μM as monomer) in 25 mM phosphate buffer, pH 7.0, ionic strength 0.1 M (NaCl), 25.0°C. Wavelength: 279 nm, open circle; 287 nm, closed circle; 293 nm, open square; 300 nm, closed square.

and 293 nm, because there were detected two separate bands at 293 nm and 300 nm at 0.13% (w/v) SDS concentration. The shape and intensity of the difference spectra were not altered up to 5% (w/v) SDS from that obtained at 0.17% (w/v) SDS. The 300 nm band and 293 nm band are due to charge effect and solvent or denaturation effect on a tryptophyl residue (*46,47,97,98*), respectively (see Discussion 4.4).

The magnitudes of the difference spectra at 279, 287, 293, and 300 nm were plotted against the concentration of SDS, as shown in Fig. 4.6. The absorptivity differences at the four wavelengths increases in parallel with the increase of the SDS concentration in 0 - 0.1% (w/v), but at the SDS concentration of 0.1% (w/v) a big change occurred. The difference spectrum should reflect the effect of SDS binding to SSI, dissociation of SSI by SDS, and denaturation of SSI by SDS. Therefore, the big change in the titration curve of absorptivity difference and deviation from a single saturation curve seems to be due to the conformational change such as dissociation into monomer or denaturation of SSI. It is noteworthy that the dependence of absorptivity difference at 300 nm on the SDS concentration is approximately a single saturation curve, whereas absorptivity difference at 293 nm starts to increase above 0.04% (w/v) SDS, and steeply increases in the range, $[SDS]_o$ = 0.08 - 0.14% (w/v), corresponding to that of the cell average molecular weight of SSI (Fig. 4.4), which is indicative of dissociation of SSI into monomers. The unusual changes in $\Delta\varepsilon_{279}$ and $\Delta\varepsilon_{287}$ seems to be the influence of the big change in $\Delta\varepsilon_{293}$. It is proposed that when SSI dissociates into monomers, a tryptophyl residue of SSI monomer become more exposed to the solvent.

The time dependent change of the difference spectrum of the bind-

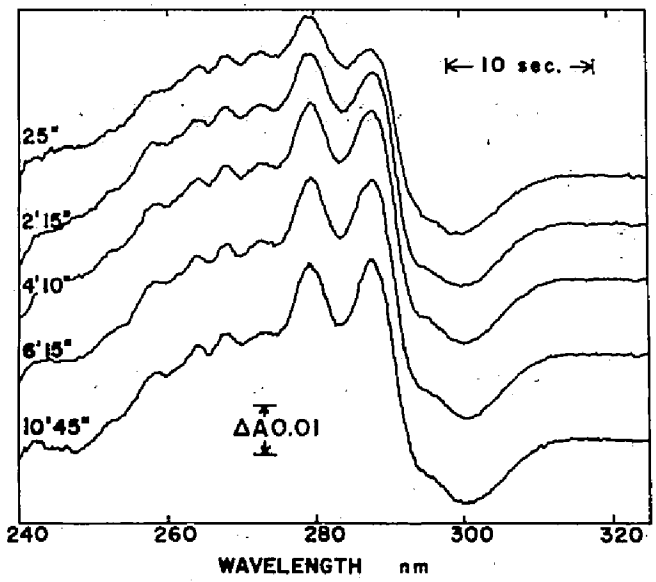

Fig. 4.7. Time dependence of the difference spectrum observed on the binding of SSI and SDS. $[SSI]_o$ = 1.00 mg/ml (87.0 μM as monomer), and $[SDS]_o$ = 0.10% (w/v) in 25 mM phosphate buffer, pH 7.0, ionic strength 0.1 M (NaCl), 25.0°C. Each scanning was started at the time shown in the figure after the mixing of the SSI and SDS solutions (see Experimental Procedures 4.2).

---

ing of SSI and SDS was obtained by recording repeatedly on a Union SM-401 recording spectrophotometer at a scanning speed of 2 nm/sec from 240 nm to 340 nm as shown in Fig. 4.7, which was obtained at the SDS concentration of 0.10% (w/v). The time-dependent absorptivity difference at 300, 279, and 287 nm is shown in Fig. 4.8. Most of the spectral change at the respective wavelengths is shown to be completed within 30 sec after mixing of SSI and SDS, but there are rather slow increases in the molar absorptivity difference at 279 and 287 nm with half-time of 1 and 2 min, respectively, whereas there is no such slow change at 300 nm. From this disagreement in the time-dependent change in absorptivity difference, the interaction between SSI and SDS is suggested to be rather

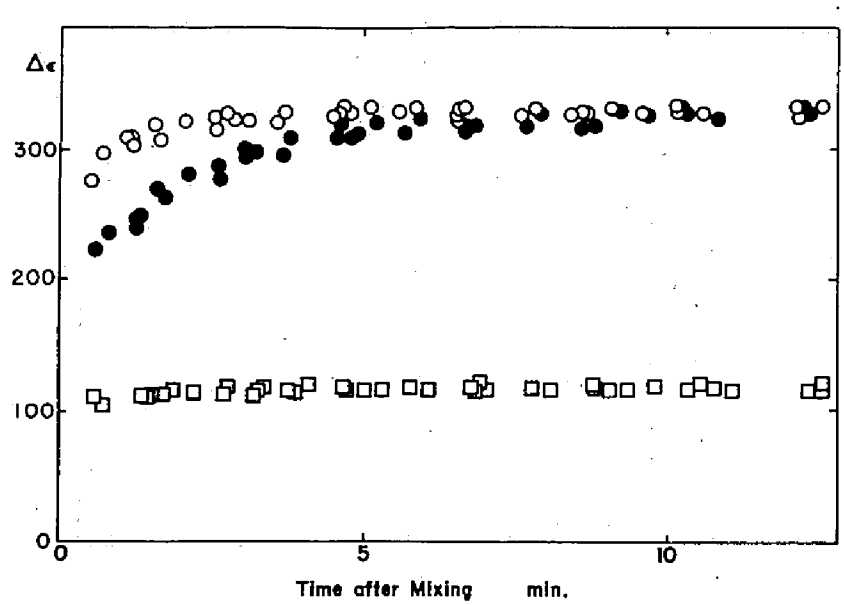

Fig. 4.8. Time dependence of the molar absorptivity difference of the difference spectrum observed on the binding of SSI and SDS. $[SSI]_o$ = 1.00 mg/ml (87.0 μM as monomer), and $[SDS]_o$ = 0.10% (w/v) in 25 mM phosphate buffer, pH 7.0, ionic strength 0.1 M (NaCl), 25.0°C. Wavelength: 279 nm, open circle; 287 nm, closed circle; 300 nm, open square. The $\Delta\varepsilon_{300}$ values are essentially negative, thus $-\Delta\varepsilon_{300}$ was plotted as $\Delta\varepsilon$.

---

complicated.

The change in state of a tryptophyl residue on diasociation of SSI into monomers was also confirmed by comparison of the absorption and differential absorption spectra obtained in the presence and absence of SDS with each other (Fig. 4.9). In the presence of SDS, the absorption spectrum of SSI becomes smoother than that obtained without SDS, especially at 276, 282, and 293 nm. The differential spectrum in 280 - 310 nm region is due to the difference spectrum caused by the red-shift of a tryptophyl residue (*98*). In the presence of SDS, there is a remarkable change in this region.

Inhibitory activity of SSI against subtilisin BPN' in the presence

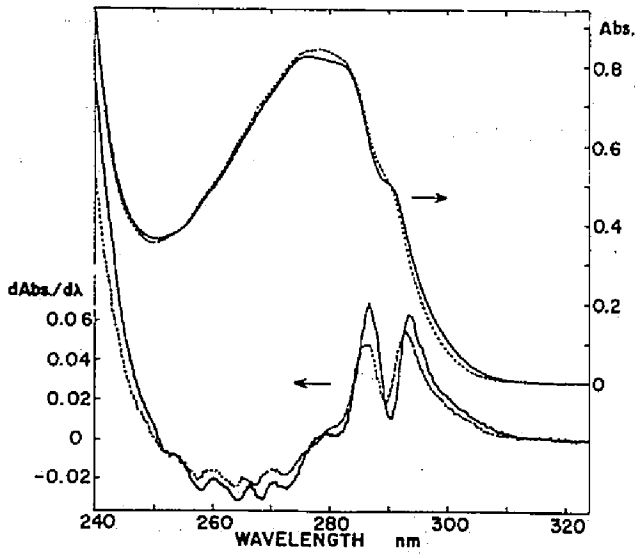

Fig. 4.9. Effect of SDS on the absorption and differential absorption spectra of SSI. $[SSI]_o$ = 1.00 mg/ml (87.0 μM as monomer), $[SDS]_o$ = 0% (w/v), solid line; 0.15% (w/v), dotted line, in 25 mM phosphate buffer, pH 7.0, ionic strength 0.1 M (NaCl), 25.0°C. $\Delta\lambda$ = 1.0 nm for the differential spectra.

---

of SDS. Prior to investigating the effect of SDS on the inhibitory activity of SSI, the influence of SDS on the enzyme activity of subtilisin BPN' was examined. Figure 4.10 shows the SDS concentration dependence of initial velocity for pNPA hydrolysis which was obtained by adding the enzyme solution to the pNPA-SDS mixture solution (see Experimental Procedures 4.2). As shown in Fig. 4.10, the initial velocity, v_o, raises up at the low SDS concentration until 0.015% (w/v), the maximum v_o ($[SDS]_o$ = 0.015% (w/v)) is 1.12 fold larger than that obtained at $[SDS]_o$ = 0%. When SDS concentration increases more than 0.015% (w/v), v_o decreases gradually, and v_o at $[SDS]_o$ = 0.25% (w/v) is 0.8 fold of v_o at $[SDS]_o$ = 0%.

When the enzyme solution was added to the pNPA-SDS-SSI mixture

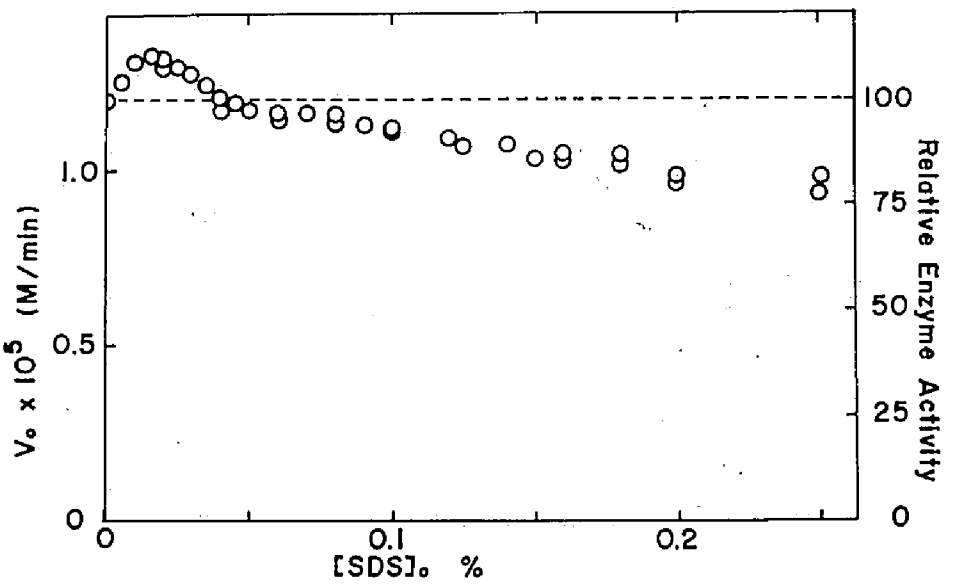

Fig. 4.10. Effect of SDS on the hydrolysis of *p*-nitrophenyl acetate by subtilisin BPN'. [subtilisin BPN']$_o$ = 4.49 μM, and [*p*-nitrophenyl acetate]$_o$ = 0.394 mM in 25 mM phosphate buffer, pH 7.0, ionic strength 0.1 M (NaCl) containing 5.0% (v/v) isopropanol at 25.0°C.

---

solution, the time course of *p*-nitrophenol liberation has a lag phase of 1 - 2 min followed by a steady-state phase, and the similar SDS concentration dependence of the initial velocity of the latter phase, v_i, was obtained under the same conditions used in Fig. 4.10 except for the presence of SSI (Figure not shown). In this case, SSI solutions used had been incubated with SDS for either 25 min or 6 hr in 25 mM phosphate buffer, pH 7.0, ionic strength 0.1 M (NaCl) at 25.0°C. In Fig. 4.11 is shown the relative inhibitory activity, RIA, of SSI against subtilisin BPN' in the presence of various concentration of SDS which is defined as $(1 - v_i/v_o) \times 100$ (%) at each SDS concentration. The dependence of RIA on the SDS concentration is the same in either incubation time (25 min or 6 hr) with SDS. As the concentration of SDS increases, RIA in-

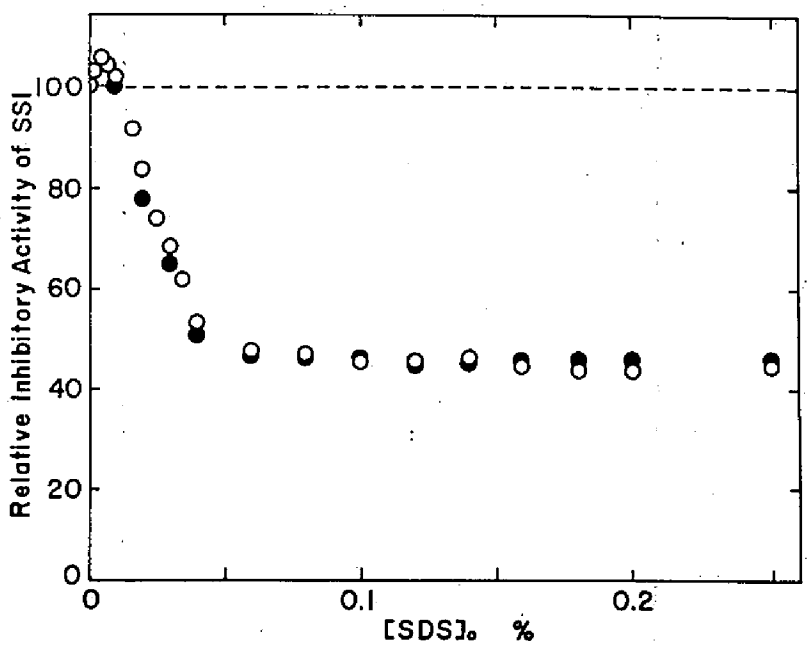

Fig. 4.11. Effect of SDS on the inhibitory activity of SSI against subtilisin BPN' catalyzed hydrolysis of *p*-nitrophenyl acetate. [subtilisin BPN']$_0$ = 4.49 μM, [SSI]$_0$ = 3.15 μM (as monomer), and [*p*-nitrophenyl acetate]$_0$ = 0.394 mM in 25 mM phosphate buffer, pH 7.0, ionic strength 0.1 M (NaCl) containing 5.0% (v/v) isopropanol at 25.0°C. SSI had been treated with SDS for 6 hr (open circle) or 25 min (closed circle) before used for the inhibitory activity assay. Data for the steady-state phase but not for the lag phase were plotted.

---

creases slightly in the SDS concentration range up to 0.005% (w/v), but above this concentration it decreases steeply reaching the saturation level of 50% at the SDS concentration of 0.04% (w/v). If RIA is plotted using the initial rate, v_i, of the lag phase in place of that of the steady-state phase, the saturation level is 70% (Figure not shown).

Figure 4.12 shows that the SSI concentration for complete inhibition against subtilisin BPN' in the presence of SDS (0.10%, w/v) ([SSI monomer]$_0$/[subtilisin BPN']$_0$ = 2 (M/M)) is considerably larger than that

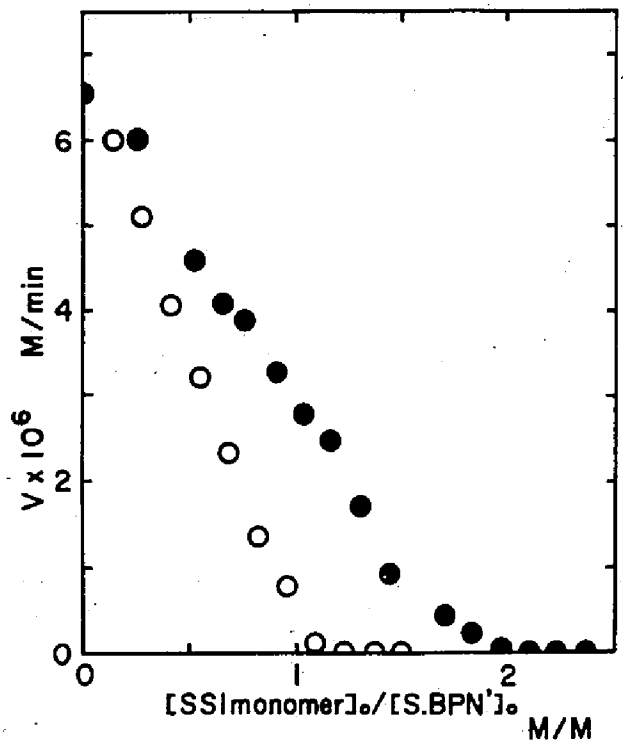

Fig. 4.12. Inhibition of SSI against the hydrolysis of *p*-nitrophenyl acetate catalyzed by subtilisin BPN'. [subtilisin BPN']$_o$ = 1.86 μM, [*p*-nitrophenyl acetate]$_o$ = 0.393 mM, and [SDS]$_o$ = 0% (w/v), open circle; 0.10% (w/v), closed circle, in 25 mM phosphate buffer, pH 7.0, ionic strength 0.1 M (NaCl) containing 5.0% (v/v) isopropanol at 25.0°C.

---

in the absence of SDS ([SSI monomer]$_o$/[subtilisin BPN']$_o$ = 1.0 (M/M)). The titration data in the former case (●) scatter rather than those of the latter case (O), suggesting the complicated effect of SDS on the assay system used for the inhibitory activity of SSI, e.g., the effect of SDS on the structures of subtilisin BPN' and SSI, on the binding of pNPA toward the active site of the enzyme, and on the electrostatic environment of the interacting region of SSI and subtilisin BPN'.

4.4 Discussion

SDS binding to SSI, dissociation of SSI into monomers, and inhibitory activity of monomeric SSI. The measurements of SDS binding to SSI (Fig. 4.2), molecular weight of SSI in the presence of SDS (Fig. 4.4), and difference spectral titration observed on the binding of SSI and SDS (Fig. 4.6) were carried out under the same conditions and the same SSI concentration ([SSI monomer]$_o$ = 87.0 μM). These behaviors depending on the SDS concentration are in good agreement. On the other hand, the relative inhibitory activity measurement of SSI against subtilisin BPN' was performed at [SSI monomer]$_o$ = 3.15 μM. Although this concentration is 1/30 as large as that used in the molecular weight measurement, the inhibitory activity remains about a half even at the concentration of SDS of 0.12% (w/v) at which all SSI molecules exist as monomer. When the relative inhibitory activity (Fig. 4.11) and the molecular weight (Fig. 4.4) of SSI are plotted against the molar ratio of [SDS]$_o$/[SSI monomer]$_o$ (M/M) in the same co-ordinate (Figure not shown) as done by Nakagawa and Jirgensons (*99*) and Sogami *et al.* (*100*), it is shown that at [SDS]$_o$/[SSI]$_o$ = 6 - 12 (M/M) (which corresponds to [SDS]$_o$ = 0.15 - 0.30% (w/v) in Fig. 4.4, and 0.005 - 0.010% (w/v) in Fig. 4.11) SSI exists as monomer and it has full inhibitory activity against subtilisin BPN'. From these considerations, it is concluded that SSI monomer has at least 50% inhibitory activity against subtilisin BPN' of that native dimeric SSI.

Effect of SDS on the conformation of SSI. An atypical trough around 300 nm observed for SSI at very low concentration of SDS (Fig. 4.5) is interpreted as a result of the change in electrostatic environ-

ment of tryptophyl residues by Ananthanarayanan and Bigelow (*46,47*). The extrema (troughs or peaks) around 300 nm were found in the difference spectra reported previously on bovine serum albumin at low concentration of SDS (0.006 - 0.025%, w/v) (*100,101*). To the author's knowledge at least, it is unknown that such absorption difference around 300 nm is observed in proteins other than SSI and bovine serum albumin in the presence of SDS. Elödi and Lakatos (*102*) showed that in the difference spectrum of *N*-acetyl-tryptophan-ethyl ester induced by the cationic detergent, cetyl pyridinium iodide, the anomalous positive absorption difference around 300 nm was observed, while in the difference spectrum induced by the anionic detergent, SDS, the negative trough around 300 nm was observed. From this result, they concluded that a blue-shift, i.e., a depression in the difference spectrum around 300 nm, is observed when the groups of polarizable molecule induce an electrostatically negative field relative to the indole nitrogen, and a red-shift, i.e., an asymmetry or tailing on the longer wavelength side of the major peak appeared in the opposite case. On the other hand, in the case that the indole chromophore contains ionizable groups in the neighborhood, such as tryptophan solution of about pH 1, it exhibits negative absorption difference around 300 nm as measured against a neutral reference. Furthermore, the absorption of tryptophan-ethyl ester appeared to be insensitive to acidic pH, whereas that of *N*-acetyl-tryptophan was not changed by increasing the pH above neutrality (*46,47,98*). In this connection, the trough around 300 nm shown in Fig. 4.5 is considered to be due to the direct interaction of SDS with a tryptophyl residue of SSI. The negative absorption difference at 293 nm which is typically known as denaturation blue-shift is observed at the SDS concentration above about

0.005% (w/v); this means that the conformation of SSI around the tryptophyl residue changes at the concentration of SDS above 0.005% (w/v). And this behavior is corresponding to the dissociation of SSI into monomers.

Effect of SDS on the inhibitory activity of SSI. (a) Effect on enzyme. When subtilisin BPN' was added to the mixture of SDS and substrate, pNPA (without preincubation of the enzyme with SDS), no or little loss of subtilisin BPN' activities was observed (Fig. 4.10). Thus, it seems that either the affinity of the substrate to the enzyme is higher than that of SDS, or the substrate has protective action, or both. The enzyme activity is slightly enhanced (about 10%) with very low SDS concentrations (0 - 0.04%, w/v). The enzyme activity enhancement in SDS was reported by Nakagawa and Jirgensons (*99*), that is, the peptidase activity of bovine carboxypeptidase B was lost at a faster rate, but the esterase activity was enhanced with increasing incubation time, although the esterase activity was decreased in the initial period. As in the present study, the dependence of the enzyme activity on the incubation time has not been examined, it is difficult to compare the data shown in Fig. 4.10 with that reported by Nakagawa and Jirgensons (*99*), but it seems that the increase of the enzyme activity in the presence of SDS at low concentration is significant. The resistance of subtilisin BPN' against denaturants is also demonstrated by Ikai (*103*), in spite that it lacks disulfide bridges.

(b) Effect on SSI. In the case of the dependence of the inhibitory activity of SSI against subtilisin BPN' on SDS concentration, the inhibitory activity is also enhanced slightly in the SDS concentration range of 0 - 0.010% (w/v), but above 0.010% (w/v) SDS, it decreases

steeply to 50% of the relative inhibitory activity, and holds constant level up to 0.25% (w/v) SDS. This means that SSI loses half of the inhibitory activity as the consequence of SDS binding, the dissociation of SSI into monomers, and the conformational change of SSI including denaturation, but the remaining half is maintained in the presence of SDS at rather high concentration.

As shown in Fig. 4.12, the ratio of [SSI monomer]$_o$/[subtilisin BPN']$_o$ (M/M) for the complete inhibition of the enzyme increases as increasing the SDS concentration in the reaction medium. In order to account for this effect of SDS, there are possible two reasons; namely, the increase of the inhibition or binding stoichiometry of SSI against subtilisin BPN', and the decrease of the inhibitor constant, K_i, of SSI against subtilisin BPN' or the dissociation constant, K_d, of the SSI-subtilisin BPN' complex. As a reactive site of SSI against the enzyme and an active site of the enzyme for substrate binding have been characterized definitely, the increase of K_i or K_d value in the interaction between subtilisin BPN' and SSI is most plausible as the effect of SDS on the system. The K_i value of SSI against subtilisin BPN' in the presence of 0.10% (w/v) SDS was roughly estimated to be 1×10^{-6} M from Fig. 4.12, and this value is 10^3 or more times larger than that obtained without SDS ($K_i < 10^{-9}$ M) (see Chapter Two).

4.5 Summary

Streptomyces subtilisin inhibitor, SSI, exists as a dimer of molecular weight of 23,000 in 25 mM phosphate buffer, at pH 7.0, ionic strength 0.1 M (NaCl), 25.0°C in the concentration range of 0.01 - 10

mg/ml (Chapter Three). In the present Chapter has been examined the effects of an anionic detergent, sodium dodecyl sulfate (SDS), on the structure and function of SSI.

The molecular weight of SSI was measured in the SDS solution with the sedimentation equilibrium method of the multicomponent-polydisperse system, and thereby it has been shown that SSI dissociates into monomers with SDS of 0.03% - 0.12% (w/v) when the concentration of SSI is 1.00 mg/ml (87.0 μM as monomer). As SSI dissociates into monomers, there observed a blue-shift due to a tryptophyl residue in the absorption difference spectrum induced by the binding of SSI and SDS.

Secondly, the inhibitory activity of SSI against subtilisin BPN'-catalyzed hydrolysis of *p*-nitrophenyl acetate, was measured under the conditions that SSI is in monomer in the SDS solution. It is concluded that monomeric SSI has at least 50% in the initial velocity for the hydrolysis of *p*-nitrophenyl acetate of the maximum value obtained without SDS.

Chapter Five

The Interaction of *Streptomyces* Subtilisin Inhibitor with α-Chymotrypsin *

5.1 Introduction

Streptomyces subtilisin inhibitor, SSI, has been believed unique in that it inhibits only microbial alkaline proteinases (*21-23*). The active site structure of subtilisin BPN', which is one of the alkaline serine proteinases of microbial origin, has been found by X-ray crystallography to resemble that of α-chymotrypsin, a neutral serine proteinase of mammalian digestive juice (*32*) (Table 1.1).

In this respect, the finding that SSI does not inhibit α-chymotrypsin whereas it strongly inhibits subtilisin BPN' with casein as substrate suggests that this inhibitor can discriminate the difference in the active site structure between α-chymotrypsin and subtilisin BPN'. The mechanism of this apparently very rigorous discrimination seems to deserve detailed investigation. In the present Chapter will be reported the study on the interaction between α-chymotrypsin and SSI through (1) inhibition of the hydrolysis of *p*-nitrophenyl acetate, pNPA, (2) ultraviolet absorption difference spectrum observed on the binding of both proteins, and (3) visible absorption difference spectrum due to the interaction of SSI with proflavine-α-chymotrypsin complex (*104*). The

---

* A part of this study was presented at the Annual Meeting of the Biophysical Society of Japan (Sapporo, October 1974), and published in *Agric. Biol. Chem.* (1975) 39, 1159-1161 (*d,e*).

interaction of SSI and trypsin will be also described.

5.2 Experimental Procedures

Proteins. A three times crystallized and lyophilized preparation of *Streptomyces* subtilisin inhibitor, SSI, was a generous gift of Professor S. Murao. A three times crystallized and lyophilized preparation of bovine α-chymotrypsin [EC 3.4.21.1] (Lot No. CDl 34D698), a two times crystallized and lyophilized preparation of bovine trypsin [EC 3.4.21.4] (Lot No. TRL 34C952) and a three times crystallized and lyophilized preparation of chymotrypsinogen A (Lot No. CGlBA) were purchased from Worthington Biochemical Corporation, Freehold, New Jersey.

Protein concentrations were determined spectrophotometrically by using the following absorptivities at pH 7.0; $E_{1\ cm}^{0.1\%}$(276 nm) = 0.829 for SSI (Experimental Procedures 2.2), $E_{1\ cm}^{0.1\%}$(282 nm) = 2.05 for α-chymotrypsin and chymotrypsinogen A (*105*), and $E_{1\ cm}^{0.1\%}$(280 nm) = 1.50 for trypsin (*106*). The molecular weight of SSI (monomer), α-chymotrypsin, chymotrypsinogen A, and trypsin were assumed to be 11,500 (*27*, Chapters Three and Four), 25,000 (*105*), 25,000 (*105*), and 24,000 (*106*), respectively.

The purities of α-chymotrypsin and trypsin preparations were determined to be 89.5% and 87.3%, respectively, according to the method described previously (*35*, Experimental Procedures 2.2) using *p*-nitrophenyl acetate and *N-trans*-cinnamoyl imidazole as titrants.

All of the experiments were carried out in 25 mM phosphate buffer, pH 7.0, ionic strength 0.1 M (NaCl), at 25.0°C.

Chemicals. *p*-Nitrophenyl acetate, pNPA (Lot No. FCFOl) was pur-

chased from Tokyo Kasei Kogyo Co. Ltd., Tokyo; proflavine hemisulfate (Lot No. M2K7686) of guaranteed reagent grade was from Nakarai Chemicals Ltd., Kyoto, and recrystallized from water before use. The concentrations of pNPA and proflavine were determined spectrophotometrically at pH 7.0 by using the molar absorptivity: $\varepsilon_{405} = 7.73 \times 10^3\ M^{-1}cm^{-1}$ ($pK_a = 7.14$) after complete hydrolysis, and $\varepsilon_{444} = 3.89 \times 10^4\ M^{-1}cm^{-1}$, respectively.

Inhibitory activity measurement. The inhibitory activity of SSI against α-chymotrypsin and trypsin was measured spectrophotometrically by using pNPA as substrate (see Discussion 5.4). The reaction was initiated by mixing equal volumes of enzyme solution and mixture solution of SSI and pNPA in 25 mM phosphate buffer, pH 7.0, ionic strength 0.1 M (NaCl), 25.0°C. The mixture solution of SSI and pNPA had been prepared by mixing equal volumes of aqueous solution of pNPA containing 10.0% (v/v) isopropanol and SSI solution in 50 mM phosphate buffer, pH 7.0, and immediately used for inhibitory activity assay. Increase in absorption at 405 nm due to the liberation of *p*-nitrophenol was monitored on a Shimadzu UV-200 recording spectrophotometer. The molar absorptivity at 405 nm of *p*-nitrophenol at pH 7.00 was taken to be $7.73 \times 10^3\ M^{-1}cm^{-1}$ which was determined by the author. The inhibitor constant, K_i, was determined by plotting the experimental data according to Lineweaver and Burk (*107*), and Dixon (*108*).

Ultraviolet absorption difference spectroscopy. Ultraviolet absorption difference spectra observed on the binding of SSI and α-chymotrypsin were recorded on a Hitachi Model 323-2000 recording spectrophotometer with an expanded scale (0.04 absorbance/full scale) using two pairs of matched cuvettes of 1.0-cm light path length at 25.0°C. To an

α-chymotrypsin solution of 32.4 μM (taking into account the purity of the preparation) in 25 mM phosphate buffer, pH 7.0, ionic strength 0.1 M (NaCl) was added at 25.0°C the equal volume of SSI solution in the same buffer at various concentrations up to 0.152 mM (as monomer). The ultraviolet absorption difference spectra were recorded after keeping the mixture at 25.0°C for 10 min.

Visible absorption difference spectrum of proflavine. Visible absorption difference spectra due to a change in the environment of proflavine (*104*) were observed on (1) adding SSI to α-chymotrypsin-proflavine mixture or (2) adding proflavine to α-chymotrypsin-SSI mixture. The difference spectra were measured with a Shimadzu UV-200 recording spectrophotometer with an expanded scale (0.2 absorbance/full scale) using a pair of tandem cuvettes of 1.0-cm light path length at 25.0°C. In the case of (1), equal volumes of an α-chymotrypsin-proflavine mixture solution ($[\alpha\text{-chymotrypsin}]_o$ = 38.6 μM, $[\text{proflavine}]_o$ = 71.4 μM) in 25 mM phosphate buffer, pH 7.0, ionic strength 0.1 M (NaCl) and a SSI solution in the same buffer of various concentrations up to 0.48 mM (as monomer) were mixed in the optical cuvette. In the case of (2), equal volumes of an α-chymotrypsin-SSI mixture solution ($[\alpha\text{-chymotrypsin}]_o$ = 31.8 μM, $[\text{SSI monomer}]_o$ = 87.2 μM) in 25 mM phosphate buffer, pH 7.0, ionic strength 0.1 M (NaCl) and a proflavine solution in the same buffer of the various concentrations up to 0.14 mM were mixed in the optical cuvette. It was estimated from the dissociation constant of α-chymotrypsin-SSI complex (K_d = 3.0 x 10^{-6} M) (see Results 5.3) that 93% of the enzyme used was bound to SSI in the final conditions.

Equilibrium dialysis experiment on the binding of proflavine with α-chymotrypsin or α-chymotrypsin-SSI complex. The binding of proflavine

to α-chymotrypsin or α-chymotrypsin-SSI complex was measured by equilibrium dialysis technique described in Experimental Procedures 4.2. Five dialysis units were placed in a reciplocating shaker (130 reciplocation per min.) at 25°C for 45 hr. In the inner solution the concentrations of α-chymotrypsin were between 0.108 mM and 54.3 μM in 25 mM phosphate buffer, pH 7.0, ionic strength 0.1 M (NaCl), and the concentration of SSI in the same buffer was so selected that SSI could bind more than 98% (in molarity) of α-chymotrypsin used assuming the dissociation constant of α-chymotrypsin-SSI complex to be 3.0×10^{-6} M (see Results 5.3); namely, SSI concentration was between 0.395 mM and 0.200 mM. The initial concentration of proflavine in the inner and the outer solutions were varied in a range below 0.5 mM. The proflavine concentration was determined spectrophotometrically by using the molar extinction coefficient at the wavelength (405 nm) of isosbestic point of proflavine, α-chymotrypsin-proflavine complex, and α-chymotrypsin-SSI-proflavine complex, $\varepsilon_{450} = 3.71 \times 10^{4}$ $M^{-1}cm^{-1}$.

5.3 Results

Inhibition. In the previous study of inhibition by SSI, casein was used as substrate (*23*). Since casein is a specific substrate with strong affinity for serine proteinases, weak inhibition of SSI against some proteinases may have been overlooked. The relative value of the inhibitor constant, K_i, to the Michaelis constant, K_m, is important in order to detect the competitive inhibition. By using pNPA as substrate ($K_m = 1.34 \times 10^{-5}$ M) it was found that SSI competitively inhibits α-chymotrypsin as shown in Fig. 5.1. The inhibitor constant, K_i, of SSI

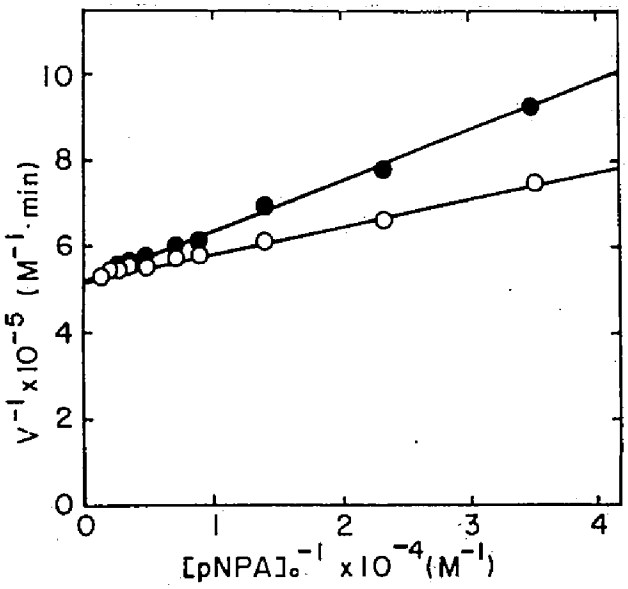

Fig. 5.1. Inhibition of SSI toward the hydrolysis of *p*-nitrophenyl acetate, pNPA, catalyzed by α-chymotrypsin. The Lineweaver-Burk plot (*107*). $[\alpha\text{-chymotrypsin}]_o$ = 3.58 μM; $[SSI\ monomer]_o$ = 0 μM, open circle; 10.9 μM, closed circle, in 25 mM phosphate buffer, pH 7.0, ionic strength 0.1 M (NaCl) containing 5.0% (v/v) isopropanol, 25.0°C. The initial velocity of the reaction, v, was measured by following the increase in absorption at 405 nm. The type of inhibition was determined to be competitive, and the inhibitor constant, K_i, of SSI against α-chymotrypsin, to be 3.8×10^{-6} M.

---

to α-chymotrypsin was determined to be 3.8×10^{-6} M. It was found by using pNPA as substrate ($K_m = 7.7 \times 10^{-5}$ M) that SSI also inhibits trypsin competitively (the Lineweaver-Burk plot not shown) with the inhibitor constant of 1.1×10^{-4} M, which was determined from the Dixon plot shown in Fig. 5.2.

Ultraviolet difference spectrum. Difference spectrum (red shift) attributable mainly to tryptophyl residues was observed on mixing the solutions of SSI and of α-chymotrypsin (Fig. 5.3).

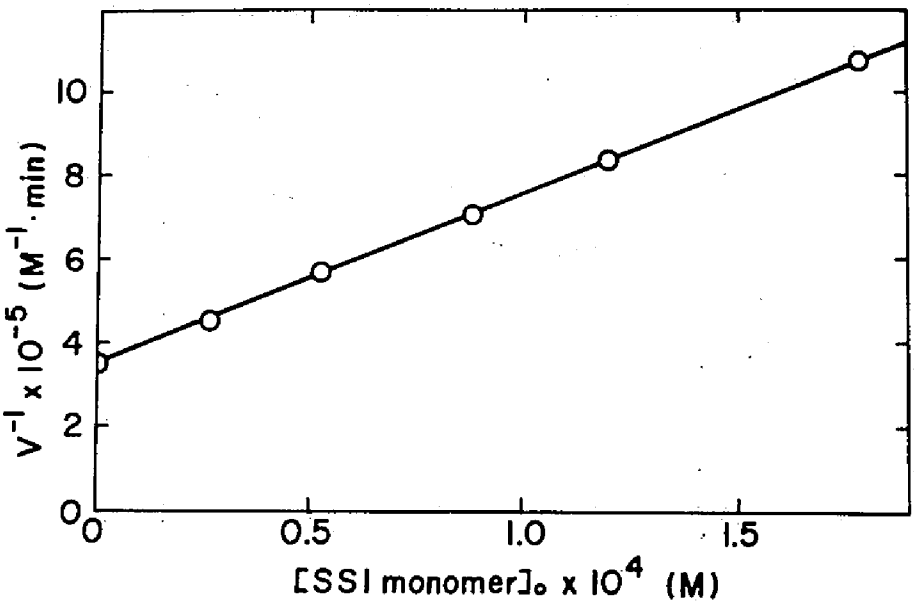

Fig. 5.2. Inhibition of SSI toward the hydrolysis of *p*-nitrophenyl acetate, pNPA, catalyzed by trypsin. The Dixon plot (*108*). $[trypsin]_o$ = 9.19 μM; $[pNPA]_o$ = 81.8 μM, in 25 mM phosphate buffer, pH 7.0, ionic strength 0.1 M (NaCl) containing 5.0% (v/v) isopropanol, 25.0°C. The initial velocity of the reaction, v, was measured by following the increase in absorption at 405 nm. The type of inhibition was determined from the Lineweaver-Burk plot (Figure not shown) to be competitive, and the inhibitor constant of SSI against trypsin, to be 1.1×10^{-4} M.

The plot of absorptivity difference, $\Delta A_{292.5} - \Delta A_{289.5}$ or $\Delta A_{287.0} - \Delta A_{289.5}$, against the concentration of SSI monomer with a constant concentration of α-chymotrypsin (16.2 μM) gave a saturation curve as shown in Fig. 5.4, from which the dissociation constant for the enzyme-inhibitor complex, K_d, was determined to be 2.2×10^{-6} M.

Proflavine difference spectrum. Proflavine is known to bind stoichiometrically at the active site of α-chymotrypsin or trypsin and to produce difference absorption spectrum in the region of 400 - 500 nm (*104*). This spectral change has been used as a probe to detect the

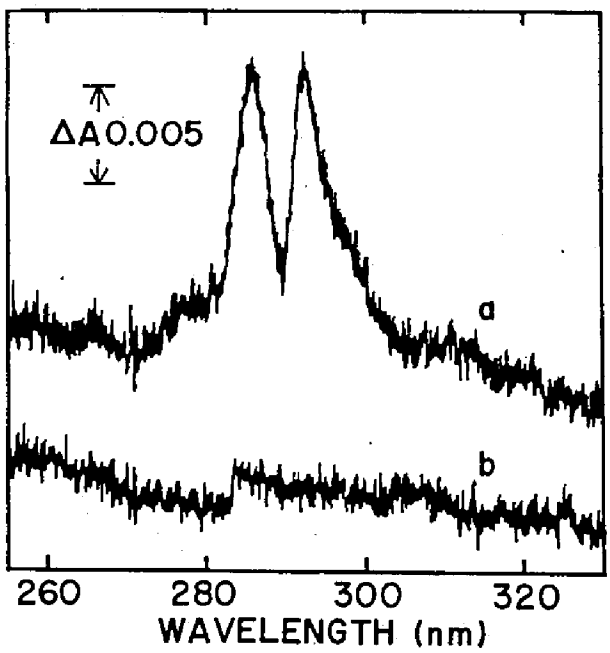

Fig. 5.3. Ultraviolet absorption difference spectra observed on the binding of SSI and α-chymotrypsin. $[\alpha\text{-chymotrypsin}]_o$ = 16.2 μM; $[SSI\ monomer]_o$ = (A) 26.8 μM; (B) 0 μM (base line), in 25 mM phosphate buffer, pH 7.0, ionic strength 0.1 M (NaCl), 25.0°C.

---

binding of substrates and analogues to the enzyme which displaces proflavine (*109*). Figure 5.5 shows the essentially the same shape of the difference spectra as those produced upon substrate binding was observed when SSI was added to the α-chymotrypsin-proflavine system. From the change in absorptivity difference at 465.0 nm with increasing SSI concentration, the dissociation constant of the α-chymotrypsin-SSI complex, K_d, was determined to be 2.9×10^{-6} M, and the maximum change in absorptivity difference, $\Delta A_{465.0} - \Delta A_{425.0}$, was determined to be 0.155 ± 0.03 (Fig. 5.6). The absorptivity difference ($\Delta A_{465.0} - \Delta A_{425.0}$) which was obtained on binding of proflavine and α-chymotrypsin under the same conditions is 0.240 ± 0.05. Thus it is suggested that proflavine bound to

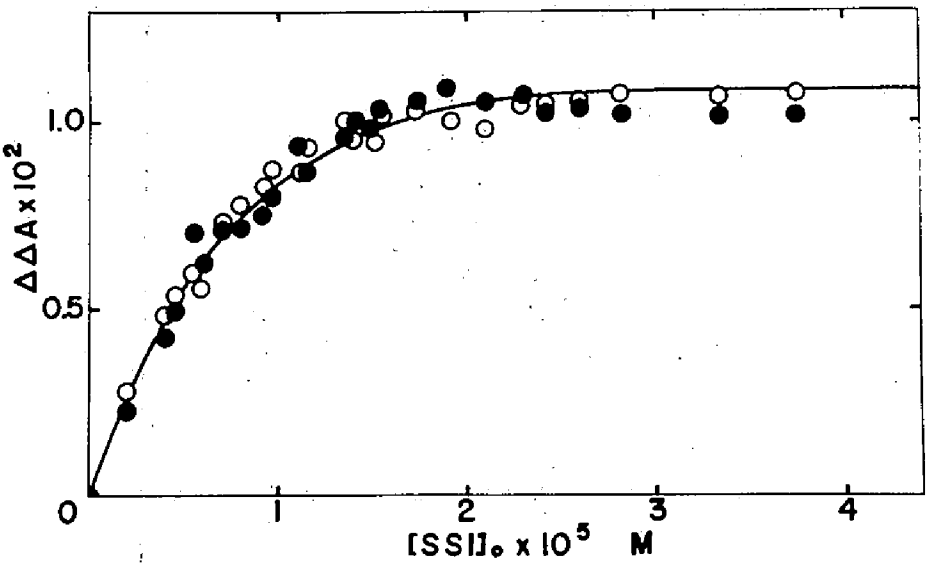

Fig. 5.4. Dependence of the absorptivity difference observed on the binding of SSI and α-chymotrypsin on the concentration of SSI monomer. $[\alpha\text{-chymotrypsin}]_0$ = 16.2 μM; $[\text{SSI monomer}]_0$ = 0 - 38.0 μM, in 25 mM phosphate buffer, pH 7.0, ionic strength 0.1 M (NaCl), 25.0°C. ΔΔA: $\Delta A_{287.0} - \Delta A_{289.5}$, open circle; $\Delta A_{292.5} - \Delta A_{289.5}$, closed circle. Solid line, the theoretical curve obtained with K_d of 2.2×10^{-6} M.

α-chymotrypsin could not completely be displaced even with large excess of SSI. Apparently 60% at most of the proflavine bound to the enzyme is displaced by SSI.

The same type of difference spectra which were produced on the binding of proflavine and α-chymotrypsin was observed upon adding proflavine solution to α-chymotrypsin-SSI mixture solution. The titrations of the absorptivity differences at 465.0 nm with proflavine at fixed concentrations of the enzyme and SSI are shown in Fig. 5.7. By applying the method of non-linear least squares to the data in Fig. 5.7, the dissociation constant of α-chymotrypsin-proflavine complex and the maximum change in absorptivity difference ($\Delta A_{465.0} - \Delta A_{425.0}$) for the α-chymo-

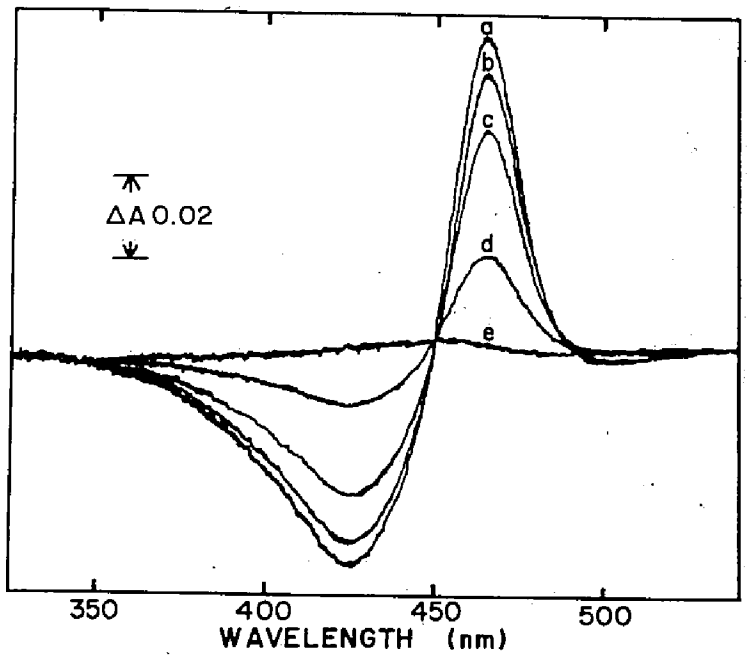

Fig. 5.5. Visible absorption difference spectra observed on adding SSI to the proflavine-α-chymotrypsin complex. $[\alpha\text{-chymotrypsin}]_o$ = 19.3 μM; $[\text{proflavine}]_o$ = 35.7 μM; $[\text{SSI monomer}]_o$ = (a) 91.2 μM, (b) 74.6 μM, (c) 49.6 μM, (d) 16.6 μM, (e) 0 μM (base line), in 25 mM phosphate buffer, pH 7.0, ionic strength 0.1 M (NaCl), 25.0°C.

---

trypsin-proflavine system were determined to be $(5.1 \pm 0.1) \times 10^{-5}$ M and 0.52 ± 0.12 (Abs./cm) ($[\alpha\text{-chymotrypsin}]_o$ = 15.9 μM), respectively. For the proflavine-(α-chymotrypsin-SSI) system in which 93% (in molarity) of the enzyme used is saturated by SSI, by assuming the dissociation constant of α-chymotrypsin-SSI complex to be 3×10^{-6} M, the dissociation constant of proflavine-α-chymotrypsin-SSI complex into proflavine and α-chymotrypsin-SSI complex was evaluated to be $(13.2 \pm 0.8) \times 10^{-5}$ M, and the maximum change in absorptivity difference $(\Delta A_{465.0} - \Delta A_{425.0})$, to be 0.36 ± 0.08 (Abs./cm) ($[\alpha\text{-chymotrypsin-SSI complex}]_o$ = 14.8 μM). It is supposed that proflavine bind α-chymotrypsin-SSI complex to form

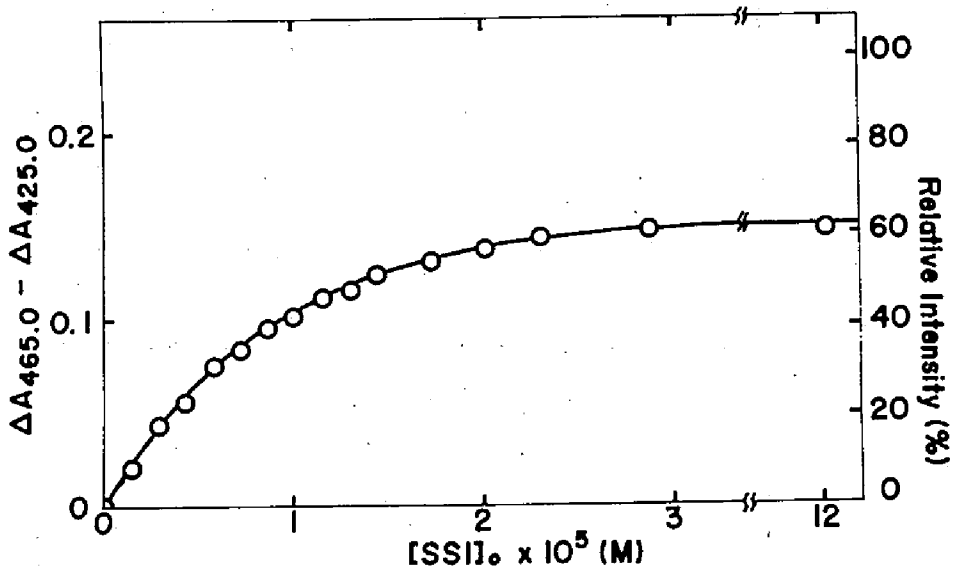

Fig. 5.6. The relationship between the absorptivity difference observed on adding SSI to the proflavine-α-chymotrypsin complex and the concentration of SSI monomer. The difference between $\Delta A_{465.0}$ and $\Delta A_{425.0}$ was plotted against the concentration of SSI monomer. $[\alpha\text{-chymotrypsin}]_o$ = 19.3 μM; $[\text{proflavine}]_o$ = 35.7 μM; $[\text{SSI monomer}]_o$ = 0 - 0.12 mM, in 25 mM phosphate buffer, pH 7.0, ionic strength 0.1 M (NaCl), 25.0°C. Solid line, the theoretical curve obtained with K_d of 2.9×10^{-6} M.

---

a ternary complex with affinity weaker than that for α-chymotrypsin.

Figure 5.8 shows the Scatchard plots of proflavine binding against α-chymotrypsin and α-chymotrypsin-SSI complex obtained by equilibrium dialysis. In the latter system, 98% (in molarity) of the enzyme was bound by SSI. The data were treated by the method of linear least squares to evaluate the dissociation constants, K_d, and binding number, n, of proflavine against α-chymotrypsin and α-chymotrypsin-SSI complex. Proflavine binds to α-chymotrypsin with $K_d = (6.4 \pm 0.5) \times 10^{-5}$ M and $n = 1.01 \pm 0.12$, and to α-chymotrypsin-SSI complex with $K_d = (16.0 \pm 0.8) \times 10^{-5}$ M and $n = 1.05 \pm 0.23$. From these results, it was revealed that

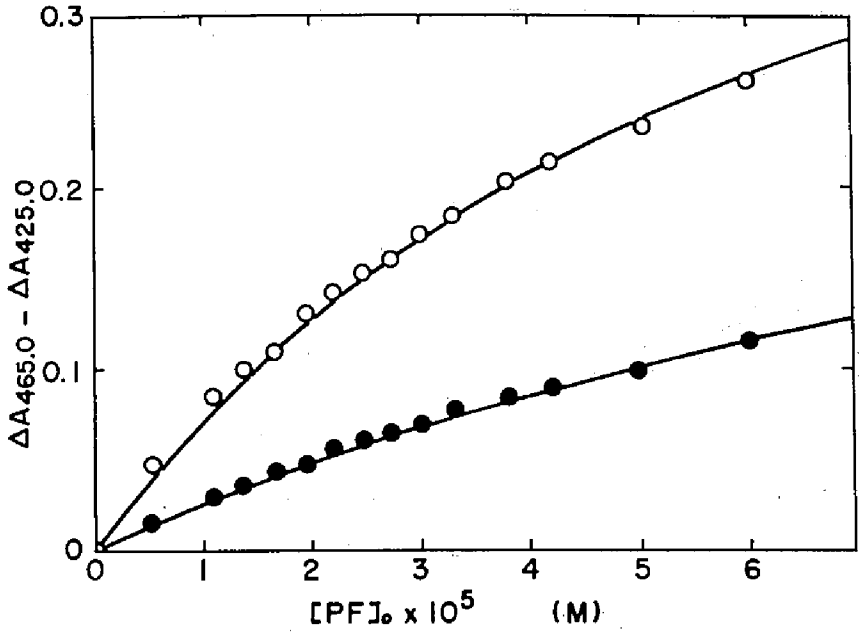

Fig. 5.7. The relationship between the absorptivity difference observed on the binding of proflavine and α-chymotrypsin or α-chymotrypsin-SSI complex and the concentration of proflavine. $[\alpha\text{-chymotrypsin}]_o$ = 15.9 μM; $[\text{SSI monomer}]_o$ = 21.8 μM; $[\text{proflavine}]_o$ = 0 - 60.0 μM, in 25 mM phosphate buffer, pH 7.0, ionic strength 0.1 M (NaCl), 25.0°C. The difference between $\Delta A_{465.0}$ and $\Delta A_{425.0}$ was plotted against the concentration of proflavine. α-Chymotrypsin-proflavine system: open circle, the solid line is the theoretical curve with K_d of 5.1 x 10^{-5} M and $(\Delta A_{465.0} - \Delta A_{425.0})_{max}$ of 0.52. (α-Chymotrypsin-SSI)-proflavine system: closed circle, the solid line is the theoretical curve with K_d of 13.2 x 10^{-5} M and $(\Delta A_{465.0} - \Delta A_{425.0})_{max}$ of 0.36.

---

proflavine can bind to α-chymotrypsin-SSI complex stoichiometrically, forming a ternary complex, with affinity less than that for α-chymotrypsin. The K_d values obtained from spectrophotometric titration of proflavine (Fig. 5.7) and equilibrium dialysis (Fig. 5.8) for both proflavine-α-chymotrypsin and proflavine-(α-chymotrypsin-SSI) systems are in good agreement with each other.

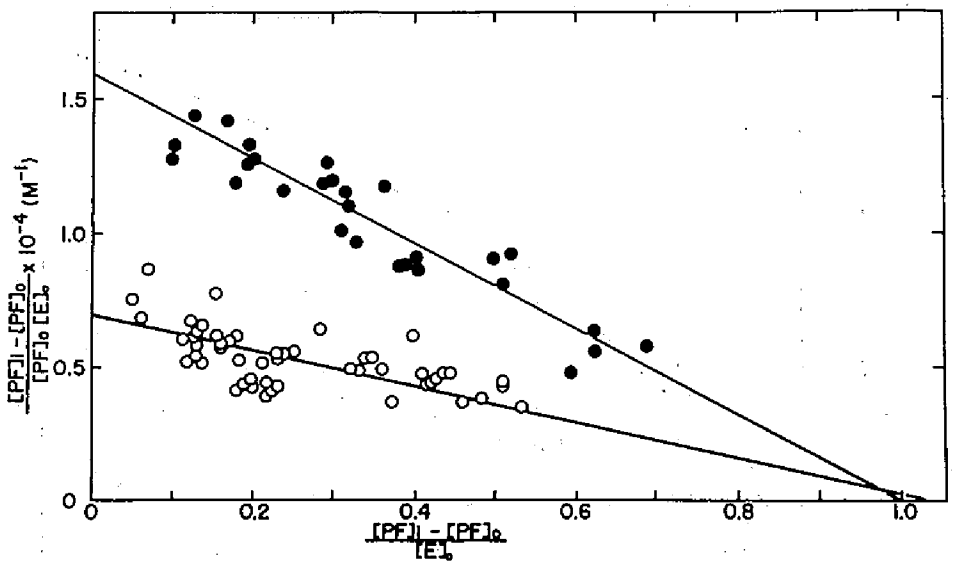

Fig. 5.8. The Scatchard plots of the binding of proflavine with α-chymotrypsin and α-chymotrypsin-SSI complex. The binding was measured by equilibrium dialysis in 25 mM phosphate buffer, pH 7.0, ionic strength 0.1 M (NaCl), 25°C. α-Chymotrypsin-proflavine system: closed circle, the solid line was drawn theoretically with K_d of 6.4 x 10^{-5} M and the number of proflavine bound to the enzyme, n, of 1.01. (α-Chymotrypsin-SSI)-proflavine system: open circle, the solid line was drawn theoretically with K_d of 16.0 x 10^{-5} M and n of 1.03.

5.4 Discussion

Inhibition and binding. In the previous study on inhibition by SSI using casein as substrate was reported that SSI inhibited neither α-chymotrypsin nor trypsin (Table 1.1) (*23*). In the present study, however, by using pNPA as substrate (K_m = 1.34 x 10^{-5} M), the inhibition of SSI against α-chymotrypsin could be detected obviously (K_i = 3.8 x 10^{-6} M). The interaction between SSI and α-chymotrypsin was detected by ultraviolet difference spectroscopy and proflavine difference spectro-

scopy by using proflavine as a probe; the dissociation constant of the α-chymotrypsin-SSI complex, K_d, was determined from these measurements to be 2.2×10^{-6} M and 2.9×10^{-6} M, respectively. From these results, it is unequivocally concluded that SSI can specifically bind and competitively inhibit α-chymotrypsin. The inhibitor constant, K_i, and the dissociation constant, K_d, obtained in the three independent methods are in reasonable agreement with each other giving the average value of $(3.0 \pm 0.7) \times 10^{-6}$ M. This value is larger by about four orders of magnitude than the inhibitor constant estimated for subtilisin BPN' (3×10^{-10} - 7×10^{-11} M: B. Tonomura, T. Azuma, and K. Hiromi; Y. Uehara, B. Tonomura, and K. Hiromi, unpublished results). Recent finding that α-chymotrypsin is bound to SSI immobilized on a Sepharose column (*110*) is consistent with the present conclusion.

Proflavine binding. A dye proflavine has been believed to bind stoichiometrically at the active site "tosyl anion hall" of α-chymotripsin or of trypsin, and to produce visible absorption difference spectrum (*104,109*). This spectral change has been used as a probe to detect the binding of the enzyme with substrates and analogues which displace proflavine (*104,109,111-114*). The same type of difference spectrum was observed on the binding of SSI with proflavine-α-chymotrypsin complex. However, it was shown by the spectrophotometric titration of the binding of proflavine to the α-chymotrypsin-SSI complex and of SSI to the proflavine-α-chymotrypsin complex, and by equilibrium dialysis, that SSI does not displace the dye in the active site of the enzyme but forms an α-chymotrypsin-proflavine-SSI ternary complex. To the author's knowledge at least, this is the only case in which a substrate analogue interacts with the active site of α-chymotrypsin without displacing pro-

flavine from it. Proflavine binds α-chymotrypsin with the dissociation constant, K_d, of (5.8 ± 0.7) x 10^{-5} M and the maximum molar absorptivity difference, $(\Delta\varepsilon_{465.0} - \Delta\varepsilon_{425.0})_{max}$, of (3.3 ± 0.8) x 10^4 $M^{-1}cm^{-1}$, and binds α-chymotrypsin-SSI complex with K_d of (14.6 ± 1.4) x 10^{-5} M and $(\Delta\varepsilon_{465.0} - \Delta\varepsilon_{425.0})_{max}$ of (2.4 ± 0.5) x 10^4 $M^{-1}cm^{-1}$. These differences may demonstrate that some change is induced in the environment of proflavine in the binding site of α-chymotrypsin when the enzyme binds SSI. It is rather astonishing that there is a space to accomodate proflavine in the α-chymotrypsin-SSI complex. This loose binding at the interacting areas of the proteins must have resulted in the weaker inhibition such as shown in the present study (K_i = 3.0 x 10^{-6} M).

The X-ray crystallographic study (*32*) has shown that the active site structure of subtilisin BPN' resembles that of α-chymotrypsin, in spite of the difference of their origins. In the present study it was suggested that SSI could discriminate strictly the small difference in the active site structure between subtilisin BPN' and α-chymotrypsin.

Notes for Chapter Five

The binding rate of SSI and α-chymotrypsin was measured preliminarily by the use of the difference absorption produced on the binding of SSI and α-chymotrypsin-proflavine complex with a Union SF-70 stopped-flow spectrophotometer (Fig. 5.9). The progress curve was observed at 465.0 nm. The final concentrations were 17.6 μM α-chymotrypsin, 49.0 μM SSI monomer, and 45.5 μM proflavine, in 25 mM phosphate buffer, pH 7.0, ionic strength 0.1 M (NaCl), 25.0°C. Figure 5.10 shows the second-order plot of the progress curve shown in Fig. 5.9, and the bimolecular rate constant, k, was determined to be 2.3 x 10^6 $M^{-1}sec^{-1}$, which is consist-

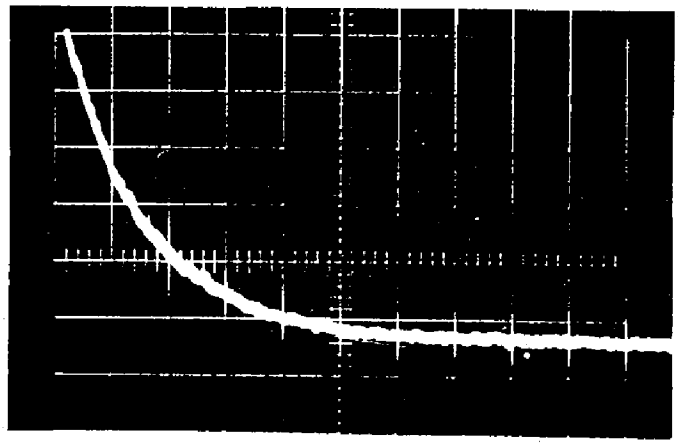

Fig. 5.9. Stopped-flow oscillogram for the binding of SSI and α-chymotrypsin-proflavine complex. $[\alpha\text{-chymotrypsin}]_o$ = 17.6 μM; $[\text{SSI monomer}]_o$ = 49.0 μM; $[\text{proflavine}]_o$ = 45.5 μM, in 25 mM phosphate buffer, pH 7.0, ionic strength 0.1 M (NaCl), 25.0°C. Scale: horizontal, 10 msec/div.; vertical, 0.01 Abs./div. Wavelength, 465.0 nm.

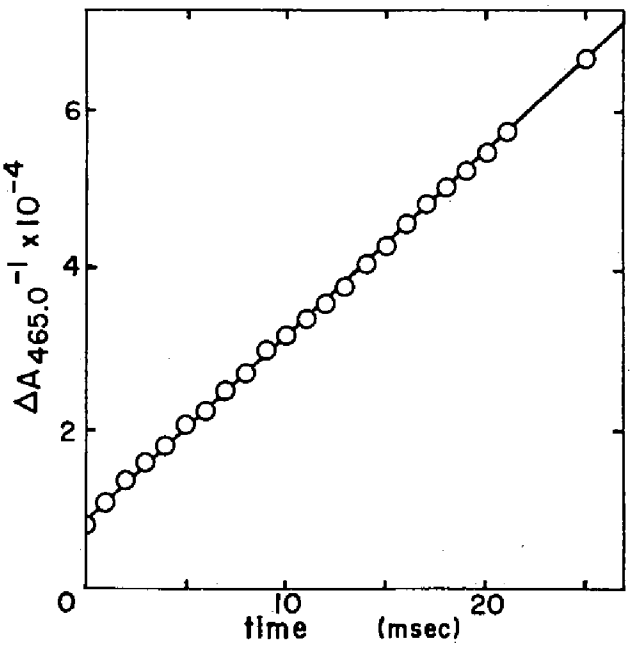

Fig. 5.10. The second-order plot of the binding curve shown in Fig. 5.9. Conditions are as in Fig. 5.9. The bimolecular rate constant, k, of the binding between SSI and α-chymotrypsin is calculated from the slope to be 2.3×10^6 $M^{-1}sec^{-1}$.

ent with the supposition that the rate of the binding of SSI and α-chymotrypsin is diffusion-controlled (see Discussion 7.4 in Chapter Seven).

5.5 Summary

In the present Chapter was described studies on the inhibition and the binding of *Streptomyces* subtilisin inhibitor, SSI, against α-chymotrypsin. Both α-chymotrypsin and trypsin have been reported not to be inhibited by SSI using a specific substrate, casein (Table 1.1) (*23*). However, in this study SSI was shown to inhibit α-chymotrypsin competitively with an inhibitor constant, K_i = 3.8 x 10^{-6} M by using *p*-nitrophenyl acetate as substrate. The dissociation constant, K_d, of α-chymotrypsin-SSI complex was determined from static titration to be 2.2 x 10^{-6} M by ultraviolet absorption difference spectra observed on the binding of the enzyme and the inhibitor, and to be 2.9 x 10^{-6} M by visible absorption difference spectra of proflavine bound to the active site of the enzyme. The K_i and K_d values are in reasonable agreement with each other giving the average value of (3.0 ± 0.7) x 10^{-6} M. This value is larger by almost four orders of magnitude than the inhibitor constant estimated for subtilisin BPN' (see Chapter Two).

It was demonstrated by spectrophotometric titration and equilibrium dialysis that proflavine bound at the active site of α-chymotrypsin is not displaced by SSI binding but forms a ternary complex with the enzyme.

SSI was also found to competitively inhibit trypsin with the inhibitor constant of 1.1 x 10^{-4} M.

Chapter Six

The States of Tyrosyl and Tryptophyl Residues of *Streptomyces* Subtilisin Inhibitor *

6.1 Introduction

Streptomyces subtilisin inhibitor, SSI, is a unique protein proteinase inhibitor in that it inhibits very strongly the alkaline serine proteinases of subtilisin family (*21,23*). It has been shown that the native SSI usually exists in a dimer form (see Chapter Three) and it binds and inhibits two molecules of subtilisin BPN' (see Chapter Two).

The complete primary structure of SSI has been determined (*27*); it contains a tryptophyl residue and three tyrosyl residues per monomer (113 amino acid residues, MW = 11,500) (Fig. 1.1).

An ultraviolet absorption difference spectrum produced on the interaction of SSI with subtilisin BPN' indicates changes in the environment of tyrosyl and tryptophyl residues (Fig. 2.6). Information on the states of these chromophoric amino acid residues would provide us with a clue for understanding the nature of specific interaction between the two proteins.

In the present Chapter, the investigation of the states of tyrosyl and tryptophyl residues of SSI and subtilisin BPN' by solvent perturba-

---

* A part of this study was presented at the Annual Meeting of the Agricultural Chemical Society of Japan (Tokyo, April 1974) and at the 25th Forum on Protein Structure (Osaka, October 1974), and published in *J. Biochem.* (1977) 82, 1207-1215 (*f*).

tion and spectrophotometric titration in the alkaline pH region are reported.

6.2 Experimental Procedures

Materials. A three times crystallized and lyophilized preparation of SSI was a generous gift from Professor S. Murao. A three times crystallized subtilisin BPN' preparation (Lot No. 206006) was purchased from Nagase & Co. Ltd., Osaka, and *N*-acetyl-L-tryptophan ethyl ester from Protein Research Foundation, Osaka. *N*-Acetyl-L-tyrosine ethyl ester (Lot No. VOP8931), ethylene glycol, and guanidinium hydrochloride of spectral grade, and other chemicals of analytical or better grade were obtained from Nakarai Chemicals Ltd., Kyoto. Deuterium oxide (99.83%) was the product of CEA-SACLAY DRA Bureau des Isotopes Stables, France. Unless otherwise noted, the buffer solution used for all experiments was 25 mM phosphate buffer, pH 7.00±0.01 (ionic strength was adjusted to 0.1 M with NaCl).

Concentrations of proteins and model compounds were all estimated spectrophotometrically with a Shimadzu UV-200 recording spectrophotometer. The absorptivities of the proteins calculated from the amino acid compositions (*25,27*) are as follows (Chapter Two): $E_{1\ cm}^{0.1\%}$(276 nm) = 0.829 for SSI, and $E_{1\ cm}^{0.1\%}$(278 nm) = 1.063 for subtilisin BPN'. Concentrations of the model compounds were determined using the following molar absorptivities (*42,115*): 1,340 $M^{-1}cm^{-1}$ for *N*-acetyl-L-tyrosine ethyl ester at 275.5 nm and 5,550 $M^{-1}cm^{-1}$ for *N*-acetyl-L-tryptophan ethyl ester at 280 nm. The purity of the subtilisin BPN' preparation used was determined to be 75.4% according to the method described in Chapter Two (Experimen-

tal Procedures 2.2).

Ultraviolet difference spectra. The procedures followed essentially the methods described by Herskovits and Laskowski, Jr. (*116*). All measurements were made with a Shimadzu UV-200 recording spectrophotometer with an expanded scale (0.1 absorbance/full scale). Two pairs of matched cuvettes with 1.0 cm optical path length were used, each pair in series in the sample and reference compartments thermostated at 25.0 °C. Concentrations of the proteins and the model compounds were always chosen not to exceed 1.5 in absorbance unit in the spectrophotometric measurements (*117*).

Solvent perturbation. Difference absorption spectra caused by solvent perturbation (*118*) were measured at 25.0°C as described above after keeping a mixture of the sample and a perturbant for 30 min at 25.0°C. Methanol, ethylene glycol, polyethylene glycol (#300) and deuterium oxide(D_2O) were used as perturbant, and their mean molecular diameters were assumed to be 2.8 A, 4.4 A, 9.2 A, and 2.0 A, respectively (*119*). The final concentrations of the perturbants were in the range of 0 - 50% (v/v) except for D_2O, which was used only at 90% (v/v). Caution was taken so as to avoid temperature difference between the sample and the reference cells, which may affect the difference spectra.

Spectrophotometric titration of tyrosyl residues. The phenolic hydroxyl groups of tyrosyl residues of SSI were titrated by directly measuring the difference in absorbance at 295 nm and 245 nm between a given alkaline and the neutral solution at pH 7.0. A 33mM phosphate-NaOH buffer was used for pH 9.0 - 11.4, a 67 mM carbonate-bicarbonate buffer for pH 11.0 - 12.0, and a mixture of 1.0 N NaOH and 1.0 M NaCl in various ratios for pH 11.5 - 13.0. NaCl was added to maintain the ionic

strength of the buffer solutions constant at 0.2 M. Time dependence of the absorbance difference was examined at 245 nm and 295 nm. To 1.5 ml of the unbuffered aqueous solution of protein in an optical cuvette, 1.5 ml of alkaline or buffer solution of various pH's was added, and the change in absorbance was followed usually for 25 min. The mixture solutions after the pH-jump were kept at 25.0°C also for about 24 hr, and the difference spectra were taken again. All the pH values were checked after the mixing using a Hitachi-Horiba F-5 pH meter. The final SSI concentration used for the titration was in the range between 5.03 μM and 12.2 μM.

For the titration in the presence of guanidinium hydrochloride, 2.7 ml of SSI solution with 4.55 M guanidinium hydrochloride at pH 7.00 which had been kept at 25.0°C for 24 hr was mixed with 0.3 ml of a mixture of 4.0 N NaOH and 4.0 M NaCl in various ratios, giving desired pH values. The tyrosyl residues were titrated in the same way as in the absence of guanidinium hydrochloride. The final protein concentration was 27.8 μM. The difference in molar absorptivity at 295 nm between an alkaline and the neutral solution is considered identical regardless the presence of 4 M guanidinium hydrochloride (*120*).

Analysis of titration data. The titration data in a given pH range were analyzed as suggested previously (*121,122*) by a linear plotting in terms of the molar absorptivity difference at a given pH, $\Delta\varepsilon$, according to the following equation, where $\Delta\varepsilon_{max}$ is the difference in molar absorptivity after complete ionization of all relevant tyrosines, and K_a is the apparent ionization constant.

$$[H^+]\cdot\Delta\varepsilon = \Delta\varepsilon_{max}\cdot K_a - \Delta\varepsilon\cdot K_a \qquad (6.1)$$

The method of least squares was used to obtain the $\Delta\varepsilon_{max}$ value and the

apparent pK_a. The molar absorptivity differences used for the ionization of a tyrosyl phenolic group were: $\Delta\varepsilon_{295} = 2.31 \times 10^3$ $M^{-1}cm^{-1}$, $\Delta\varepsilon_{245} = 1.066 \times 10^4$ $M^{-1}cm^{-1}$. These values were obtained by the author with *N*-acetyl-L-tyrosine ethyl ester and agree with the values reported by other investigators (*120-123*).

Examination of a rapid change in absorbance by the pH-jump. The pH-jump stopped-flow experiments were performed using a Union SF-70 stopped-flow apparatus with an optical path of 1.0 cm and about 1.5 msec of dead-time according to the previously reported method (*124*). The optical changes at 295 nm and 245 nm were recorded with a Riken Denshi QSC-8C quick signal converter equipped with an X-Y recorder, F-3D.

6.3 Results

Solvent perturbation. Figure 6.1 shows the molar absorptivity difference, $\Delta\varepsilon_\lambda$, of *N*-acetyl-L-tryptophan ethyl ester of a tryptophan maximum, λ = 291.0 nm, and that of *N*-acetyl-L-tyrosine ethyl ester at a tyrosine maximum, λ = 284.5 nm, plotted against the final concentration of ethylene glycol (%, v/v). The similar plots were obtained also for the other perturbants employed. In the perturbant concentration range between zero and 30% (v/v) the plots were linear, above which upward deviation from the linearity was observed. The molar absorptivity differences of the model compounds at the perturbant concentration of 20% (v/v) (except in the case of D_2O, 90%, v/v) have been determined as shown in Table 6.1, which are in satisfactory agreement with those obtained by Herskovits and Sorensen (*119*) except for one case (*N*-acetyl-L-tryptophan ethyl ester in D_2O at 285.5 nm). Calculations described in

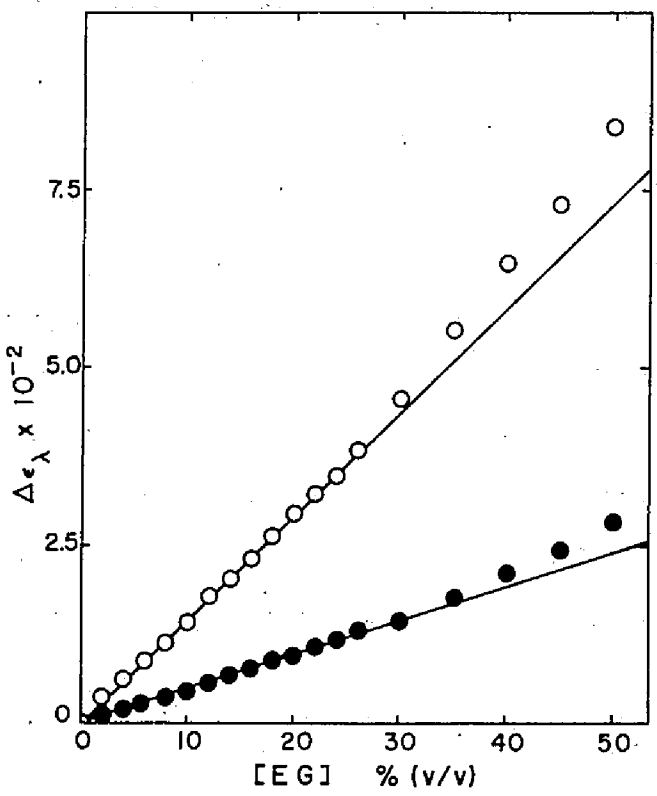

Fig. 6.1. Effect of the concentration of ethylene glycol on the solvent perturbation difference spectrum of *N*-acetyl-L-tryptophan ethyl ester and that of *N*-acetyl-L-tyrosine ethyl ester. [*N*-acetyl-L-tryptophan ethyl ester]$_o$ = 0.240 mM, λ = 291.0 nm, open circle; [*N*-acetyl-L-tyrosine ethyl ester]$_o$ = 1.26 mM, λ = 284.5 nm, closed circle, in 25 mM phosphate buffer, pH 7.00, ionic strength 0.1 M (NaCl), 25.0°C.

---

the following sections were made using the values obtained by the author.

Figures 6.2 (A - D) show the solvent perturbation difference spectra of SSI obtained with 20% (v/v) methanol, 20% (v/v) ethylene glycol, 20% (v/v) polyethylene glycol (#300), and 90% (v/v) D_2O, respectively. Examples of the plots of $\Delta\epsilon_\lambda$ at 285 nm and 294 nm against the perturbant concentration are presented in Fig. 6.3, in which upward deviation from

Table 6.1. Parameters of perturbants and model chromophores in water.[a]

perturbant (%, v/v)	mean diameter (A)	wavelength (λ) of a Trp max (nm)	$\Delta\varepsilon_\lambda$ Ac-Trp-OEt	$\Delta\varepsilon_\lambda$ Ac-Tyr-OEt	wavelength (λ) of a Tyr max (nm)	$\Delta\varepsilon_\lambda$ Ac-Trp-OEt	$\Delta\varepsilon_\lambda$ Ac-Tyr-OEt
D_2O (90)	2.0	292.0	-160.1 (-203.6)[d]	-11.0 (-12.2)[d]	285.5	-71.2 (-120.0)[d]	-60.3 (-67.1)[d]
methanol (20)	2.8	291.5	231.3 (235.4)[d]	16.8 (16.8)[d]	285.5	133.5 (135.9)[d]	75.5 (75.5)[d]
EG[b] (20)	4.4	292.0	294.0 (305.1)[d]	16.1 (16.1)[d]	285.5	165.9 (172.2)[d]	92.2 (92.2)[d]
PEG[c] (20)	9.2	291.0	512.5 (518.7)[d]	57.0 (57.1)[d]	286.0	90.1 (94.3)[d]	178.6 (187.0)[d]

[a] 25 mM phosphate buffer, pH 7.00, ionic strength 0.1 M (NaCl), 25.0°C.
[b] EG, ethylene glycol. [c] PEG, polyethylene glycol (#300). [d] $\Delta\varepsilon_\lambda$ values shown in ( ) are cited from Herskovits and Sorensen (1968) (*125*).

---

linearity was also detected in each plot at the perturbant concentration above 30% (v/v). Values of the molar absorptivity difference of SSI at 20% (v/v) (in the case of D_2O, 90%, v/v) of the perturbant concentration are summarized in Table 6.2.

In the difference spectra of SSI obtained by polyethylene glycol (Fig. 6.2, C) no shoulder was detected at the 292 nm region. This was a unique feature of the polyethylene glycol perturbation, which was not found with other perturbants. This suggests that there was no or little, if any, contact between polyethylene glycol molecules and the tryptophyl residue of SSI. The extent of exposure of tryptophyl and tyrosyl residues was estimated using the following simultaneous equations (*125*).

$$\Delta\varepsilon_{291-293}(\text{protein}) = a\cdot\Delta\varepsilon_{291-293}(\text{Trp}) + b\cdot\Delta\varepsilon_{291-293}(\text{Tyr}) \qquad (6.2)$$

$$\Delta\varepsilon_{286-288}(\text{protein}) = a\cdot\Delta\varepsilon_{286-288}(\text{Trp}) + b\cdot\Delta\varepsilon_{286-288}(\text{Tyr}) \qquad (6.3)$$

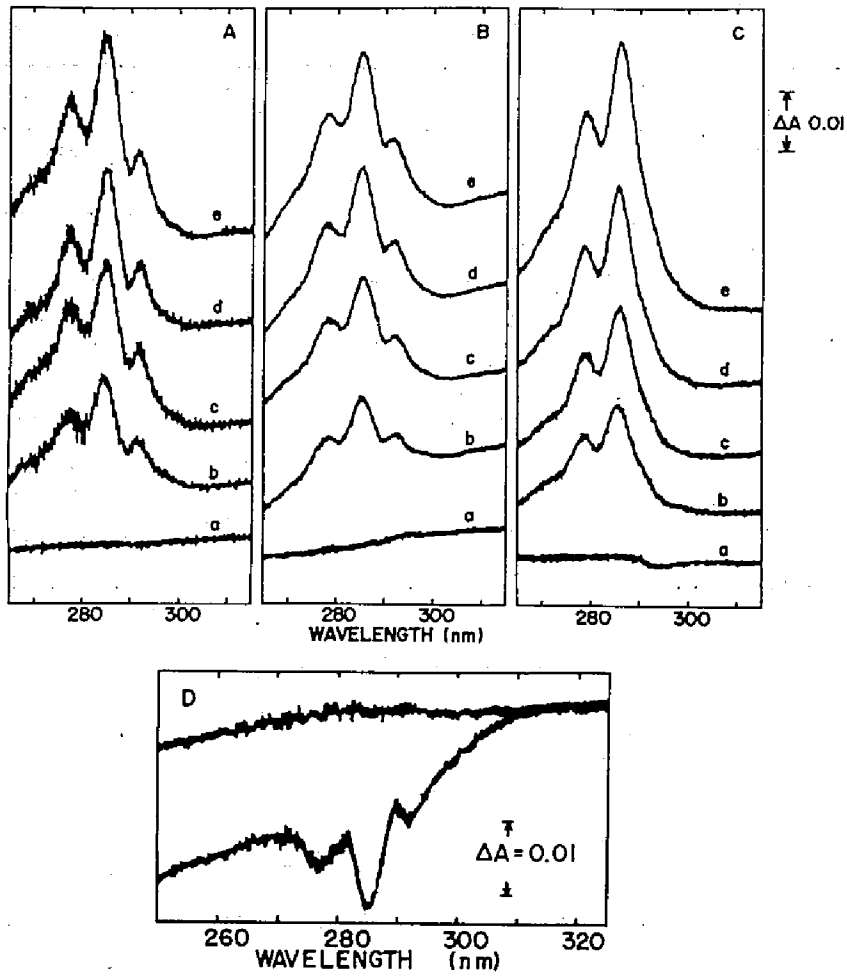

Fig. 6.2. Difference spectra of SSI produced by adding (A) methanol, (B) ethylene glycol, (C) polyethylene glycol, and (D) deuterium oxide. SSI dimer: (A) 59.7 μM; (B) 46.8 μM; (C) 49.7 μM; (D) 44.0 μM. (A) methanol (v/v): (a) 0%; (b) 12%; (c) 16%; (d) 20%; (e) 22%. (B) ethylene glycol (v/v): (a) 0%; (b) 12%; (c) 16%; (d) 20%; (e) 22%. (C) polyethylene glycol (v/v): (a) 0%; (b) 8%; (c) 12%; (d) 16%; (e) 20%. (D) deuterium oxide (v/v): 90%. SSI was in 25 mM phosphate buffer, pH 7.00, ionic strength 0.1 M (NaCl), at 25.0°C.

---

where coefficients a and b respectively represent the apparent number of exposed tryptophyl (Trp) and tyrosyl (Tyr) residues in the protein under investigation. Here $\Delta\varepsilon_\lambda$ values refer to the molar absorptivity differ-

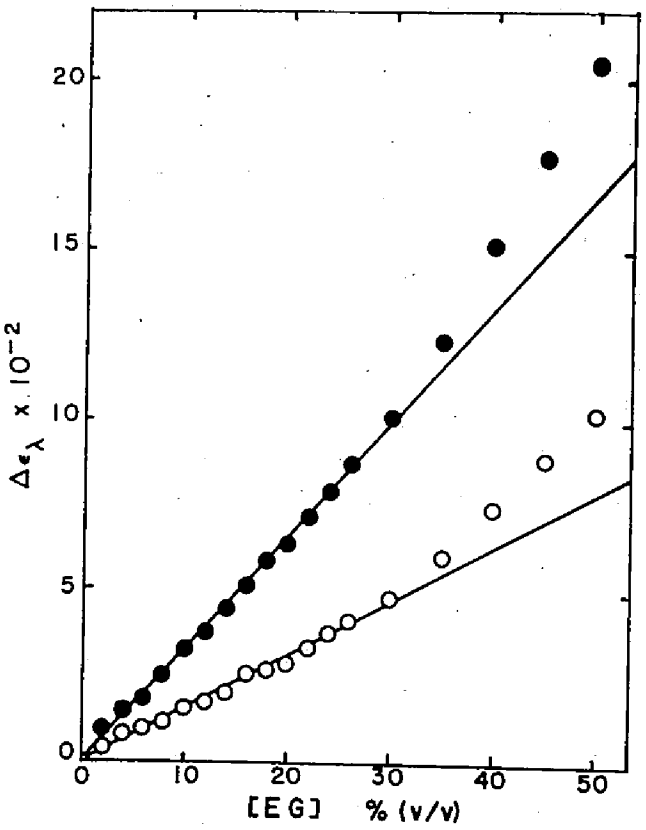

Fig. 6.3. Effect of ethylene glycol concentration on the solvent perturbation difference spectra of SSI. λ = 292.0 nm, open circle; λ = 286.0 nm, closed circle. [SSI dimer]$_o$ = 46.8 μM, in 25 mM phosphate buffer, pH 7.00, ionic strength 0.1 M (NaCl), 25.0°C.

---

ences of the protein and the model compounds at the peak wavelengths of the difference spectrum (291-293 nm and 286-288 nm). The results are summarized in Tables 6.1, 6.2, and 6.3. The coefficients a and b and the ratios of the exposed chromophoric residues to the total chromophoric residues are listed in Tables 6.2 and 6.3.

Curves A - C of Fig. 6.4 show the solvent perturbation difference spectra of subtilisin BPN' caused by 20% (v/v) methanol, 20% (v/v) ethylene glycol, and 20% (v/v) polyethylene glycol (#300), respectively.

Table 6.2. Difference spectral parameters of SSI.[a]

perturbant (%, v/v)	mean diameter (A)	molar absorptivity difference ($\Delta\varepsilon_\lambda$) λ:290-293nm	λ:284-288nm	apparent no. of exposed groups[d] Trp	Tyr	fraction of residues exposed (%) Trp	Tyr
D_2O (90)	2.0	-329.9	-568.8	1.54	7.58	77.0	126.3
methanol (20)	2.8	251.3	544.5	0.65	6.07	32.3	101.2
EG[b] (20)	4.4	279.8	651.5	0.63	5.94	31.5	99.0
PEG[c] (20)	9.2	322.0	915.5	0.06	5.09	3.0	88.8

[a] 25 mM phosphate buffer, pH 7.00, ionic strength 0.1 M (NaCl), 25.0°C. [b] EG, ethylene glycol. [c] PEG, polyethylene glycol (#300). [d] values are calculated according to Eqs. 6.2 and 6.3.

The number and the fraction of the exposed tryptophyl and tyrosyl residues are shown in Table 6.3.

Spectrophotometric titration of tyrosyl groups. Figure 6.5 shows the ultraviolet absorption spectra of SSI at pH's 7.0 and 13.1. No spectral change was observed between pH 6 and 8. Above pH 8, the spectra showed gradual increase in molar absorbance concomitant with the red shift, as pH values increased, reaching the spectrum of pH 13.1. These spectral changes were due almost exclusively to ionization of tyrosyl phenolic groups. No conformational change of SSI seems to have taken place; the identical profile of ORD spectra of SSI was obtained between pH's 7.0 and 13.1, and no cleavage of disulfide bond at pH 13 was detected. Figure 6.6 shows the pH-difference spectra of SSI, SSI in the presence of 4 M guanidinium hydrochloride, and *N*-acetyl-tyrosine ethyl ester. The number of ionized tyrosyl residues in SSI at pH 14.0 was calculated from Curve A to be 6.0 per mole of dimer SSI. The value is in good agreement with the results of amino acid analysis, three tyrosyl

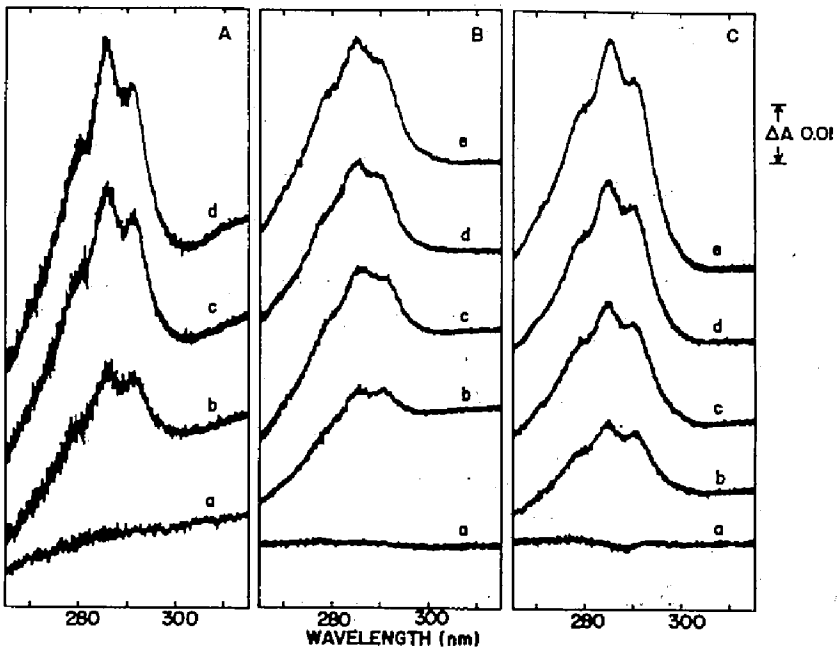

Fig. 6.4. Difference spectra of subtilisin BPN' produced by adding (A) methanol, (B) ethylene glycol, and (C) polyethylene glycol. Subtilisin BPN': (A) 42.7 μM; (B) 40.2 μM; (C) 31.4 μM. (A) methanol (v/v): (a) 0%; (b) 8%; (c) 16%; (d) 20%. (B) ethylene glycol (v/v): (a) 0%; (b) 14%; (c) 18%; (d) 20%; (e) 22%. (C) polyethylene glycol (v/v): (a) 0%; (b) 6%; (c) 10%; (d) 14%; (e) 18%. Subtilisin BPN' was in 25 mM phosphate buffer, pH 7.00, ionic strength 0.1 M (NaCl), at 25.0°C.

Table 6.3. Difference spectral parameters of subtilisin BPN'.[a]

perturbant (%, v/v)	mean diameter (A)	molar absorptivity difference ($\Delta\varepsilon_\lambda$) λ:290-293nm	λ:284-288nm	apparent no. of exposed groups[d] Trp	Tyr	fraction of residues exposed (%) Trp	Tyr
methanol (20)	2.8	704.6	869.4	2.54	7.04	84.7	70.4
EG[b] (20)	4.4	712.0	939.4	2.07	6.47	68.9	64.7
PEG[c] (20)	9.2	1083	1155	1.41	6.31	47.0	63.1

[a] 25 mM phosphate buffer, pH 7.00, ionic strength 0.1 M (NaCl), 25.0°C. [b] EG, ethylene glycol. [c] PEG, polyethylene glycol (#300). [d] values are calculated according to Eqs. 6.2 and 6.3.

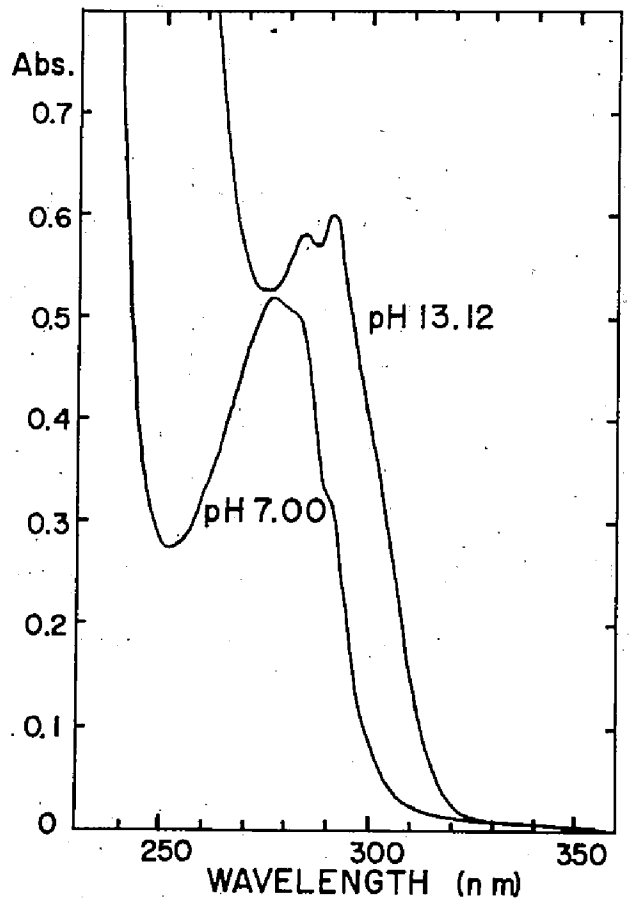

Fig. 6.5. Ultraviolet absorption spectra of SSI. [SSI dimer]$_o$ = 27.3 μM, in 25 mM phosphate buffer, pH 7.00, ionic strength 0.1 M (NaCl), and in the mixture of 1.0 M NaOH and 1.0 M HCl, pH 13.1, 25.0°C.

---

residues per SSI monomer (*27*).

Figure 6.7 shows the plots of $\Delta\varepsilon_{295}$ between neutral and alkaline solutions of SSI against respective pH. Curve A represents the ionization of the tyrosyl phenolic groups measured at 10 min after the preparation of the alkaline samples without guanidinium hydrochloride. The identical curve was obtained even when $\Delta\varepsilon_{295}$ were measured after 24 hr at 25°C. Curve D shows the phenolic hydroxyl ionization in the presence of 4.1 M guanidinium hydrochloride after keeping for 24 hr at 25°C. The

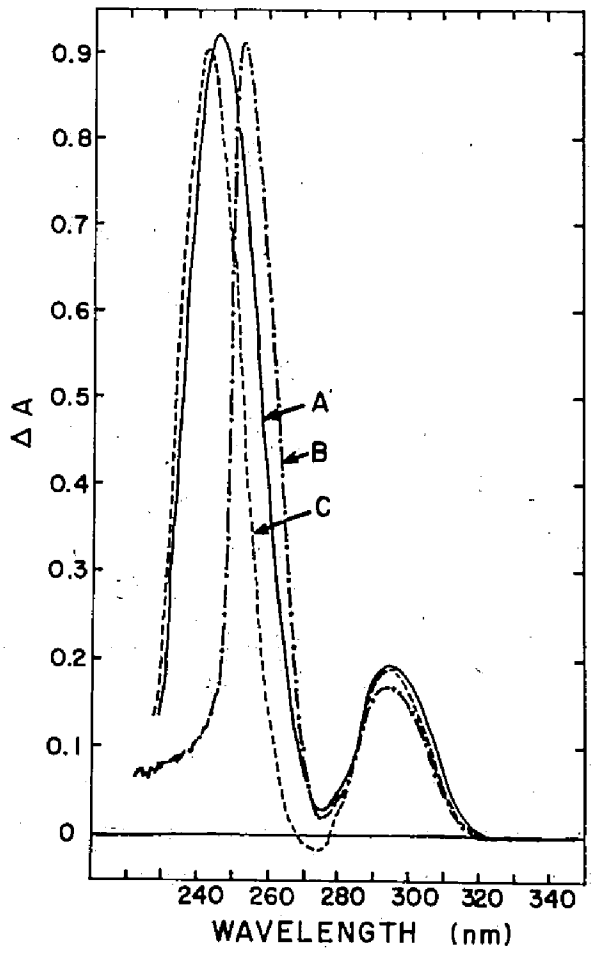

Fig. 6.6. pH-Difference spectra of SSI and *N*-acetyl-L-tyrosine ethyl ester. A (——): [SSI dimer]$_o$ = 14.1 μM, pH 14.0 vs. pH 7.00. B (—·—): [SSI dimer]$_o$ = 15.5 μM, pH 10.35 vs. pH 7.00 in the presence of 4.1 M guanidinium hydrochloride. C (---): [*N*-acetyl-L-tyrosine ethyl ester]$_o$ = 66.3 μM, pH 13.0 vs. pH 7.00.

---

plateau level of $\Delta\varepsilon_{295}$ of Curve D corresponds to the ionization of 6.0 tyrosyl phenolic groups. Curve A shows three steps of the ionization.

The pK_a values of the tyrosyl residues of SSI were determined essentially according to the procedure previously described (*121,122*). The experimental values between pH 9.0 - 10.4 of Fig. 6.7 Curve A can be best fitted to a straight line using Eq. 6.1 as shown in Fig. 6.8, A.

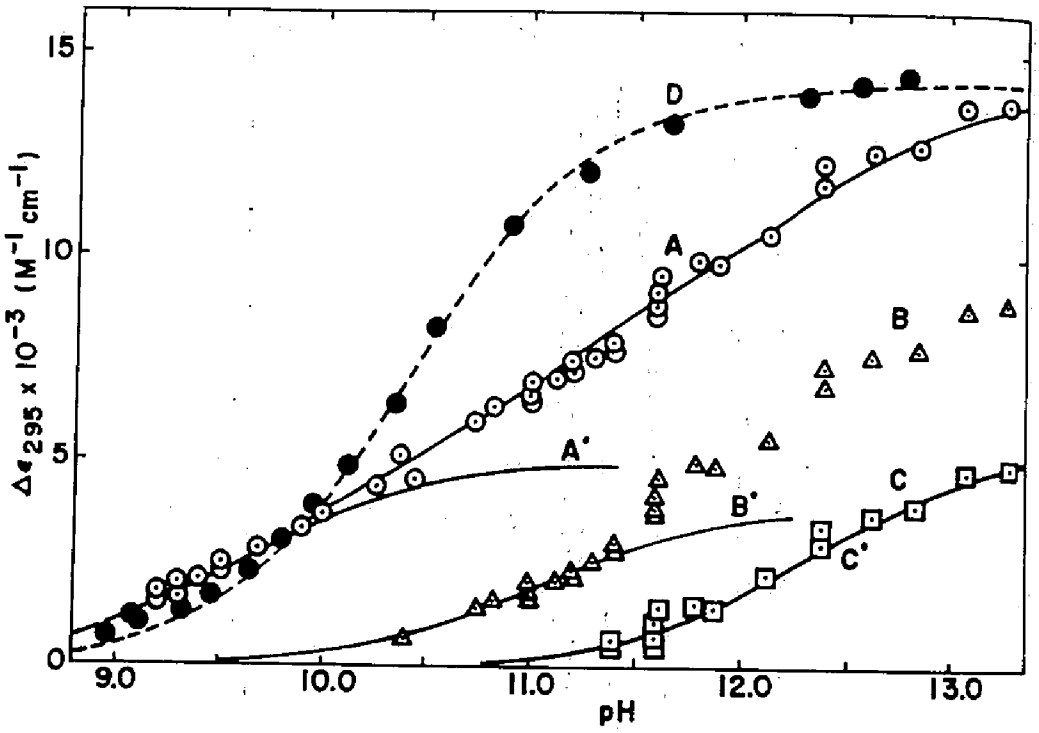

Fig. 6.7. Spectrophotometric titration curves of SSI. A (open circle): forward titration at 10 min and 24 hr after preparing alkaline sample solution. [SSI dimer]$_o$ = 5.03 μM. Solid line is the theoretical curve drawn by assigning pK_a values, 9.58, 11.10, and 12.42, respectively, to three pairs of tyrosyl residues per mole of SSI dimer. A': theoretical ionization curve for 2.15 tyrosyl residues per mole of dimer SSI with a pK_a of 9.66. B (open triangle): difference between curves A and A'. B': theoretical ionization curve for 1.68 tyrosyl residues per mole of dimer SSI with pK_a 11.02. C (open square): difference between curves B and B'. C': theoretical ionization curve for 2.26 tyrosyl residues per mole of dimer SSI with pK_a 12.33. D (closed circle): forward titration in the presence of 4.1 M guanidinium hydrochloride. [SSI dimer]$_o$ = 27.8 μM. Dotted line is the theoretical curve for six tyrosyl residues with pK_a 10.41.

A pK_a of the relevant phenolic groups was obtained from the slope to be 9.66 ± 0.10, and the number of the groups, from the intercept on the

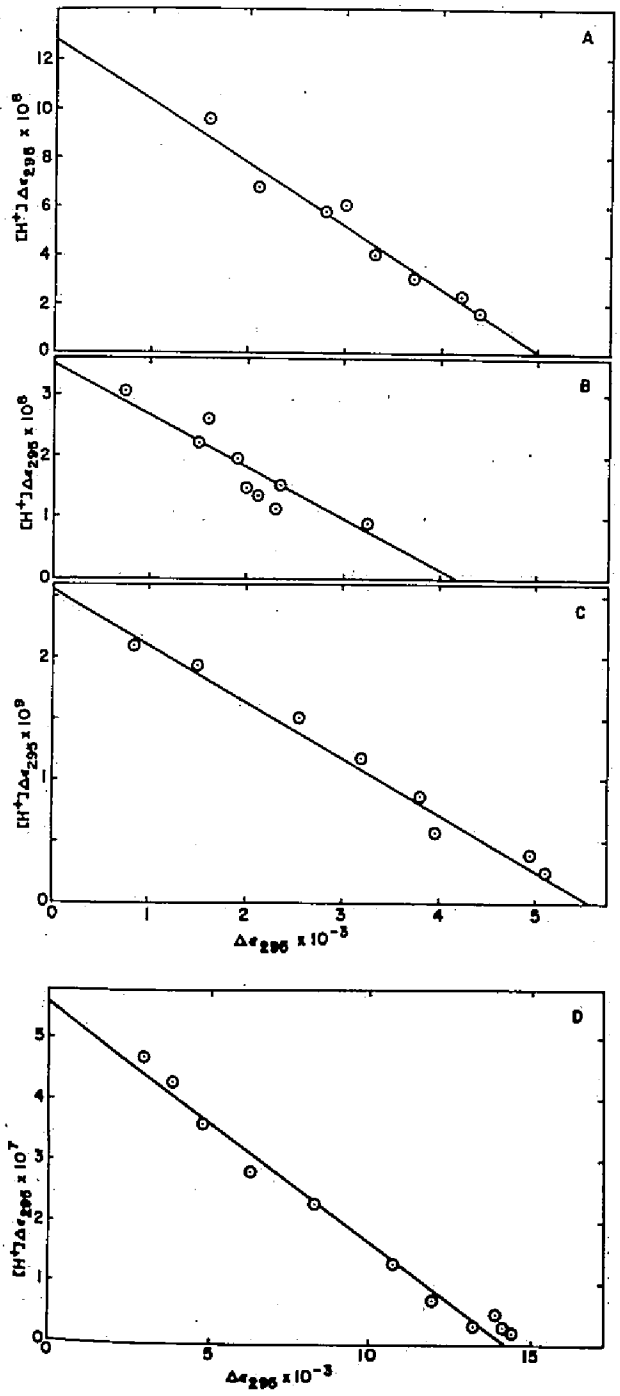

Fig. 6.8. Analysis of titration curves of SSI in terms of $[H^+]\cdot\Delta\varepsilon$ vs. $\Delta\varepsilon$ plot. Titration at 295 nm between pH 9.0 and 10.4, (A); between pH 10.4 and 11.4, (B); between pH 11.4 and 13.4, (C). Titration in the presence of 4.1 M guanidinium hydrochloride at 294 nm between pH 9.95 and 13.0, (D).

abscissa, to be 2.15 ± 0.03 per mole of SSI dimer. Curve A' in Fig. 6.7 represents a theoretical ionization curve for 2.15 phenolic groups with

a pK_a of 9.66. Subtraction of Curve A' from the experimental points of Curve A gives Curve B. The $\Delta\varepsilon_{295}$ values of Curve B between pH 10.4 and 11.4 can be best fitted, in the same manner, to a straight line (Fig. 6.8, B), which indicates ionization of 1.68 ± 0.13 phenolic groups with a pK_a of 11.02 ± 0.06 in this pH region. Curve B' of Fig. 6.7 is a theoretical titration curve for 1.68 phenolic groups with a pK_a of 11.02. Subtracting Curve B' from Curve B gives Curve C of Fig. 6.7, which can be best fitted, by the same treatment, to a straight line (Fig. 6.8, C) that indicates the ionization of 2.26 ± 0.16 tyrosyl residues with a pK_a of 12.33 ± 0.06 in the region of pH 11.4 - 13.4. Curve C' of Fig. 6.7 is a theoretical ionization curve for 2.26 phenolic groups with a pK_a of 12.33. Thus the six tyrosyl residues of a dimer SSI are to be classified into three groups: 2.15 residues with a pK_a of 9.66, 1.68 residues with a pK_a of 11.02, and 2.26 residues with a pK_a of 12.33. (see Discussion 6.4)

The experimental points of Curve D in Fig. 6.7 can be best fitted to a straight line according to Eq. 6.1 as shown in Fig. 6.8, D, which shows the ionization of six tyrosyl residues per mole of SSI dimer with a single pK_a of 10.41 in the presence of 4.1 M guanidinium hydrochloride. The dotted line of Curve D in Fig. 6.7 is a theoretical ionization curve for such phenolic groups.

Time-dependence of the phenolic ionization. The apparent ionization process of originally buried tyrosyl residues caused by conformational change due to the pH-jump can be distinguished from the ionization of originally exposed residues in terms of the time-dependence of the process (*124*). The latter process is so fast that the time-dependence should not be detectable. In the case of SSI, no time-dependent

ionization of tyrosyl residues was detected with an ordinary spectrophotometer or with a stopped-flow apparatus in the pH range pH 10 - 14. This implies that the ionization of all phenolic groups has completed within the dead-time of the apparatus, and strongly suggests that these tyrosyl residues are originally exposed.

6.4 Discussion

The states of tyrosyl residues of SSI. The solvent perturbation studies have demonstrated that all of the six tyrosyl residues in SSI dimer are exposed to the solvent for every perturbant studied. This is consistent with the fact that all of the tyrosyl phenolic groups ionize very rapidly within the dead-time of the stopped-flow apparatus.

The results obtained from laser Raman spectroscopy (M. Nakanishi and M. Tsuboi, personal communication) and from X-ray crystallographic analysis with 2.3 A resolution (*29*) also support this inference.

Three apparent pK_a's of tyrosyl residues. The spectrophotometric titration of tyrosyl residues at the alkaline pH region has shown that the six tyrosyl residues in a dimer SSI can be classified into three groups in terms of the pK_a of the ionization. If the tyrosyl residues of SSI ionize independently, the number of the residues of a certain pK_a should be an integer. This condition has not been considered for the calculation described in Results 6.3. When Curve A in Fig. 6.7 is analyzed with a fixed number of tyrosyl residues, i.e., two for each group with the same molar absorptivity difference, the pK_a values become 9.58 ± 0.10, 11.10 ± 0.19, and 12.42 ± 0.30 for each group. These values are in agreement with those described in Results 6.3, though somewhat larger

deviations are included here. The solid line of Fig. 6.7, Curve A is a theoretical curve drawn for pK_a's 9.58, 11.10, and 12.42 for each two residues. Thus, the six tyrosyl residues of SSI dimer are to be separated into three groups, each including two residues. Since SSI is composed of two identical subunits as shown in the previous studies (*27,28, 49*), the pK_a's of the three tyrosyl residues of monomer SSI are thus separately evaluated. The three tyrosyl residues must locate in different environment from each other, although they all appear to be on the surface of the molecule as described above. Difference in microscopic electrostatic field or the presence of hydrogen bonds could be the reason for the observed difference in pK_a values.

The titration of SSI in the presence of guanidinium hydrochloride was carried out without cleaving the disulfide bonds, since the contribution of reducing agents such as 2-mercaptoethanol to the molar absorptivity difference was thought difficult to be accurately estimated. The obtained pK_a value (10.41) is slightly higher than the case of proteins free of disulfide bond, subtilisin BPN' and subtilisin Carlsberg (pK_a 9.97 in the presence of 5 M guanidinium hydrochloride) (*122*). The difference between those values might be due to that two of the three tyrosyl residues of SSI monomer locate in a disulfide loop (*27*).

The states of tryptophyl residues of SSI. The results of solvent perturbation experiments suggest also that the tryptophyl residues (two per dimer SSI) are not accessible to polyethylene glycol, the mean molecular diameter of which is 9.2 A, whereas about a third of the tryptophyl residue contact with methanol and ethylene glycol, the diameters of which are 2.8 A and 4.4 A, respectively. Since each of the chromophores in a dimer SSI is expected to be in a homologous part in the sub

nit (*27,28,49*), it is concluded that the tryptophyl residue is partially buried in the molecule of SSI. The state of the tryptophyl residue thus estimated seems to be closely related to the unique properties of SSI that the intrinsic protein fluorescence due to tryptophyl residues is strongly quenched in the native SSI (*126*).

The states of tyrosyl and tryptophyl residues of subtilisin BPN'. One molecule of subtilisin BPN' (275 amino acid residues, MW = 27,500) contains three tryptophyl and ten tyrosyl residues (*25*), and the states of those chromophores have been investigated by several methods: spectrophotometric titration (*122*), chemical modification (*26,127-129*), X-ray crystallography (*26*), and solvent perturbation (*130*).

The states of these chromophoric amino acid residues of the subtilisin BPN' preparation used had to be confirmed for further investigation on the interaction between SSI and the enzyme. The number of exposed tyrosyl and tryptophyl residues of subtilisin BPN' obtained in the present Chapter (Table 6.3) are essentially consistent with the published results from the spectrophotometric titration and from the reactivities of those residues toward chemical modification reagents, though the present results give somewhat larger extent of exposure than the values of Herskovits and Fuchs (*130*).

All of the six tyrosyl residues of SSI dimer and about six of the ten residues of subtilisin BPN' have been found in the exposed state by the solvent perturbation study. Some of them must be involved in the enzyme-inhibitor complex formation resulting in the ultraviolet absorption difference spectrum (Fig. 2.6). Whether the tyrosyl residues of the both proteins or of either one of the two proteins participate in the complex formation remains to be clarified, and further studies along

this line are described in the following Chapters.

6.5 Summary

The states of tyrosyl and tryptophyl residues of a dimeric protein proteinase inhibitor, *Streptomyces* subtilisin inhibitor, were studied by solvent perturbation difference spectroscopy with methanol, ethylene glycol, polyethylene glycol (#300), and deuterium oxide as perturbant, and by spectrophotometric titration at alkaline pH. It was indicated that all three tyrosyl residues per monomer of the inhibitor were exposed on the surface of the molecule, and their pK_a values were separately estimated to be 9.66(± 0.10), 11.02(± 0.06), and 12.33(± 0.06). The only one tryptophyl residue per monomer of the inhibitor seemed to be buried in a cleft of the molecule.

The solvent perturbation study of subtilisin BPN', which is a main target enzyme of this inhibitor, indicated that seven tyrosyl and two or three tryptophyl residues of the enzyme molecule were accessible to methanol molecule.

Chapter Seven

A Tyrosyl Residue Involved in the Specific Interaction between *Streptomyces* Subtilisin Inhibitor and Subtilisin BPN' ——— Static and Kinetic Studies *

7.1 Introduction

Protein proteinase inhibitors like soybean trypsin inhibitor (Kunitz) and bovine pancreatic trypsin inhibitor (Kunitz) have drawn attention as the most "natural" substrate analogues of trypsin. The crystallographic studies on the complexes of these inhibitors and trypsin provided a plenty of information as an excellent model for the true binding mode of a specific substrate on the enzyme in general (*10,11*). *Streptomyces* subtilisin inhibitor, SSI, is a protein proteinase inhibitor with such a prospect for subtilisins, against which only very few specific protein inhibitors have been found.

An SSI molecule, which exists as a dimer under the usual conditions consisting of two identical subunits (see Chapters Two, Three, and Four) (*27,28*), binds and inhibits two molecules of subtilisin BPN' (see Chapter Two). The inhibitor contains a tryptophyl and three tyrosyl residues per monomer (113 amino acid residues, MW = 11,500) (*27*); the tryptophyl residue is believed to be partially buried in the molecule and all tyrosyl residues to be exposed on the surface of the protein, from the results of the solvent perturbation and the spectrophotometric

* A part of this study was presented at the 26th Forum on Protein Structure (Nagasaki, October 1975) (*g*).

titration. On the other hand, it has been found that in a molecule of subtilisin BPN', seven out of ten tyrosyl residues and almost all three tryptophyl residues are accessible to methanol (see Chapter Six). Changes in the environment of those chromophoric residues on the association of SSI and subtilisin BPN' have been suggested by the ultraviolet absorption difference spectra (see Chapter Two).

In the present Chapter, changes in the solvent accessibility of those chromophoric amino acid residues accompanied by the enzyme-inhibitor complex formation are studied to obtain evidence for the involvement of such chromophoric residues in the specific interaction between SSI and subtilisin BPN'.

7.2 Experimental Procedures

Materials. A three times crystallized and lyophilized preparation of *Streptomyces* subtilisin inhibitor, SSI, was a generous gift from Professor S. Murao. A three times crystallized and lyophilized preparation subtilisin BPN' [EC 3.4.21.14] (Lot No. 206006) was purchased from Nagase & Co. Ltd., Osaka. The purity of the enzyme preparation used was determined to be 75.4% according to the method described in Chapter Two. A three times crystallized subtilisin Carlsberg [EC 3.4.21.14] preparation (Lot No. 28B-2340) was purchased from Sigma Chemical Co., and its purity was determined to be 92.7%. A three times crystallized bovine pancreatic α-chymotrypsin [EC 3.4.21.1] (Lot No. CDI 34D698) and a twice crystallized bovine pancreatic trypsin [EC 3.4.21.4] (Lot No. TRL 34C-952) are from Worthington Biochemical Corporation (see Experimental Procedures 5.2).

Concentrations of the protein solutions were determined using the following absorptivities at pH 7.00: $E^{0.1\%}_{1\ cm}$(276 nm) = 0.829 for SSI, $E^{0.1\%}_{1\ cm}$(278 nm) = 1.063 for subtilisin BPN' (Chapter Two), $E^{0.1\%}_{1\ cm}$(280 nm) = 0.96 for subtilisin Carlsberg (*131*), $E^{0.1\%}_{1\ cm}$(282 nm) = 2.05 for α-chymotrypsin (*105*), and $E^{0.1\%}_{1\ cm}$(280 nm) = 1.05 for trypsin (*106*); and the following values were also used at pH 9.70, $E^{0.1\%}_{1\ cm}$(276 nm) = 0.850 for SSI and $E^{0.1\%}_{1\ cm}$(280 nm) = 1.092 for subtilisin BPN'. The molecular weights were taken to be 11,500 for SSI monomer (*27*), 27,500 for subtilisin BPN' (*25*), 27,300 for subtilisin Carlsberg (*131*), 25,000 for α-chymotrypsin (*105*), and 24,000 for trypsin (*106*). All spectrophotometric measurements were performed with a Shimadzu UV-200 recording spectrophotometer.

Ethylene glycol of spectral grade and other chemicals of analytical reagent or better grade were obtained from Nakarai Chemicals Ltd., Kyoto.

For the experiment of solvent perturbation difference spectroscopy 25 mM phosphate buffer, pH 7.00±0.01 (ionic strength was adjusted to 0.1 M with NaCl) was used. For the experiments of the difference spectroscopy on the binding of the enzyme and SSI in the alkaline pH range, 25 mM carbonate buffer was used. pH of the buffer was adjusted to a desired value within ±0.01 pH unit with 0.1 N HCl or NaOH solutions, and the ionic strength was adjusted to 0.1 M with NaCl. A Hitachi-Horiba F-5 pH-meter was used for all pH measurements. All the experiments were carried out at 25.0°C.

Notes for the symbols used. In the following description, the molecule of subtilisin BPN' and that of SSI subunit will be indicated by E and I, respectively, and the suffixes, 1 and 2 will stand for their number; accordingly, the binding stoichiometry described in Chapter Two

can be written as $I_2 + 2E_1 \longrightarrow E_2I_2$. Symbols, I_1 and E_1I_1 will be also used representing $\frac{1}{2}(I_2)$ and $\frac{1}{2}(E_2I_2)$, respectively, for convenience of interpreting the interaction between the two proteins simply in terms of the reaction per binding site, although no molecular species such as I_1 and E_1I_1 have been actually detected under the conditions employed in the present study (see Chapter Four).

Solvent perturbation. The solvent perturbation experiments were carried out at pH 7.00, 25.0°C according to the method described in Experimental Procedures 6.2 in Chapter Six. The solvent perturbation difference spectra of the mixture of SSI and subtilisin BPN' solutions rather than the isolated complex were examined.** Methanol and ethylene glycol, their mean diameters being 2.8 A and 4.2 A, respectively, were used as perturbant.

The estimation of the number of tryptophyl and tyrosyl residues involved in the binding of SSI and subtilisin BPN' by solvent perturbation. The following symbols were used.

d : purity of the subtilisin BPN' preparation used.

X, Y : total number of tryptophyl and tyrosyl residues, respectively, in one molecule of the complex of monomer SSI and subtilisin

---

** Inactive protein fraction in the enzyme preparation used may be perturbed by the solvent to the same degree as the active enzyme. This effect, however, does not hamper the estimation of the number of chromophoric residues involved in the interaction between SSI and subtilisin BPN', because the effect of the inactive fraction is cancelled out so far as the mixture of subtilisin BPN' and SSI solutions are used.

BPN' (E_1I_1).

x, y : number of solvent-accessible (exposed) tryptophyl and tyrosyl residues, respectively, in one molecule of the protein, SSI (I_1) or subtilisin BPN' (E_1).

$\bar{x}$, $\bar{y}$: number of solvent-inaccessible (buried) tryptophyl and tyrosyl residues, respectively, in one molecule of the protein, SSI (I_1) or subtilisin BPN' (E_1).

x^*, y^* : number of tryptophyl and tyrosyl residues, respectively, whose accessibility to the solvents was changed on the formation of the complex (E_1I_1).

C_e, C_i : initial concentrations of subtilisin BPN' (active and inactive fractions) and SSI monomer, respectively, in the mixture of the enzyme and the inhibitor solutions. Accordingly dC_e stands for the concentration of the active enzyme.

C_{ei} : concentration of the complex (E_1I_1) formed in the mixture of subtilisin BPN' and SSI solutions, which is equal to dC_e under the conditions used.

The suffices, e, i, and ei represent subtilisin BPN', SSI and the enzyme-inhibitor complex, respectively. The concentrations of tryptophyl (C_x) and tyrosyl residues (C_y) which are perturbed by the solvent perturbants in the mixture of subtilisin BPN' and SSI solutions are expressed by Eqs. 7.2 and 7.3.

$$X = x + \bar{x}, \quad Y = y + \bar{y} \tag{7.1}$$

$$C_x = C_e x_e + C_i x_i - C_{ei} x^* \tag{7.2}$$

$$C_y = C_e y_e + C_i y_i - C_{ei} y^* \tag{7.3}$$

The absorptivity differences, ΔA_λ(E-I mixture), in which λ represents the wavelength, 292 nm and 286 nm, caused by solvent perturbation are

given by Eqs. 7.4 and 7.5.

$$\Delta A_{292}(\text{E-I mixture}) = C_x \cdot \Delta\varepsilon_{292,x} + C_y \cdot \Delta\varepsilon_{292,y} \quad (7.4)$$

$$\Delta A_{286}(\text{E-I mixture}) = C_x \cdot \Delta\varepsilon_{286,x} + C_y \cdot \Delta\varepsilon_{286,y} \quad (7.5)$$

where $\Delta\varepsilon_{\lambda,x}$ and $\Delta\varepsilon_{\lambda,y}$ are the molar absorptivity differences at the wavelength, λ nm, of tryptophyl and tyrosyl residues, respectively. The values of $C_{ei}x^*$ and $C_{ei}y^*$ can be given by solving Eqs. 7.2 - 7.5 simultaneously:

$$C_{ei}x^* = (C_e x_e + C_i x_i) - C_x$$

$$C_x = \frac{\Delta A_{292}(\text{E-I mixture}) \cdot \Delta\varepsilon_{286,y} - \Delta A_{286}(\text{E-I mixture}) \cdot \Delta\varepsilon_{292,y}}{\Delta\varepsilon_{292,x} \cdot \Delta\varepsilon_{286,y} - \Delta\varepsilon_{286,x} \cdot \Delta\varepsilon_{292,y}} \quad (7.6)$$

$$C_{ei}y^* = (C_e y_e + C_i y_i) - C_y$$

$$C_y = \frac{\Delta A_{292}(\text{E-I mixture}) \cdot \Delta\varepsilon_{286,x} - \Delta A_{286}(\text{E-I mixture}) \cdot \Delta\varepsilon_{292,x}}{\Delta\varepsilon_{292,y} \cdot \Delta\varepsilon_{286,x} - \Delta\varepsilon_{286,y} \cdot \Delta\varepsilon_{292,x}} \quad (7.7)$$

Difference spectra on the binding of subtilisin BPN' and SSI at alkaline pH. Difference spectra were observed on the binding of SSI and subtilisin BPN' in the pH region between 8.4 and 10.2 using a Shimadzu UV-200 recording spectrophotometer with an expanded scale (0.1 absorbance/full scale) and a cell holder thermostated at 25.0°C. Two pairs of matched quartz cells (optical path, 1.0 cm) were used.

Kinetics of binding of subtilisin BPN' and SSI at alkaline pH. The rate of the binding of subtilisin BPN' and SSI was measured at 25.0° C with a Union SF-70 stopped-flow spectrophotometer monitoring the absorbance difference at 245 nm, with an Iwatsu MS-5019A storage oscilloscope. The second order rate constant for the binding of subtilisin

BPN' was determined from the progress curve using an equal concentration of the active enzyme and of SSI as monomer. In this case the second-order rate constant, k, is given by Eq. 7.8,

$$(t_{1/2})^{-1} = k[\text{SSI monomer}]_o \qquad (7.8)$$

where $t_{1/2}$ is the half-time of the binding and [SSI monomer]$_o$ is the initial concentration of SSI monomer. The measurements were repeated under the same conditions at least seven times, and the rate constants were determined by the least square method from the plots of ΔA_{245}^{-1} vs. time.

Binding of subtilisin BPN' and SSI at neutral pH. The difference spectrum and the stopped-flow oscillogram observed on the binding of subtilisin BPN' and SSI at alkaline pH were compared with those observed at neutral pH. The ultraviolet absorption difference spectrum was measured with a Union SM-401 recording spectrophotometer, and the binding of the both proteins was measured in 25 mM phosphate buffer, pH 7.00, ionic strength 0.1 M (NaCl), 25.0°C.

7.3 Results

States of tryptophyl and tyrosyl residues affected by the interaction between subtilisin BPN' and SSI. Figure 7.1 shows the difference spectra observed on the solvent perturbation of the mixture of SSI and subtilisin BPN' by ethylene glycol. The final concentration of SSI as monomer (C_i) and of total subtilisin BPN' (C_e) were 26.3 μM and 0.602 mg/ml (21.9 μM assuming the enzyme to be 100% active), respectively. Figure 7.2 depicts the relationship between the absorptivity difference and the concentration of ethylene glycol at 292 nm and 286 nm. The ab-

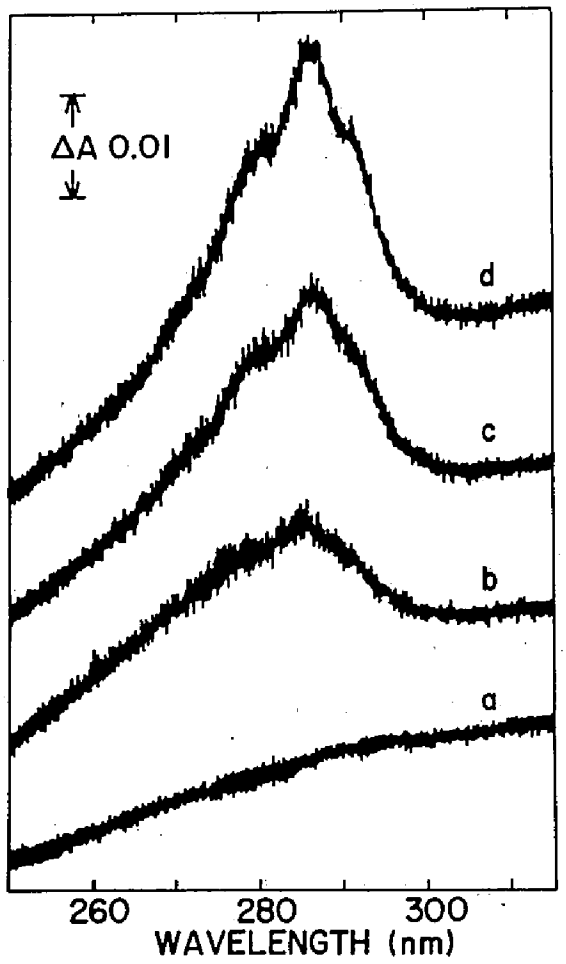

Fig. 7.1. Absorption difference spectra observed on the solvent perturbation of the mixture solution of subtilisin BPN' and SSI with ethylene glycol in 25 mM phosphate buffer, pH 7.00, ionic strength 0.1 M (NaCl), at 25.0°C. [SSI monomer]$_o$ = 26.3 μM; [subtilisin BPN']$_o$ = 16.5 μM (taking the purity of the preparation, 75.4% into account). ethylene glycol (v/v): (a) 0%; (b) 5%; (c) 15 %; (d) 25%.

---

sorptivity differences, ΔA_{292}(E-I mixture) and ΔA_{286}(E-I mixture), at 20% (v/v) ethylene glycol were determined from this plot to be 1.35 x 10^{-2} cm^{-1} and 1.95 x 10^{-2} cm^{-1}, respectively, by the method of least squares. The absorptivity differences at 292 nm and 286 nm with 20% (v/v) methanol as perturbant were determined to be 1.50 x 10^{-2} cm^{-1} and 2.31 x 10^{-2} cm^{-1}, respectively in the same manner. Since the dissociation constant, K_i, of the subtilisin BPN'-SSI complex is below 10^{-9} M (see Chapter Two), the concentration of the complex (E_1I_1) in the mixture of subtilisin BPN' and SSI (C_{ei}) can be taken to be equal to the

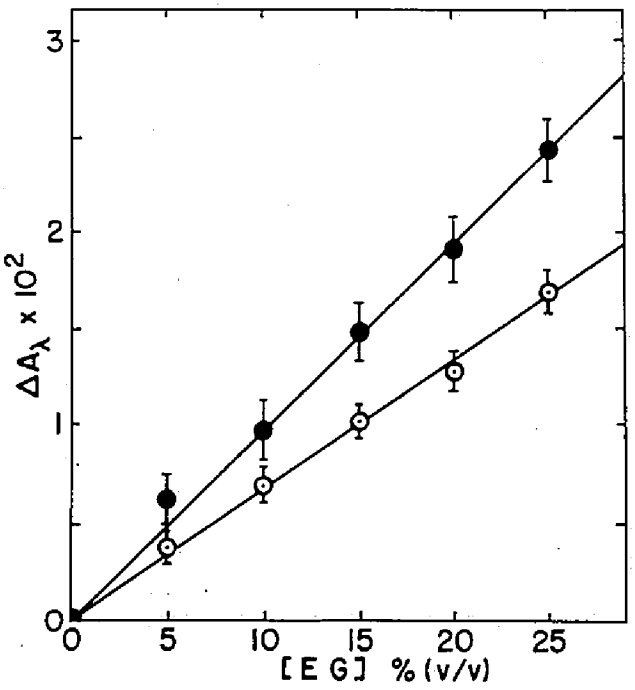

Fig. 7.2. The relationship between the absorptivity differences observed on the solvent perturbation of the mixture solution of subtilisin BPN' and SSI with ethylene glycol and the concentration of ethylene glycol. $[\text{subtilisin BPN'}]_o$ = 16.5 μM; $[\text{SSI monomer}]_o$ = 26.3 μM, in 25 mM phosphate buffer, pH 7.00, ionic strength 0.1 M (NaCl), 25.0°C. Wavelength: 292 nm, open circle; 286 nm, closed circle.

---

concentration of the active form of the enzyme, dc_e, which was 16.5 μM by using the purity of the enzyme preparation, 75.4%. The molar absorptivity differences for solvent perturbation shown in Table 6.1 (Chapter Six), which were determined with model compounds, *N*-acetyl-L-tryptophan ethyl ester and *N*-acetyl-L-tyrosine ethyl ester, were used for calculating the numbers of tryptophyl and tyrosyl residues in the proteins, respectively. The total numbers of the solvent-accessible tryptophyl and tyrosyl residues contained in one molecule of monomer SSI (I_1) and one molecule of subtilisin BPN' (E_1) are shown in Table 7.1. By solving

Table 7.1. The number of the solvent-accessible (exposed) tryptophyl and tyrosyl residues of SSI, subtilisin BPN', and their complex.[a]

	proteins	(a) SSI (I_1)	(b) S. BPN' (E_1)	(c)[d] -	(d) complex (E_1I_1)	(e)[e] -
tryptophyl residues	total number of residues	1	3	4	4	-
	with perturbant					
	20% (v/v) EG[b]	0.315	2.06	2.38	1.43	-0.95
	20% (v/v) Met[c]	0.323	2.54	2.86	1.95	-0.91
tyrosyl residues	total number of residues	3	10	13	13	-
	with perturbant					
	20% (v/v) EG[b]	2.97	6.47	9.44	4.83	-4.61
	20% (v/v) Met[c]	3.04	7.04	10.08	9.10	-0.98

[a] 25 mM phosphate buffer, pH 7.00, ionic strength 0.1 M (NaCl), 25.0°C.
[b] EG, ethylene glycol. [c] Met, methanol. [d] (c) = (a) + (b).
[e] (e) = (d) - (c).

Eqs. 7.6 and 7.7 using the parameters given above, the numbers of tryptophyl (x*) and tyrosyl (y*) residues whose accessibility to the solvent changed on the formation of the complex (E_1I_1) were obtained. The results show that 0.95 tryptophyl and 4.61 tyrosyl residues become inaccessible to ethylene glycol, and 0.91 tryptophyl and 0.98 tyrosyl residues to methanol, upon binding of SSI and subtilisin BPN'.

Difference spectrum observed on the binding of subtilisin BPN' and SSI at alkaline pH. Figure 7.3 shows the difference spectrum observed on the binding of subtilisin BPN' and SSI at pH 9.70. This is a typical difference spectrum that is observed when the ionized tyrosyl residues are protonated. This indicates undoubtedly that some ionized tyrosyl residue(s) of SSI and/or subtilisin BPN' at pH 9.70 become protonated by

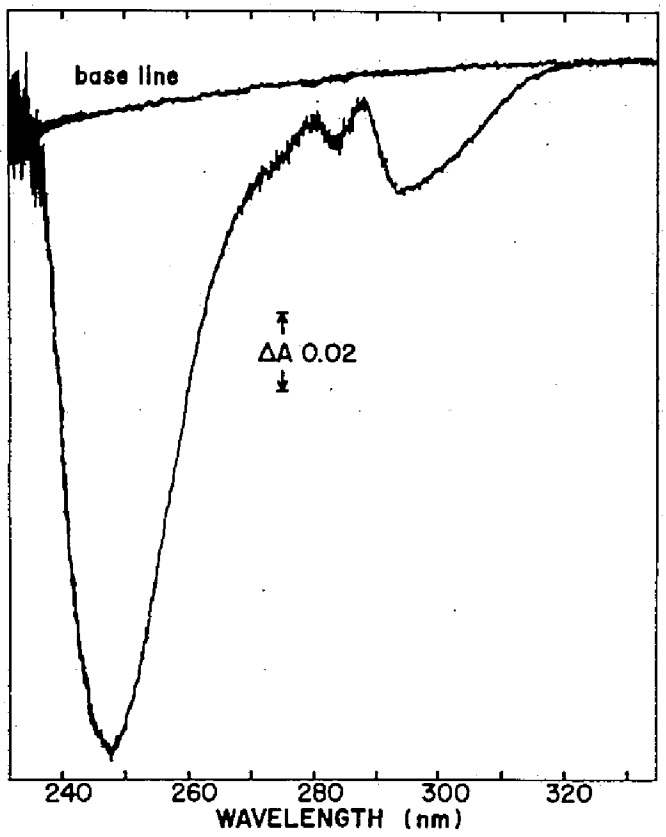

Fig. 7.3. Ultraviolet absorption difference spectrum observed on the binding of SSI and subtilisin BPN'. $[\text{subtilisin BPN'}]_o$ = 24.5 μM; $[\text{SSI monomer}]_o$ = 28.5 μM, in 25 mM carbonate buffer, pH 9.70, ionic strength 0.1 M (NaCl), 25.0°C.

---

the binding of the two protein molecules.

The molar absorptivity differences calculated from Fig. 7.3 are $\Delta\varepsilon_{245} = -7.21 \times 10^3\ M^{-1}cm^{-1}$ and $\Delta\varepsilon_{295} = -1.27 \times 10^3\ M^{-1}cm^{-1}$. Since the molar absorptivity differences for the ionization of a tyrosyl residue determined with *N*-acetyl-L-tyrosine ethyl ester are $\Delta\varepsilon_{245} = 10.66 \times 10^3\ M^{-1}cm^{-1}$ and $\Delta\varepsilon_{295} = 2.31 \times 10^3\ M^{-1}cm^{-1}$ (see Chapter Six), the spectral change in Fig. 7.3 corresponds to the change which would be expected when half-ionized 1.2 tyrosyl residues or 40% ionized one tyrosyl

Table 7.2. The states of the tyrosyl residues and their pK_a values of SSI (I_1), subtilisin BPN', and subtilisin Carlsberg.[a]

		SSI			subtilisin BPN'		subtilisin Carlsberg	
		no. of tyrosyl residues	pK_a		no. of tyrosyl residues	pK_a	no. of tyrosyl residues	pK_a
Class I	exposed	1.08	9.66	exposed	5.30	9.74	6.38	9.92
Class II	exposed	0.84	11.02	buried	2.65	11.25	3.58	11.61
Class III	exposed	1.13	12.33	buried	2	12.5	3	12.5

[a] Data on subtilisin BPN' and subtilisin Carlsberg are cited from Markland (1969) (*122*), and data on SSI from Chapter Six.

---

residue become fully protonated on the formation of the complex (E_1I_1) at pH 9.70. This implies that pK_a of about one tyrosyl residue considerably shifted upwards. The pK_a values of tyrosyl residues of SSI, subtilisin BPN', and subtilisin Carlsberg are listed in Table 7.2. There are six candidate residues with pK_a 9.7 which could be responsible for this shift in pK_a.

The difference spectra at alkaline pH were observed at various ratios of the concentration of monomer SSI (I_1) to that of subtilisin BPN' (E_1); the observed absorptivity differences increased with the increase in the ratio and reached a saturated level at the ratio of 1.0 (M/M) (Figure not shown).

The pH-profile of the absorptivity difference at 245 nm is shown in Fig. 7.4 (plot a) (see Fig. 7.5, a).

The similar difference spectrum as shown in Fig. 7.3 was observed on the binding of subtilisin Carlsberg and SSI at pH 9.70 (Fig. 7.6), and the molar absorptivity differences at 245 nm and 295 nm were - 5.93

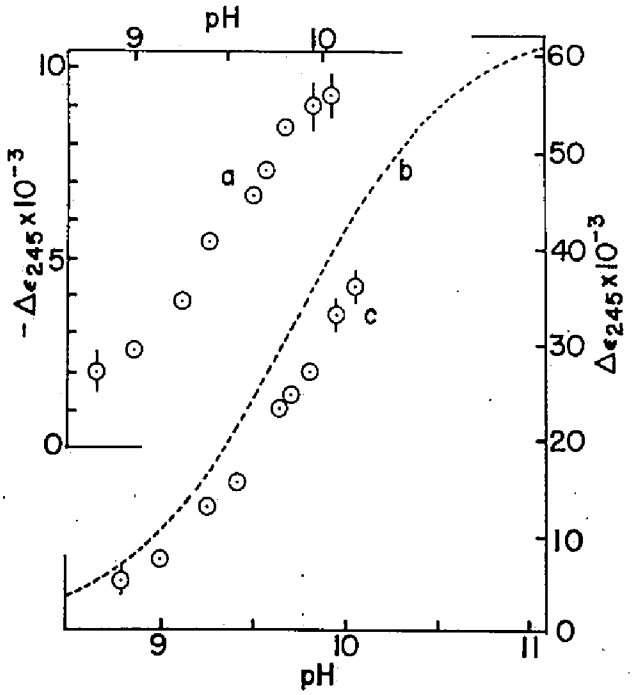

Fig. 7.4. Spectrophotometric titration of tyrosyl residues of the SSI-subtilisin BPN' complex. (a): absorptivity differences at 245 nm observed on the binding of SSI and subtilisin BPN' at alkaline pH's, in 25 mM carbonate buffer, ionic strength 0.1 M (NaCl), 25.0°C. (b): theoretical titration curve of 6 tyrosyl residues of pK_a 9.7 (see text). (c): absorptivity differences obtained by subtracting those of (a) from (b) (see text).

---

x 10^3 $M^{-1}cm^{-1}$ and - 1.29 x 10^3 $M^{-1}cm^{-1}$, respectively. The number of tyrosyl residues with pK_a 9.92 - 9.66 (Table 7.2) converted to the fully protonated form by the complex formation (E_1I_1) was calculated to be between 0.9 and 1.1. However, no difference spectra of this type were observed at pH 9.70 with α-chymotrypsin and trypsin (Fig. 7.7), although these proteinases have been found to interact with and be inhibited by SSI at neutral pH (see Chapter Five).

The kinetics of association between SSI and subtilisin BPN'. The

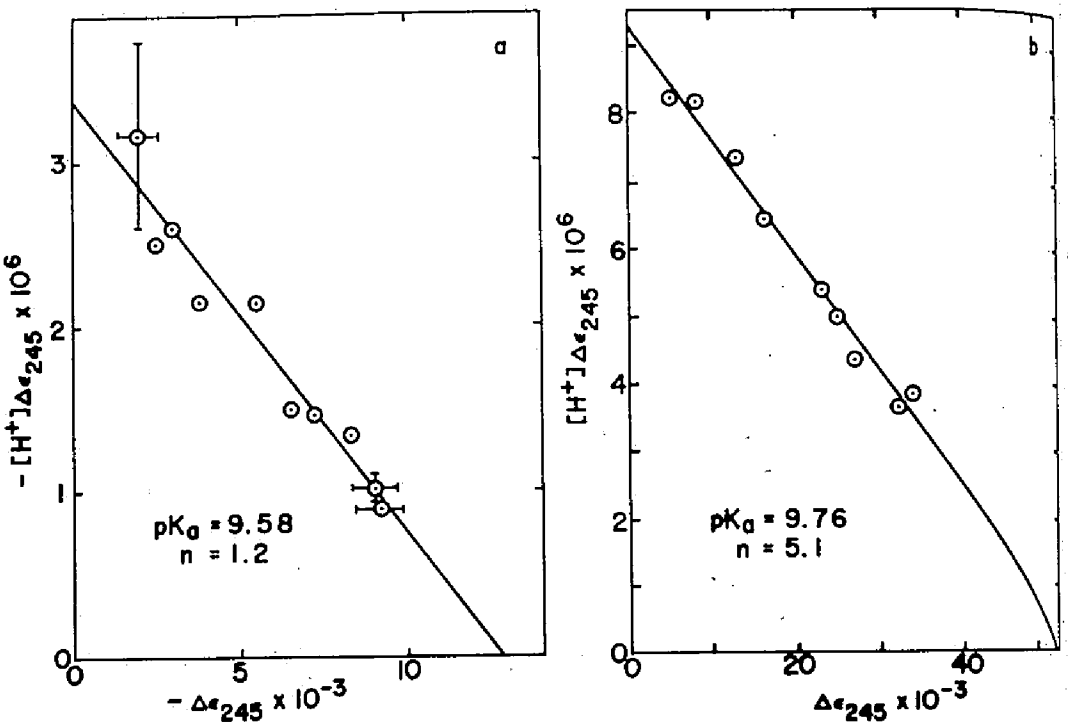

Fig. 7.5. The relationship between $\Delta\varepsilon_{245}[H^+]$ and $\Delta\varepsilon_{245}$. Plots (a) and (b) were made based on the values of plots (a) and (b) in Fig. 7.4, respectively. (see Discussion 7.4).

---

absorptivity difference at 245 nm shown in Fig. 7.3 could be a good probe for studying the binding kinetics of SSI with subtilisin BPN'. Figure 7.8 shows an oscilloscope trace of the time course of the binding between SSI and subtilisin BPN' measured with a stopped-flow apparatus. The concentrations of SSI monomer and subtilisin BPN' were equal (2.61 μM). The second-order rate constant was determined to be 3.1×10^6 M^{-1} sec^{-1} from the second-order plot $(\Delta A_{245}{}^{-1}$ vs. time) in Fig. 7.9. The dependence of the reciprocal of half-time $(t_{1/2})^{-1}$ of the binding time course at pH 9.70 on the protein concentrations is shown in Fig. 7.10. The good linear relationship observed in Figs. 7.9 and 7.10 suggests that the binding proceeded through a simple bimolecular step in the

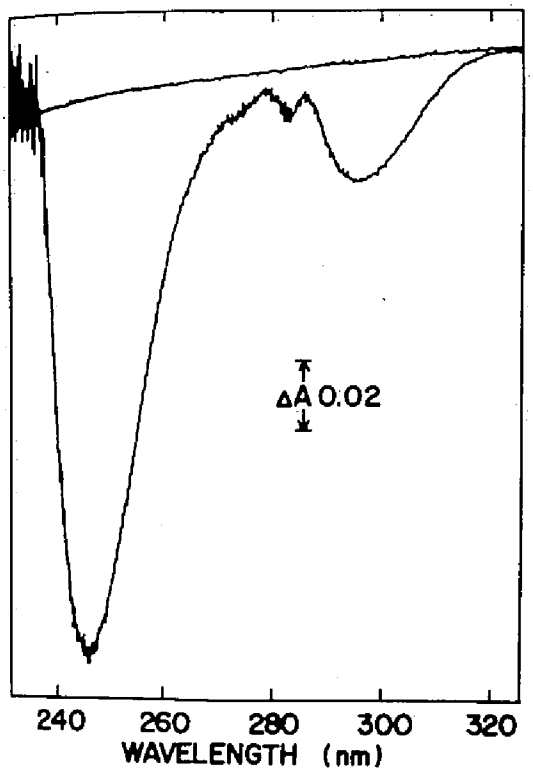

Fig. 7.6. Ultraviolet absorption difference spectrum observed on the binding of SSI and subtilisin Carlsberg. [subtilisin Carlsberg]$_o$ = 25.8 μM; [SSI monomer]$_o$ = 32.3 μM, in 25 mM carbonate buffer, pH 9.70, ionic strength 0.1 M (NaCl), 25.0°C.

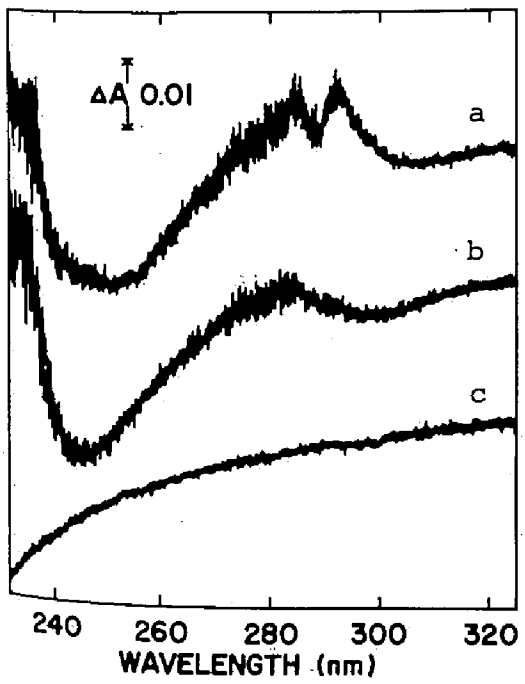

Fig. 7.7. Ultraviolet absorption difference spectra observed on the binding of SSI with α-chymotrypsin and trypsin. (a): α-chymotrypsin-SSI system. (b): trypsin-SSI system. (c): base line. [SSI monomer]$_o$ = 38.1 μM; [α-chymotrypsin]$_o$ = 20.3 μM; [trypsin]$_o$ = 20.0 μM, in 25 mM carbonate buffer, pH 9.70, ionic strength 0.1 M (NaCl), 25.0°C.

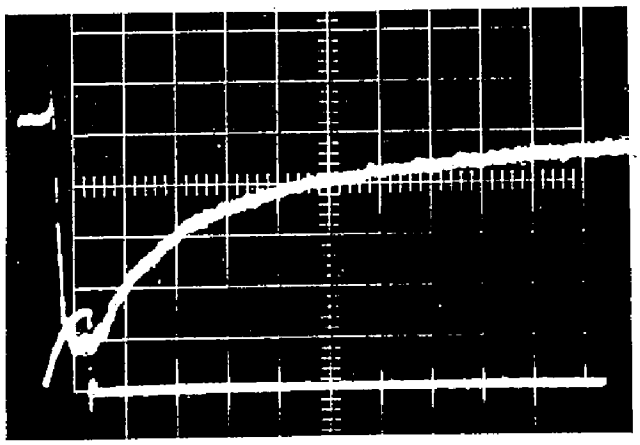

Fig. 7.8. An oscilloscope trace of a time course of absorbance change at 245 nm on the binding of SSI and subtilisin BPN' observed with a stopped-flow apparatus at pH 9.70. [subtilisin BPN']$_o$ = [SSI monomer]$_o$ = 2.61 μM, in 25 mM carbonate buffer, pH 9.70, ionic strength 0.1 M (NaCl), 25.0°C. Scale: horizontal, 50 msec/div.; vertical, 0.00465 Abs./div. The lower curve is the flow velocity trace.

---

range of the protein concentration studied: [active enzyme]$_o$ = [SSI monomer]$_o$ = 2.61 μM - 0.127 mM; and the second-order rate constant was determined from the slope of the plot in Fig. 7.10 to be (3.0 ± 0.2) x 10^6 $M^{-1}sec^{-1}$ showing a good agreement with the one obtained for the progress curve (Fig. 7.9).

The pH-dependence of the second-order rate constants was studied in the range of the protein concentrations, [active enzyme]$_o$ = [SSI monomer]$_o$ = 5.2 μM - 24.2 μM, and in the pH-region, pH 9.0 - 11.3. The logarithms of the rate constants are plotted against pH in Fig. 7.11. The rate constant, k, decreased with the increase of pH with a slope, (log k / pH), of -1 above pH 10.4.

Comparison of the difference spectrum and the stopped-flow oscillogram observed on the binding of SSI and subtilisin BPN' at pH 9.70

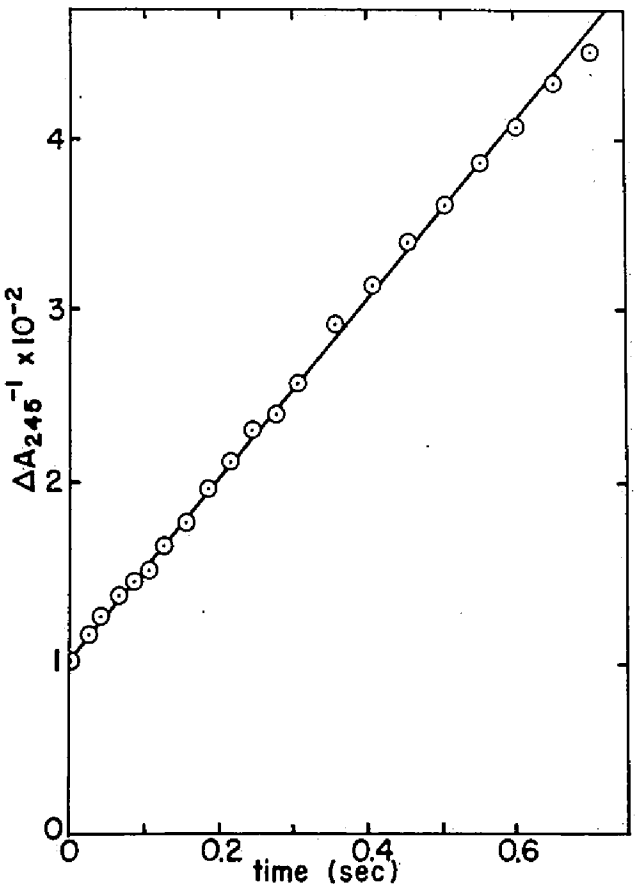

Fig. 7.9. Second-order plot (ΔA_{245}^{-1} vs. time) for the binding of SSI and subtilisin BPN' in 25 mM carbonate buffer, pH 9.70, ionic strength 0.1 M (NaCl), 25.0°C. [subtilisin BPN']$_o$ = [SSI monomer]$_o$ = 2.61 μM. The second-order rate constant was estimated to be 3.1×10^6 $M^{-1}sec^{-1}$.

---

with those at pH 7.00. Figure 7.12 shows an absorption difference spectrum observed on the binding of SSI and subtilisin BPN' at pH 7.00, 25.0 °C. The maximum spectral change is about 1/15 of that in Fig. 7.3 which was obtained on the binding at pH 9.70. In Fig. 7.13 is shown the time course of the binding observed at pH 7.00 by the use of this small absorbance change with a Union RA-401 stopped-flow spectrophotometer with data averaging equipment. A single run (upper one) is too noisy to

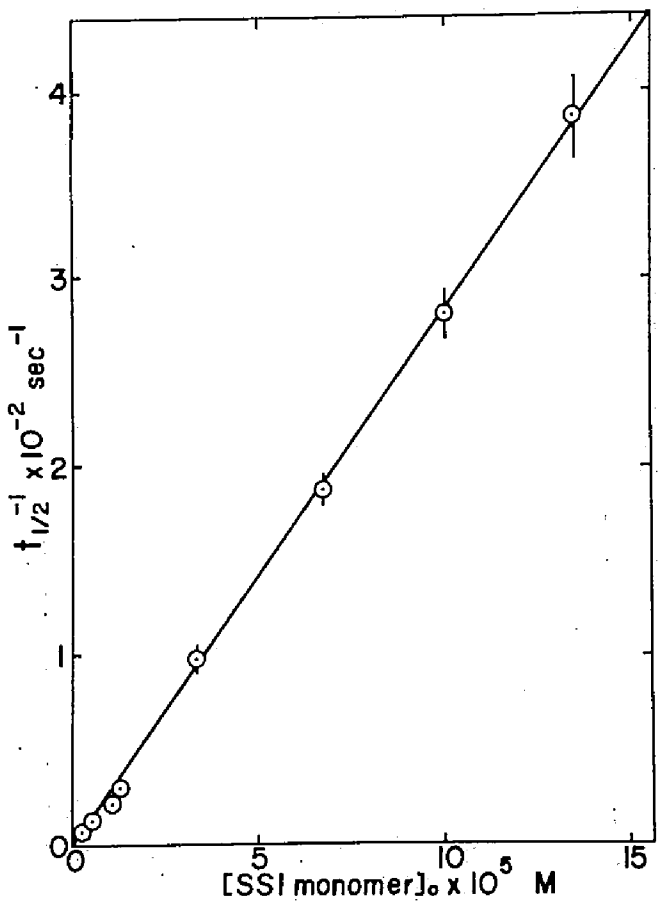

Fig. 7.10. Dependence of the reciprocal of half-time of the binding time course on protein concentration in 25 mM carbonate buffer, pH 9.70, ionic strength 0.1 M (NaCl), at 25.0°C. The final concentration of SSI monomer and that of the active form of subtilisin BPN' were equal. The second order rate constant obtained from the slope was (3.0 ± 0.2) x 10^6 $M^{-1}sec^{-1}$.

---

estimate the rate constant. The lower curve, which was obtained by accumulating and averaging 14 binding curves, has a sufficient signal to noise ratio for the analysis. By comparing the binding curves in Fig. 7.13 with that in Fig. 7.9, it would be clear how the absorptivity difference at 245 nm of Fig. 7.3 (at pH 9.70) is a good probe for studying

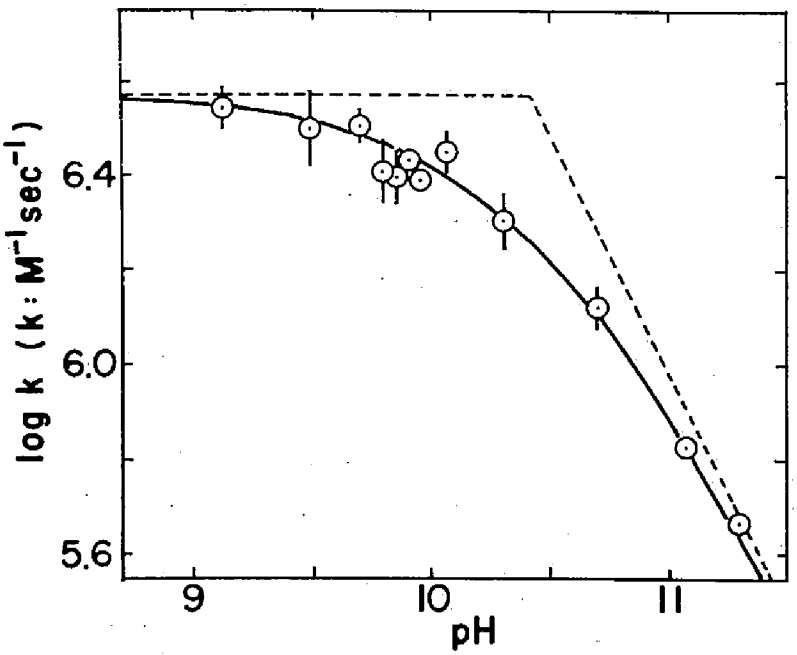

Fig. 7.11. pH-Dependence of the second-order rate constants of the binding of SSI and subtilisin BPN' in 25 mM carbonate buffer, ionic strength 0.1 M (NaCl), at 25.0°C. The solid line is the theoretical curve drawn according to Eq. 7.10 with a pK_a value of 10.40 and $\tilde{k}$ = 3.80 x 10^6 $M^{-1}sec^{-1}$.

---

binding kinetics between subtilisin BPN' and SSI.

7.4 Discussion

Solvent perturbation difference spectroscopy. It can be deduced from the solvent perturbation study with ethylene glycol that four or five tyrosyl residues out of ten exposed tyrosyl residues (of total 13 residues) and one tryptophyl residue out of total four in a molecule of SSI monomer (I_1) and subtilisin BPN' (E_1) are located at or near the binding sites of the two proteins. Only one tyrosyl residue among those five at the binding region could be approached by methanol.

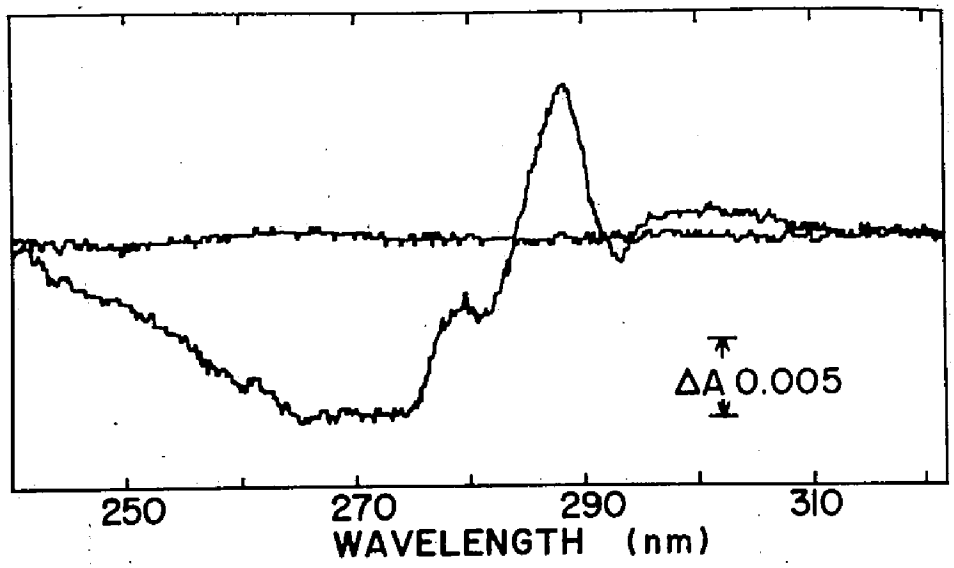

Fig. 7.12. Ultraviolet absorption difference spectrum observed on the binding of subtilisin BPN' and SSI at pH 7.00. [subtilisin BPN']$_o$ = 20.8 μM; [SSI monomer]$_o$ = 41.0 μM, in 25 mM phosphate buffer, pH 7.00, ionic strength 0.1 M (NaCl), 25.0°C. (refer also to Figs. 2.6 and 7.3)

Difference spectroscopy of the binding between subtilisin BPN' and SSI at alkaline pH. From the difference spectrum observed on the binding of subtilisin BPN' and SSI (Fig. 7.3), it is suggested that apparently one tyrosyl residue of pK_a 9.7 ("normal" tyrosyl residue) in either SSI or the enzyme undergoes a change from the half-ionized to the completely protonated form on the binding at pH 9.70. In order to determine whether really only one tyrosyl residue is subjected to the pK_a shift or a sum of the changes of more than one residue comes up to a value corresponding to the change of one residue, the difference spectra on the binding of subtilisin BPN' and SSI were measured at various pH's (plot (a) in Fig. 7.4). In the region of pH 8.4 - 10.2 the changes in the ionization of only the tyrosyl residues of pK_a 9.7 among those shown in Table 7.2 should be selectively observed. Five tyrosyl residues of

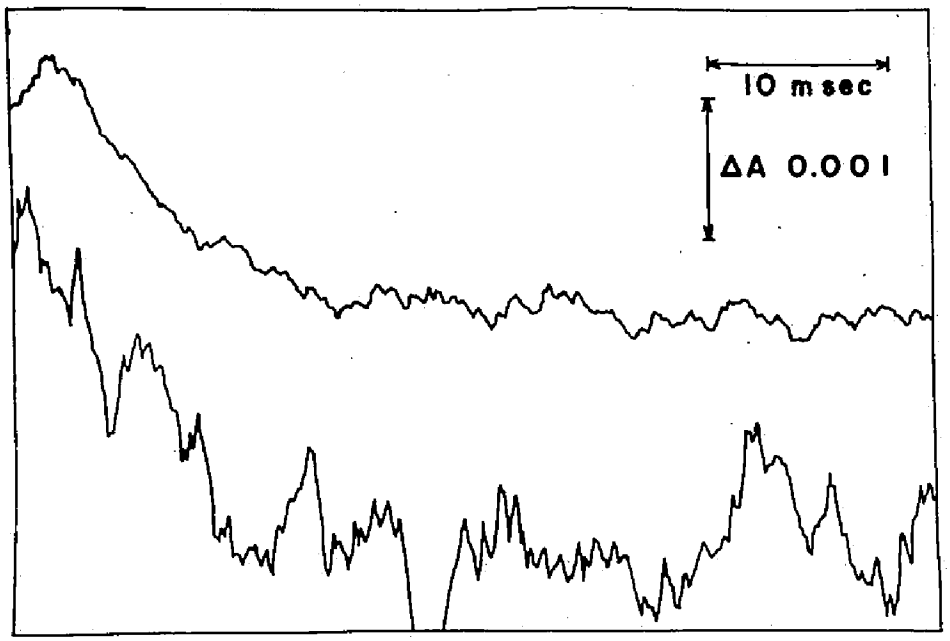

Fig. 7.13. Stopped-flow oscillograms of a time course of absorbance change at 288 nm on the binding of subtilisin BPN' and SSI at pH 7.00. [subtilisin BPN']$_o$ = 11.2 μM; [SSI monomer]$_o$ = 45.7 μM, in 25 mM phosphate buffer, pH 7.00, ionic strength 0.1 M (NaCl), 25.0°C. Lower curve: a single scanning. Upper curve: an average of 14 times accumulated scannings.

---

subtilisin BPN' (E_1) and one residue of SSI monomer (I_1) have pK_a 9.7, and accordingly six residues out of the total 13 tyrosyl residues in the complex (E_1I_1) would be half-ionized and the others be fully protonated at pH 9.70, if simple additivity is applicable. A theoretical pH-titration curve can be drawn for these supposedly six "normal" tyrosyl residues in the complex (E_1I_1) as shown in Fig. 7.4 (curve b). The true titration curve of "normal" tyrosyl residues in the complex (E_1I_1) can be obtained, therefore, by subtracting $\Delta\varepsilon$ value of plot (a) in Fig. 7.4 from that of curve (b). The difference is shown as plot (c) in Fig. 7.4. The titration data shown in plots (a) and (c) in Fig. 7.4 were

analyzed by a linear plotting ($\Delta\varepsilon[H^+]$ vs. $\Delta\varepsilon$; Eq. 6.1) according to the method described previously (Experimental Procedures 6.2, *Analysis of titration data*). The number of tyrosyl residues with a pK_a value which is indicated by the slope of the plot ($\Delta\varepsilon_{245}[H^+]$ vs. $\Delta\varepsilon_{245}$) can be given by dividing the value of intercept on the abscissa, $\Delta\varepsilon_{245}^{max}$, by the molar absorptivity difference for the ionization of a tyrosyl residue ($\Delta\varepsilon_{245}$ = 10.66×10^3 $M^{-1}cm^{-1}$; see Chapter Six). In Fig. 7.5, a, $\Delta\varepsilon_{245}[H^+]$ are plotted against $\Delta\varepsilon_{245}$ using the values of plot (a) in Fig. 7.4. This linear plot corresponds to the titration curve of 1.2 tyrosyl residues with pK_a 9.58. Thus we may expect a titration curve of five "normal" tyrosyl residues for plot (c) in Fig. 7.4. The plot shown in Fig. 7.5, b, which was drawn by using the values of plot (c) in Fig. 7.4, actually showed that it corresponds to a titration curve of 5.1 tyrosyl residues with pK_a 9.76. It has been shown, therefore, that one "normal" tyrosyl residue must have turned into untitrable at the pH region examined (pH 8.4 - 10.2) due to a pK_a shift probably to above 11.5.

That the similar difference spectra due to change in the protonation of a tyrosyl residue were observed on the binding of SSI with subtilisin BPN' and subtilisin Carlsberg but not with α-chymotrypsin or trypsin suggests the similarity in the active site structure between the two subtilisins. It may be related in some way to the remarkable difference in K_i values of SSI against α-chymotrypsin (3.0×10^{-6} M), trypsin (1.1×10^{-4} M), and subtilisin BPN' (3×10^{-10} - 7×10^{-11}) (see Chapters Two and Five).

Kinetics of association between subtilisin BPN' and SSI. The large absorptivity difference at 245 nm due to the pK_a shift of tyrosyl residues upon the binding of the two proteins is an excellent probe for

monitoring the reaction with a stopped-flow apparatus (Fig. 7.8). This is much more superior to the small absorptivity differences in 260 - 300 nm region observed at neutral pH (Fig. 7.12), which have been used for the kinetic studies in the case of the interaction between trypsin and soybean trypsin inhibitor (Kunitz) (*132*). The only limitation of this difference spectrum by tyrosine ionization is that it cannot be used at lower pH region, for which the fluorescence method has been successfully employed in the case of SSI and subtilisin BPN' (Uehara, Y., Tonomura, B., and Hiromi, K., unpublished results).

The second-order rate constants obtained in the present study, k = 4×10^6 - 5×10^5 $M^{-1}sec^{-1}$ at pH 9.0 - 11.3, are in the order of magnitude of the rate constants obtained for the association between some other proteinases and their specific protein inhibitors: e.g., bovine β-trypsin and bovine basic pancreatic trypsin inhibitor (*133*), bovine α-chymotrypsin and bovine basic pancreatic trypsin inhibitor (*114*), and trypsin or chymotrypsin and pancreatic trypsin inhibitors (Kunitz and Kazal) (*134*). These values may be considered to be those of a diffusion controlled reaction (*135*), if the effective fractions of surface area involved in the specific interaction of the two proteins (estimated to be between 1 and 3%) are taken into consideration. If a reaction occurs every time there is an encounter and subsequent collisions no longer contribute to the reaction, it is called a diffusion-controlled reaction. For the case of uncharged molecules in solution, the encounter rate constant, k_e, can be calculated from

$$k_e = \frac{4\pi N(D_A + D_B)(r_A + r_B)}{1{,}000} \quad M^{-1}sec^{-1} \qquad (7.9)$$

The units are those of a second-order reaction, N is Avogadro's number,

and D and r are the diffusion constants and reaction radii of molecules A and B, respectively. For subtilisin BPN' and SSI dimer, $D_{20,w}$ were determined to be 9.04 x 10^{-7} cm^2/sec (*131*) and 9.32 x 10^{-7} cm^2/sec (*49*), respectively; and respective values of r are calculated to be 21.7 A and 20.4 A, assuming the molecules to be sphere. For the E_1I_2 complex, $D_{20,w}$ and r were calculated to be 7.16 x 10^{-7} cm^2/sec and 24.4 A, respectively. According to Eq. 7.9, k_e for the binding: $E + I_2 \longrightarrow E_1I_2$ is calculated to be 5.9 x 10^9 $M^{-1}sec^{-1}$, and that for the binding: $E + E_1I_2 \longrightarrow E_2I_2$ to be 5.6 x 10^9 $M^{-1}sec^{-1}$. As the maximum value of the second-order rate constant for the binding of SSI and subtilisin BPN' is 4 x 10^6 $M^{-1}sec^{-1}$, the effective fraction of surface area for the binding can be estimated to be 3% for each protein. This value, 3%, of the effective fraction is in good agreement with that estimated by the author based on the results of the X-ray crystallographic study on the complex of porcine trypsin and soybean trypsin inhibitor (Kunitz) (*11*).

The pH-dependence of the binding rate constant, k (Fig. 7.11), is consistent with the following equation:

$$k = \tilde{k} \frac{1}{1 + \frac{K_a}{[H^+]}} \qquad (7.10)$$

where $\tilde{k}$ is a pH independent rate constant. The result suggests that an amino acid residue with pK_a 10.4 participates directly in controlling the binding rate. The amino acid could be a tyrosyl residue in either subtilisin BPN' and SSI.

Tyrosyl residues have been postulated to be involved, through hydrogen bonding, or hydrophobic interactions, in the intermolecular interactions between proteins: tabacco-mosaic-virus protomers (*136-138*),

the leuteinizing hormone (*139*), Bence-Jones protein protomers (Rei) (*140*), the flagellin subunits (*141*), and trypsin and soybean trypsin inhibitor (Kunitz) (*142*).

In the case of the binding of subtilisin BPN' and SSI, evidence has been obtained in this study that a tryptophyl residue and about five tyrosyl residues are in or near the contact area of the two proteins, and that one of the latter with pK_a 9.7 is directly involved on the binding. At the present stage, it remains to be clarified whether or not this tyrosyl residue is identical with the one that changes the extent of accessibility to methanol molecule, or the ionizable group having pK_a = 10.4 that affect the binding rate constant.

7.5 Summary

Changes in the states of tyrosyl and tryptophyl residues on the formation of a complex between subtilisin BPN' and *Streptomyces* subtilisin inhibitor, SSI, were studied. The solvent perturbation study with ethylene glycol and methanol as perturbant showed that, on the complex formation, a tryptophyl and about five tyrosyl residues become inaccessible to ethylene glycol, and a tryptophyl and a tyrosyl residues to the smaller perturbant, methanol. The ultraviolet absorption difference spectra at 245 nm observed at alkaline pH indicated that a tyrosyl residue of either one of the two proteins shifted its pK_a value considerably upwards (9.7 $\longrightarrow$ > 11.5) on the complex formation. The kinetics of association of these two protein molecules were studied with the difference absorbance mentioned above as monitoring probe. A typical bimolecular reaction was observed in the protein concentration range, 2.61 μM -

127 μM; and the second-order rate constant of association was 3.1×10^6 $M^{-1}sec^{-1}$ at pH 9.70. The pH-dependence of the second-order rate constants suggested the involvement of a residue with pK_a 10.4 in the association.

Chapter Eight

The Interaction of Carboxyl Groups and a Tyrosyl Residue in the Specific Interaction between *Streptomyces* Subtilisin Inhibitor and Subtilisin BPN' —— Chemical Modification Studies *

8.1 Introduction

In the previous Chapter, it was suggested that there are four or five tyrosyl residues at or near the binding sites of SSI and subtilisin BPN' from the solvent perturbation study with ethylene glycol. An absorption difference spectra characteristic of protonation of tyrosyl residues was observed on the complex formation between subtilisin BPN' and SSI at alkaline pH, and it was indicated that a tyrosyl residue in either one of the two proteins shifts its pK_a value considerably upwards (pK_a 9.7 $\longrightarrow$ > 11.5). This difference spectra may serve as a clue to elucidate the molecular mechanism of the interaction between subtilisin BPN' and SSI.

The present work was initiated in order to determine in which protein, SSI or subtilisin BPN', the tyrosyl residue in question exists and what kind of functional group are responsible for the pK_a shift. Chemical modification methods perturbing the ionization states of tyrosyl residues and carboxyl groups are considered useful for this purpose.

---

* A part of this study was presented at the Annual Meeting of the Japanese Biochemical Society (Sapporo, September 1976) (*h*).

8.2 Experimental Procedures

Proteins. A three times crystallized and lyophilized preparation of SSI was a generous gift from Professor S. Murao. Three times crystallized and lyophilized preparation of subtilisin BPN' [EC 3.4.21.14] (Lot No. 7370935) and subtilisin Carlsberg [EC 3.4.21.14] (Lot No. 28B-2340) were purchased from Nagase & Co. Ltd. and Sigma Chemical Co., respectively, and their respective purities were determined to be 80.9% and 92.7% by the method previously described (Experimental Procedures 2.2). Their concentrations were determined spectrophotometrically at pH 7.00 using the absorptivity coefficients and molecular weights shown in Experimental Procedures 7.2.

Chemicals. 3-Nitrotyrosine was obtained from Aldrich Chemical Co., Milwaukee, *p*-nitrophenyl acetate (pNPA) was from Tokyo Kasei Kogyo Ltd. Co., and tetranitromethane (TNM), 1-ethyl-3-(3-dimethylaminopropyl) carbodiimide (EDPC), 1-cyclohexyl-3-(2-morpholinoethyl) carbodiimide metho *p*-toluenesulfonate (CMEC), glycine methyl ester, and other chemicals of analytical reagent or better grade were from Nakarai Chemicals Ltd., Kyoto.

Amino acid analyses. Amino acid analyses were performed with a Hitachi KLA-3 amino acid analyzer according to the procedure of Spackman *et al.* (*143*) following hydrolysis with 6 M boiling HCl in evaculated sealed tubes at 110°C for 22 hr. For the determination of tryptophan the protein was hydrolyzed in the presence of 4% thioglycolic acid by the same procedure as above (*144*).

Inhibitory activity measurement. Inhibitory activities of native and chemically modified SSI's towards subtilisin BPN' were measured as

described in Experimental Procedures 5.2, using pNPA as substrate with a Shimadzu UV-200 recording spectrophotometer in 25 mM phosphate buffer, pH 7.00, ionic strength 0.1 M (NaCl), containing 5.0% isopropanol, 25.0 °C.

Inhibitor constant, K_i, of SSI and its derivatives against subtilisin BPN' were determined according to the following equations describing the steady-state kinetics of an enzyme with tightly bound inhibitors (*41,145*) (see Chapter Two).

$$E + S \underset{k_{-1}}{\overset{k_1}{\rightleftharpoons}} ES \xrightarrow{k_2} E + P$$

$$E + I \underset{k_{-3}}{\overset{k_3}{\rightleftharpoons}} EI$$

Kinetic parameters were defined as follows:

$$K_i = \frac{[E] \cdot [I]}{[EI]} = \frac{k_{-3}}{k_3}, \qquad K_m = \frac{k_{-1} + k_2}{k_1}$$

$$\alpha = \frac{v_i}{v_o}$$

Thus, we have:

$$K_i = \frac{\alpha}{1 - \alpha} \cdot \frac{K_m}{s_o + K_m} \{i_o - e_o(1 - \alpha)\}$$

where e_o, i_o, and s_o are the initial concentrations of enzyme, inhibitor, and substrate, respectively; K_m is the Michaelis constant; v_o and v_i are the initial velocities without and with inhibitor, respectively. The slope of the plot, $\{i_o / (1 - \alpha)\}$ vs. $\{(1 + s_o/K_m) / \alpha\}$, gives the K_i value.

Nitration of SSI and subtilisin BPN' with tetranitromethane. Nitration of SSI and subtilisin BPN' was carried out by adding a suitable aliquot of a 0.65 M ethanolic TNM solution to protein solution (5 -

20 mg/ml) in 50 mM Tris-HCl buffer, pH 8.0. The reaction mixture was kept at 25°C for a suitable period and the reaction was stopped by gel filtration on a Bio-Gel P-4 column equilibrated with the same buffer or with 25 mM carbonate buffer, pH 9.7, ionic strength 0.1 M (NaCl). The degree of nitration was determined by amino acid analysis or by absorbance at 381 nm using the molar absorptivity of 2,200 $M^{-1}cm^{-1}$ (*146*).

Modification of carboxyl groups of SSI with water soluble carbodiimide. SSI (ca. 10 mg/ml) and glycine methyl ester hydrochloride were dissolved in 0.1 M NaCl aqueous solution, and the pH of the solution was immediately adjusted to 6.5 with HCl and NaOH. The reaction was initiated by addition of either 1-cyclohexyl-3-(2-morpholinoethyl) carbodiimide metho *p*-toluenesulfonate (CMEC) or 1-ethyl-3-(3-dimethylaminopropyl) carbodiimide (EDPC) of respective concentration of 0.10 M or 0.13 M. The reaction mixture was kept at 25°C for a suitable period. The pH of the mixture did not alter during the reaction. The mixture was then subjected to dialysis against 0.10 M NaCl aqueous solution at pH 7.0 to remove excess reagents at 5°C. The number of glycyl residues incorporated was determined by amino acid analysis.

Polyacrylamide gel electrophoresis. In order to determine homogeneity and molecular weights of the modified proteins, polyacryl amide gel electrophoresis under denaturating conditions (sodium dodecyl sulfate plus 2-mercaptoethanol) was carried out according to Weber and Osborn (*147*).

Gel chromatography. Gel chromatography to estimate molecular weights of the modified proteins was performed according to Andrews (*148*) on a column (100 x 1.6 cm) of Sephadex G-100, calibrated with standard proteins, equilibrated with 25 mM phosphate buffer, pH 7.0,

ionic strength 0.1 M (NaCl).

Ultraviolet absorption difference spectroscopy. Ultraviolet absorption difference spectra observed on the binding between native or modified SSI and native or modified subtilisin BPN' were measured as described in Experimental Procedures 7.2 with a Shimadzu UV-200 recording spectrophotometer in 25 mM carbonate buffer, pH 9.70, ionic strength 0.1 M (NaCl), or in 25 mM pyrophosphate buffer, pH 8.00, ionic strength 0.1 M (NaCl), 25.0°C.

As demonstrated in Chapter Seven, this difference spectrum results from the shift of ionization state of a tyrosyl residue of pK_a 9.7 either in SSI or in subtilisin BPN' to the fully protonated state on the interaction between the both proteins. Here, the number, n, of tyrosyl residues whose ionization states were converted from ionized to protonated ones on the interaction between SSI (or modified SSI) and subtilisin BPN' (or modified subtilisin BPN') was evaluated from the difference absorbance at 245 nm. In the case of interaction between carboxyl-group-modified SSI and subtilisin BPN', n value was calculated using the molar absorptivity difference, $\Delta\varepsilon_{245} = 1.066 \times 10^4\ M^{-1}cm^{-1}$, obtained for the ionization of *N*-acetyl-L-tyrosine ethyl ester (Results 7.3). In the cases of the interaction between nitrated SSI and subtilisin BPN' and that between SSI and nitrated subtilisin BPN', there should be contribution in the absorbance difference at 245 nm from 3-nitrotyrosyl residues in addition to that from tyrosyl residues. Figure 8.1 shows a difference spectrum of 3-nitrotyrosine in aqueous solution at pH 5.56 against pH 6.90. From the pH-dependence of the difference spectra, the molar absorptivity differences, $\Delta\varepsilon$, at 245 nm and 427 nm for the ionization of 3-nitrotyrosine were determined to be $7.56 \times 10^3\ M^{-1}cm^{-1}$ and

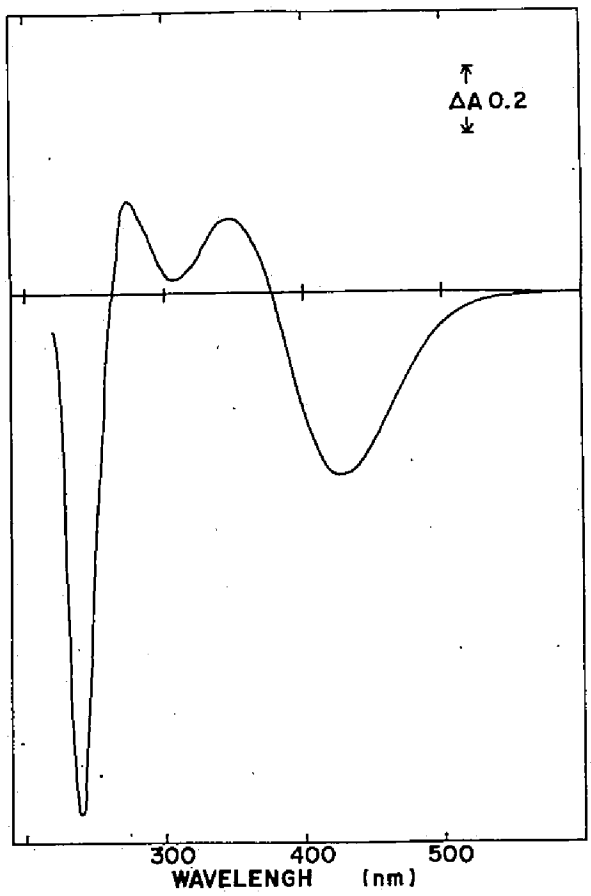

Fig. 8.1. Absorption difference spectrum of 3-nitrotyrosine produced due to the difference in pH. $[3\text{-nitrotyrosine}]_o$ =27.6 μM. Sample solution, pH 5.56; reference solution, pH 6.90, in 0.1 M NaCl aqueous solution, 25.0°C. The value of pK_a of 3-nitrotyrosine was determined to be 6.83.

2.63×10^3 $M^{-1}cm^{-1}$, respectively, and the pK_a value was determined to be 6.83. Using these values, the absorptivity difference at 245 nm due to the ionization of tyrosyl residues was estimated separately.

8.3 Results

Nitration of SSI. At 1.5 hr after the addition of a 200 fold

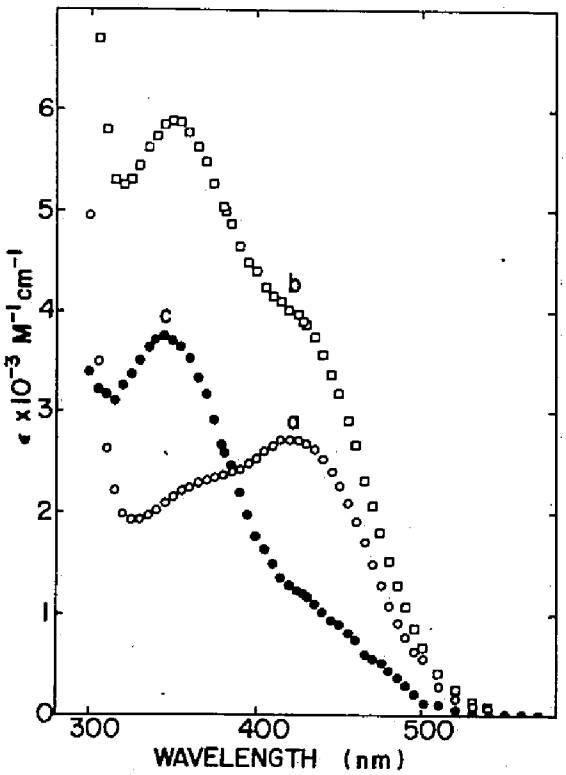

Fig. 8.2. Absorption spectra of the tyrosyl-residues-nitrated SSI derivatives in visible region in 25 mM pyrophosphate buffer, pH 8.00, ionic strength 0.1 M (NaCl), 25.0°C. (a) one-tyrosyl-residue-nitrated SSI; (b) two-tyrosyl-residue-nitrated SSI; (c) absorption spectrum obtained subtracting (a) from (b), which is corresponding to the absorption spectrum of a nitrotyrosyl residue secondarily modified. The pK_a values of the nitrotyrosyl residues of primarily and secondarily nitrated were estimated to be 7.95 ± 0.11, and 8.56 ± 0.10, respectively.

---

excess of TNM to a 0.46 mM solution of SSI monomer in 50 mM Tris-HCl buffer, pH 8.0, 25°C, 1.1 out of three tyrosyl residues of the protein were converted to 3-nitrotyrosyl residues, and at 20 hr after, 2.3 residues were converted. Figure 8.2 shows the absorption spectra of (a) 1.1-tyrosyl-residue-nitrated SSI, (b) 2.3-tyrosyl-residue-nitrated SSI, and (c) the difference spectrum between (a) and (b). Spectrum (a)

is considered to be the absorption spectrum of the mono-nitrotyrosyl residue modified first, and spectrum (c) is that of the mono-nitrotyrosyl residue modified second. From these spectra, the pK_a values of the nitrotyrosyl residues were calculated to be 7.95 ± 0.11 for spectrum (a) and 8.56 ± 0.10 for spectrum (c) in comparison with the spectrum of model compound, 3-nitrotyrosine (Fig. 8.1, pK_a 6.83), using the values: $\varepsilon_{427} = 4.10 \times 10^3\ M^{-1}cm^{-1}$ at absorption maximum of nitrophenolate ion, $\varepsilon_{360} = 2.79 \times 10^3\ M^{-1}cm^{-1}$ at absorption maximum of unionized nitrophenol, and $\varepsilon_{381} = 2.20 \times 10^3\ M^{-1}cm^{-1}$ at the isosbestic point.

It has been reported that native SSI is composed of two identical subunits under the usual conditions, and gel filtration on a Sephadex G-100 column and SDS-polyacrylamide gel electrophoresis of SSI give molecular weights of 23,000 (dimer) and 11,500 (monomer), respectively (see Chapter Three). One-tyrosyl-residue-nitrated SSI shows the same pattern in the gel filtration and the electrophoresis. Gel filtration of two-tyrosyl-residue-nitrated SSI, however, shows two main bands of molecular weights of 69,000 and 23,000 in the ratio of 4 : 3 in protein amount, and SDS-disc electrophoresis shows three bands of molecular weights of 45,000, 23,000, and 11,500. By densitometry with a Shimadzu CS-9000 dual-wavelength TLC scanner, the ratio of the protein amount of the three bands was determined as 2 : 5 : 10. The molecular sizes determined above demonstrate that the most reactive tyrosyl residue of SSI monomer can be nitrated without polymerization, but that the nitration of the second-reactive residue is accompanied with polymerization of SSI probably due to the internal cross-linking by TNM.

Absorption difference spectra observed on the binding of nitrated SSI and subtilisin BPN'. Figure 8.3 shows the absorption difference

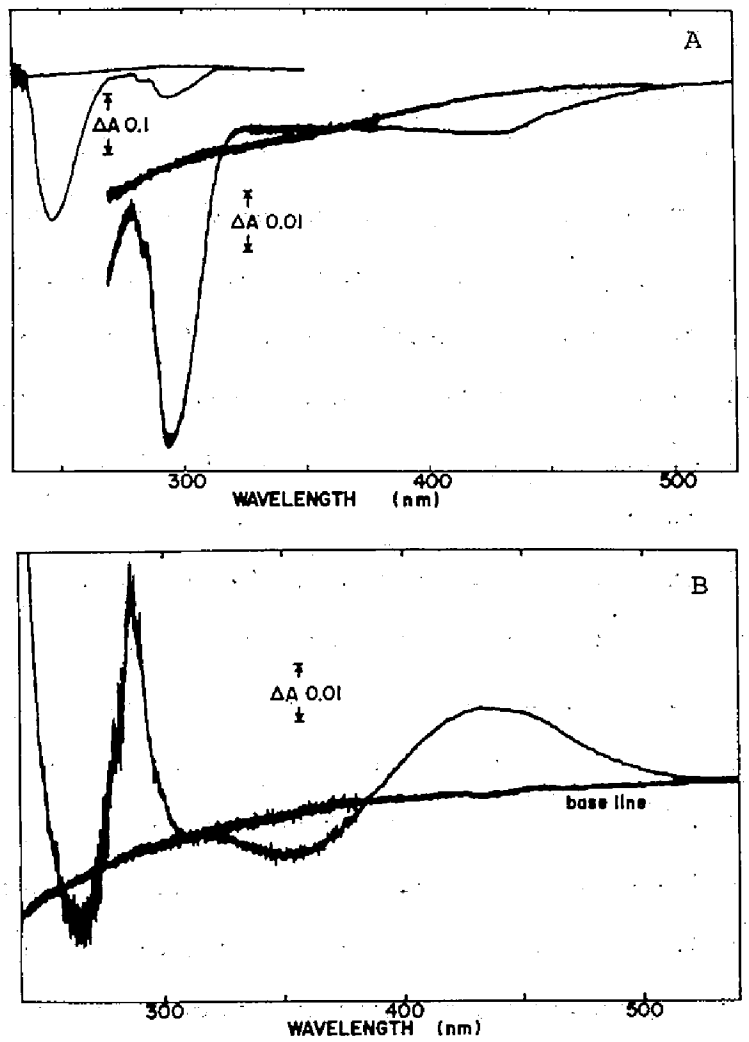

Fig. 8.3. Difference spectra observed on the binding of tyrosyl-residue-nitrated SSI and subtilisin BPN'. (A) [subtilisin BPN']$_o$ = 24.2 μM; [one-tyrosyl-residue-nitrated SSI monomer]$_o$ = 28.1 μM, in 25 mM carbonate buffer, pH 9.70, ionic strength 0.1 M (NaCl), 25.0°C. (B) [subtilisin BPN']$_o$ = 31.9 μM, [one-tyrosyl-residue-nitrated SSI monomer]$_o$ = 66.2 μM, in 25 mM pyrophosphate buffer, pH 8.00, ionic strength 0.1 M (NaCl), 25.0°C.

---

spectra observed on the binding of one-tyrosyl-residue-nitrated SSI and subtilisin BPN' at (A) pH 9.70 and (B) pH 8.00. The molar absorptivity

difference at 245 nm, $\Delta\varepsilon_{245}$, of spectrum (A) was - 7.21 x 10^3 $M^{-1}cm^{-1}$, which corresponds to that of 1.1 tyrosyl residue of pK_a 9.70 shifted to the completely protonated state. Absorptivity differences at 428 nm and 360 nm demonstrates that the pK_a of the nitrotyrosyl residue (7.95 ± 0.11) shifts up to pK_a 8.60 on the formation of enzyme-inhibitor complex. On the other hand, the direction of the difference absorptivities in spectrum (B) at 428 nm and 360 nm are inverted in comparison with those of spectrum (A). This shows that the pK_a of the nitrotyrosyl residue shifts down to pK_a 7.77.

The difference spectra observed on the binding between two-tyrosyl-residue-nitrated SSI and subtilisin BPN' were measured at pH 9.70 and pH 8.00. They are almost the same as those obtained with one-tyrosyl-residue-nitrated SSI (Figure not shown). $\Delta\varepsilon_{245}$ was determined to be - 7.49 x 10^3 $M^{-1}cm^{-1}$ from the spectrum observed at pH 9.70.

These results shown here indicate that the microenvironment of a nitrotyrosyl residue changes on the formation of enzyme-inhibitor complex, and the inversive direction in the absorptivity differences at pH 9.70 and pH 8.00 shows the difference in the environment of the nitrotyrosyl residue at these pH's. It should be noticed, however, that a large upward pK_a-shift of a tyrosyl residue of pK_a 9.7 was observed at either pH.

Nitration of subtilisin BPN' and difference spectra on the binding between SSI and nitrated subtilisin BPN'. The modification conditions and the results are summarized in Table 8.1. These nitrated enzyme derivatives show no remarkable changes in hydrolizing activity towards pNPA (k_{cat} = 2.58 ± 0.22 min^{-1}, K_m = (3.40 ± 0.33) x 10^{-4} M in 25 mM phosphate buffer, pH 7.0, ionic strength 0.1 M (NaCl), 25.0°C).

Table 8.1. Nitration of tyrosyl residues of subtilisin BPN' with tetranitromethane (TNM).[a]

$\frac{[TNM]_o}{[S.\ BPN']_o}$ (M/M)	Reaction time (hr)	# of nitrated Tyr	n
		0	1.1
56	0.5	0.5	1.1
56	1.0	0.8	0.9
218	0.5	1.8	0.8
218	1.5	4.1	0.4
218	3.0	6.7	0.0

[a] Nitration was carried out at pH 8.0, 25°C in 50 mM %ris-HCl buffer solution. $[subtilisin\ BPN']_o$ = 0.285 mM.

n : number of tyrosyl residues of pK_a 9.7 which are converted to fully unionized form on the complex formation at pH 9.70, 25.0°C.

Svendsen (*129*) reported that even 8.2 out of 10 tyrosyl residues can be nitrated without loss of activity towards protein and synthetic substrates.

The difference spectra observed on the binding between SSI and nitrated subtilisin BPN' at pH 9.70 are shown in Fig. 8.4. As the degree of nitration of tyrosyl residues increased, the molar absorptivity difference at 245 nm decreased and the one at 428 nm increased. Finally with 6.7 tyrosyl residues nitrated, the difference spectrum shows only the changes in nitrotyrosyl residues (as Fig. 8.1), and the contribution of tyrosyl residues has disappeared. The results shown here strongly suggest that the tyrosyl residue of pK_a 9.7, which converts itself to fully protonated form on the formation of the enzyme-inhibitor complex, is one of the five tyrosyl residues of pK_a 9.7 of subtilisin BPN'.

Modification of carboxyl groups of SSI with water-soluble carbodi-

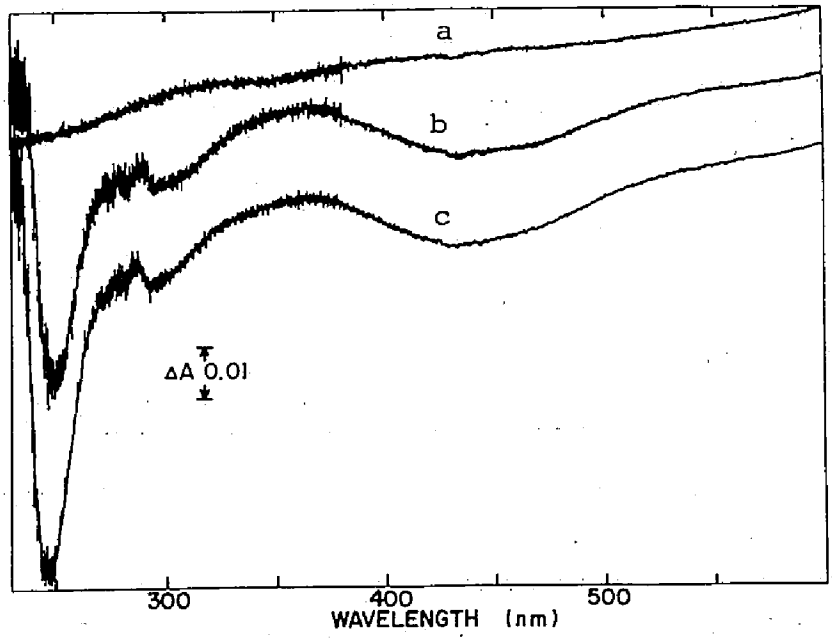

Fig. 8.4. Difference spectra observed on the binding of SSI and tyrosyl-residue-nitrated subtilisin BPN' derivative. [tyrosyl-residue-nitrated subtilisin BPN']$_o$ = 15.2 μM; [SSI monomer]$_o$ = 44.9 μM, in 25 mM carbonate buffer, pH 9.70, ionic strength 0.1 M (NaCl), 25.0°C. (a) base line. (b) 6.7; (c) 4.1 tyrosyl residues of subtilisin BPN' are nitrated.

---

imide. The effect of electrostatic field on the difference spectra upon the binding of SSI and subtilisin BPN' was examined through modification of carboxyl groups by binding covalently glycine methyl ester with the aid of water-soluble carbodiimide. There are 12 carboxyl groups (6 aspartyl and 5 glutamyl residues and a carboxyl terminus) and 10 glycyl residues in a monomeric SSI (Fig. 1.1) (*27*). The modification conditions and the results are shown in Table 8.2. Behaviors of the SSI derivatives on Sephadex G-100 gel filtration and SDS-polyacrylamide gel electrophoresis are the same as those of native SSI. The difference spectra observed on the binding between subtilisin BPN' and carboxyl-

Table 8.2. Blocking of carboxyl groups of SSI with glycine methyl ester (GME) using water-soluble carbodiimide (WSC).[a]

$[SSI]_o$ (M)	GME (M)	WSC (M)	Reaction time (hr)	# of blocked carboxyls	n
				0	1.1
2.61×10^{-4}	0.25	CMEC 0.10	2.0	3.3	1.1
0.82×10^{-4}	0.25	CMEC 0.10	22.0	4.7	0.5
1.70×10^{-4}	0.33	EDPC 0.13	3.0	4.0	0.8
1.70×10^{-4}	0.33	EDPC 0.13	6.0	5.3	0

[a] Chemical modification was carried out at pH 6.5, 25°C in 0.1 M NaCl aqueous solution. CMEC: 1-cyclohexyl-3-(2-morpholinoethyl) carbodiimide metho *p*-toluene sulfate. EDPC: 1-ethyl-3-(3-dimethylaminopropyl) carbodiimide. n: number of tyrosyl residues of pK_a 9.7 which are converted to fully unionized form on the complex formation at pH 9.70, 25.0°C.

group-modified SSI at pH 9.70 are shown in Fig. 8.5. The difference spectra were measured quickly (within 15 min) after adjusting pH of the solution to 9.70 to avoid alkaline hydrolysis of the glycine methyl esters blocking carboxyl groups of SSI; the rate constant, k, of the alkaline hydrolysis was determined to be 4.6×10^{-5} sec^{-1} ($t_{1/2}$ = 250 min). As the modification of carboxyl groups proceeds, the molar absorptivity differences at 245 nm are decreased. The difference spectrum obtained with 5.3-carboxyl-group-modified SSI is almost the same as that observed on the binding between native SSI and subtilisin BPN' at pH 7.0 (Figs. 2.6 and 7.12), and the number of tyrosyl residues of pK_a 9.7 which are converted to fully unionized form on the complex formation, the n value, was calculated to be zero.

The difference spectrum produced on the binding between subtilisin

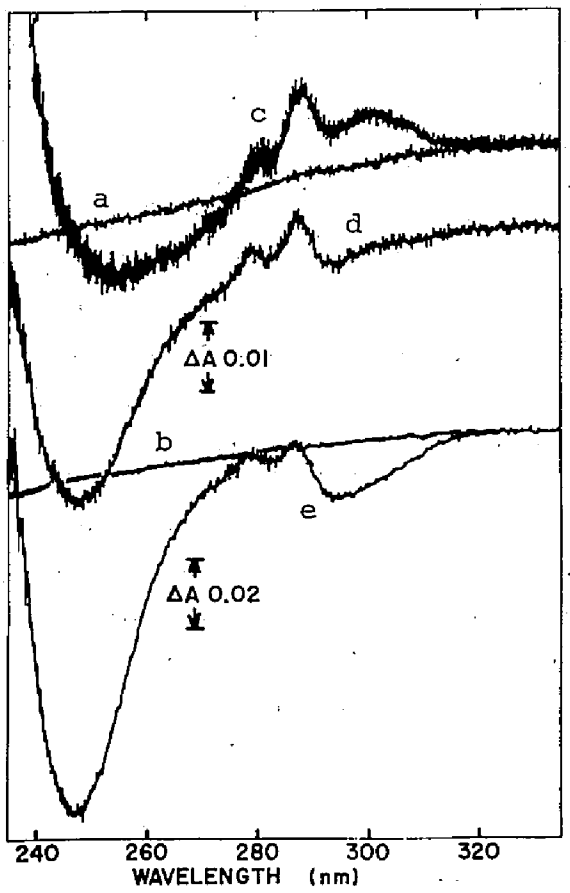

Fig. 8.5. Difference spectra observed on the binding of subtilisin BPN' and carboxyl-group-modified SSI. [subtilisin BPN']$_o$ = 16.8 μM; [carboxyl-group-modified SSI monomer]$_o$ = 27.6 μM, in 25 mM carbonate buffer, pH 9.70, ionic strength 0.1 M (NaCl), 25.0°C. (a), base line for spectra (c) and (d); (b), base line for spectrum (e). (c) 5.3; (d) 4.7; (e) 3.3 carboxyl groups of SSI monomer are modified.

BPN' and 5.3-carboxyl-group-modified SSI was also measured at pH 9.70 after incubating the SSI derivative at the same pH, 25.0°C for 12 hr (Figure not shown). Under these conditions, 5.3 glycine methyl esters incorporated into SSI must have been hydrolysed as follows:

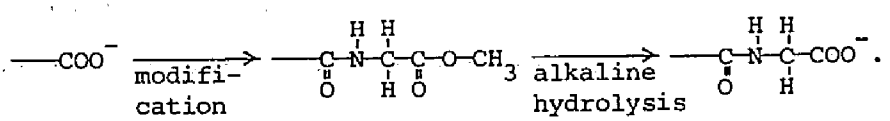

And there should appear again 5.3 carboxyl groups of glycyl residues. The difference spectrum gives the n value of 0.6. The fractional value of n may be due to the steric hindrance by the glycyl residues coupled.

The difference spectrum measured immediately after the binding

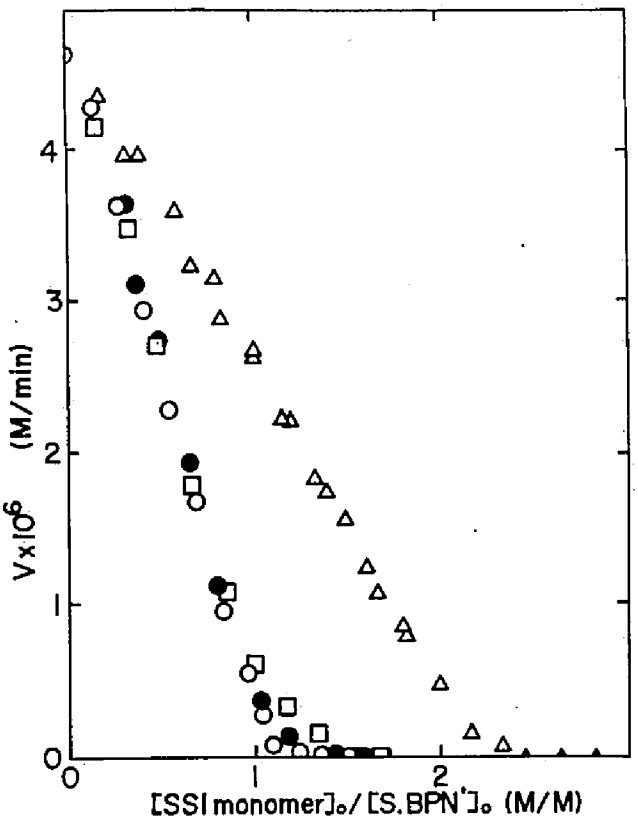

Fig. 8.6. Inhibition of subtilisin BPN'-catalyzed hydrolysis of *p*-nitrophenyl acetate by chemically modified SSI derivatives. [subtilisin BPN']$_0$ = 74.0 μM; [pNPA]$_0$ = 0.502 mM; SSI: native SSI (open circle); one-tyrosyl-residue-nitrated SSI (closed circle); two-tyrosyl-residue-nitrated SSI (open triangle); 5.3-carboxyl-group-modified SSI (open square), in 25 mM phosphate buffer, pH 7.00, ionic strength 0.1 M (NaCl), containing 5.0% (v/v) isopropanol, 25.0°C.

---

between 5.3-carboxyl-group-modified SSI and subtilisin Carlsberg at pH 9.70 and the one measured with the SSI derivative incubated 12 hr at pH 9.70 give the n value of zero and 0.5, respectively.

The results suggest that the negative charges of carboxyl group(s) in SSI are involved in the upward pK_a-shift of a tyrosyl residue of subtilisin BPN' or subtilisin Carlsberg on their interaction.

Inhibitory activities of chemically modified SSI derivatives. Figure 8.6 shows the inhibitory activities of native SSI, one-tyrosyl-residue-nitrated SSI, two-tyrosyl-residue-nitrated SSI, and 5.3-carboxyl-group-modified SSI against subtilisin BPN' activity using pNPA as substrate (K_m = 4.98 x 10^{-4} M at pH 7.0, 25.0°C). Except for the two-tyrosyl-residue-nitrated SSI, the inhibitory stoichiometry is 1 : 1 (M/H) with inhibitor costants, K_i, of (3.8 ± 1.5) x 10^{-10} M for native SSI, (7.8 ± 2.0) x 10^{-10} M for one-tyrosyl-residue-nitrated SSI, and (4.5 ± 0.6) x 10^{-9} M for 5.3-carboxyl-group-modified SSI. Two-tyrosyl-residue-nitrated SSI has an unusual stoichiometry. This unusual stoichiometry seems to correspond to the decrease of the reactive site of SSI against subtilisin BPN' due to the polymerization of SSI by TNM.

8.4 Discussion

Nitration of SSI. There are three tyrosyl residues (Tyr 7, Tyr 75, and Tyr 93) in SSI monomer (*27*). All of them are located on the molecular surface according to the results of solvent perturbation difference spectroscopy, and their pK_a values are determined to be 9.66, 11.02, and 12.33 by spectrophotometric titration at alkaline pH (Chapter Six). Tyr 75 locates near the reactive site of SSI towards α-chymotrypsin, i.e., Met 73 - Val 74 (*27*). By X-ray crystallographic study of SSI at 2.3 Å resolution, it was shown that Tyr 93 is near the contact region of subunits, and Tyr 7 is almost a diagonal region to the reactive site (*29*). It can be expected that Tyr 75 might interact with subtilisin BPN', and this tyrosyl residue could be responsible for the difference spectral change on the complex formation between subtilisin BPN' and SSI.

As the reactivity of a tyrosyl residue toward TNM should decrease in the order of pK_a (*146*), a tyrosyl residue of pK_a 9.66 must be nitrated at first. As shown in Fig. 8.3, a spectral change is observed at visible region (400 - 500 nm region) on the binding of the one-tyrosyl-residue-nitrated SSI derivative and subtilisin BPN', and this made us speculate that the difference spectral change is most probably due to the environmental change of Tyr 75 and that pK_a of the residue is 9.66. Even upon the interaction of subtilisin BPN' with the two-tyrosyl-residue-nitrated SSI (probably those of pK_a 9.66 and 11.02), there remains the large absorptivity difference at 245 nm in the difference spectrum observed (Fig. 8.3). Therefore, the tyrosyl residue of pK_a 9.7 which shifts upward to > 11.5 on the binding of subtilisin BPN' and SSI is supposed to be in subtilisin BPN' but not in SSI, for a tyrosyl residue remains not to be nitrated must have a high pK_a value.

Nitration of subtilisin BPN'. Markland and his coworkers (*149-151*) have demonstrated that 5 tyrosyl residues in subtilisin BPN' react readily with TNM. Tyr 6, 21, 104, 217, and 262 are fully nitrated, whereas Tyr 91 and 263 are only partially nitrated; it is not yet clear whether residue 167 and 171 are nitrated at all. Presumably the five residues that are readily nitrated are those titrated normally (pK_a = 9.7) in spectrophotometric titration at alkaline pH (Table 7.3), and those that are partially nitrated may be the residues that are titrated with slightly higher pK_a. Svendsen (*128,129*) has reported that with exhaustive nitration 8 out of 10 tyrosyl residues in subtilisin BPN' are nitrated without a loss of enzymic activity. Svendsen (*128,129*) also found the same number of accessible tyrosyl residues on iodination.

Weber and Kraut (*152*) have found that Tyr 104 is the first to be

iodinated. Other iodinated residues appear to be 21, 167 or 171, and 217 (*26*). Preliminary results by Markland (*151*)indicated that nitration of subtilisin BPN' with a five-fold excess of TNM resulted in one most readily nitrated tyrosyl residue identified as Tyr 104. Tyr 104 is common to the two subtilisins, BPN' and Carlsberg. Svendsen (*153*) has obtained an identical result with nitration of subtilisin Carlsberg.

At the active site of subtilisin BPN', there are two tyrosyl residues of pK_a 9.7, Tyr 104 and 217, and they are located in the each side of the catalytic residue Ser 221. X-ray crystallographic studies so far examined on subtilisin BPN'-inhibitor complexes provide evidence for two alternative binding sites. While active-site directed reagents like ZAGPCK (*N*-benzyloxycarbonyl-L-alanyl-glycyl-L-phenylalanine chloromethyketone) are found in a shallow hydrophobic cleft, *Site A* (*31,32*); irreversible inhibitors such as phenylmethane sulphonyl fluoride (PMSF), good acylating agents like *N-trans*-cinnamoyl imidazole (TCI), and *N*-benzoyl-L-arginine (BA) are all located at the second site, *Site B* (*154*). These two sites are about 12 A apart, but are at approximately the same distance from the active Serine 221 (*155*). The former studies by Kraut *et al.* (*31*) and Robertus *et al.* (*32*) have demonstrated that Tyr 104 exists at *Subsite 4* which is involved in the formation of hydrophobic environment, *Site A*, and that the tyrosyl residue interacts with the benzyloxycarbonyl group. Tyr 104 moves 1 - 2 A on this interaction. The latter studies by Wright *et al.* (*154*) have showed that an aromatic ring of the inhibitor, BA, interacts with Tyr 217 through van der Waals contacts. It seems to be very difficult to determine which *Site A* or *B* is a real binding site for protein substrate by using only synthetic inhibitors such as ZAGPCK and BA. It can be expected to solve this

problem by using a naturally occurring protein inhibitor, such as SSI. If spectral changes of Tyr 104 and Tyr 217 of subtilisin BPN' on the binding with SSI can be discriminated from each other, it is possible to infer the interacting mode between a protein substrate and the enzyme.

As shown in Table 8.1, even if the most reactive tyrosyl residue of subtilisin BPN' towards TNM (which is assigned to Tyr 104 according to Markland) has been nitrated, the difference spectrum observed on the binding of SSI and the nitrated enzyme at pH 9.70 is the same as that obtained on the binding of SSI and native enzyme. Thus, it is most reasonably considered that Tyr 104 is excluded from the candidates of a tyrosyl residue whose pK_a shifts upwards ($9.7 \longrightarrow > 11.5$) on the formation of subtilisin BPN'-SSI complex, and that Tyr 217 can be most likely the tyrosyl residue in question.**

Modification of carboxyl groups of SSI. Table 8.2 shows that negative charges on carboxyl groups of SSI, especially that modified fifth, are a direct origin of raising up the pK_a value of a normal tyrosyl residue (presumably Tyr 217) on the active site of subtilisin BPN'. The

---

** *N*-Benzoyl-L-arginine, BA, is a competitive inhibitor toward the hydrolysis of pNPA by subtilisin BPN' and the inhibitor constant, K_i, was determined to be 18.3 mM. Nitration of subtilisin BPN' was carried out preliminary under the same condition as shown on the line 5 in Table 8.1 in the presence of 30 mM BA. The results, however, are completely the same as those obtained without BA, leading us to conclude that this inhibitor does not protect tyrosyl residues (especially Tyr 217) from nitration by TNM, though it is believed to bind near Tyr 217.

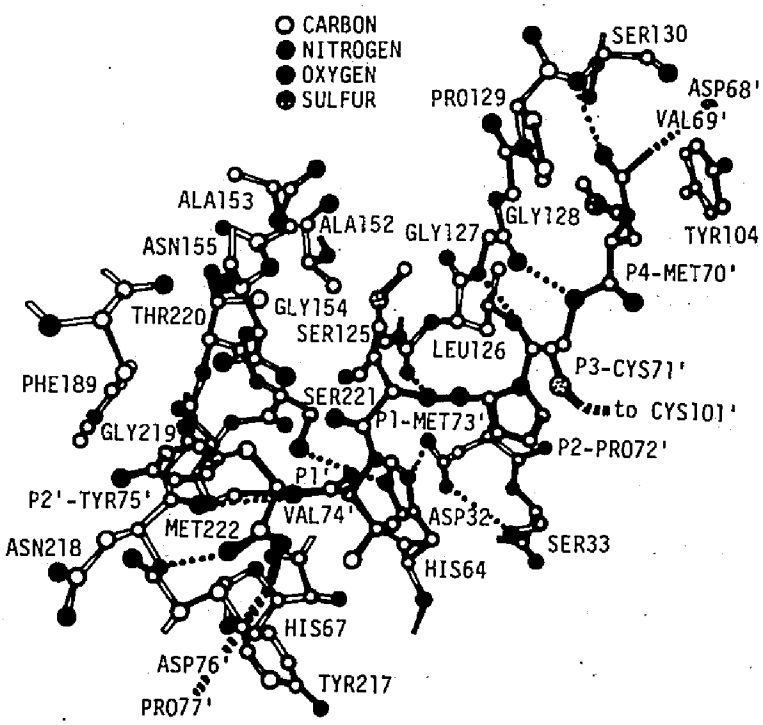

Fig. 8.7. Skeletal model of interface structure between SSI and subtilisin BPN'. This Figure is cited from the Doctoral Thesis of Y. Satow submitted to the University of Tokyo (1977). Black bars and white bars show the back bones (covalent structures) of SSI and subtilisin BPN', respectively.

---

reactive site of SSI against α-chymotrypsin has been proposed to be Met 73' - Val 74' (prime shows the residue in SSI). Although the site against subtilisin BPN' has not yet been determined, Met 73' - Val 74' can be reasonably considered to be the reactive site also against subtilisin BPN' on the basis of resemblance in substrate specificity and active site structure between the two enzymes. If the sequence around the reactive site of SSI is placed over the subsites of subtilisin BPN' (*30,156*) mimicking the binding mode revealed by the X-ray crystallo-

graphic study of subtilisin BPN'-ZAGPCK complex (*32*), there are two conceivable interactions between tyrosyl residues and carboxyl groups, i.e., Tyr 104 - Asp 68' and Tyr 217 - Asp 76' (Fig. 8.7). The latter interaction is supposed to be the one involved in the strong and specific interaction between SSI and subtilisin BPN' accompanied with the pK_a-shift of a tyrosyl residue.

The interaction between a tyrosyl residue and carboxyl group(s) (presumably Tyr 217 - Asp 76') should contribute somewhat to the stability of an enzyme-inhibitor complex. In fact, this interaction was shown to amount to a tenth of the total affinity (~1.5 kcal/mol out of 14 kcal/mol in free energy) between the both proteins from the comparison of the inhibitor constants of native and the chemically modified SSI's.

8.5 Summary

An absorption difference spectra typical of a change in ionization state (pK_a 9.7 ⟶ > 11.5) of a tyrosyl residue has been observed upon the binding between SSI and subtilisin BPN' at alkaline pH (Chapter Seven). Nitration of tyrosyl residues of SSI and those of subtilisin BPN' were performed with tetranitromethane, TNM. By the measurements of the difference spectra observed on the binding of the tyrosyl-residue-nitrated SSI and the native subtilisin BPN', or the native SSI and the tyrosyl-residue-nitrated subtilisin BPN' at alkaline pH, the tyrosyl residue in question was revealed to be one out of the five tyrosyl residues of pK_a 9.7 of the enzyme. This tyrosyl residue was assigned to Tyr 217 by taking into consideration the reactivities of tyrosyl residues against TNM.

Carboxyl groups of SSI were modified by covalently binding glycine methyl ester with aid of water-soluble carbodiimide, in order to cross out the negative charges on SSI. The difference spectrum which was observed on the binding of subtilisin BPN' and the 5.3-carboxyl-group-modified SSI at alkaline pH is almost the same as that observed on the binding of the native SSI and the enzyme at neutral pH. This phenomenon indicates that the pK_a of a tyrosyl residue of the enzyme is shifted upwards by interacting with carboxyl group(s) of SSI on the formation of the enzyme-inhibitor complex.

By placing the sequence around the reactive site of SSI (Met 73 - Val 74) over the active site structure of subtilisin BPN', the interacting pair of a tyrosyl residue and a carboxyl group is suggested to be that of Tyr 217 of the enzyme and Asp 76 of SSI.

Chapter Nine

The Interaction of *Streptomyces* Subtilisin Inhibitor and Thiolsubtilisin BPN' *

9.1 Introduction

It has been demonstrated that *Streptomyces* subtilisin inhibitor, SSI, tightly binds subtilisin BPN' and inhibits its enzyme activity with the inhibitor constant, K_i, less than 10^{-9} M (Chapter Two). On the other hand, chromatographic study showed that SSI does not interact with chemically modified inactive enzymes such as diisopropylphosphorylated (DIP) and carbobenzoxy-L-alanyl-glycyl-L-phenylalanine-chloromethyl-ketone-treated (ZAGPCK) subtilisins (*45*), suggesting that SSI binds subtilisin BPN' at or near the active site of the enzyme (Chapter Two). It remains obscure, however, whether or not the proteolytic activity of the enzyme is essential for the enzyme-inhibitor interaction, since introduction of a bulky group such as DIP and ZAGPCK to the active site of the enzyme may lead to a steric hindrance in the specific interaction with SSI, making the complex formation impossible. In order to make this point clear, a study was attempted on the interaction between SSI and thiolsubtilisin BPN' (*157-159,127*) in which Ser 221 of the native enzyme has been converted artificially to Cys 221.

The present Chapter describes the spectrophotometric analyses of

---

* A part of this study was presented at the 28th Forum on Protein Structure (Tokyo, October 1977), and published in *J. Biochem.* (1977) 82, 125-130 (*i,j*).

of the interaction of SSI with thiolsubtilisin BPN'. The results indicated that conversion of the active serine residue to cysteine residue induces a large increase in the dissociation constant of the enzyme-SSI complex and a definite decrease in the extent of upward pK_a-shift of a tyrosyl residue of the enzyme upon binding with SSI. These results were compared with those obtained for natural subtilisin BPN'-SSI interaction in Chapter Seven.

9.2 Experimental Procedures

Proteins. A three times crystallized and lyophilized preparation of SSI was a generous gift from Professor S. Murao. The lyophilized preparation of thiolsubtilisin BPN', which was prepared from subtilisin BPN' [EC 3.4.21.14] purchased from Nagase & Co. Ltd., Osaka (Lot No. 7370935), was kindly supplied by Professor D. Tsuru. Protein concentrations were determined spectrophotometrically at pH 7.0 by using the absorptivity coefficients $E_{1\ cm}^{0.1\%}$(276 nm) = 0.829 for SSI, and $E_{1\ cm}^{0.1\%}$(278 nm) = 1.063 for subtilisin BPN' and thiolsubtilisin BPN'; and the molecular weights 11,500 for SSI monomer, and 27,500 for subtilisin BPN' and thiolsubtilisin BPN' (Experimental Procedures 2.2).

The purity of the thiolsubtilisin BPN' preparation used was checked with various criteria. The preparation showed no caseinolytic activity but definite esterolytic activity toward pNPA (see Results 9.3 and Fig. 9.2). The esterase activity was inhibited by incubation with *p*-chloromercuribenzoate, pCMB, at a molar ratio of 1 : 1, in sharp contrast with that of subtilisin BPN', to which pCMB was completely inert. Amino acid analysis gave 0.9 mole of cysteic acid per mole of enzyme,

and 1.1 mole free sulfhydryl groups were titrated with pCMB. No gross conformational change was detected on this modification as observed with optical rotatory dispersion, ORD, and circular dichroism, CD, spectral measurements (Fig. 9.1) (see later). The purity of the used preparation of thiolsubtilisin BPN' was determined to be (99 ± 3)% by the method described in Experimental Procedures 2.2 using pNPA as titrant.

Inhibitory activity measurement. Inhibitory activity of SSI against thiolsubtilisin BPN' was measured as described in Experimental Procedures 5.2 using pNPA as substrate in 25 mM phosphate buffer containing 5.0% (v/v) isopropanol, pH 7.00, (the ionic strength adjusted to 0.1 M with NaCl), 25.0°C. The concentrations of the enzyme and the inhibitor in the reaction solution were 3.00 μM and 13.0 μM, respectively, and pNPA concentration was between 9.38 μM and 0.563 mM.

Ultraviolet absorption difference spectra. Difference spectra observed on the binding of SSI and thiolsubtilisin BPN' at alkaline pH were measured with a Union SM-401 recording spectrophotometer (0.01 absorbance/full scale) equipped with a Union SM-4012 spectral data processor and a cell holder thermostated at 25.0°C. A pair of quarz cuvettes divided into two compartments of 4 mm light path length was used. Eqaul volumes of 33.4 μM thiolsubtilisin BPN' and SSI of various concentration up to 0.36 mM in 25 mM carbonate buffer, pH 9.0 - 10.4, ionic strength 0.1 M (naCl) were mixed in the optical cuvette (Experimental Procedures 7.2 and 8.2). A Hitachi-Horiba F-5 pH-meter was used for all pH measurements.

ORD and CD spectra. Optical rotatory dispersion, ORD, and circular dichroism, CD, spectra were measured with subtilisin BPN' and thiolsubtilisin BPN' by using a JASCO ORD/UV-5 spectropolarimeter and a JASCO

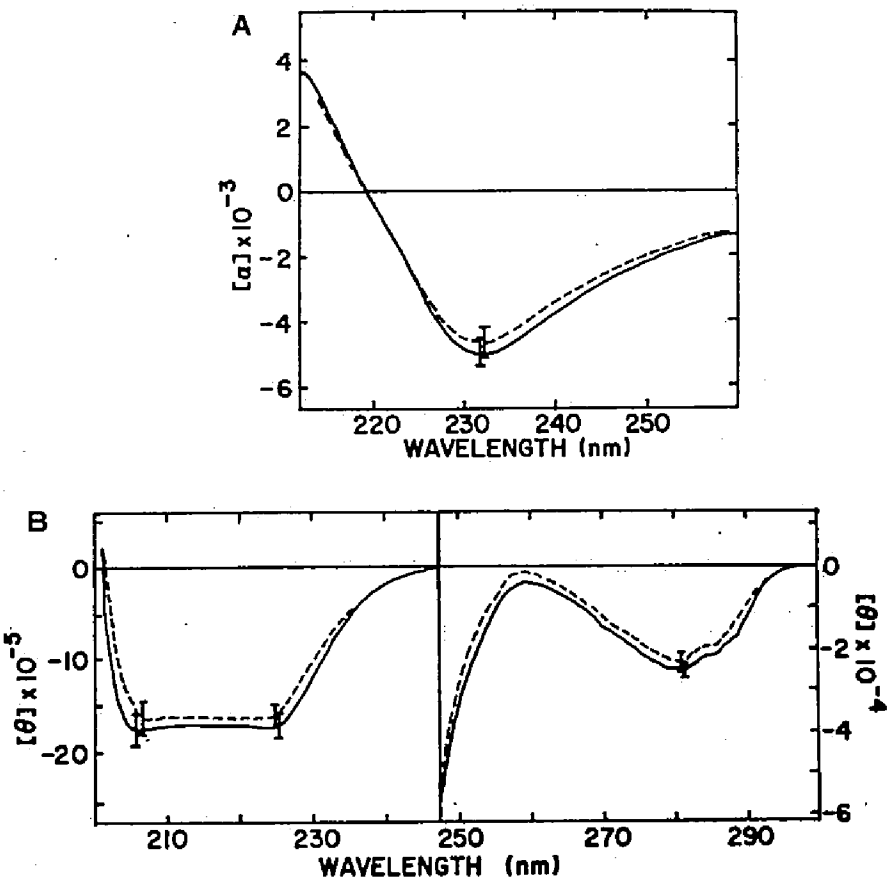

Fig. 9.1. Optical rotatory dispersion (A) and circular dichroism (B) of the native subtilisin BPN' and thiolsubtilisin BPN'. The enzymes were dissolved in 25 mM phosphate buffer, pH 7.00, ionic strength 0.1 M (NaCl). The measurements were performed at 25.0°C. The solid line and the broken line refer to thiolsubtilisin BPN' and native subtilisin BPN', respectively. The bar shows the noise level. The protein concentrations and optical paths are (A) 3.25 μM, 10 mm; (B) 5.13 μM, 1 mm (200 - 250 nm) and 2.31 μM, 10 mm (260 - 300 nm), respectively.

Model J-20 automatic recording spectropolarimeter equipped with CD attachment, respectively. The both apparatus were calibrated with sucrose (Schwarz-Mann, ultra pure) and *d*-10-camphoresulfonic acid (Eastman Kodak) (*160-162*).

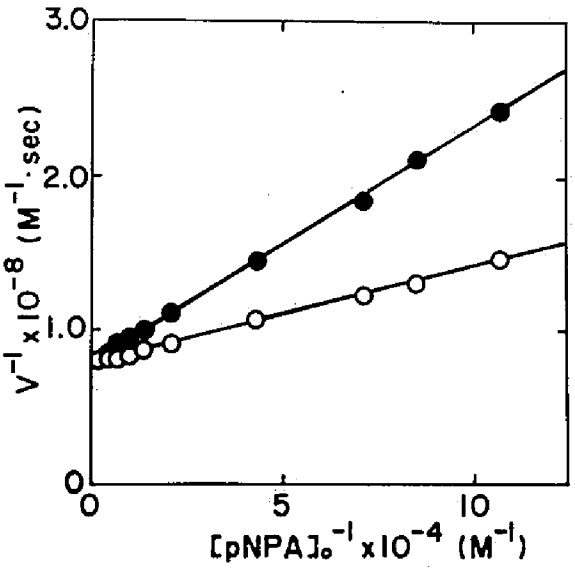

Fig. 9.2. Inhibition of SSI toward the hydrolysis of *p*-nitrophenyl acetate, pNPA, catalyzed by thiolsubtilisin BPN'. The Lineweaver-Burk plot (*107*). [thiolsubtilisin BPN']$_o$ = 3.00 μM; [SSI monomer]$_o$ = 0 μM (open circle); 13.0 μM (closed circle), in 25 mM phosphate buffer, pH 7.00, ionic strength 0.1 M (NaCl), containing 5.0% (v/v) isopropanol, 25.0°C. The initial velocity of the reaction, v, was measured by following the increase in absorbance at 405 nm. The type of inhibition was determined to be competitive, and the inhibitor constant, K_i, of SSI against thiolsubtilisin BPN', to be 1.31 x 10^{-5} M. (see Text)

9.3 Results

Inhibition of SSI against thiolsubtilisin BPN'. *p*-Nitrophenyl acetate has proved to be a suitable substrate to study the enzymatic activity of thiolsubtilisin BPN' (*158*). The kinetics of the thiolsubtilisin BPN'-catalyzed hydrolysis of pNPA is similar to that of α-chymotrypsin, subtilisin, and papain, and the hydrolysis presumably takes place according to the three-step mechanism shown in Chapter Two (Eq.

2.1). In a presteady-state reaction an initial burst of *p*-nitrophenol was observed corresponding to rapid formation of acetyl-enzyme. The burst was followed by a steady-state (zero-order) reaction, indicating a rate-determining deacylation. The reaction was carried out at the enzyme concentration of 13.5 μM (assuming the purity of the preparation used to be 100%), and the pNPA concentration between 1.56 mM and 0.521 mM, in 25 mM phosphate buffer containing 5.0% (v/v) isopropanol, pH 7.00, ionic strength 0.1 M (NaCl), 25.0°C. The purity of the thiolsubtilisin BPN' preparation used was estimated to be (99 ± 3)% by measuring the burst of *p*-nitrophenol liberation (see Experimental Procedures 9.2). The steady-state portion of the hydrolysis obeys Michaelis-Menten kinetics. The Lineweaver-Burk plots (*107*) are shown in Fig. 9.2. The kinetic parameters, k_{cat} and K_m, were calculated from the plot (open circle) to be 4.35×10^{3} sec^{-1} and 8.42×10^{-6} M at pH 7.00, 25.0°C, respectively. The plot (closed circle) in Fig. 9.2 is a Lineweaver-Burk plot in the presence of SSI, indicating that the type of inhibition is competitive, and the competitive inhibitor constant, K_i, was calculated to be 1.31×10^{-5} M at pH 7.00, 25.0°C.

Difference spectra observed on the binding at alkaline pH. Figure 9.3 shows an ultraviolet absorption difference spectrum observed on the binding of SSI and thiolsubtilisin BPN' at pH 9.70, 25.0°C. This is of the same shape as that observed on the binding of SSI and subtilisin BPN' (Fig. 7.3); therefore, the difference spectrum in Fig. 9.3 should be attributable to the upward pK_a-shift of a tyrosyl residue (Chapter Seven). Although the molar absorptivity difference, $\Delta\varepsilon_{245}$, under the conditions studied (-1.10×10^{3} $M^{-1}cm^{-1}$) is considerably smaller than that (-7.21×10^{3} $M^{-1}cm^{-1}$) obtained from Fig. 7.3 for the native enzyme

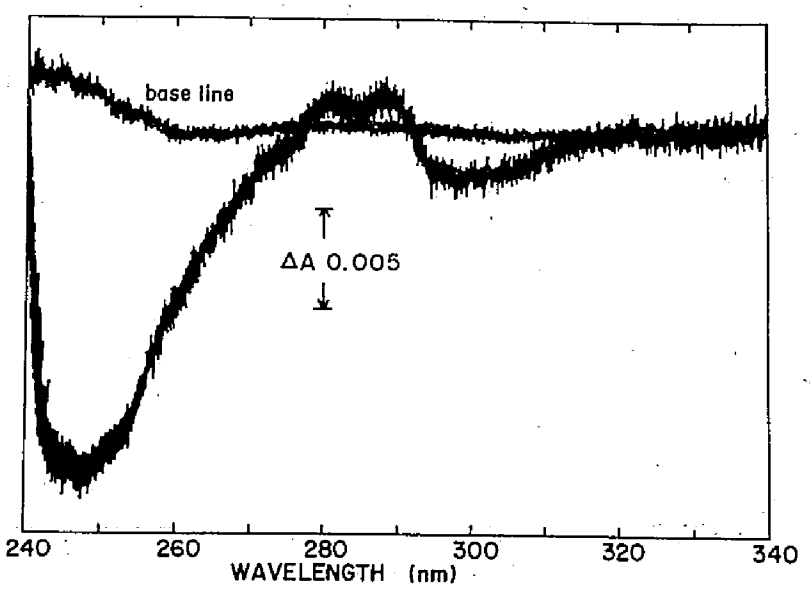

Fig. 9.3. Ultraviolet absorption difference spectrum observed on the binding of SSI and thiolsubtilisin BPN'. $[\text{thiolsubtilisin BPN'}]_o$ = 16.7 μM; $[\text{SSI monomer}]_o$ = 24.1 μM, in 25 mM carbonate buffer, pH 9.70, ionic strength 0.1 M (NaCl), 25.0°C.

---

under the same conditions, the molar absorptivity difference at 245 nm was used for the spectrophotometric titration to estimate the dissociation constant, K_d, of SSI-thiolsubtilisin BPN' complex. The dependence of $\Delta\varepsilon_{245}$ on SSI concentration were measured at pH 10.20, 9.70, and 9.20 (Fig. 9.4). Each titration curve was analyzed by the use of non-linear least squares method (*163*) giving K_d values and limiting values of $\Delta\varepsilon_{245}$ in large excess of SSI, $\Delta\varepsilon_{245}^{max}$, as shown in Table 9.1. The K_d values can be assumed to be constant (~40 μM) between pH 9.2 and 10.2.

pH-Dependence of the molar absorptivity difference at 245 nm. Figure 9.5 shows the pH-dependence of $\Delta\varepsilon_{245}$ which was measured for the binding of thiolsubtilisin BPN' (16.7 μM) and SSI (0.150 mM as monomer) in the pH region 9.0 - 10.4, 25.0°C. Under these conditions, the con-

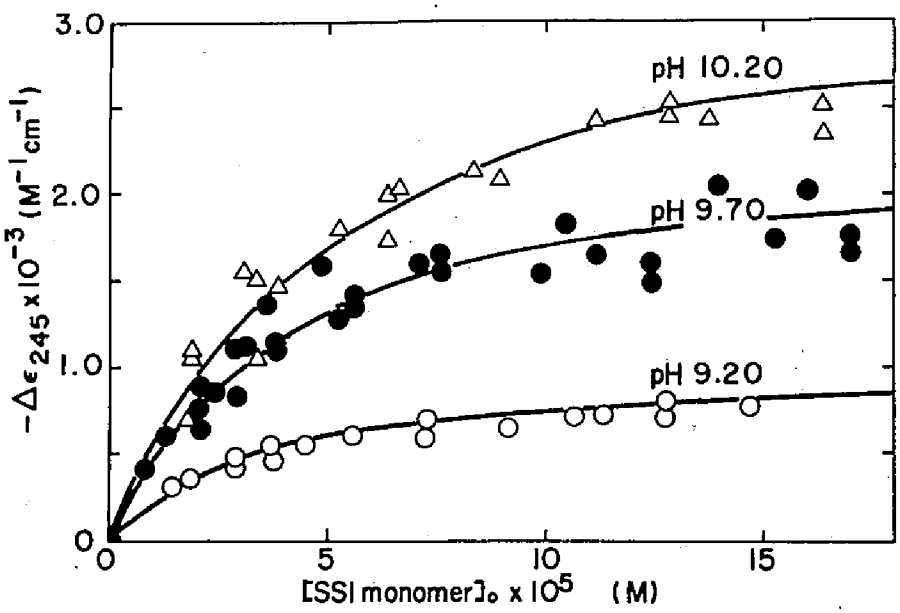

Fig. 9.4. Relationship between the molar absorptivity difference at 245 nm observed on the binding of thiolsubtilisin BPN' and SSI, $\Delta\varepsilon_{245}$, and the concentration of SSI monomer. [thiolsubtilisin BPN']$_o$ = 16.7 μM; [SSI monomer]$_o$ = 0 - 0.20 mM, in 25 mM carbonate buffer; pH 9.20 (open circle), pH 9.70 (closed circle), and pH 10.20 (open triangle); ionic strength 0.1 M (NaCl), 25.0°C. (see Table 9.1)

Table 9.1. The dissociation constant of the thiolsubtilisin BPN'-SSI complex, K_d, and the maximum value of the molar absorptivity difference at 245 nm, $\Delta\varepsilon_{245}^{max}$, determined from the titration of the absorptivity difference at 245 nm observed on the binding of thiolsubtilisin BPN' and SSI shown in Fig. 9.4. [thiolsubtilisin BPN']$_o$ = 16.7 μM.

pH	Kd x 10^5 (M)	$-\Delta\epsilon_{245}^{max} \times 10^{-3}$ ($M^{-1}cm^{-1}$)
10.20	4.3 ± 0.5	3.40 ± 0.20
9.70	3.5 ± 0.4	2.28 ± 0.08
9.20	3.8 ± 0.3	1.03 ± 0.04

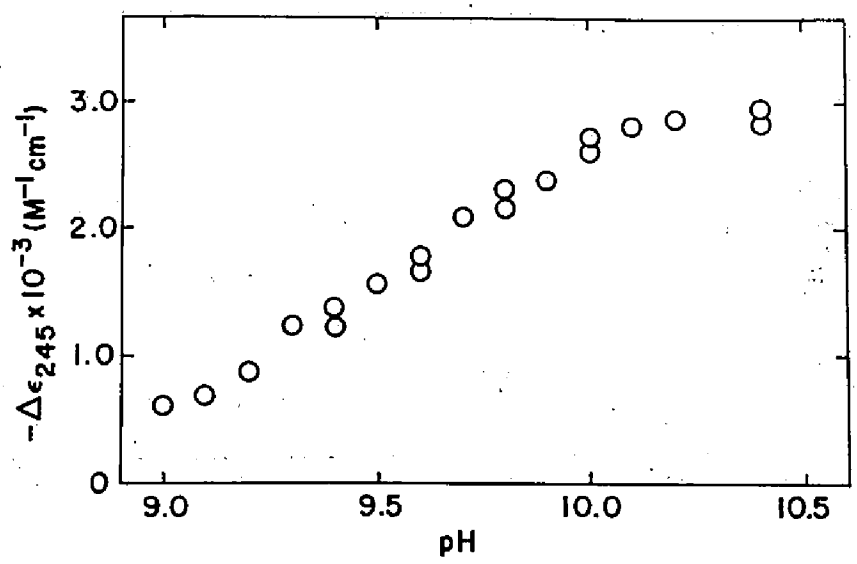

Fig. 9.5. pH-Dependence of the molar absorptivity difference at 245 nm observed on the binding of thiolsubtilisin BPN' and SSI. [thiolsubtilisin BPN']$_o$ = 16.7 μM; [SSI monomer]$_o$ = 0.150 mM, in 25 mM carbonate buffer, pH 9.00 - 10.40, ionic strength 0.1 M (NaCl), 25.0°C.

---

centration of the enzyme-inhibitor complex was estimated to be 13.4 μM in the mixture solution from the value K_d = 40 μM.

As has been described on Chapters Seven and Eight, a pK_a value of a tyrosyl residue of subtilisin BPN' shifts from 9.7 to > 11.5 on the formation of the complex between SSI and subtilisin BPN'. This tyrosyl residue can be presumed to exist in the same state in thiolsubtilisin BPN' also as in subtilisin BPN'. The plots in Fig. 9.5 would correspond to the difference titration curve of this tyrosyl residue between before and after the complex formation (pK_a = 9.7 for the tyrosyl residue in free enzyme). Thus, the pH titration curve of the tyrosyl residue in the enzyme-inhibitor complex (data represented by open circles in Fig. 9.6) was obtained by subtracting $\Delta\varepsilon_{245}$ value in Fig. 9.5 at each pH from

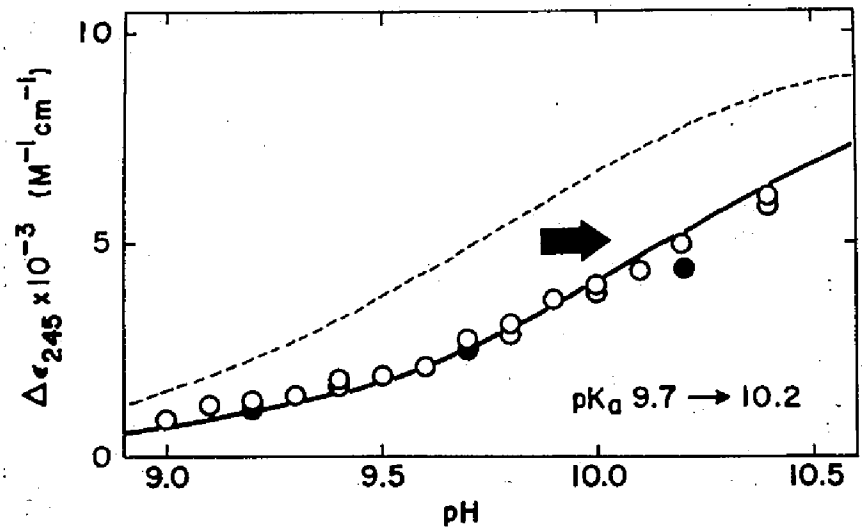

Fig. 9.6. The shift of the ionization state of a tyrosyl residue of pK_a 9.7 (most probably Tyr 217 of thiolsubtilisin BPN') on the binding of thiolsubtilisin BPN' and SSI, in 25 mM carbonate buffer, pH 9.00 - 10.40, ionic strength 0.1 M (NaCl), 25.0°C. Open circle: data obtained with $[\text{thiolsubtilisin BPN'}]_o$ = 16.7 μM and $[\text{SSI monomer}]_o$ = 0.150 mM; under the condition, 80% of the enzyme was assumed to be bound with SSI with $K_d = 4 \times 10^{-5}$ M (Table 9.1); pK_a 9.7 ⟶ 10.2. Closed circle: data obtained by assuming that 100% of the enzyme is bound with SSI; pK_a 9.7 ⟶ 10.3.

---

the titration curve of the residue of pK_a 9.7 (Fig. 9.6). A titration curve with pK_a 10.2 was best fitted to the titration data according to the equation (Experimental Procedures 6.2, Eq. 6.1):

$$[H^+] \cdot \Delta\epsilon_{245} = K_a \cdot \Delta\epsilon_{245}^{max} - K_a \cdot \Delta\epsilon_{245}$$

The closed circles in Fig. 9.6 were obtained by using $\Delta\epsilon_{245}^{max}$ in Table 9.1 instead of $\Delta\epsilon_{245}$ in Fig. 9.5 which was smaller than $\Delta\epsilon_{245}^{max}$, because it was measured under the conditions that 80% of the enzyme exists as the enzyme-inhibitor complex. The calculated values of $\Delta\epsilon_{245}^{max}$ obtained by multiplying $\Delta\epsilon_{245}$ values in Fig. 9.5 by 1.25 (= 1/0.8) (the reciprocal

of the degree of saturation of the enzyme with SSI) were used as well as $\Delta\varepsilon_{245}^{max}$ shown in Table 9.1 to evaluate the pK_a value more precisely. The pK_a value of the tyrosyl residue in the thiolsubtilisin BPN'-SSI complex was thus determined to be 10.3.

9.4 Discussion

Thiolsubtilisin BPN'. The alteration of the active site of an enzyme may give mechanistically meaningful information. Thiolsubtilisin BPN', an SH analog of the serine proteinase subtilisin BPN', can be produced by the conversion of the hydroxyl group of the reactive serine residue at the active site into a sulfhydryl group by chemical modification. Thiolsubtilisin BPN' can be regarded as a model of thiol proteinases, such as papain, inasmuch as both thiolsubtilisin BPN' (*164*) and papain (*165*) have an imidazole ring in the immediate vicinity of the thiol group, as clearly indicated by X-ray diffraction studies. However, thiolsubtilisin BPN' has no proteinase activity: it can only catalyze the hydrolysis of pNPA and imidazole amides (*157,158*) and it is inactive toward other ester and amide substrates (*166*). In serine proteinases in general, a serine hydroxyl group at the active site of subtilisin BPN' serves as a nucleophile during enzymatic catalysis, with the intermediate formation of an acyl-enzyme in which the acyl group is attached to this serine hydroxyl group. The SH group of cysteine possesses steric and chemical properties similar to those of the OH group of serine. The van der Waals radii of oxygen and sulfur are 1.40 and 1.85 A, respectively, and the covalent radii are 0.66 and 1.04 A, respectively (*167*). Since the two groups react similarly in hydrolyses of

esters such as pNPA, the conversion of an OH group to an SH group would be a minimal modification, in both chemical and sterical sense. The SH group is, in general, somewhat more reactive than the OH group either as an attacking nucleophile or as a leaving group (*168-170*). However, the catalytic activity of thiolsubtilisin BPN' towards pNPA is significantly lower than that of subtilisin BPN': K_m = 8.42 x 10^{-6} M and k_{cat} = 4.35 x 10^{-3} sec^{-1} for thiolsubtilisin BPN', and K_m = 4.98 x 10^{-4} M and k_{cat} = 9.25 x 10^{-2} sec^{-1} for subtilisin BPN' in 25 mM phosphate buffer, pH 7.0, ionic strength 0.1 M (NaCl), 25.0°C. The decrease in K_m value counteracts the low k_{cat}, so the specificity constant, k_{cat}/K_m, of thiolsubtilisin BPN' toward pNPA is about the same as in the subtilisin BPN' system.

Inhibition and binding of SSI against thiolsubtilisin BPN'. The results obtained here show that the proteolytic activity of the enzyme is not necessarily essential for the enzyme-inhibitor interaction. The inhibitor constant, K_i (1.3 x 10^{-5} M at pH 7.0), of SSI against thiolsubtilisin BPN' and dissociation constant, K_d (4 x 10^{-5} M at pH 9.2 - 10.2), of the SSI-thiolsubtilisin BPN' complex are more than 10^5-fold greater than those for subtilisin BPN'. The slight conversion of the active seryl residue of subtilisin BPN' to a cysteinyl residue was found to decrease the affinity between the enzyme and the inhibitor to a considerable extent, by about 7 kcal/mole in free energy units. It is noteworthy that the small difference in atomic radii of oxygen and sulfur could result in such a big change in binding affinity, and it seems likely that SSI strictly discriminates the fine structure around the region of active site serine residue of the target enzyme.

The interaction between a tyrosyl residue and carboxyl group(s).

It has been described in Chapters Seven and Eight that on the complex formation between subtilisin BPN' and SSI a tyrosyl residue of the enzyme interacts with carboxyl group(s) of SSI and that the pK_a of the tyrosyl residue shifts upwards from 9.7 to > 11.5. As has been shown in the present Chapter, however, presumably the same tyrosyl residue of thiolsubtilisin BPN' shifts its pK_a from 9.7 to only 10.2 - 10.3 upon the interaction with SSI.

A quantitative formulation of the electrostatic effect of a charged group on the acidity of a neighboring group was given by Bjerrum (*171*) based on point charge model. If a group of charge $Z\varepsilon$ —— where Z is the valence of the group, and ε is the proton unit of charge —— is assumed to be immersed in a continuous medium of dielectric constant, D, and if it is at a distance, r, from an acidic group, then the contribution of the charged group to the electrical work done per mole under the influence of the potential, Ψ, at the acidic group is

$$\Delta W = N\varepsilon\Psi = \frac{NZ\varepsilon^2}{Dr} \qquad (9.1)$$

where N is Avogadro's number. If the free energy of ionization of an acid containing a charged substituent group is compared with that of a similar acid containing no such substituent, the difference in $\Delta G°$, namely the difference in pK_a, for the two acids may be set equal to ΔW. Thus, it may be written, making use of Eq. 9.1 as:

$$\Delta W = \Delta(\Delta G°) = 2.303 \cdot \Delta pK_a = \frac{N\varepsilon^2}{RTDr} \qquad (9.2)$$

where R and T are gas constant and absolute temperature in K, respectively. Using the numerical values $\varepsilon = 4.80 \times 10^{-10}$ esu, $N = 6.02 \times 10^{23}$, $R = 8.31 \times 10^7$ erg $deg^{-1} mol^{-1}$, and T = 298 K, we have:

$$r = \frac{24.32 \times 10^{-7}}{D \cdot \Delta pK_a} \quad (cm) \qquad (9.3)$$

This relationship was applied to the interaction between a tyrosyl residue of the enzyme and carboxyl group(s) of the inhibitor on the complex formation between SSI and subtilisin BPN' or between SSI and thiol-subtilisin BPN'. When the value of D for water, 78.3, is used (since the effective dielectric constants around the interacting residues are unknown), r is calculated to be less than 1.72 A for the SSI-subtilisin BPN' interaction and 6.21 - 5.17 A for the SSI-thiolsubtilisin BPN' interaction. The former value, r < 1.72 A, seems to be unconceivably small for the distance between a tyrosyl phenolic hydroxyl group and a carboxyl group. If the formation of an hydrogen bond is postulated between the tyrosyl hydroxyl group of subtilisin BPN' and the carboxyl group of SSI, 2.76 A can be reasonably assigned to the value of r, and then the D value is caluculated to be less than 49.0 from Eq. 9.3. Making use of this effective dielectric constant, the distance between the tyrosyl hydroxyl group of thiolsubtilisin BPN' and the carboxyl group of SSI was estimated to be > 9.93 A (ΔpK_a 0.5) - 8.27 A (ΔpK_a 0.6).**

** The D values on the molecular surface of lysozyme were estimated on the basis of the previously reported titration data of Glu 35 and Asp 52 obtained by Kuramitsu *et al.* (*173*) and those of His 15 obtained by Kangawa *et al.* (*174*). From the former data, D was determined to be 34 - 48 by the use of the atomic coordinate obtained by the X-ray crystallographic studies (*175*), and from the latter data, D of about 40 was estimated from the plot as shown in Fig. 9 in Ref. (*173*).

It is obvious that Bjerrum's treatment can be only an approximation (*172*). However, it is clear that the considerably small pK_a-shift of the tyrosyl residue on the interaction between SSI and thiolsubtilisin BPN' compared with that between SSI and subtilisin BPN' could be an extension of the distance between the tyrosyl residue and the carboxyl group. The tyrosyl residue and the carboxyl group are most probably assigned to Tyr 217 of subtilisin BPN' and thiolsubtilisin BPN' and Asp 76 of SSI, respectively (Chapter Eight). It is noteworthy that the small change in the active site structure of subtilisin BPN' (Ser 221 $\longrightarrow$ Cys 221) leads to a considerable extension (about three times in so far as the effective dielectric constant is unchanged in the Bjerrum's equation, Eq. 9.3) of the distance between Tyr 217 of the enzyme and Asp 76 of SSI.

9.5 Summary

The interaction between SSI and thiolsubtilisin BPN', in which Ser 221 of subtilisin BPN' is converted to Cys 221, was examined.

SSI competitively inhibits the esterolytic activity of thiolsubtilisin BPN' towards *p*-nitrophenyl acetate with the inhibitor constant, K_i, of 1.3×10^{-5} M at pH 7.00, 25.0°C. Spectrophotometric analysis of the interaction between SSI and thiolsubtilisin BPN' yielded the dissociation constant of the SSI-thiolsubtilisin BPN' complex, K_d, of 4×10^{-5} M at pH 9.20 - 10.20. These values are more than 10^5-fold greater than those for subtilisin BPN' (see Chapter Two). This indicates that the small change in the active site structure of subtilisin BPN' leads to a considerable decrease in the binding affinity (by about 7 kcal/mole

in free energy units) to SSI.

The spectrophotometric titration of the difference spectra observed on the binding of SSI and thiolsubtilisin BPN' at alkaline pH demonstrated that a tyrosyl residue of the enzyme shifts its pK_a value from 9.7 to 10.2 - 10.3 on the complex formation with SSI. This extent of pK_a-shift is considerably smaller compared with that observed on the interaction between SSI and subtilisin BPN' (pK_a 9.7 $\longrightarrow$ > 11.5). This large difference in the pK_a-shift suggests that the small change (of 0.45 A) at the active site of subtilisin BPN' leads to a great increase in the distance between the tyrosyl residue of the enzyme and the carboxyl group(s) of SSI.

Chapter Ten

Concluding Remarks

The present studies were carried out to clarify the physical-chemical properties of *Streptomyces* subtilisin inhibitor, SSI, and to elucidate the mechanism of interaction of SSI and proteinases, especially the unusually tight binding between SSI and subtilisin BPN'. The experimental results are summarized as follows:

i) One molecule of SSI (MW 23,000; dimer) binds and inhibits two molecules of subtilisin BPN' (MW 27,500) strongly. The inhibitor constant, K_i, against subtilisin BPN' was estimated to be less than 10^{-9} M at pH 8.5 and pH 7.0, 25.0°C.

ii) SSI exists as a stable dimer of molecular weight of 23,000 in the wide concentration range, 0.010 - 10 mg/ml, which includes the range used for the various studies employed; spectrophotometric, kinetic, and inhibition measurements. The molecular weight of the subtilisin BPN'-SSI complex is about 78,000 (77,300 - 87,300), which indicates that one molecule of dimeric SSI binds two molecules of the enzyme to form a stable complex of E_2I_2 type.

iii) SSI molecules, at 1.0 mg/ml, are in the equilibrium between monomeric and dimeric form in the presence of 0.03 - 0.12% (w/v) SDS at pH 7.0, ionic strength 0.1 M (NaCl), 25.0°C. The SSI monomer, in the presence of SDS, has at least 50% of the inhibitory activity against subtilisin BPN' obtained without SDS.

iv) SSI binds stoichiometrically and inhibits competitively α-chymotrypsin with the inhibitor constant, $K_i = (3.0 \pm 0.7) \times 10^{-6}$ M, when

p-nitrophenyl acetate is used as substrate at pH 7.0, 25.0°C. These values which are 10^3-fold or more greater than those for subtilisin BPN', suggest much weaker binding for α-chymotrypsin. This indicates that SSI can discriminate strictly the difference between the active site structure of α-chymotrypsin and subtilisin BPN'. Proflavine bound at the active site of α-chymotrypsin is not displaced by SSI but forms a ternary complex with the enzyme and SSI. SSI also inhibits competitively trypsin with K_i = 1.1 x 10^{-4} M.

v) It was demonstrated by solvent perturbation difference spectroscopy that all three tyrosyl residues per monomer SSI are exposed on the surface, and their individual pK_a values were estimated to be 9.66 ± 0.10, 11.02 ± 0.06, and 12.33 ± 0.06 by spectrophotometric titration at alkaline pH. The single tryptophyl residue per monomer SSI seemed to be in a cleft of the molecule, as it is only 30% accessible to ethylene glycol and inaccessible to polyethylene glycol.

vi) The solvent perturbation study with ethylene glycol and methanol as perturbants showed that a tryptophyl and about five tyrosyl residues become inaccessible to ethylene glycol and that a tryptophyl and a tyrosyl residues to the smaller perturbant, methanol upon the complex formation. The ultraviolet absorption difference spectra at 245 nm observed at alkaline pH indicated that a tyrosyl residue of either one of the two proteins shifted its pK_a value considerably upwards (9.7 $\longrightarrow$ > 11.5) on the complex formation. A typical second-order kinetics was observed for the binding by monitoring the difference absorbance mentioned above, and the second-order rate constant of the association was obtained to be 3.1 x 10^6 $M^{-1}sec^{-1}$.

vii) Chemical modification studies showed that a tyrosyl residue of

subtilisin BPN' shifts its pK_a upwards on the complex formation, which is brought about by carboxyl group(s) of SSI. The interacting tyrosyl residue and carboxyl group(s) are most probably assigned to Tyr 217 of subtilisin BPN' and Asp 76 of SSI, respectively.

vii) SSI inhibits competitively the esterolytic activity of thiolsubtilisin BPN' towards *p*-nitrophenyl acetate with the inhibitor constant, K_i, of 1.3×10^{-5} M at pH 7.0, 25.0°C. An ultraviolet difference spectrum was observed on the binding of SSI and thiolsubtilisin BPN' at alkaline pH which is similar to that observed on the binding of SSI and subtilisin BPN'. From the concentration dependence of the difference spectra, the dissociation constant, K_d, of the SSI-thiolsubtilisin BPN' complex was determined to be 4×10^{-5} M, and the pH-dependence of the difference spectra demonstrated that a tyrosyl residue shifts its pK_a upwards from 9.7 to 10.2 - 10.3, which is considerably lower than the pK_a-shift for the SSI-subtilisin BPN' interaction. This tyrosyl residue is reasonably assumed to be Tyr 217 of the enzyme based on the results obtained with the binding of SSI and subtilisin BPN'. These results indicate that the small change in the active site of subtilisin BPN' (Ser 221 ⟶ Cys 221) leads to a considerable loosening of the binding with SSI, which is reflected upon the decrease in the pK_a-shift due to an extension of the distance between the interacting tyrosyl residue of the enzyme and the carboxyl group(s) of SSI.

Three dimensional model of SSI. Figure 10.1 shows a tentative sketch of the SSI subunit established recently by the X-ray crystallographic studies at 2.3 A resolution by Mitsui *et al.* (*29*). At this stage, it seems to be interesting to compare the results mentioned above with those obtained from the X-ray crystallographic studies (*28,29,31,*

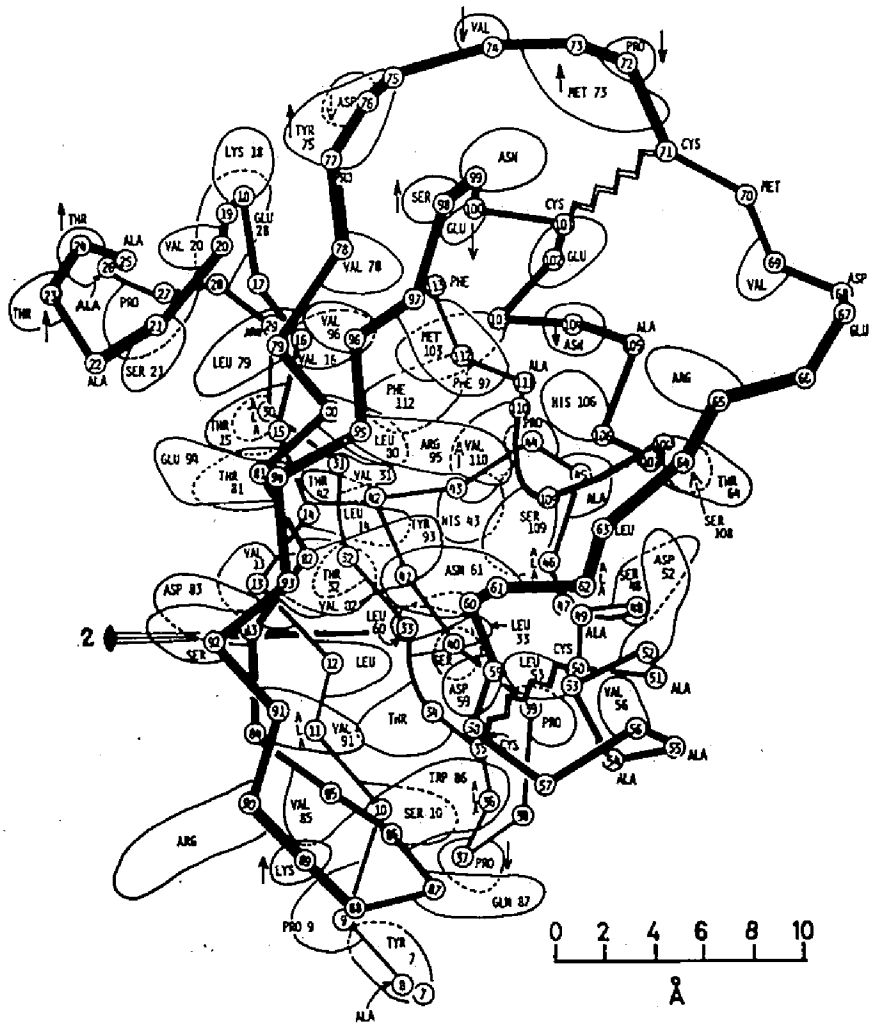

Fig. 10.1. A tentative sketch of the SSI subunit, which is cited from Mitsui *et al.* (*29*). The circles with residue numbers represent the rough positions of α-carbon atoms. Residues without the names of amino acids are glycines. The assignments of the side-chains of Phe 113 and Arg 29 are tentative. Disulfide bridges are denoted by zig-zag double lines. Upward and downward arrows indicate the direction of extension of the side-chain moieties perpendicular to the plane of the paper. The other subunit belonging to the same molecule is related to this subunit by a diad marked by 2 which is inclined at an angle of 60° to the plane of the paper.

32).

It is one of the unique characteristics of SSI that it exists as a dimer and it forms a stable E_2I_2 complex under the usual conditions (see Chapters Three and Four). At the contact region of subunits, as shown in Fig. 10.1, five segments of the polypeptide chain, i.e., residues 40-42, 29-34, 12-15, 78-84, and 91-97, form an antiparallel β-sheet. The β-sheet of a subunit faces directly toward that of the other, related by the diad shown in Fig. 10.1, and the plane of the two β-sheets are roughly parallel. About a fourth of total amino acid residues are involved in the β-sheet formation, and this explains the strong binding between SSI subunits. The solvent accessibilities of three tyrosyl and a tryptophyl residues per SSI monomer measured by the solvent perturbation method are consistent with their states revealed by the X-ray crystallographic studies. The N-terminal side and C-terminal side of the region around the reactive site, Met 73 - Val 74, seem to be held tightly by the 71-101 disulfide bridge and by the β-sheet, respectively. Mitsui *et al.* (*29*) indicate that the residues Met 70, Cys 71, Pro 72, Met 73, Val 74, and Tyr 75 in SSI seem to fit reasonably, respectively, the S_4, S_3, S_2, S_1, S_1', and S_2' sites of subtilisin BPN' (*30-32*). The conformation of the part containing these residues in SSI seems to be closely related to those of the corresponding parts of trypsin inhibitors, bovine pancreatic trypsin inhibitor (BPTI) and soybean trypsin inhibitor (STI), although the over-all conformation of SSI is completely different from those of the latter two inhibitors (*8-11,29*).

Homology in the region surrounding the reactive site and in a disulfide bridge can be pointed out (*27*) between SSI and the pancreatic secretory trypsin inhibitor (PSTI; Kazal-type trypsin inhibitor) from

bovine (*176,177*), porcine (*178,179*), ovine (*180*), and human (*181*) pancreas. Recent investigations revealed a considerable homology among animal and plant proteinase inhibitors (*182*). The case of SSI and PSTI provides an interesting example of the homology between two entirely distinct organisms, a bacterium and a mammal.

Inhibitory specificity of SSI. The rather narrow inhibitory specificity is another unique feature of SSI as a protein proteinase inhibitor. Some protein proteinase inhibitors which inhibit subtilisin BPN', e.g., plasminostreptin (Kakinuma, A., Sugino, H., and Isono, M., unpublished results) and potato inhibitors (*183-185*) inhibit as well trypsin and/or plasmin and α-chymotrypsin.

On the other hand, SSI can strictly discriminate the subtle difference in the active site structure of subtilisin BPN' and α-chymotrypsin or trypsin, and surprisingly, it can recognize even the minute difference between the active site structures of subtilisin BPN' and thiolsubtilisin BPN'. Judging from the large decrease in the binding affinity (large increase in K_i), it can be pointed out that the structures of contact-areas of the two proteins do not fit well in the weak interaction between SSI and α-chymotrypsin and that between SSI and thiolsubtilisin BPN'.

A dye, proflavine bound at the active site of α-chymotrypsin is not displaced by the binding of SSI to the active site of the enzyme. This is, to the author's knowledge, the first observation of the formation of a ternary complex among α-chymotrypsin, proflavine, and a substrate analog (in this case, SSI). This implies that SSI does not occupy the part of the active site to which proflavine binds, presumably the "tosyl anion hole" of the enzyme. In the weak interaction

between SSI and thiolsubtilisin BPN', the distance between Tyr 217 in the substrate binding site of thiolsubtilisin BPN' and Asp 76 of SSI is estimated to be about three times longer than that in the interaction between SSI and native subtilisin BPN'.

It has been known, by the subsite mapping method (*30,156*), that the substrate specificity of subtilisin BPN' is broader than that of α-chymotrypsin, trypsin, and elastase, and the X-ray crystallographic studies (*32,39*) revealed that subtilisin BPN' has no definite specificity determining site as the latter three enzymes. The interaction with substrate at the specificity determining site of α-chymotrypsin, trypsin and elastase, in which a favorable amino acid side chain can be accomodated, appears to contribute largely to the total affinity between the enzymes and the substrate. In the interaction between trypsin and soybean trypsin inhibitor (Kunitz) (*11*), the interaction at the primary binding site, P_1, was estimated to be 4 kcal/mole out of total 15 kcal/mole. In subtilisin BPN', however, because of the lack of the definite specificity determining site, the interaction with a substrate at the subsites, so called "secondary interaction", should have more significant than in α-chymotrypsin, trypsin, and elastase. In this sense, there could be a distinct difference between the interaction of subtilisin BPN' and SSI and that of trypsin and STI or BPTI (*8-11*).

The X-ray crystallographic studies on the BPTI-bovine trypsin complex and the STI-porcine trypsin complex indicated strongly that the both complexes exist as the tetrahedral adducts. In order to stabilize energetically unfavorable tetrahedral intermediate with the oxyanion of the inhibitors, some very strong and energetically favorable binding must be required elsewhere. Some binding forces can be identified which

are probably strongest in the tetrahedral form, in particular the hydrogen bonds to the oxyanion and the contacts made at the P_1'-site, e.g., Ile 64 in STI, Ala 16 in BPTI, and Val 74 in SSI. In addition, there are other strong interactions nearby. Some of these attractive contacts in the complex will be destroyed and others will be weakened if the enzyme and the inhibitor are forced apart in order to form either the acyl enzyme or the Michaelis complex. Thus, the tightly bound tetrahedral intermediate, which allows these numerous interactions, becomes the most stable form. In the interaction between SSI and subtilisin BPN', it is not yet known whether or not the tetrahedral intermediate is formed.

The central question about SSI system is to be: Why does the inhibitor bind so strong ? What have to be explained is the binding constant of SSI which corresponds to 15 - 20 kcal/mole of free energy decrement ? In the present thesis, the interaction of SSI with subtilisin BPN' and that with thiolsubtilisin BPN' are especially stressed. The ultraviolet absorption difference spectral change due to the pK_a shift of tyrosyl residue resulted from the interaction of tyrosyl residue and carboxyl group was used as a probe for investigating the protein-protein interaction. By using this method, it was demonstrated that a slight structural change (0.45 A) in the active site of subtilisin BPN' by converting the active Ser 221 to Cys 221 artificially (OH $\longrightarrow$ SH) leads to a remarkable decrease in the binding affinity to SSI. It is unambiguously concluded that the strong binding between SSI and subtilisin BPN' is caused by the topographical fitness between the contact areas of the both proteins. The method employed above is useful, if applicable, for the investigation on the protein-protein inter-

action at the molecular aspects, and provides us with the meaningful evidence as well as X-ray crystallography and NMR (nuclear magnetic resonance) spectroscopy.

*

Acknowledgments

The author wishes to express his sincere gratitude to Dr. Keitaro Hiromi, Professor of Kyoto University, for his invaluable guidance, generous suggestions, and constant encouragement throughout the course of this graduate work and preparation of this dissertation.

The author is deeply grateful to Dr. Ben'ichiro Tonomura, Associate Professor of Kyoto University, for his constant and valuable advice and discussions during the course of these studies and his critical reading of the manuscript.

The author is greatly indebted to Professor Sawao Murao and Dr. Sakae Sato (University of Osaka Prefecture) for their kind gift of the crystallized preparation of *Streptomyces* subtilisin inhibitor, and also indebted to Professor Daisuke Tsuru and Dr. Kunio Fujiwara (Nagasaki University) for their generous gift of the preparation of thiolsubtilisin BPN'.

Acknowledgments are also made to Professor Hiroshi Inagaki (Kyoto University) and Professor Tadao Kotaka (Osaka University) for their helpful suggestions and discussions on the sedimentation studies. The author should like to thank two institutes of Kyoto University: Institute for Chemical Research and Research Institute for Food Science, for allowing the use of the Beckman Spinco Model E analytical ultracentrifuge and the Hitachi UCA-1A analytical ultracentrifuge and UVC scanner, respectively.

Thanks are due to all the members of the Laboratory of Enzyme Chemistry, Department of Food Science and Technology, College of Agriculture, Kyoto University, for their support and discussions throughout

these studies. A word of gratitude to friends is small recognition for their time and expertise in discussing and criticizing the experimental data.

Last but not least the author owes a particular debt to his parents and his wife for starting him off and for their patience and encouragement untill he finished. Without them, these studies would not have been completed.

References

1. Kunitz, M. and Northrop, J. H. (1936) *J. Gen. Physiol.* 19, 991
2. Ham, W. E. and Standstedt, R. M. (1944) *J. Biol. Chem.* 154, 505
3. Bowman, D. E. (1944) *Proc. Soc. Exp. Biol. Med.* 57, 139
4. Kunitz, M. (1947) *J. Gen. Physiol.* 30, 311
5. Lineweaver, H. and Murray, C. W. (1947) *J. Biol. Chem.* 171, 565
6. Laskowski, M., Sr. and Laskowski, M., Jr. (1954) *Adv. Protein Chem.* 9, 203
7. Laskowski, M., Sr. (1955) *Methods Enzymol.* 2, 8
8. Huber, R., Kukla, D., Rühlmann, A., Epp, O., and Formanek, H. (1970) *Naturwissenschaften* 57, 389
9. Huber, R., Kukla, D., Rühlmann, A., and Steigemann, W. (1971) *Cold Spring Harbor Symp. Quant. Biol.* 36, 141
10. Rühlmann, A., Kukla, D., Schwager, P., Bartels, K., and Huber, R. (1973) *J. Mol. Biol.* 77, 417
11. Sweet, R. M., Wright, H. T., Janin, J., Chothia, C. H., and Blow, D. M. (1974) *Biochemistry* 13, 4212
12. Liener, I. E. and Kakade, M. L. (1969) in *Toxic Constituents of Plant Foodstuffs* (Liener, I. E., ed.) p. 7, Academic Press, New York
13. Pusztai, A. (1967) *Nutr. Abstr. Rev.* 37, 1
14. Weyer, E. M. (1968) *Ann. N. Y. Acad. Sci.* 146, 361
15. Laskowski, M., Jr. and Sealock, R. W. (1971) *Enzymes, 3rd Ed.* 3, 375
16. Perlmann, G. E. and Lorand, L. (1970) *Methods Enzymol.* 19, 807
17. Lorand, L. (1976) *Methods Enzymol.* 45, 639

18. Vogel, R., Trautschold, I., and Werle, E. (1966) *Natürliche Proteinasen-Inhibitoren*, Georg Thieme Verlag, Stuttgart

19. Fritz, H. and Tschesche, H. (1971) *Proceedings of the International Conference on Proteinase Inhibitors*, Walter de Gruyter, Berlin

20. Fritz, H., Tschesche, H., Greene, L. J., and Truscheit, E. (1974) *Proteinase Inhibitors, Proceedings of the 2nd International Research Conference*, Springer Verlag, Berlin

21. Murao, S. and Sato, S. (1972) *Agric. Biol. Chem.* 36, 160

22. Murao, S., Sato, S., and Muto, N. (1972) *Agric. Biol. Chem.* 36, 1737

23. Sato, S. and Murao, S. (1973) *Agric. Biol. Chem.* 37, 1067

24. Smith, E. L., Markland, F. S., Kasper, C. B., DeLange, R. J., London, M., and Evans, W. H. (1966) *J. Biol. Chem.* 241, 5974

25. Markland, F. S. and Smith, E. L. (1967) *J. Biol. Chem.* 242, 5198

26. Wright, C. S., Alden, R. A., and Kraut, J. (1969) *Nature* 221, 235

27. Ikenaka, T., Odani, S., Sakai, M., Nabeshima, Y., Sato, S., and Murao, S. (1974) *J. Biochem.* 76, 1191

28. Satow, Y., Mitsui, Y., Iitaka, Y., Murao, S., and Sato, S. (1973) *J. Mol. Biol.* 75, 745

29. Mitsui, Y., Satow, Y., Sakamaki, T., and Iitaka, Y. (1977) *J. Biochem.* 82, 295

30. Morihara, K., Oka, T., and Tsuzuki, H. (1969) *Biochem. Biophys. Res. Commun.* 35, 210

31. Kraut, J., Robertus, J. D., Birktoft, J. J., Alden, R. A., Wilcox, P. E., and Powers, J. C. (1972) *Cold Spring Harbor Symp. Quant. Biol.* 36, 117

32. Robertus, J. D., Alden, R. A., Birktoft, J. J., Kraut, J., Powers,

J. C., and Wilcox, P. E. (1972) *Biochemistry* 11, 2439

33. Murachi, T. (1971) *Kagaku to Seibutsu* (in Japanese) 9, 74

34. Mathews, B. W., Singer, P. B., Henderson, R., and Blow, D. M. (1967) *Nature* 214, 652

35. Bender, M. L., Begue-Canton, M. L., Blakeley, R. L., Brubacher, L. J., Feder, J., Gunter, C. R., Kezdy, F. J., Killheffer, J. V., Jr., Marshall, T. H., Miller, C. G., Roeske, R. W., and Stoops, J. K. (1966) *J. Am. Chem. Soc.* 88, 5890

36. Gutfreund, H. and Sturtevant, J. M. (1956) *Biochem. J.* 63, 656

37. Guggenheim, E. A. (1926) *Philos. Mag.* 2, 538

38. Olaitan, S. A., DeLange, R. J., and Smith, E. L. (1968) *J. Biol. Chem.* 243, 5296

39. Robertus, J. D., Alden, R. A., and Kraut, J. (1971) *Biochem. Biophys. Res. Commun.* 42, 334

40. Green, N. M. and Work, E. (1953) *Biochem. J.* 54, 347

41. Henderson, P. J. F. (1972) *Biochem. J.* 127, 321

42. Wetlaufer, D. B. (1962) *Adv. Protein Chem.* 17, 303

43. Matsubara, H., Kasper, C. B., Brown, D. M., and Smith, E. L. (1965) *J. Biol. Chem.* 240, 1125

44. Dixon, M. and Webb, E. C. (1964) *Enzymes* 2nd Ed., p. 331, Longmans Green & Co., London

45. Sato, S. and Murao, S. (1974) *Agric. Biol. Chem.* 38, 2227

46. Ananthanarayanan, V. S. and Bigelow, C. C. (1969) *Biochemistry* 8, 3717

47. Ananthanarayanan, V. S. and Bigelow, C. C. (1969) *Biochemistry* 8, 3723

48. Itani, N., Kuramitsu, S., Ikeda, K., and Hamaguchi, K. (1975) *J.*

Biochem. 78, 705

49. Sato, S. and Murao, S. (1974) *Agric. Biol. Chem.* 38, 587

50. Kassell, B. (1970) *Methods Enzymol.* 19, 853

51. Schachman, H. K. (1957) *Methods Enzymol.* 4, 32

52. McMeekin, T. L. and Marshall, K. (1952) *Science* 116, 142

53. Haschmeyer, R. H. and Haschmeyer, A. E. V. (1970) *Proteins, A Guide to Chemical Methods*, p. 160, John Wiley & Sons, New York

54. Schachman, H. K. and Edelstein, S. J. (1966) *Biochemistry* 5, 2681

55. Yphantis, D. A. (1964) *Biochemistry* 3, 297

56. Richards, E. G. and Schachman, H. K. (1959) *J. Phys. Chem.* 63, 1578

57. Richards, E. G., Teller, D. C., and Schachman, H. K. (1968) *Biochemistry* 7, 1054

58. Creeth, J. M. and Pain, R. H. (1967) *Prog. Biophys. Mol. Biol.* 17, 217

59. Fujita, H., Kotaka, T., and Uchiyama, H. (1968) in *Butsuriteki Sokutei-hou* II (The Biophysical Society of Japan, ed.) (in Japanese), p. 131, Yoshioka Shoten, Kyoto

60. Adams, E. T., Jr. (1967) *Fractions* 3, 1

61. Sophianopoulos, A. J. and Van Holde, K. A. (1964) *J. Biol. Chem.* 239, 2516

62. Koide, T. and Ikenaka, T. (1973) *Eur. J. Biochem.* 32, 417

63. Birk, Y. (1976) *Methods Enzymol.* 45, 695

64. Haynes, R. and Feeney, R. E. (1967) *J. Biol. Chem.* 242, 5378

65. Krahn, J. and Stevens, F. C. (1971) *FEBS Lett.* 13, 339

66. Sakura, J. D. and Timasheff, S. N. (1973) *Arch. Biochem. Biophys.* 159, 123

67. Harry, J. B. and Steiner, R. F. (1969) *Biochemistry* 8, 5060

68. Miller, D. B. S., Willick, G. E., Steiner, R. F., and Frattali, V. (1969) *J. Biol. Chem.* 244, 281

69. Ventura, M. M., Filho, J. X., Moreira, R. A., Aquino, A. M., and Pinheiro, P. A. (1971) *An. Acad. Bras. Cienc.* 43, 233

70. Melville, J. C. and Ryan, C. A. (1972) *J. Biol. Chem.* 247, 3445

71. Kiyohara, T., Iwasaki, T., and Yoshikawa, M. (1973) *J. Biochem.* 73, 89

72. Belitz, H.-D., Kaiser, K.-P., and Santarius, K. (1971) *Biochem. Biophys. Res. Commun.* 42, 420

73. Gennis, L. S. and Cantor, C. R. (1976) *J. Biol. Chem.* 251, 747

74. Gennis, L. S. and Cantor, C. R. (1976) *J. Biol. Chem.* 251, 754

75. Seidl, D. S. and Liener, I. E. (1972) *J. Biol. Chem.* 247, 3533

76. Rhode, M. B., Bennett, N., and Feeney, R. E. (1960) *J. Biol. Chem.* 233, 1686

77. Joly, M. (1965) *A Physicochemical Approach to the Denaturation of Proteins*, p. 76, Academic Press, New York

78. Meyer, M. L. and Kauzmann, W. (1962) *Arch. Biochem. Biophys.* 99, 348

79. Jirgensons, B. (1967) *J. Biol. Chem.* 242, 912

80. Tanford, C. (1973) *The Hydrophobic Effect: Formation of Micelles and Biological Membranes*, p. 12, John Wiley & Sons, New York

81. Jirgensons, B. (1973) *Optical Activity of Proteins and Other Macromolecules* 2nd Ed., p. 121, Springer Verlag, Berlin

82. Jirgensons, B. and Capetillo, S. (1970) *Biochim. Biophys. Acta* 214, 1

83. Visser, L. and Blout, E. R. (1971) *Biochemistry* 10, 743

84. Darnall, D. W. and Barela, T. D. (1971) *Biochim. Biophys. Acta* 236, 593

85. Anthony, J. S. and Moscarello, M. A. (1971) *Biochim. Biophys. Acta* 243, 429

86. Sund, H., Weber, K., and Mölbert, E. (1967) *Eur. J. Biochem.* 1, 400

87. Reynolds, J. A. and Tanford, C. (1970) *J. Biol. Chem.* 245, 5161

88. Nelson, C. A. (1971) *J. Biol. Chem.* 246, 3895

89. Reynolds, J. A. and Tanford, C. (1970) *Proc. Nat. Acad. Sci. U. S. A.* 66, 1002

90. Wilhelmy, L. (1863) *Ann. Phys. (Leipzig)* 119, 186

91. Takagi, T., Tsujii, K., and Shirahama, K. (1975) *J. Biochem.* 77, 939

92. Casassa, E. F. and Eisenberg, H. (1964) *Adv. Protein Chem.* 19, 287

93. Hersh, R. T. and Schachman, H. K. (1958) *Virology* 6, 234

94. Tanford, C., Nozaki, Y., Reynolds, J. A., and Makino, S. (1974) *Biochemistry* 13, 2369

95. Carusi, E. A. and Sinsheimer, R. L. (1963) *J. Mol. Biol.* 7, 388

96. Shibata, K. (1974) *Supekutoru Sokutei to Bunkoukoudokei* (in Japanese), p. 232, Kodansha, Tokyo

97. Scheraga, H. A. (1961) *Protein Structure*, p. 217, Academic Press, New York

98. Donovan, J. W., Laskowski, M., Jr., and Scheraga, H. A. (1961) *J. Am. Chem. Soc.* 83, 2686

99. Nakagawa, Y. and Jirgensons, B. (1973) *Biochim. Biophys. Acta* 328, 42

100. Sogami, M., Uyeda, M., and Ogura, S. (1973) *Biochim. Biophys. Acta*

310, 487

101. Bigelow, C. C. and Sonenberg, M. (1962) *Biochemistry* 1, 197

102. Elödi, P. and Lakatos, S. (1973) *Eur. J. Biochem.* 36, 45

103. Ikai, A. (1976) *Biochim. Biophys. Acta* 445, 182

104. Bernhard, S. A., Lee, B. F., and Tashjian, Z. H. (1966) *J. Mol. Biol.* 18, 405

105. Wilcox, P. E. (1970) *Methods Enzymol.* 19, 64

106. Walsh, K. A. (1970) *Methods Enzymol.* 19, 41

107. Lineweaver, H. and Burk, D. (1934) *J. Am. Chem. Soc.* 56, 658

108. Dixon, M. (1953) *Biochem. J.* 55, 170

109. Bernhard, S. A. and Gutfreund, H. (1965) *Proc. Nat. Acad. Sci. U. S. A.* 53, 1238

110. Sato, S., Kimura, T., and Murao, S. (1975) *Agric. Biol. Chem.* 39, 415

111. Guillain, F. and Thusius, D. (1970) *J. Am. Chem. Soc.* 92, 5534

112. Brandt, K. D., Himoe, A., and Hess, G. P. (1967) *J. Biol. Chem.* 242, 3973

113. Quast, U., Engel, J., Heumann, H., Krause, G., and Steffen, E. (1972) *Biochemistry* 13, 2512

114. Engel, J., Quast, U., Heumann, H., Krause, G., and Steffen, E. (1974) in *Proteinase Inhibitors, Proceedings of the 2nd International Research Conference* (Fritz, H., Tschesche, H., Greene, L. J., and Truscheit, E., eds.), p. 412, Springer Verlag, Berlin

115. Beaven, G. H. and Holliday, E. R. (1952) *Adv. Protein Chem.* 7, 319

116. Herskovits, T. T. and Laskowski, M., Jr. (1962) *J. Biol. Chem.* 237, 2481

117. Eyzaguirre, J. (1974) *Biochem. Biophys. Res. Commun.* 60, 35

118. Herskovits, T. T. (1967) *Methods Enzymol.* 11, 748

119. Herskovits, T. T. and Sorensen, S. M. (1968) *Biochemistry* 7, 2523

120. Inada, Y. (1961) *J. Biochem.* 49, 217

121. Tachibana, A. and Murachi, T. (1966) *Biochemistry* 5, 2756

122. Markland, F. S. (1969) *J. Biol. Chem.* 244, 694

123. Crammer, J. L. and Neuberger, A. (1943) *Biochem. J.* 37, 302

124. Hiromi, K., Ohnishi, M., Kanaya, K., and Matsumoto, T. (1975) *J. Biochem.* 77, 957

125. Herskovits, T. T. and Sorensen, S. M. (1968) *Biochemistry* 7, 2533

126. Uehara, Y., Tonomura, B., Hiromi, K., Sato, S., and Murao, S. (1976) *Biochim. Biophys. Acta* 453, 513

127. Neet, K. E., Nanci, A., and Koshland, D. E., Jr. (1968) *J. Biol. Chem.* 243, 6392

128. Svendsen, I. (1968) *Compt. Rend. Trav. Lab. Carlsberg* 36, 235

129. Svendsen, I. (1968) *Compt. Rend. Trav. Lab. Carlsberg* 36, 347

130. Herskovits, T. T. and Fuchs, H. H. (1972) *Biochim. Biophys. Acta* 263, 468

131. Ottesen, M. and Svendsen, I. (1970) *Methods Enzymol.* 19, 199

132. Luthy, J. A., Praissman, M., Finkenstadt, W. R., and Laskowski, M., Jr. (1973) *J. Biol. Chem.* 248, 1760

133. Finkenstadt, W. R., Hamid, M. A., Mattis, J. A., Shrode, J., Sealock, R. W., Wang, D., and Laskowski, M., Jr. (1974) in *Proteinase Inhibitors, Proceedings of the 2nd International Research Conference* (Fritz, H., Tschesche, H., Greene, L. J., and Truscheit, E., eds.), p. 389, Springer Verlag, Berlin

134. Lazdunski, M., Vincent, J. P., Schweitz, H., Péron-Renner, M., and Pudles, J. (1974) in *Proteinase Inhibitors, Proceedings of the 2nd*

International Research Conference (Fritz, H., Tschesche, H., Greene, L. J., and Truscheit, E., eds.), p. 420, Springer Verlag, Berlin

135. Gutfreund, H. (1972) *Enzymes, Physical Principles*, p. 157, John Wiley & Sons, London

136. Fairhead, S. M., Steel, J. S., Wreford, L. J., and Walker, I. O. (1969) *Biochim. Biophys. Acta* 194, 584

137. Budzynski, A. Z. (1972) *Biochim. Biophys. Acta* 251, 292

138. Vogel, D. and Jaenicke, R. (1974) *Eur. J. Biochem.* 41, 607

139. Combarnous, Y. and Maghuin-Rogister, G. (1974) *Eur. J. Biochem.* 42, 7

140. Epp, O., Colman, P., Fehlhammer, H., Bode, W., Schiffer, M., Huber, R., and Palm, W. (1974) *Eur. J. Biochem.* 45, 513

141. Schalch, W. and Bode, W. (1975) *Biochim. Biophys. Acta* 405, 292

142. Kowalski, D., Leary, T. R., McKee, R. E., Sealock, R. W., Wang, D., and Laskowski, M., Jr. (1974) in *Proteinase Inhibitors, Proceedings of the 2nd International Research Conference* (Fritz, H., Tschesche, H., Greene, L. J., and Truscheit, E., eds.), p. 311, Springer Verlag, Berlin

143. Spackman, D. H., Stein, W. H., and Moore, S. (1958) *Anal. Chem.* 30, 1190

144. Matsubara, H. and Sasaki, R. M. (1969) *Biochem. Biophys. Res. Commun.* 35, 175

145. Bieth, J. (1974) in *Proteinase Inhibitors, Proceedings of the 2nd International Research Conference* (Fritz, H., Tschesche, H., Greene, L. J., and Truscheit, E., eds.), p. 463

146. Sokolovsky, M., Riordan, J. F., and Vallee, B. L. (1966) *Biochem-*

istry 5, 3582

147. Weber, K. and Osborn, M. (1969) *J. Biol. Chem.* 244, 4406

148. Andrews, P. (1965) *Biochem. J.* 96, 595

149. Markland, F. S. (1969) *Fed. Proc., Fed. Am. Soc. Exp. Biol.* 28, 877

150. Smith, E. L., Markland, F. S., and Glazer, A. N. (1970) in *Structure-Function Relationships of Proteolytic Enzymes* (Desnuelle, P., Neurath, H., and Ottesen, M., eds.), p. 160, Munksgaard, Copenhagen

151. Markland, F. S. and Smith, E. L. (1971) *Enzymes, 3rd Ed.* 3, 561

152. Weber, B. H. and Kraut, J. (1968) *Biochem. Biophys. Res. Commun.* 33, 280

153. Svendsen, I. (1974) *Compt. Rend. Trav. Lab. Carlsberg* 39, 375

154. Wright, C. S., Alden, R. A., and Kraut, J. (1972) *J. Mol. Biol.* 66, 283

155. Wright, C. S. (1972) *J. Mol. Biol.* 67, 151

156. Schechter, I. and Berger, A. (1967) *Biochem. Biophys. Res. Commun.* 27, 157

157. Polgar, L. and Bender, M. L. (1966) *J. Am. Chem. Soc.* 88, 3153

158. Polgar, L. and Bender, M. L. (1967) *Biochemistry* 6, 610

159. Philipp, M., Polagar, L., and Bender, M. L. (1970) *Methods Enzymol.* 19, 215

160. Cassim, J. Y. and Yang, J. T. (1969) *Biochemistry* 8, 1947

161. Chen, Y.-H., Yang, J. T., and Martinez, H. M. (1972) *Biochemistry* 11, 4120

162. DeTar, DeLos F. (1969) *Anal. Chem.* 41, 1406

163. Sakoda, M. and Hiromi, K. (1976) *J. Biochem.* 80, 547

164. Alden, R. A., Wright, C. S., Westall, F. C., and Kraut, J. (1970) in *Structure-Function Relationships of Proteolytic Enzymes* (Desnuelle, P., Neurath, H., and Ottesen, M., eds.), p. 173, Munksgaard, Copenhagen

165. Drenth, J., Jansonius, J. N., Koekoek, R., and Wolthers, B. G. (1971) *Adv. Protein Chem.* 25, 79

166. Neet, K. E. and Koshland, D. E., Jr. (1966) *Proc. Nat. Acad. Sci. U. S. A.* 56, 1606

167. Pauling, L. (1960) *The Nature of the Chemical Bond* 3rd Ed., Cornell University Press, Ithaca

168. Jencks, W. P. and Carriuolo, J. (1959) *J. Biol. Chem.* 243, 1280

169. Jencks, W. P. and Carriuolo, J. (1960) *J. Am. Chem. Soc.* 82, 1778

170. Swain, C. G. and Scott, C. B. (1953) *J. Am. Chem. Soc.* 75, 141

171. Bjerrum, N. (1923) *Z. Physik. Chem.* 106, 219

172. Edsall, J. T. and Wyman, J. (1958) *Biophysical Chemistry* I, p. 460, Academic Press, New York

173. Kuramitsu, S., Ikeda, K., and Hamaguchi, K. (1977) *J. Biochem.* 82, 585

174. Kangawa, K., Matsuo, H., and Narita, K. (1976) *Seibutsubutsuri* (in Japanese) 16, 145

175. Imoto, T., Johnson, L. N., North, A. C. T., Phillips, D. C., and Rupley, J. A. (1972) *Enzymes, 3rd Ed.* 7, 665

176. Kazal, L. A., Spicer, D. A., and Brahinsky, R. A. (1948) *J. Am. Chem. Soc.* 70, 3034

177. Greene, L. J. and Bartelt, D. C. (1969) *J. Biol. Chem.* 244, 2646

178. Bartelt, D. C. and Greene, L. J. (1971) *J. Biol. Chem.* 246, 2218

179. Tschesche, H. and Wachter, E. (1970) *Eur. J. Biochem.* 16, 187

180. Tschesche, H., Wachter, E., Kupfer, S., Obermeier, R., Reidel, G., Haenisch, G., and Schneider, M. (1971) in *Proceedings of the International Conference on Proteinase Inhibitors* (Fritz, H. and Tschesche, H., eds.), p. 207, Walter de Gruyter, Berlin

181. Bartelt, D. C., Shapanka, R., and Greene, L. J. (1977) *Arch. Biochem. Biophys.* 179, 189

182. Laskowski, M., Jr., Kato, I., Leary, T. R., Schrode, J., and Sealock, R. W. (1974) in *Proteinase Inhibitors, Proceedings of the 2nd International Research Conference* (Fritz, H., Tschesche, H., Greene, L. J., and Truscheit, E., eds.), p. 597, Springer Verlag, Berlin

183. Iwasaki, T., Kiyohara, T., and Yoshikawa, M. (1973) *J. Biochem.* 73, 1039

184. Iwasaki, T., Kiyohara, T., and Yoshikawa, M. (1973) *J. Biochem.* 74, 335

185. Kiyohara, T., Fujii, M., Iwasaki, T., and Yoshikawa, M. (1973) *J. Biochem.* 74, 675

a. Inouye, K., Tonomura, B., Hiromi, K., Sato, S., and Murao, S. (1977) *J. Biochem.* 82, 961; Tonomura, B., Inouye, K., Hiromi, K., Sato, S., and Murao, S. (1973) The abstract of papers, The Annual Meeting of the Agricultural Chemical Society of Japan, Tokyo, p. 163

b. Inouye, K., Tonomura, B., Hiromi, K., Kotaka, T., Inagaki, H., Sato, S., and Murao, S. (1973) The abstract of papers, 12th Annual Meeting of the Biophysical Society of Japan, Tokyo, p. 47

c. Inouye, K., Tonomura, B., and Hiromi, K. (1976) The abstract of papers, The Annual Meeting of the Agricultural Chemical Society of Japan, Kyoto, p. 227

d. Inouye, K., Tonomura, B., and Hiromi, K. (1975) *Agric. Biol. Chem.* 39, 1159

e. Inouye, K., Tonomura, B., and Hiromi, K. (1974) The abstract of papers, 13th Annual Meeting of the Biophysical Society of Japan, Sapporo, p. 228

f. Inouye, K., Tonomura, B., Hiromi, K., Sato, S., and Murao, S. (1977) *J. Biochem.* 82, 1207; Inouye, K., Tonomura, B., Hiromi, K., Sato, S., and Murao, S. (1974) The abstract of papers, The Annual Meeting of the Agricultural Chemical Society of Japan, Tokyo, p. 391; Tonomura, B., Inouye, K., Uehara, Y., Hiromi, K., Sato, S., Murao, S., and Miwa, M. (1974) The abstract of papers, 25th Forum on Protein Structure, Osaka, p. 125

g. Inouye, K., Tonomura, B., and Hiromi, K. (1975) The abstract of papers, 26th Forum on Protein Structure, Nagasaki, p. 117; Tonomura, B., Inouye, K., Uehara, Y., and Hiromi, K. (1975) *Seikagaku* (in Japanese) 47, 399

h. Inouye, K., Tonomura, B., and Hiromi, K. (1976) *Seikagaku* (in Japanese) 48, 542

i. Fujiwara, K., Inouye, K., Tonomura, B., Murao, S., and Tsuru, D. (1977) *J. Biochem.* 82, 125

j. Inouye, K., Tonomura, B., Hiromi, K., Fujiwara, K., and Tsuru, D. (1977) The abstract of papers, 28th Forum on Protein Structure, Tokyo, p. 105